Development of an Indirect Forced Convection Solar Dryer for Cassava Chips

Article · December 2014

Akindele Folarin Alonge
University of Uyo

Aims and Scope

The main aim of the Journal of Agricultural Engineering and Technology (JAET) is to provide a medium for dissemination of high quality Technical and Scientific information emanating from research on Engineering for Agriculture. This, it is hoped will encourage researchers in the area to continue to develop cutting edge technologies for solving the numerous engineering problems facing agriculture in the third world in particular and the world in general.

The Journal publishes original research papers, review articles, technical notes and book reviews in Agricultural Engineering and related subjects. Key areas covered by the journal are: Agricultural Power and Machinery; Agricultural Process Engineering; Food Engineering; Post-Harvest Engineering; Soil and Water Engineering; Environmental Engineering; Agricultural Structures and Environmental Control; Waste Management; Aquacultural Engineering; Animal Production Engineering and the Emerging Technology Areas of Information and Communications Technology (ICT) Applications, Computer Based Simulation, Instrumentation and Process Control, CAD/CAM Systems, Biotechnology, Biological Engineering, Biosystems Engineering, Bioresources Engineering, Nanotechnology and Renewable Energy. The journal also considers relevant manuscripts from related disciplines such as other fields of Engineering, Food Science and Technology, Physical Sciences, Agriculture and Environmental Sciences.

The Journal is published by the Nigerian Institution of Agricultural Engineers (NIAE), A Division of Nigerian Society of Engineers (NSE). The Editorial Board and NIAE wish to make it clear that statements or views expressed in papers published in this journal are those of the authors and no responsibility is assumed for the accuracy of such statements or views. In the interest of factual recording, occasional reference to manufacturers, trade names and proprietary products may be inevitable. No endorsement of a named product is intended nor is any criticism implied of similar products that are not mentioned.

Submission of an article for publication implies that it has not been previously published and is not being considered for publication elsewhere. The Journal's peer review policy demands that at least two reviewers give positive recommendations before the paper is accepted for publication. Prospective authors are advised to consult the Guide for Authors which is available in each volume of the Journal. Four copies of the manuscript should be sent to:

The Editor-In-Chief
Journal of Agricultural Engineering and Technology (JAET)
℅ The Editorial Office
National Centre for Agricultural Mechanization (NCAM)
P.M.B. 1525
Ilorin, Kwara State,
Nigeria.

Papers can also be submitted directly to the Editor-In-Chief or any of the Sectional Editors. Those who have access to the internet can submit electronically as an attached file in MS Word to aponwualu@niae.net; ponwualu@yahoo.com. All correspondence with respect to status of manuscript should be sent to the Technical Assistant to the Editor-In-Chief at ifeeolife@yahoo.com.

TABLE OF CONTENTS

GUIDELINES, PROCESSES, OPERATIONAL TECHNIQUES AND FACTORS TO CONSIDER IN MECHANIZED AGRICULTURAL BUSH CLEARING IN NIGERIA

J. C. Adama
Department of Agricultural and Bioresouces Engineering,
College of Engineering and Engineering Technology,
Michael Okpara University of Agriculture, Umudike, Nigeria.
Email: adamajoseph@yahoo.com

ABSTRACT

Bush clearing for any purpose causes environmental degradation when improperly done. To reduce this effect, there are guidelines to be followed. This paper presents the guidelines, processes operational techniques and factors to be considered in mechanized agricultural bush clearing in the tropics.

The author relied on literature, interaction with farmers and machinery operators and his experience as field officer in National Agricultural Land Development Authority of Nigeria (NALDA) to develop a system for mechanized agricultural bush clearing in the tropics. Some of the recommendations are that the site should have a slope and stoniness of less than 5% and 20% respectively, depth to compact layer and bedrock should be greater than 40 cm and 75 cm respectively, a band of between 5 m – 10 m of vegetation must be left along both sides of rivers and streams where they exist, and where a bulldozer is used for windrowing, a maximum depth of 80 mm and a maximum lateral movement of 1 m of the soil are allowed. Areas that are poorly drained with sandy gravel and silty clay loam should not be cleared mechanically.

In all cases, mechanized agricultural bush clearing must be properly planned and executed. Also, the operation should be supervised by experts who must include soil scientists and agricultural engineers. This is to ensure that the operators adhere strictly to the guidelines.

KEYWORDS: Bush clearing, agriculture, mechanization, machinery, soil.

1. INTRODUCTION

Bush clearing for crop production such as construction is different from bush clearing for other purposes. This is because, the cardinal objective in clearing for other purposes is not only the removal of all bush, rubbish, debris and other objectionable materials, but the top soil is also removed and may be replaced with sub soil (laterite) and where necessary, compacted or stabilized depending on the type of project. In agricultural bush clearing, the top soil must be preserved. The top soil contains nutrients needed by crops for optimum performance. Agricultural bush clearing is therefore defined as the process of scientific removal and disposal of existing material, vegetation, rubbish and other obstructions from the land by manual, mechanical and chemical means for agricultural food production (Anazodo, 1986; NALDA, 1992; Adama, 2013). Agricultural bush clearing operation is effective only when all the unwanted vegetation including all roots and stumps are removed with minimum disturbance to the top soil (Nwuba, 1984).

The basic objectives of mechanized agricultural bush clearing and land development are to remove unwanted materials from the land and to increase the size of land to be cultivated_ Unwanted materials include trees, boulders, stumps and tree trunks. These materials cause obstructions to smooth field operations during subsequent tillage and other operations on the land. Tall trees also prevent rain and sunlight from getting to the soil by shielding. The area to be cultivated could be limited by presence of unwanted vegetation and undulating terrain, and stumps which could be easily removed using mechanical means.

Bush clearing in general increases erosion and sedimentation of waterways and reduces water quality. Also, the operation removes habitats leading to the direct loss of native animals and plants. To reduce the negative effects of mechanized agricultural bush clearing especially in the tropics, the operation requires to be properly supervised and guidelines followed. This is because soils in the tropics are known to be delicate and low in organic matter content both down the depth and in profiling (FAO, 1990; Adama, 2013). In Nigeria for instance, about 63% of the soils are low in productivity and over 90% of them are alfisols and ultisols which are low in organic matter and have low activity clays (Ojeniyi, 1997).

A number of researchers have conducted field studies on agricultural bush clearing in the tropics. For instance, Anazodo, (1986) developed appropriate methods and equipment for agricultural land clearing and development in Nigeria. Oni and Adeoti (1994) conducted field experiment to determine the effects of mechanized land clearing and tractor traffic on agricultural soils and crop growth. Okore, et al. (2006) carried out field studies on impact of land clearing methods and cropping systems on labile Soil C and N pools in the Humid zone Forest of Nigeria. Fagbemi and Gana (1994) attempted to produce guidelines for agricultural bush clearing in Nigeria. Couper, 1996 working under the International Institute for Tropical Agriculture, produced a guide for agricultural land clearing in the tropics. Although these works are useful and relevant, they are limited in scope. They failed to give comprehensive approach to mechanized agricultural bush clearing. Also documents to guide farmers, field officers, machinery operators, etc on operational guidelines and specifications for mechanized agricultural bush clearing existed mostly as technical bulletins and abridged guides in government agencies. Peer reviewed publications in reputable journals in this field are scarcely available.

The objective of this study is to develop a comprehensive approach for mechanized agricultural bush clearing in the tropics. The approach includes guidelines, processes, operational techniques and factors to consider before embarking on mechanized agricultural bush clearing in the tropics. The approach is intended to serve large scale farmers, agronomists, agricultural engineers, machinery operators and other stake holders in crop production industry.

2. METHODOLOGY

Part of the information and data used in this study were sourced from relevant literature. Other information and data were gathered from field experience and interview of farmers, machinery operators and field engineers/officers of Agricultural Development Programme, River Basin Development Authority, Federal Department of Rural Development and National Directorate of Employment in South East and South South geopolitical zones of Nigeria. The interview was conducted using questionnaire and the enumerators were the 2013/2014 set of final year students of the Department of Agricultural and Bioresources Engineering, Michael Okpara University of Agriculture Umudike Nigeria. The interviews were conducted in the first semester of 2013/2014 session.

The field experience was acquired during bush clearing operations in the project sites of the National Agricultural Land Development Authority (NALDA) in Nigeria. The literatures were sourced from the National Agricultural Land Development Authority (NALDA) and International Institute for Tropical Agriculture (IITA).

3. RESULTS AND DISCUSSION

3.1 Processes and Unit Operations in Mechanized Agricultural Bush Clearing

The processes and unit operations for mechanized agricultural bush clearing were identified which include the following:

(a) Acquisition of land: In areas where land is donated by the community, the first step is to acquire the land and then follow necessary steps to register it.

(b) Notification of availability of land: The first major step is for the farmer to know where land is available. This can be obtained through agents or land owners, In National Agricultural Land Development Authority, it was required that land owners (donors) should notify the authority of the availability of land and their willingness to give such land for mechanized agricultural bush clearing in writing through the Local Government Chairman.

(c) Site visitation and selection: The farmer then visits the site to observe the location, condition and suitability of the land.

(d) Site evaluation: The site will be evaluated to obtain its suitability for crop production. This will involve surveys such as perimeter, contour and soil to determine the nutrient status; demarcation of the farm and mapping out the roads; indication of permanent features such as rivers, valleys, hills and hanging cliffs; show the topography of the land depth to bedrock, drainage ability, percent slope, percent stoniness, surface stone and rock outcrops.

Table 1 gives soil suitability criteria for mechanized agricultural bush clearing. Soils having components falling within the "Not recommended" category in the Table should not be cleared because such areas are prone to accelerated erosion or surface ponding.

Table 1: Soil suitability selection criteria for mechanized agricultural bush clearing

S/N	Soil factors	Good	Fair	Not recommended
1	Surface Texture	Sandy Loam, Loam, Silt Loam	Loamy Sand, Clay Loam	Sandy Gravel, Silty, Clay Loam
2	Depth to Compact Layer	Greater than 40 cm	20 to 40 cm	Less than 20 cm
3	Depth to Bedrock	Greater than 75 cm	40 to 75 cm	Less than 40 cm
4	Drainage	Well Moderately	Rapid, imperfect	Poor
5	Slope (%)	Less than 5%	5% to 10%	Greater than 10%
6	Stoniness (%)	Less than 20%	20% to 30%	Greater than 30%
7	Surface stone (%)	Less than 0.1%	0.1 to 3%	Greater than 3%
8	Rock Outcrops (%)	0%	Less than 10%	Greater than 10%

Source: (Brunswick, 2008)

(e) Tree count and tree size:
The tree count involves taking a census of the trees in the area. The result will be the density (population per hectare) of trees in the area. The tree size is then determined by measuring circumference ''Cs'' of each tree at a height of 1.37m from the ground using the Rome Job Industries formula (Elesa, 2003). The diameter ''D'' of each tree is then calculated from the formula, $D = Cs/\pi$. After getting the diameter, the basal area ''A'' is calculated from the formula $A = \pi(D^2)/4$. Before undertaking the above exercises, a section of the field should be mapped out in blocks and the blocks divided into plots. The tree count and the tree circumferences are done within the plots in each block. It is also required that the trees in the plots should be grouped in diameter ranges (Adama, 2013)

(f) Machinery sourcing and mobilization to the site:
After the above operations, the next operation is to source for suitable machinery. Crawler tractor which should not be more than model D7 or its equivalent should be sourced to reduce soil compaction problem. Crawler tractors can be sourced from road construction firms and adopted for the operation in absence of specialized agricultural bush clearing companies to provide such specialized agricultural bush clearing machinery like brush rake, tree pusher, anchor chains etc.

The next step is machinery mobilization to site for the clearing.

(g) Bush clearing, monitoring and inspection.
In the field, as bush clearing is going on, the operation is closely monitored by experts to ensure that proposed guidelines are adhered to (Figure 1).

Figure 1: Crawler tractor bulldozer in agricultural bush clearing operation under supervision (Adama, 2013)

3.2 Guidelines and Specifications for Mechanized Agricultural Bush Clearing

The following guidelines are to be observed in bush clearing for crop production (NALDA, 1994a and b; Brunswick, 2008; Miscellaneous, 2009). They are applicable for all mechanized agricultural bush clearing project irrespective of the clearing machinery.

(a) The vegetation should be cleared in such a way that minimum disturbance is caused to the top soil to a depth of not more than 80 mm. In fact, the clearing should limit the movement of top soil from the area being cleared. This is to ensure that the top soil which contains the nutrients is retained as much as possible.

(b) All standing dry trees must be knocked down and all shrubs, stumps, large stones and other obstacles to the normal subsequent field operations like ploughing, harrowing and ridging must be completely removed. It is dangerous to leave dry trees in the farms as they could fall anytime damaging crops and/or causing injury if they fall on workers.

(c) Economic trees must as much as possible be left in place, but they should be at least 20 m apart. Where there are clusters of such trees, the older ones that are spent should be cleared leaving only the ones that shall be identified by the field engineer or supervisor. The older ones are removed so that they will give way to young ones.

(d) When a bulldozer (where clearing rake, chains or tree pusher is not available) is used for windrowing, a maximum depth of 80 mm and a maximum lateral movement of 1 m of the soil are allowed. The depth limit should be strictly observed to avoid digging out the subsoil which has little nutrient. The 1 m lateral movement should also be observed in order to reduce compaction during piling and /or windrowing.

(e) Windrows should be 120 m apart and the width of each should not be more than 4 m. When windrows are spaced as recommended, it will give way for proper parcellation and tractor maneuverability.

(f) Land should not be cleared on slopes above 10%. This is because clearing on lands with such slope will accelerate erosion which could jeopardize the venture.

(g) A band of between 5 m – 10 m of vegetation must be left along both sides of rivers and streams. This is necessary to preserve the stream and the habitats and prevent erosion from encroaching into the farm.

(h) Under no circumstances should felled trees or shrubs be piled across or along water way. This is to allow free flow of water thereby reducing ponding and water flow into the field.

(i) When uprooting trees using crawler tractor equipped with dozer blade, take care to control the fall of the tree to avoid breaking trees marked as economic or wind breakers.

(j) Ensure minimum top soil removal along the debris on the windrow. Wind breakers help to reduce wing erosion.

(k) Protective tractor mounted cabs, complete jungle bush clearing protection package or forest canopy should be used when extensive clearing operations are anticipated. This will protect both the perator and the machinery and thus permit greater flexibility and increase operator efficiency.

3.3 Processes and Operational Techniques for Tree Felling (Knockdown) Using Crawler Tractor Bulldozer

In Nigeria and in a number of countries in the tropics, crawler tractor bulldozer is the commonest equipment for mechanized agricultural bush clearing. In absence of specialized agricultural bush clearing machinery like anchor chains, tree pusher, brush rake, good clearing can be achieved using crawler tractors. Farmers in these adopt this category of machinery. The machinery are sourced from road construction firms in absence of specialized agricultural equipment hiring firms. Research has shown that under proper supervision, crawler tractor bulldozer can serve as agricultural bush clearing (Adama, 2013). The greatest challenge when crawler tractor bulldozer is used is experienced when the equipment is uprooting a tree and during windrowing (Adama, 2014). With specialized machinery like anchor chains, tree pusher, brush rake as listed earlier, good clearing is achieved with minimum disturbance to the soil system. But where tractor bulldozer is used, the following processes and techniques are recommended to be followed (Miscellaneous, 2009; Adama, 2013). This will ensure good clearing and thus achieve the objective of minimum disturbance to the top soil.

In thick vegetation with trees that have diameters between 0.15 m and 0.3 m the machinery should be operated with the blade raised as high as possible to gain added leverage (Figure 2) As the tree falls, the implement is backed up quickly to clear the roots. As the implement is lowered, the machine travels forward again to dig the roots (Figure 3).

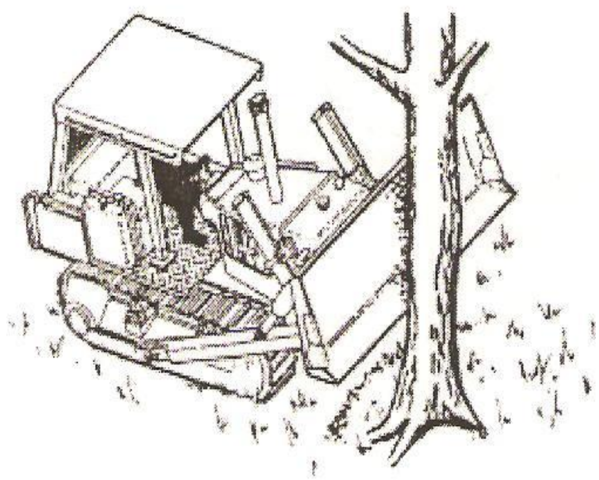

Fig 2: Crawler tractor with the bulldozer in a raised position to fell a tree
Source: (Miscellaneous, 2009).

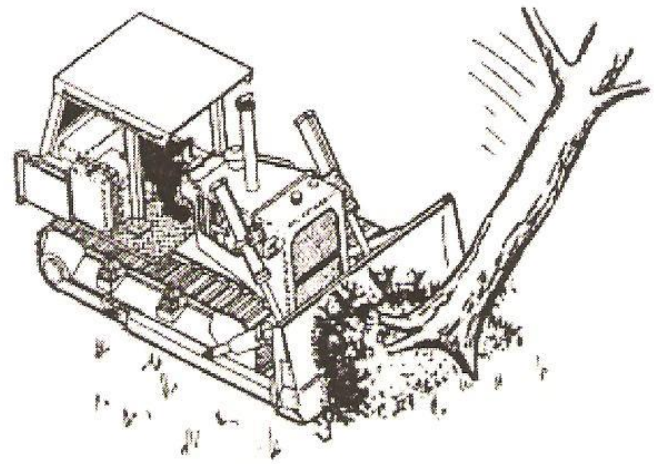

Fig 3: Crawler tractor traveling forward with the bulldozer to dig out tree roots
Source: (Miscellaneous, 2009).

The process and techniques for removing large trees 1.00 m diameter and above is slower and more difficult (Miscellaneous, 2009). First, gently and cautiously probe the tree for dead limbs that could fall and injure the operator or other workers or damage the machine and/or the components. Then, position the implement for maximum leverage. Determine the direction of fall before pushing. The direction of lean is usually the direction of fall. When this is determined, the following steps are followed:

Step 1: Opposite the direction of fall, make a cut deep enough to cut some of the large roots as shown in Figure 4(a)

Step 2: Cut side two as shown in Figure 4(b)

Step 3: Cut side three as shown in Figure 4(c)

Step 4: To obtain greater pushing leverage, build an earth ramp on the same side as the original cut. The tree is pushed over as shown in Figure 4(d)

As the tree starts to fall, reverse the tractor quickly to get away from rising roots mass. After fall, fill the hole created so that water will not collect in it. As the tree starts to fall, the operator should watch to ensure that the tree does not fall on him and the machine. As these processes are going on, experienced professionals namely, agricultural engineer, soil scientist and technical assistants should be on the watch to ensure that clearing including the tree felling operations are done in accordance with lay-down procedure.

The operational techniques have been demonstrated in a field trial at Ako Nike and Agu Ukehe Enugu state Nigeria (Adama, 2013).

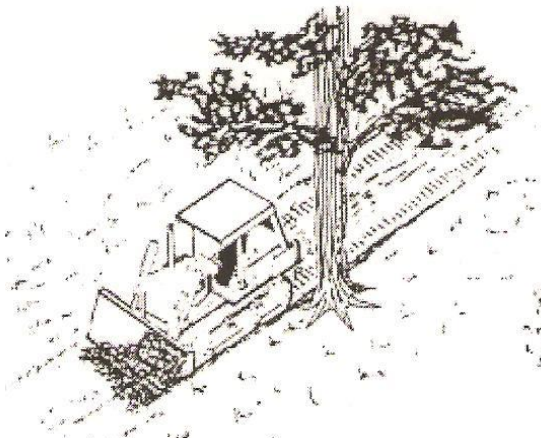

Fig 4a: The Technique of Felling a Tree (Step 1)

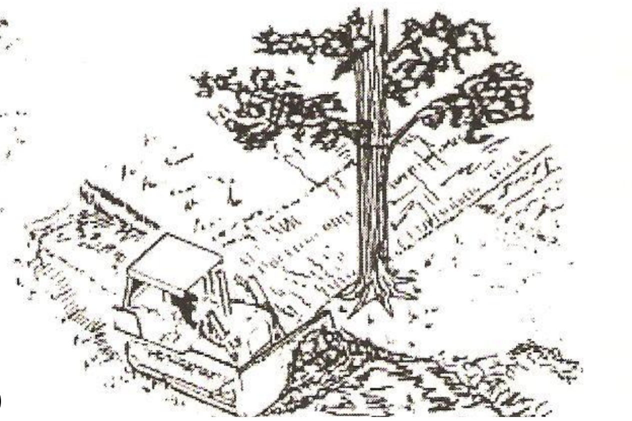

Fig 4b: The Technique of Felling a Tree (Step 2)

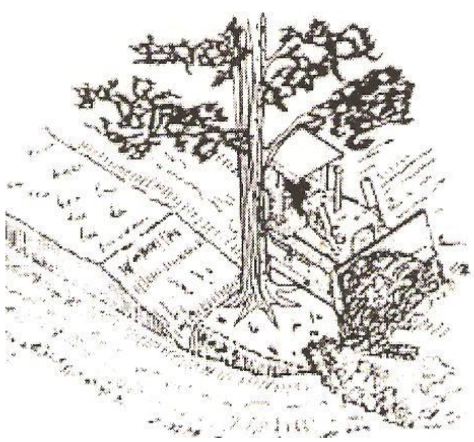

Fig 4c: The Technique of Felling a Tree (Step 3): The Bulldozer Cutting Roots at Side Three

Source: (Miscellaneous, 2009)

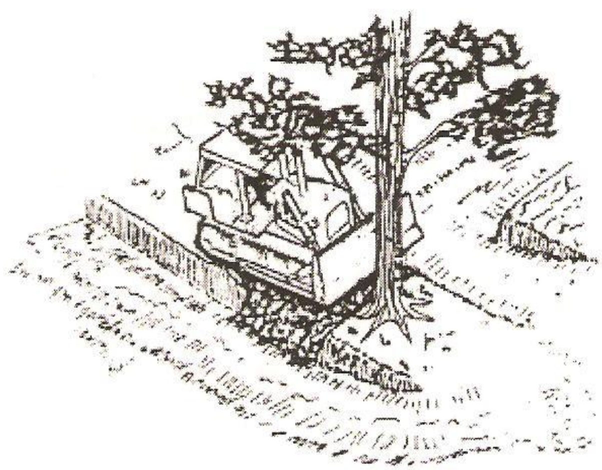

Fig 4d: The Technique of Felling a Tree (Step IV)

3.5 Factors to Consider in Planning and Undertaking Integrated Agricultural Land Development Project

Agricultural bush clearing can be carried out as a single operation but the planning is integrated with other operations involved in large scale crop production. These other operations include surveys, mapping, bush clearing, tillage, erosion control, irrigation design and management. All these operation including bush clearing are referred to as integrated agricultural land development project.

The factors to consider before planning and embarking on mechanized agricultural land development project can be grouped into four areas, namely: environmental, social or institutional, cost- price and end users (Anazodo, 1986; Onwualu et al; 2006). These operations which are necessary in large scale crop production include:

3.4.1 Environmental Factors

The environmental factors can be divided as follows:

(i) Land: soils, topography, size and shape of land.

(ii) Temperature: annual extremes and length of growing seasons.

(iii) Water: control, rainfall amount and distribution, availability of irrigation water, disruption of natural watersheds.

(iv) Location: access roads, farm stead, market, electricity load centre and service areas.

(v) Vegetative: cover, type and density and possibility of re-growth after initial clearing.

The type of trees, vegetation, soil, and terrain of the site must be determined as accurately as possible. This could be done through climatic geological maps, intelligent reports, aerial and ground reconnaissance. The density of the trees as earlier described is determined by conducting a tree count and recording the tree diameters at breast height which is taken at 1.37 m (4.5 ft) above the ground. Record also the species and number of trees.

3.4.2 Social or Institutional

The social or institutional factors to consider are:

(i) The place accorded land in the overall scope of national development.

(ii) Willingness and /or ability of the government to support agriculture through fiscal tax policy: adequate transportation facilities: favorable policies on land tenure, land reform and settlement project development.

(iii) Willingness and /or ability of the government to support research interpret research findings and disseminate information on various aspects of land development.

(iv) Availability and willingness of the government to provide training at all levels to foster extension programme and to use mass media such as radio, television and print in helping to attain the objectives of agricultural land development.

3.4.3 Cost - price Factors

The cost-price factors referred to as economic considerations to be borne in mind in integrated agricultural land development operations are as follow;

(i) Return on investment. That is the price received by the farmer on the crops he produces.

(ii) Cost of input required. These include; land development, tools, hired labour, agro chemicals, seeds and seedlings and taxes on land, availability and cost of credit which may either be long term credit to finance land, construction of major buildings, machinery or intermediate credit to finance establishment of tree crops, major land development operations such as surveys, bush clearing and tillage and erosion control.

(iii) Availability and cost of transport, storage, processing and market facilities.

(iv) Benefits available from the state such as subsidies, price support and assured markets.

3.4.4 The End User

Another important factor to consider is the ability of the end user (owner or manager of the project) to make proper use of the developed land. Closely related to the end user's ability is the level of his specialized training in the area, of his venture, (crop production, reforestation program, highway construction, etc). Moreover, success of a project whether large or small, depends on favorable cost/ price relationships, favorable environment, and owner or managers skills. Since a range of factors must be considered, those involved in any land development projects must have sufficient amount of information which must be gathered before undertaking a project.

4. CONCLUSIONS AND RECOMMENDATIONS

An approach to mechanized agricultural bush clearing in the tropics has been developed. The approach includes guidelines, processes, operational techniques, specifications and factors to consider in mechanized agricultural bush clearing.

The approach if followed will ensure the preservation of the soil for sustainable crop production; protect both the operator and the machinery and thus permit greater flexibility and increase in operator efficiency.

The operational techniques as demonstrated in the study are limited to crawler tractor bulldozer. Other bush clearing machinery such as chains, tree pusher, the rake, etc are designed to cause minimum disturbance to the soil if the machine is handled by experienced machinery operator and under the supervision of professionals.

It is recommended that:
Mechanized agricultural bush clearing as an integral part of agricultural land development must be properly planned and executed jointly with such other operations as surveys, erosion control, tillage and irrigation.

Mechanized agricultural bush clearing machinery should be carefully selected. The selection should be based on a number of factors which include type of soil, availability of the equipments, cost of available machinery, size of land available, type and density of the vegetation, tree rooting system, terrain and income level of the farmer.

Although field experimental results (Adama, 2013) showed that crawler tractor bulldozers model D6, D7 and D8 when used for agricultural bush clearing did not significantly affect the yield and growth performance of maize when compared with manual clearing, models D6 and D7 are the most suitable for agricultural bush clearing and therefore, selection should be within D6 and D7 ranges.

Also agricultural bush clearing operation should be supervised by experts who must include soil scientists and agricultural engineers as this will ensure that the operators adhere strictly to the guidelines and specifications.

REFERENCES

Adama, 2013. Cost components for mechanized agricultural bush clearing. Unpublished Ph. D Thesis. Department of Agricultural and Bioresources Engineering, University of Nigeria, Nsukka, 133 pages.

Anazodo, U. G. N. 1986. Appropriate methods and equipment for agricultural land clearing and development in Nigeria: basic considerations. An invited paper presented at the National Workshop on Soil Erosion and Land Clearing and Soil Testing. Centre for Rural Development and Co-operatives, University of Nigeria, Nsukka. 24 pages.

Brunswick, A. S. 2008. Land clearing. Department of Agriculture and Acqua-culture. Home Francaise. Retrieved 21/ 09/ 08

Couper, D.C. 1996 Land Clearing for Agricultural Research Stations. IITA Research Guide 5. Ibadan Nigeria. 16 pages.

Fagbemi, A. A. and Gana, G. I. 1994. The sequence of NALDA land development activities. National Agricultural Land Development Authority. Abuja, Nigeria.1- 10 pages.

FAO, 1990 Food and Agriculture Organization. The conservation and rehabilitation of African lands. An International Scheme: Towards Sustainable Agriculture. ARC/90/4. Pg 8.

Miscellaneous, 2009. Clearing, grubbing and stripping. Field manual http//www.globalsecurity.org/military/library. 5-430-00-1. Accessed, August 2009.

NALDA. 1992. National Agricultural Land Development Authority. Blue Print. Abuja, Nigeria. 102 pages.

NALDA 1994a. National Agricultural Land Development Authority Programme Implementation Manual. Abuja, Nigeria.72 pages.

NALDA 1994b. National Agricultural Land Development Authority. Guidelines and Specifications for Land Development Activities in NALDA Farms. pp 15.

Nwuba, E.I.U. 1984. Agricultural land clearing practices in Nigeria: an appraisal. Proceedings of NSAE Symposium on Soil and Water Management. pp 68-87

Ojeniyi, S. O. 1997. Soils and tillage for sustainable agricultural productivity. In Tillage Research and Agricultural Development in Sub-Sahara Africa. Proceedings of Nigeria Branch of International Soil Tillage Research Organization pg. 21.

Okore, I. K; Tijani-Eniol H; Agboola. A. A. and Aiyelari, E.A. 2006. Impact of land clearing methods and cropping systems on labile soil C and N pools in the humid zone forest of Nigeria. Agriculture, Ecosystems and Environment, ELSEVIER 120 (2007), 250-258.

Oni, K .C and Adeoti, J. S. 1994. Mechanized land clearing and tractor traffic effects on agricultural soil and crop growth. Agricultural Mechanization in Asia, Africa and Latin America. 36 (4). 25-29.

Onwualu, A.P. Akubuo, C.O. and Ahaneku, I. E. 2006, Fundamentals of Engineering for Agriculture. Immaculate Publications Limited. Enugu, Nigeria.

FIELD CAPACITIVE PERFORMANCE STUDY OF PLOUGHING OPERATION IN LAFIA L.G.A, NASARAWA STATE, NIGERIA

J. K. Yohanna[1], S. O. Ode and M. B. Ibrahim
Department of Agricultural Engineering Technology,
College of Agriculture, PMB 33, Lafia, Nasarawa State-Nigeria
[1]Email: engrkuje@yahoo.com

ABSTRACT

In field machinery selection, the most pertinent variable is size or capacity of the machine. Size selection of agricultural machinery should be based on anticipated performance. A field capacitive performance study of ploughing operations was carried out on a small field of 0.49ha using a 3 x 1.5m- disc plough pulled by an MF 375 (56kW) tractor. The analysis of the data generated from the time and motion studies yielded a mean field efficiency of about 67%. The average effective width of cut of the ploug was 1.39m as against the theoretical width of plough of 1.5m. Analysis of the man- machine combination performance yielded a maximum man-machine activity of 90% and a minimum of 85.9%. the mean man-machine performance obtained was 0.2ha/hr. an average of 33% of total yield time was spent on non-productive activities while 67% was spent on productive (harrowing) activities. It is concluded that high effective field capacities could be obtained with high speeds. Proper preventive maintenance will minimize the number of field adjustments and also help in increasing implement width of utilization; hence increase in field capacities.

KEYWORDS: Field capacitive performance, operational speed, effective field capacity, field efficiency, total field time.

1. INTRODUCTION

All machines are designed to perform a given task at a specified time. If this design objective is not met, it only means that the machine setting is wrong or the machine of the machine and the power unit is not correct (Kepner et al; 2005). Field machine performance or capacity is the rate at which it can cover a field while performing its intended function or useful work. It is usually measured by the rate of work and the speed of travel with the allowance for are the width of useful work and the speed of travel with the allowance for lost time in turning and servicing the machine (Yohanna and Ifem, 2004).

The theoretical field capacity of an implement is the rate at which it will perform its intended function if it is operated continuously at its rated width. It is the hectare covered per hour or rate of field coverage possible if the machine works all the time at the recorded speed and utilized its entire width of operation. There is no allowance for loss of time or serving. The theoretical field capacity is calculated by multiplying the forward speed in km/hr by the operating width of the implement (Kepner et al; 2005). Culpin (1976) mentioned equation of theoretical field capacity as follows:

$$C_T = \frac{SW}{C}$$

Where, C_T = Theoretical field capacity, ha/hr; S = Speed, km/hr; W = Implement width, m; C = Constant = 10

The effective field capacity of an implement is the average rate at which it covers a field expressed in ha/hr or the actual rate of coverage by the machine. This includes an allowance for loss of time in turning and servicing. The effective field capacity of a machine in ha/hr is determined by multiplying the product of the speed in km/hr and the rated width by the field efficiency expressed in decimal fraction. It can be calculated in area base as follows:

$$C = \frac{Sw\ Ef}{10}$$

Where, C_e = Effective field capacity, ha/hr; S = Field Speed, km/hr; W = Implement working width, m; E_f = Field efficiency, decimal

It was found that effective capacity is affected by the implement size (Moayad et al; 2014). Ahmed and Haffar (1993) reported that heavy disc harrow showed higher effective field capacity than light disc harrow. Field efficiency of a machine is the ratio of the effective field capacity or productivity of a machine under key condition to the theoretical field capacity or theoretical maximum productivity and multiply by 100% (ASAE, 2003), Kumar et al; 2012). The efficiency of machine is always less than 100 and is influence by various factors involved in the effective capacity. Field efficiency account for failure to utilize the theoretical operating width of the machine, time lost because of operator capacity and habits and operating policy and field characteristics. Travel to and fro a field, major repairs, preventive maintenance and daily service activities are not constant for a particular machine but vary with the size and shape of the field, pattern of field operation, crop yield, moisture and crop conditions (ASAE, 2003). The field efficiency of a plough may have a typical range of 74-84 (ASAE, 1988). This value includes all effects of time and width of utilization and might be considered to represent the percentage of time that a machine spends actually doing what it is supposed to be doing. Actual width measurement from field observation of a 3-disc plough is 150cm (1.5m). Doubling the size of a machine does not double the theoretical or effective field capacities; instead it may decrease the field efficiency (Smith, 1965). Field efficiency is expressed by Kumar et al (2012) as;

$$E = \frac{C_e}{C_T} = 100 \quad \text{To} \quad E_f = \frac{X100}{T_e + T_h + T_a}$$

Where, T_o = Theoretical Time per ha; T_e = Effective Operating Time = $\frac{T_o}{k}\ x\ 100$; K = The percentage of Implement width actually used; T_h = the time loss per ha due to interruptions and is not proportional to the area

Witney (1988) indicated that the implement might be selected depending on the width for getting sufficient capacity so that work needed to be done within allotted time, and getting the maximum net profit can be estimated as follows:

$$W = \frac{C_e\ x\ C_f}{SE_f}$$

Where, W = optimum width, m; C_e = effective field capacity, ha/hr; CF = Correction factor; S = Field Speed, km/hr; Ef = Field efficiency, decimal

Studies on the field performance of agricultural machinery provide information for machinery design, selection and for the improvement of machinery use. Over the years different types and sizes of agricultural machi9nes have been imported into Nigeria; most often without regards for their adaptability to local needs (Gwarzo, 1991; Onwualu et al; 2006). According to them, some of these machines come without proper information on the design capabilities and the conditions under which they are best utilized. These have posed serious problem to machinery managers especially in the area of optimization of machinery selection for any given situation. It has therefore become necessary for proper performance evaluation to be carried out under different local conditions in order to have the required information on all available machinery and machinery systems.

Morghan and Bolarin (1976) carried out work on disc ploughing, disc harrowing and chiseling operations. The results obtained were respectively 0.13, 0.61 and 0.61ha/hr. in this performance studies of field machinery for crop production, Gwarzo (1991) reported a mean operating speed for ploughing operation of 5.66km/hr using CAT D4E tractor equipped with a 4.32m Rome plough and 9.97km/hr for harrowing using a CASE 2590 tractor equipped with 1 3.7m offset disc harrow. The corresponding values of effective field capacities obtained were 2.34ha/hr and 3.42 ha/hr with field utilization was above 90% during all observations.

The studies conducted during ploughing operations and the information obtained are quantitative values of operation's productive and non-productive times, the field capacity, field efficiency and man-machine performance for the operation.

The main aim of the study was to conduct field performance studies of ploughing operation on small farms. Specific objectives include to: obtain accurate records of ploughing time, turning timer and delay time (idle travel, machine facture and management stops/adjustment) during a ploughing operation; analysis and evaluate the performance of the man-machine combination and obtain the required capacitive performance criteria values of effective field capacity, field efficiency, operating speed and man- machine characteristics.

2. MATERIALS AND METHODS

The machine combination used comprised of Massey Ferguson, MF 375 (56KW) real-wheel driven tractor equipped with a 3-disc furrow 150cm disc plough (or 3 x 1.5m disc plough). The studies were conducted on sandy loan fallow farm lands that have not been under continuous cultivation for more than five (5) years in college of Agriculture, Lafia, Nasarawa State. The time and motion studies were conducted following the procedures in Ullah and Kofoed (1987) and taking into consideration one of the recommendations in Gwarzo (19910, which called for the use of 3 persons equipped with stop watches to record the activity times. The parameters measured included:

1. Ploughing time, support function time or turning time and delay activity times (idle travel, machine failure and management stops (adjustments, repairs etc).
2. Field row length, actual or effective width of cut of plough as well as the ploughing depths. For the measurement of activity times, three stop watches (hever club master 1/5type) were employed. All lengths were measured with a 100m-surveyor type while ploughing depths and widths of cut were measured with crown 3.5m/12FT 16mm pocket steel tape-1k-3H 93W.

During the observations the primary function activity began when the plough was lowered at the starting point and actual ploughing began and ended as soon as the plough was raised at the end of the field now. Time for stoppages (if any) were summed up and deducted from the total times spent on the entire row length. At the end of a filed row just where the plough was raised, the timing activity began. The time spent in making the turn was recorded as the turning activity time. All field adjustments or servicing during operations that exceeds 10 minutes were considered major breakdowns and were therefore excluded from delay activity time following the recommendations of Barnes (1960), Ojha and Michael 2003, 2011). The length of each field row was later measured and the number of passes (trips) made to cover the entire field recorded. Other information collected for each field included soil type and condition and weather condition during every operation. Over the period of study, a total number of ten (10) field outings were made.

3. RESULTS AND DISCUSSION

The results of the activity times for each field row recorded were summed up and the mean values of each field are presented in Table 1. The fields were all rectangular in shape so that all rows in each field were of equal length. The length of field rows varied from 35 to 37. The actual or effective width of cut of plough ranged between 1.36m and 1.41m against a theoretical rated width of 1.5m. Over the entire operations, an average width of plough utilized was 1.39m, which is 93%. This compares favorably with data in Morghan and Bolarin (1976), Gwarzo (1991) and Sahay (2004).

Table 2 shows analysis of data on performance criteria for the tractor plough combination. It can be seen that the size of the field varied between 0.48ha and 0.50ha or a mean ploughed area of 0.49ha, which according to Rahamoo (1983), is about the average plot size in the area. Average ploughing speed varied between a minimum of 6.6 km/hr. this mean value for ploughing operation is well within the ranges recommended in ASAE (1988), Ojha and Michael, (2003) and (2011), Sahay (2004) and Kumar et al, (2012). The turning times recorded were low to mean turning time at row end of 6.3 minutes. The average delay times, due to preventive maintenance (adjustment, minor servicing, greasing etc) during the whole operations was 3.53 minutes.

The theoretical field capacities ranged from 1.29ha/hr to 1.73ha/hr while the effective field capacity of the operations ranged between 0.90ha/hr and 1.12ha/hr with an average of 1.0ha/hr. ideally, the effective field capacity should be the same or as close as possible to the theoretical field capacity; however, in practice this is not because it is not possible to utilize the full width of operation of a machine without any overlap and it is not always possible to work at the speed because of the condition of the field, the judgment and efficiency of the operator and the amount of power available. Considerable time is lost in turning at the ends of rows, in minor breakdown, in lubrication and in adding seed, fertilizer or spraying solution. Thus it is impossible for the machine to be working effectively all the time (Yohanna and Ifem, 2004).

The lowest field efficiency attained was 63% while the highest was 70% as shown in Table 2, with the average being 66.9%. This is within the ranges cited in smith (1965). ASAE (1988) and (2003), Ojha and Michael (2003) and (2011), Sahay, (2004), Onwualu et al, (2006) and Kumar et al, (2012).

Man-machine activity values were very high reaching up to 90%, signifying minimum delay or stoppages during operations. Ordinary, this should be an indication of good operator's performance and/or machine reliability; however, in this case it is more likely a result of the small sizes of the fields, which made operators stoppages almost unnecessary.

Table 1: Results of Field Studies

Observation	Length (m)	No. of Passes (Trips)	Effective width of cut (m)	Activity Times (Minutes)				Speed (Km/hr)	Area (ha)
1	100	36	1.37	21.4	6.5	4.6	32.5	6.6	0.49
2	98	37	1.36	22.7	5.8	3.7	32.2	6.8	0.49
3	99	35	1.44	18.2	6.2	3.6	28.0	7.4	6.49
4	100	36	1.40	20.8	6.0	3.4	30.2	7.2	0.50
5	10	36	1.38	17.8	6.8	3.6	28.2	7.7	0.50
6	99	36	1.38	22.4	6.4	3.2	32.0	6.7	0.48
7	98	36	1.38	21.0	6.2	3.2	30.2	7.0	0.49
8	98	36	1.40	17.9	6.7	3.4	28.0	7.6	0.49
9	98	36	1.41	17.3	6.2	3.2	26.7	7.9	0.50
10	99	36	1.40	20.3	6.1	3.4	29.8	70	0.50
Total	989	360	13.89	199.8	63	35.3	29.8	721	4.93
Mean	99.0	36.0	1.39	20.0	6.3	3.53	29.8	7.21	0.493

Table 2: Evaluation Values of Various Performance Criteria/Parameters

Observations	A	B	C	D	E	F	G	H	I	J	K	L	M
1	100	36	0.49	6.6	21.4	6.5	4.6	32.5	1.37	0.90	66	0.02	85.9
2	98	37	0.49	6.8	22.7	5.8	3.7	32.2	1.30	0.91	70	0.02	88.5
3	99	35	0.49	7.4	13.2	6.2	3.6	28.0	1.62	1.05	65	0.02	87.1
4	100	36	0.50	7.2	20.8	6.0	3.4	30.2	1.44	0.99	69	0.02	87.7

5	100	36	0.50	7.7	17.8	6.8	3.6	28.2	1.69	1.06	63	0.02	87.2
6	99	36	0.48	6.7	22.4	6.4	3.2	32.0	1.29	0.90	70	0.02	90.0
7	98	36	0.49	70	21.0	6.2	3.2	30.4	1.40	0.97	69	0.02	89.5
8	98	36	0.49	7.6	17.9	6.7	3.4	28.0	1.64	1.05	64	0.02	87.9
9	98	36	0.50	7.9	17.3	6.2	3.2	28.7	1.73	1.12	65	0.02	88.0
10	99	36	0.50	7.2	20.3	6.1	3.4	29.8	1.48	1.01	68	0.02	88.6
Total	989	360	4.93	721	199.8	63	35.3	298	14.96	9.96	669	0.02	880.4
Mean	99	36	0.49	7.2	20	6.3	3.5	29.8	1.50	1.00	67	0.02	88.04

Key/Legend
A = Field row length (m); B = Effective width of cut (m); C = Area ploughed (ha); D = Forward speed (km/hr); E = Ploughing time (minutes); F = Turning time (minutes); G = Delay time (minutes); H = Total Field time (E+F+G); I = Theoretical field (ha/hr) = (C x $^{60}/_{E}$); J = Effective Field capacity (ha/hr) = (C x $^{60}/_{H}$); K = Field efficiency (%) = ($^{J}/_{I}$); L = Man-Machine productivity M_{mp} [$^{C}/_{E} + {}_{F}$]; M = Man- Machine activity, Mma (%) = [100 x (E+F)/H]

Man-machines performances mean was about 0.02ha/hr lower than the mean field capacity of 1.0ha/hr. this is due to operator inexperience, capability, habit, operating policy and/or stumps present on the ploughed field as well as the small sizes of the fields. The average time lost in making turns at the ends of the rows was 9.8 minutes.

From the Table 3, it can be seen that the higher the operating speed, the higher the effective field capacity but the lower the field efficiency. This shows that speed and effective field capacity are indirectly proportional to the field efficiency. It can also be deduced that the lower the time loss, the higher the field efficiency showing that the unproductive time is inversely proportional to the field efficiency. This shows that higher field efficiencies could be obtained with lower time loss during field activities.

Table 3: Comparison between Speed of Operation and Effective Field Capacity and between Total Time Lost and Field Efficiency

Observations	Speed (km/hr)	Effective Field Capacity (ha/hr)	Total Time Lost (Mins)	Field Efficiency (%)
1	6.6	0.90	11.1	66
2	6.8	0.91	9.5	70
3	7.4	1.05	9.8	65
4	7.2	0.99	9.4	69
5	7.7	1.06	10.4	63
6	6.7	0.90	9.6	70
7	7.0	0.97	9.4	69
8	7.6	1.05	10.1	64
9	7.9	1.12	9.4	65
10	7.2	1.01	9.5	68
Total	72.1	9.96	98.2	669
Mean	7.21	0.996	9.82	66.9

4. CONCLUSION

Results from these studies show that high effective field capacities could be obtained with high operating speeds. Also as speed is increased, the total field time decreased and the effective field capacity increased while the field efficiency decreased. Proper maintenance and adjustment of machines would also help increasing width utilization and hence increased field capacities. The tractor and implement must be chosen so that the tractor is fully utilized with respect to the power available. This will ensure that the tractor-implement combination is matched to the size of work at hand. Field efficiencies can be increased with proper field time management by the machine operator. These studies showed that it is very necessary to minimize the proportion of the total field spent on non-productive activities. Proper preventive maintenance will minimize the number of field adjustment required during field operation. It is concluded that it is not necessary to have higher efficiency at higher speeds.

REFERENCES

Ahmed, M. H and M. Haffar 1993. Comparison of Five Tillage Systems for Cotton Production in Rahad Scheme. A. M.A 24 (2): 17-20.

ASAE 1988. American Society of Agricultural Engineers. Agricultural Engineer Year Book, Handbook, St. Joseph, Mich.

ASAE 2003. American Society of Agricultural Engineers, EP 4962.2 FEB 03 STANDARDS. Agricultural Machinery Management. Pp 367-372.

Barnes, K. K 1960. Proper Evaluation of Machines. Implements and Tractors. 75(8):48.

Culpin, C 1976. Profitable Farm Mechanization, 3rd Edition. Crosby Lockwood Staples Publishers London, UK.

Gwarzo, M. A. S. 1991. Capacitive Performance study of Power and Machinery on a Large Scale Farm. Ph.D Thesis, Dept. of Agric. Engineering, A.B.U Zaria-Nigeria.

Kepner, R. A, R. Bainer and E. R. Berger 1978. Principles of Farm Machinery. 3rd Edition. Avi Publishers Westport. Pp 23-47.

Kepner, R. A, R. Bainer and E.R Berger 2005. Principles of Farm Machinery. Revised Edition. Avi Publishing co. Westport. Conn.

Kumar, S; Kumar, V; and Sahu R.K 2012. Fundamentals of Agricultural Engineering. Kalyani Publishes Ladhiana-New Delhi. Pp 138.

Moayad, B.E, A. M. EINaim and T. E Mahmoud 2004. Computer Modeling for Production of Implement Field Performance Variables. World Journal of Agricultural Research. Vol. 2 (2): 37-41.

Morghan, M. J and D. A. Bolarin 1976. Mechanization of Fadama Rice at Edozigi, Niger State. Proc. of NSAE. Vol. 4: 73-80.

Ojha, T. P and A. M Michael 2003. Principles of Agricultural Engineering. Vol. 1. (4th Edition). Jain Brothers Publishers, New Delhi.

Ojha, T. P and A. M Michael 2011. Principles of Agricultural Engineering. Vol. 1. (6th Edition). Jain Brothers Publishers, New Delhi, India.

Onwualu, A. P, C. O. Akubuo and I. E Ahaneku 2006. Fundamentals of Engineering in Agriculture. Immaculate Publishing, Enugu-Nigeria.

Rahamoo, S. A 1983. Tractorization and Small Farms in Developing Countries. Nigerian Journal of Science and Technology vol. 1 (1): 45-50.

Sahay, J. 2004. Elements of Agricultural Engineering. Standard Publishes Distributions, Nai, Sarak, Delhi-India.

Smith, H. P 1965. Farm Machinery and Equipment. McGraw-Hill Book Company, New York.

Ullah, M. D and S. S Kofoed 1987. Effect of Field Dimension on Energy and Labour Consumption for Rotary Cultivating Small Sized Plots. AMA.18 (1): 22-26.

Witney, B 1988. Choosing and using Farm Machines (2nd Edition). Longman Singapore Publishers (PTC) Ltd. Singapore.

Yohanna, J. K and J. L. C. Ifem 2004. Performance Evaluation of Field Efficiencies of Farm Machinery in Nasarawa and Plateau States. Proc. Of the Nigerian Institution of Agricultural Engineers, 26:88-92.

DEVELOPMENT OF EQUATIONS FOR ESTIMATING TIME, WATER AND ENERGY REQUIREMENTS IN DOMESTIC RICE COOKING

R. Akinoso[1], A. K. Aremu[2] and T. T. Oyegunle[1]
[1]Department of Food Technology, University of Ibadan, Ibadan, Nigeria.
[2]Department of Agricultural and Environmental Engineering, University of Ibadan, Nigeria
E-mail: akinoso2002@yahoo.com

ABSTRACT

A study was conducted to develop equations for estimating the time, water and energy requirements in domestic rice cooking using electric stove. A 3 x 2 x 2 factorial experimental design was employed. Rice variety (o*fada*, *bida* and royal stabilon), cooking method (open, closed) and quantity (173, 692 g) were the variables. The responses were time, water and energy requirements. Results obtained varied between 40 - 75 minutes for time requirement, 329.3 – 1933.4 g water and 2.4 – 4.3 MJ for energy requirement. Linear regression models were found to be the most suitable for estimating time, water and energy requirements with coefficients of determination R^2 of the equations ranging from 0.718 – 0.948. Analysis of variance of the data showed significant effects of treatment on the responses at 5% level of significance. Therefore, variety of rice, cooking method and quantity determine the time, energy and water requirements in rice cooking.

KEYWORDS: Rice cooking, time, water, energy, model.

1. INTRODUCTION

Rice is an important cereal for human consumption grown in all the ecological and dietary zones of Nigeria (Sanni et al., 2005)**.** The two commonly cultivated varieties of rice in Nigeria are *Oryza sativa and Oryza glabberima* (Abulude, 2004). Processing of rice involves the following unit operations, harvesting, threshing, cleaning, drying, parboiling, dehulling, de-braning, polishing, grading, packaging and cooking. Rice has potential in a wide range of food categories. Besides having nutritional and medicinal benefits, the by-products of rice are equally important and beneficial. By-products from growing rice create many valuable and worthwhile products. On the average, a sample of milled rice grown will contain about 80% starch, 8% protein, 0.5% ash and 11% water (Adekoyeni *et al.,* 2012).

Cooking requires the transformation of the potential energy in fuel into heat energy. There are many factors influencing the efficiency of cooking like the phenomenon of heat production, heat utilization, heat transmission and heat rejection during combustion. Rice is cooked by boiling or steaming. It can be cooked in just enough water (the absorption method), or it can be cooked in a large quantity of water which is drained before serving (the rapid-boil method). Rice may also be made into rice porridge by adding excess water so that the cooked rice is saturated with water to the point that it becomes very soft, expanded, and fluffy. Rice may be soaked prior to cooking using different cooking devices that depends on energy (Osaratin and Abosede, 2007).

Energy is an indispensable commodity for the economic growth and development of any nation. Energy is also an essential input to the growth and development of the various sectors of the economy. Energy is inevitable for poverty alleviation and provides services in the areas of health, communication and productivity. Knowledge of energy consumption in food processing is useful for several purposes such as budgeting, evaluation of energy consumption for a given product, forecasting energy requirement in a plant, and for planning plant expansion. Literature on estimation of energy input in food processing includes quantification of energy requirements for sugar-beet production in Morocco (Mrini *et al.,* 2002). Cashew nut processing operations (Jekayinfa and Bamgboye, 2006), palm-kernel oil processing operations (Jekayinfa and Bamgboye, 2007), energy utilization patterns in a sugar production factory in

Nigeria (Abubakar *et al.*, 2010) and bread baking (Akinoso and Ganiu, 2011) and *gari* processing (Akinoso and Kasali, 2012)

Nigeria is endowed with a wide range of renewable and non – renewable energy sources. The non – renewable resources include crude oil, natural gas, coal, lignite, tar and nuclear fuels (Wang 2009). The renewable ones include solar and wind energy. Nigeria operates a centralized energy system where communities and individuals are connected to a common energy source and because of the cost implication of connection to this source; many poor communities live without electricity. There is energy crisis in Nigeria; the cost of producing fossil fuels, which is predominantly the source of energy used in cooking, is expensive and electric power is unreliable.

Therefore, the objective of the study was to generate mathematical equations for estimating time, water and energy requirements for domestic cooking of rice, a widely consumed cereal in Nigeria. The models will aid energy conservation studies.

2. MATERIALS AND METHODS

2.1 Experimental Design

A 3 x 2 x 2 factorial experimental design was employed, that is three varieties of rice (*ofada*, *bida*, royal stabilion), two cooking methods (open, close) and two different quantities (173 g, 692 g). The variables were coded as variety, ofada (-1), bida (1), royal (0); methods open (-1), close (1) and quantity, 173 (-1), 692 (1). Responses were water consumption, time and energy requirement (Table 1). Data obtained were analyse using historical response surface (Design- expert version 6.0.6, Stat Ease Minneapolis, Minn).

2.2 Preparation of Materials

Bida (an indigenous Nigerian variety) and royal stabilion (Thailand) were procured from Bodija market, a local market in Ibadan, Oyo State Nigeria. While *ofada* (an indigenous Nigerian variety) was sourced from Abeokuta, Ogun state Nigeria. The extraneous matters such as stone and dirt inside *ofada* and *bida* rice were blown-off and removed by hand picking before the required quantities were weighed. The Digital weighing balance (model:Gx/GF-1 3003858,A&D company Limited) used was first set to zero before 173±3g (approximately 1tin cup) of o*fada* rice, *bida* rice, royal stabilion rice was weighed separately. This was also repeated for another quantity 692±5g (approximately 4 tin cups).

Table 1. Design matrix and responses

	Actual			Coded	
Variety	Method	Quantity	Variety	Method	Quantity
Ofada	Open	173	-1	-1	-1
Ofada	Open	692	-1	-1	1
Ofada	Close	173	-1	1	-1
Ofada	Close	692	-1	1	1
Bida	Open	173	1	-1	-1
Bida	Open	692	1	-1	1
Bida	Close	173	1	1	-1
Bida	Close	692	1	1	1
Royal	Open	173	0	-1	-1
Royal	Open	692	0	-1	1
Royal	Close	173	0	1	-1
Royal	Close	692	0	1	1

2.3 Cooking Methods

The three rice varieties of *ofada*, *bida* and royal stabilion rice were washed and cooked separately inside open and closed aluminum cooking pots (3mm thickness) using 1kW temperature regulated electric cooking plate (Crown star, Model MCHP-225, Rajko Traders Ltd, Hong Kong, China). The electric cooker was put on and left for 10 minutes to initialize before it was loaded.

2.4 Determination of Cooking Time

A trial experiment was first carried out to get approximate cooking time. After which, samples of the boiling rice were examined at 5 minutes interval by an experience analysis using sensory attributes. At close of cooking time assessment period was reduced to 3 minutes interval. This was continued until it was found satisfactory.

2.5 Determination of Water Requirement

The cooked rice was drained to remove excess water using sieve. This was left to stand for about 30 minute to equilibrate with ambient temperature 29±2°C. The difference between the weight of raw rice and cooked rice was recorded as quantity of water consumed (Osaratin and Abosede, 2007).

2.6 Determination of Energy Requirement

Energy utilization was quantified as a function of electrical power and time (Equation 1) (Akinoso and Kasali, 2012)

$$En = power\ x\ time \qquad 1$$

2.7 Statistical Analysis

All the experimental procedures were repeated three times. Mean values were recorded as obtained data. These were subjected to analysis of variance (ANOVA) at 5% level of significance. Regression equations were developed using propriety software package SPSS 14.0 for windows. The models were subjected to coefficient of determination and lack of fit test at 5% level of significance.

3. RESULTS AND DISCUSSION

3.1 Time Requirement

Recorded duration for cooking the variety and quantity of rice under consideration varied between 40 and 75 minutes. Effects of treatments were found to be significant on time requirement ($p< 0.05$). Cooking *bida* rice was fastest while royal stallion rice took longest duration. For all varieties of rice, close cooking took shorter duration. This is expected because closing the pot increases pressures thus the cooking rate. Using linear regression (Equation 2) to express the relationship gave high coefficient of determination (0.974), an indication of good fitness. Variety and quantity of rice were the significant model terms (Table 2). Khatoon (2006) reported similar observation. Graphical illustration of the relationship is presented as Fig. 1.

$$T = 57.42 - 3.25V - 2.08M + 11.75Q \qquad 2$$

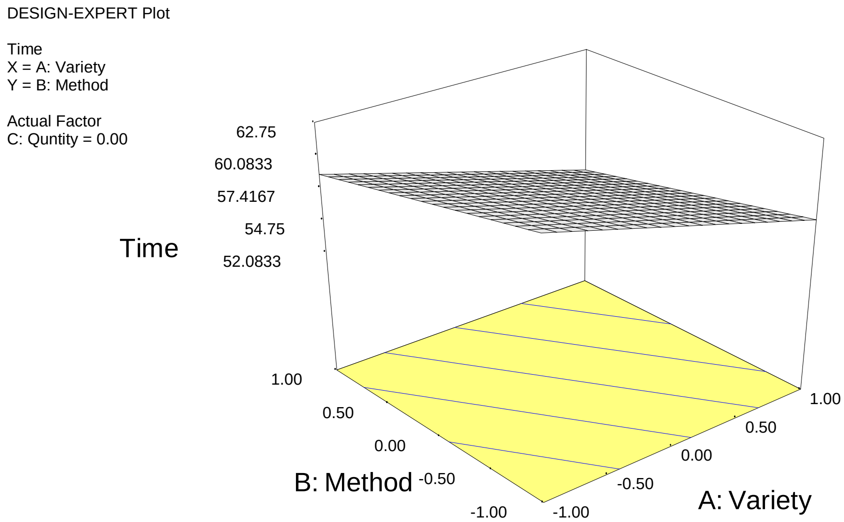

Figure 1. Response surface plot of time against cooking method and rice variety

Table 2. Analysis of variance of linear regression model for time requirement

	Un standardized coefficients		standardized coefficients		
Model	B	Std. Error	Beta	t	Sig.
Constant	57.417	1.008		56.948	0.000
Variety	-3.250	1.235	-0.211	-2.632	0.030
Method	-2.083	1.008	-0.166	-2.066	0.073
Quantity	11.750	1.008	0.936	11.654	0.000

3.2 Water Requirement

Highest quantity of water required to cook was 1933.4 g. This was recorded when 692 g of royal rice was cooked in a close pan. While the least water requirement of 329.2 g was obtained when 173 g of *ofada* rice was cooked in open pan. Level of water absorption is an indicative test for functional property. This result suggests that royal rice has highest water absorption and swelling capacities. This agreed with Osaretin and Abosede (2007) report on comparison of *ofada* and polished rice cooking rate. Analysis of variance of the data showed significant effect of treatments on water absorption capacity at 5 % level of significance. Mathematical expression of the relationship is presented as Equation 3. Coefficient of determinationR^2 of the model is 0.718. Test of significance of the model coefficients revealed quantity that quantity of cooked rice as the only independent significant model term (Table 3). This is suggesting that quantity as the major factor determining water requirement in rice cooking. Response surface plot of effects of the treatments on water requirement is shown in Figure 2.

$$W = 972.50 - 219.84V - 2.90M + 515.97Q \qquad 3$$

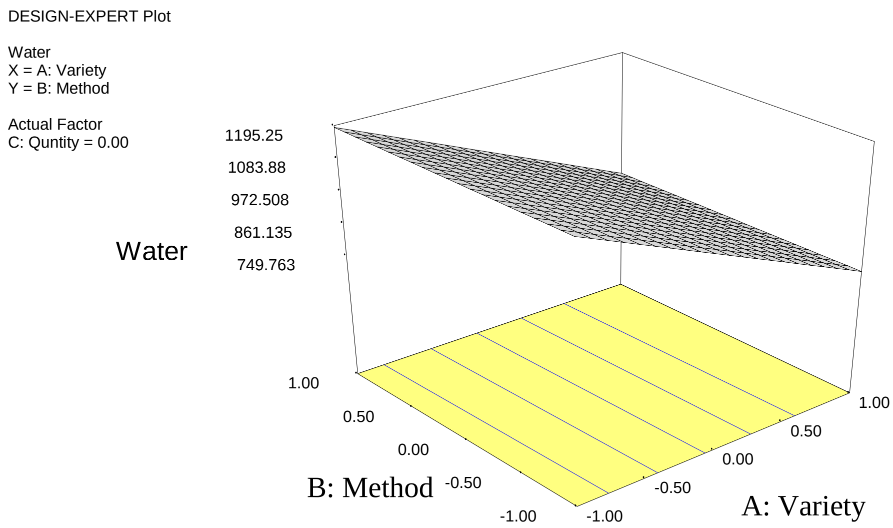

Figure 2. Response surface plot of water against cooking method and rice variety

Table 3. Analysis of variance of linear regression model for water requirement

	Un standardized coefficients		standardized coefficients		
Model	B	Std. Error	Beta	T	Sig.
Constant	972.503	121.107		8.030	0.000
Variety	-219.846	148.326	-0.278	-1.482	0.177
Method	-2.902	121.107	-0.005	-0.024	0.981
Quantity	515.978	121.107	0.800	4.260	0.003

3.3 Energy Requirements

Maximum and least energy expended were 4.3 and 2.4 MJ respectively, which is equivalent to energy intensity 6.21 MJ/kg and 13.87 MJ/kg. The energy expended was higher than 2.95 MJ/kg for bread making (Akinoso and Ganiyu, 2011). Higher energy intensity may be traced to quantity cooked, it is also an indication that electric stove consumes high energy. The treatments have significant effect on energy consumption at 5% level of significant. Linear model is fit to express the relationship (Equation 4). Coefficient of determination $R^2$of the model is high (0.948). Significant model terms of the equation were variety and quantity (Table 4). This is a revelation that variation in cooking method as no significant effect on energy demand. Figure 3 shows visual illustration of the relationship.

$$E = 3.445 - 0.195V - 0.125M + 0.705Q \qquad 4$$

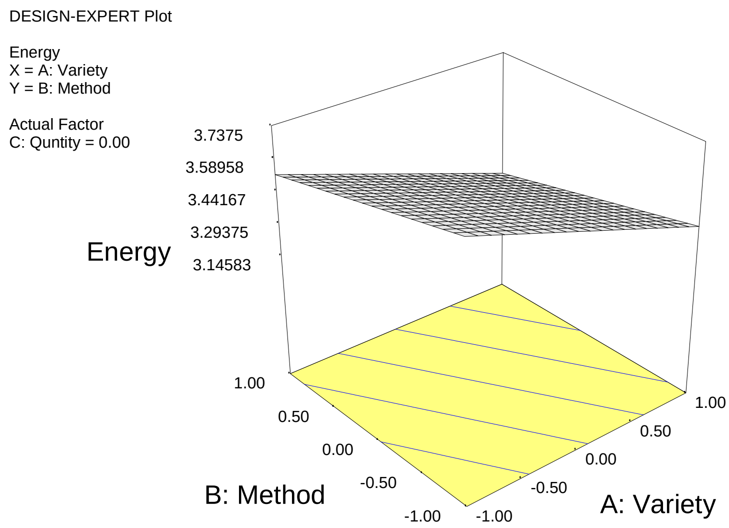

Figure 3. Response surface plot of energy against cooking method and rice variety

Table 4. Analysis of variance of linear regression model for energy requirement

	Un standardized coefficients		standardized coefficients		
Model	B	Std. Error	Beta	T	Sig.
Constant	3.445	0.060		56.949	0.000
Variety	-0.195	0.074	-0.211	-2.632	0.030
Method	-0.125	0.060	-0.166	-2.066	0.073
Quantity	0.705	0.060	0.936	11.654	0.000

4. CONCLUSION

This study has shown that variety of rice, cooking method and quantity determine the time, energy and water requirements in rice cooking. *Bida* rice cooking time was shortest while royal rice water requirement was the highest. Energy intensity of cooking the three varieties of rice using electric energy was low. Pot covering during rice cooking conserves time, water and energy. Co-efficient of determination of the regression equations (R^2) is high, indicating fitness of the model. Thus, the model is reliable and applicable.

REFERENCES

Abubakar, M. S., Umar B. and Ahmad, D. 2010. Energy use patterns in sugar production: a case study of savannah sugar company, Numan, Adamawa State, Nigeria. Journal of Applied Science and Research 6: 377-382.

Abulude, F.O. 2004. Effect of processing on nutritional composition phytate and functional properties of rice (*Oryza sativa)* floor. Nigeria Food Journal 22: 97-108.

Adekoyeni, O O, Akinoso, R and Malomo O. 2012. Some physical properties and yield of *ofada* rice. Journal of Basic and Applied Scientific Research, 2: 4098-4108.

Akinoso, R and Ganiyu, I. A. 2011. Estimation of energy requirements in small-scale bread making. LAUTECH Journal of Engineering and Technology 6: 81-85.

Akinoso, R and Kasali, W. O. 2012. Energy Expended in Processing *Gari*- Cassava (*Manihot esculenta* Crantz) Flakes - using three Levels of Mechanization. Pakistan Journal of Scientific and Industrial Research Series B Biological Sciences 55: 114 – 116.

Jekayinfa, S. O. and Bamgboye, A.I. 2006. Estimating energy requirements in cashew nut processing operations. Energy 31:1305–1320.

Jekayinfa, S. O. and Bamgboye, A.I. 2007. Development of equations for estimating energy requirements in palm-kernel oil processing operations. Journal of Food Engineering 79: 322 329.

Khatoon, R 2006. Nutritional quality of microwave and pressure cooked rice (*Oryza sativa)* varieties. Food Science and Technology International 12: 297-305

Mrini, M., Senhaji F. and Pimentel D 2002. Energy analysis of sugar beet production under traditional and intensive farming systems and impacts on sustainable agriculture in Morocco. Journal of Sustainable Agriculture 20: 5–28.

Osaratin, A.T. and Abosede, C. O. 2007. Effect of cooking and soaking on physical characteristics, nutrient composition and sensory evaluation of indigenous and foreign rice varieties in Nigeria. African Journal of Biotechnology 6: 1016-1020.

Sanni, S.A, Okeleye, K.A, Soyode, A.F and Taiwo, O. C. 2005. Physio-chemical properties of early and medium maturing and Nigerian rice varieties. Nigeria Food Journal 23: 148-152.

Wang, L. J. 2009. Energy efficiency and management in food processing facilities. CRC Press Taylor & Francis Group, LLC, Boca Raton, FL, USA.

EFFECT OF MOISTURE CONTENT ON SOME PHYSICAL AND FRICTIONAL PROPERTIES OF AFRICAN LOCUST BEAN *(PAKIA BIGLOBOSA)*

G. U. Asonye, S. N. Asoegwu and O. H. Ohaeri
Department of Agricultural Engineering, Federal University of Technology, Owerri, Nigeria
Email: u.asonye@yahoo.com, asosab49@yahoo.com

ABSTRACT

The moisture-dependent handling properties (linear dimensions, sphericity, bulk and true densities, porosity) and flow or frictional properties (angle of repose and static coefficient of friction) were investigated for African Locust Bean *(Pakia biglobosa)* at moisture contents in the range of 7.45% to 15.2% (d.b.). All the seed dimensions showed a linear response to an increase in moisture content within the range of moisture content studied. All other measured parameters increased polynomially with increased in moisture content. They are: seed equivalent diameter (11.02 to 12.73mm); seed volume (362.74mm^3 to 542.01mm^3); seed surface area (308.50mm^2 to 406.66mm^2); bulk density and true density (0.45g/cm^3 to 0.54g/cm^3 and 0.80g/cm^3 to 1.40g/cm^3 respectively); aspect ratio, sphericity and porosity (0.76 to 0.79, 0.71 to 0.70 and 0.41 to 0.61 respectively); angle of repose (21.05^o to 37.45^o); while static coefficient of friction increased for all surfaces from 0.53 to 0.92 for plywood, 0.45 to 0.84 for mild steel and 0.36 to 0.71 for aluminum with plywood giving the highest range of values. The data obtained from this study is useful in the structural design of hoppers, bins and silos for storing the seeds and the equipment for processing, sorting, sizing and other post-harvest operations.

KEYWORDS: African locust bean, moisture content, equivalent diameter, bulk density, porosity, angle of repose, static coefficient of friction.

1. INTRODUCTION

African locust bean *(Parkia biglobosa)* seed is a leguminous seed that grows on a tree common in the Savannah Zone of Nigeria. The tree is a perennial, growing where temperature is high, and relative humidity and precipitation are relatively low (Oladele *et al*., 1985). African locust bean fruit consists of bunches of pods which contain the edible part of the plant. The brownish-black seeds in each pod are enveloped in a yellow pulp, which is also edible, as it contains a high percentage of sucrose (Ogunjimi *et al*., 2002).

These seeds are extracted from the pod by plucking, cracking and tearing after which the remaining pulp is washed off and the seeds dried. Traditionally, these seeds are processed by boiling for about 8 hours to soften the testa, washing to separate the testa from the cotyledons, feet mashing, sieving in running water, boiling the cotyledons until desired moisture content is obtained for the fermentation of the resultant mash (Oje, 1993).

African locust bean (*Parkia biglobosa)* is of economic importance in Nigeria especially as it provides a cheaper source of protein for many inhabitants. The cotyledon or embryo is rich in nitrogen, phosphorus, potassium, magnesium, iron and zinc. The testa is rich in calcium, manganese and sodium when compared to that of the cotyledon, which is a rich source of lipids, carbohydrates, proteins, fibre and ascorbic acid (Alabi, 1991). The yellow powdery pulp is rich in carbohydrate (Oladele *et al*., 1985) and rich in oil suitable for the manufacture of soap (Owoyale *et al*., 1986). The husk is rich in tannins, making it a valuable source of tannins for the leather industry. The presence of fibres in the husk, together with tannins makes the husk a good raw material for the production of particle board (Owoyale *et al*., 1986).

The production of *'ogiri (iru)* condiment' (the fermented cotyledons of the seeds) has over the years remained in the hands of rural families who process these seeds for home consumption and for sale, using rudimentary tools (Odunfa and Adewuyi, 1985). Due to the hectic nature of the process of making locust bean cake (*ogiri*), mechanization of this process has been of high interest in recent times in order to increase the efficiency of the production process. However, achieving optimum mechanization of the process cannot be made with success without proper study of the various physical, frictional, and mechanical properties of the African locust bean as a function of moisture content. To design equipment for the handling, separation, conveying, drying, storing, aeration and processing of African locust bean, determining their physical and flow properties as a function of moisture content is essential.

Ogunjimi, *et al*. (2002) investigated some engineering properties of a specie of locust bean (*Parkia fillicoidea)* at a particular moisture content of 10.25% (dry basis) and generated expressions for the relationship between their dimensions. as in Eqns. 1 and 2.

$$L = 1.4W = 1.85T \qquad 1.$$

And that of its seed (kernel) to be;

$$l = 1.39w = 2.85t \qquad 2.$$

Where; L and l = length, W and w = width, T and t = thickness (the upper case letters refer to pod and lower case, seed).

Oje (1993) found out that the locust bean pod has a major diameter ranging from 76mm to 277mm as against 8mm to 12mm of the seeds and average sphericity and roundness of 67% and 65% respectively. Subukola and Onwuka (2009) on the other hand investigated the effects of moisture content on some frictional properties of *Parkia fillicoidea*. Using plywood, galvanized iron, aluminum and stainless steel respectively as experimental surfaces and varying the moisture content from 7.37% to 28.09% (dry basis), they found out that the highest static coefficient of friction and angle of repose was on plywood surface which gave 0.47 to 1.00 and 21.43^0 to 37.46^0 respectively.

However, the main features of African locust bean and other agro and food materials that make them different from mineral materials are the strong influence of moisture content on their handling, flow and mechanical behavior and the high deformability of their seeds and granules. These differences bring about certain peculiar behaviors that necessitate the adjustments of models of material, experimental techniques and technological solutions (Molenda and Horabik, 2005).. Kibar *et al*. (2010) reported that for rice grains and other commodities, increased moisture content causes notable increases of pressure on silo walls. Because the increase of pressure requires an increase in the thickness of silo construction materials, costs of construction increase. Also, flow problems in silos such as arching, rat-holing, irregular flow and segregation occur with increased moisture content.

Many studies have been reported on the effect of moisture on the physical properties of seeds: guna seeds (Aviara *et al*., 1999); Roselle or sorrel (*Hibiscus sabdariffa*) seeds (Omobuwajo *et al*., 2000a; Sánchez-Mendoza *et al*., 2008); Ackee apple (*Blighia sapida*) seeds (Omobuwajo *et al*., 2000b); pigeon pea (Baryeh and Mangope, 2002); chickpea (Masoumi and Tabil, 2003); calabash nutmeg (Omobuwajo *et al.*, 2003); lentil seeds (Amin *et al.*, 2004); dried pomegranate seeds (Kingsly *et al.*, 2006); fibered flaxseed (Wang *et al.*, 2007); soybean (Kashaninejad *et al*., 2008); African oil bean seed (Asoegwu *et al.*,2006). The moisture content range used in Literature for its effect on some physical, mechanical, aerodynamic and other properties of agricultural products has been between 5 to 39% (d.b.), varying according to product type. However, limited work seems to have been done on the physical properties of African locust bean and their relationship with moisture content.

The aim of this study was to investigate some handling and flow (frictional) properties of African locust bean(*Parkia biglobosa)* as they are affected by moisture content in the range of 7.45% to 15.2% (d.b.) and establish some regression models to predict these effects.

2. MATERIALS AND METHODS

2.1 Physical Properties

About 9.5kg of samples of processed African locust bean seeds were obtained from the Abakpa market in Enugu state in the southeastern part of Nigeria and were carefully sorted to remove dirt, debris and unwholesome seeds after which 8.4kg of whole seeds were got for proper experimental use. To determine the initial moisture content of the seeds, a laboratory oven at the Food Science and Technology Department of the Federal University of Technology Owerri was used for the experiment. The initial moisture content was determined after oven drying 45 randomly selected seeds for 18 hours at a temperature of 125^{0}C using the Eqn. 3 (ASAE Standards., 1999).

$$MC = \frac{(W_1 - W_2)}{W_2} x100\% \qquad 3.$$

Where; W_1 = Initial weight of sample; W_2 = Final weight of sample; MC = Moisture content

Firstly, a batch of 1kg (batch 1) was kept at the initial moisture content of 7.45% without any further addition of water, this was used as control. The rest of the seeds were then divided into 4 parts of 1kg each and were conditioned to obtain four different moisture content levels between 10.2% and 15.2% dry basis, hence giving a total of 5 batches. This was done by adding different calculated amounts of water to each batch of the African Locust Bean seeds (*Parkia biglobosa*), using Eqn. 4(Gamayak *et al*., 2008);

$$Q = A\frac{(b-a)}{(100-b)} \qquad 4.$$

Where; Q = mass of water to be added (g); A = Initial mass of sample (g); a = Initial moisture content of sample (% dry basis); b = Final/desired moisture content (% dry basis).

The batches were put in high density polyethylene bags and kept in a refrigerator at 2^{0}C - 5^{0}C for about 5days to allow for even distribution of water. Before each test was carried out, the sample was exposed for about 2 hours for equilibration to occur (ASAE standards, 1999). This rewetting technique to attain the desired moisture content in seeds and grains has frequently been used (Coşkun *et al*., 2005; Garnayak *et al*., 2008; Sacilik *et al*., 2003).

The principal dimensions (L_1; L_2; & L_3) of the seed were determined using a micrometer screw gauge with an accuracy of 0.02mm.

The arithmetic mean diameter (F_1), geometric mean diameter(F_2), square mean diameter(F_3), equivalent diameter (D_e) were determined respectively using the formulae by Ciro (1997) and Asoegwu *et al*., (2006);

$$F_1 = \frac{(L_1 + L_2 + L_3)}{3} \qquad 5.$$

$$F_2 = (L_1 x L_2 x L_3)^{1/3} \qquad 6.$$

$$F_3 = \left[\frac{(L_1L_2 + L_2L_3 + L_3L_1)}{3}\right]^{1/2} \qquad 7.$$

$$D_e = \frac{(F_1 + F_2 + F_3)}{3} \qquad 8.$$

The aspect ratio (A_r) was determined by using equation (9) by Seifi and Alimardani (2010);

$$A_r = \frac{L_2}{L_1} \qquad 9.$$

Seed surface area (A_s) and seed volume (V) was calculated using the following relationships (Jain and Bal, 1997; Subukola and Onwuka, 2011):

$$A_s = \frac{\pi B L_1^2}{(2L_1 - B)} \qquad 10$$

$$V = \frac{\pi B^2 L_1^2}{6(2L_1 - 3)} \qquad 11.$$

$$Where\ B = (L_2 L_3)^{½} \qquad 12.$$

The bulk density (ρ_b) which is the ratio of the mass of the seeds to its total volume was determined by filling up a 600mL beaker with samples, striking off the top level without seed being compacted in any way, weighing the set up and subtracting the weight of the beaker. Equation (13) was used (Amin *et al.*, 2004; Subukola and Onwuka, 2011);

$$\rho_b = \frac{bulk\ kernel\ mass}{600mL} \qquad 13.$$

The true density (ρ_t) was determined using toluene displacement method. Toluene was used in place of water because it is absorbed by seeds to a lesser extent and also has a low surface tension with low dissolution power too (Aydin, 2002). 500ml of toluene was put in 1000mL graduated measuring cylinder. Seeds from each batch were first weighed using an electronic weighing balance and then immersed in toluene in six replicates. The amount of displacement was recorded as the volume. Hence true density was obtained using equation (14);

$$\rho_t = \frac{weight\ of\ seed}{V_2 - V_1} \qquad 14.$$

$$Where\ V_2 = final\ volume;\ V_1 = initial\ volume$$

Porosity (ε) was determined as a function of the volume fraction ($f_v = \rho_b/\rho_t$). The porosity expressed in percentage was calculated using equation (15) (Asoegwu *et al.*, 2006; Joshi *et al.*, 1993; Deshpande *et al.*, 1993; Suthar and Das, 1996; Nelson, 2002):

$$\varepsilon = \left(1 - f_y\right) x 100\% \qquad 15.$$

Sphericity (ϕ) was calculated using equation (16) by Mohsenin (1986), Asoegwu *et al.*, (2006) and Gupta and Das (1997):

$$\phi = \frac{F_2}{F_1} \qquad 16.$$

2.2 Frictional Properties

The angle of repose (θ_r) was determined at different moisture contents using square box method. In this method, a specially constructed square box with removable front cover was used. The box was filled with the seeds from each batch; the front cover was then quickly removed, allowing the seeds to flow to its natural angle. The height (H) of the seeds was measured together as well as the length of spread (L) and the expression below (Oje and Ugbor, 1991) was used to determine the angle of repose for the different moisture contents:

$$\theta_r = tan^{-1}\left(\frac{H}{L}\right) \qquad 17.$$

Where H = maximum height of seeds in mm; L = spread length in mm

The static coefficient of friction of the various sample batches was determined against three (3) different structural materials, namely; mild steel, aluminum and plywood. A carton of St. Louis sugar was filled up to the brim with samples from each batch at a time and placed inverted on the structural surface lying on an adjustable tilting table. The carton was raised slightly so as to prevent the edges from touching the surface of the structural material. The entire set up was raised gradually using the tilt table screw device until the inverted carton of samples started to slide down and the angle of tilt (α) was read off using a protractor. Equation (18) was then used to determine the values of the static coefficient of friction (μ) on these structural surfaces at different moisture content levels (Singh and Goswami, 1996; Isik, 2007; Yalcin and Ozarslan, 2004).

$$\mu = \tan\alpha \qquad 18.$$

3. RESULTS AND DISCUSSION

It is observed that all the measured parameters were affected by increased moisture content. Table 1 shows the amount of water added to the African locust beans after being calculated with respect to mass of samples contained in each batch and the initial and desired moisture content levels.

3.1 Physical Properties

The seeds were grouped into five (5) batches of moisture content values of 7.45%, 10.2%, 11.4%, 12.9% and 15.2% respectively in dry basis. The average dimensions of volume, major, intermediate and minor diameters of each batch were determined by taking the average of the replicate values as shown in Table 2 for each of the batches.

3.2 Seed Dimensions

Table 2 shows the average major, intermediate and minor diameters for moisture content range of 7.45% to 15.2% dry basis. They were observed to vary from 15.09mm to 17.56mm, 11.50mm to 13.84mm and 7.19mm to 7.79mm respectively. Fig.1 show that they all increased linearly as moisture content increased. The following regression models (Eqns. 19 – 21) were developed for the effect of moisture content on seeds dimensions.

$$L_1 = 0.3389M + 12.588 \qquad (R^2 = 0.9568) \qquad 19.$$
$$L_2 = 0.3220M + 9.048 \qquad (R^2 = 0.9427) \qquad 20.$$
$$L_3 = 0.0872M + 6.4958 \qquad (R^2 = 0.9133) \qquad 21.$$

The increase in dimensions being moisture uptake in the intercellular spaces in the seeds, causing swelling and expansion. Hence, when these experimental values were regressed, linear and polynomial regression models gave the highest R^2-values. The linear relationship is recommended as the best that relates these properties to moisture content. Amin *et al.(*2004), Subukola and Onwuka (2011), Seifi and Alimardani (2010) and Tavakoli *et al.(*2009) all posited linear response of seed dimensions to moisture increase for lentil seeds, locust bean (*Parkia fillicoidea*), corn and barley grain respectively.

Table 1. Seed conditioning of batches

Batches	A(g)	Q (g)	b (% db)
1	1000	**Nil**	**7.45**
2	1000	18.1	10.2
3	1000	26.5	11.4
4	1000	36.9	12.9
5	1000	54.0	15.2

Table 2. Batch averages of dimensions

MC level	**L_1(mm)**	**L_2 (mm)**	**L_3(mm)**	**V(mm^3)**	**A_s (mm^2)**
M_1 (7.45%)	15.09	11.50	7.19	362.74	308.50
M_2 (10.5%)	15.51	11.99	7.29	399.78	329.69
M_3 (15.5%)	16.67	12.97	7.46	464.21	365.47
M_4 (20.5%)	17.16	13.34	7.73	507.77	388.81
M_5 (25.0%)	17.56	13.84	7.79	542.01	406.66

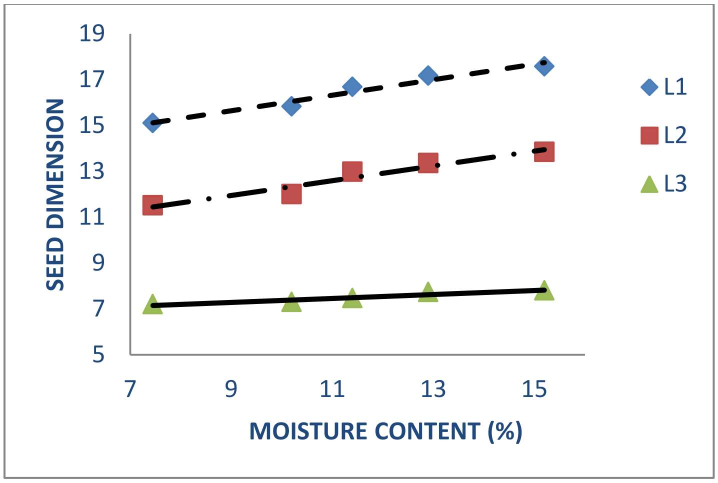

Fig 1. Effect of moisture content on seed dimensions

3.3 Seed Volume and Surface Area

Fig. 2 shows the behavior of seed volume and seed surface area with respect to changes in moisture content levels. Seed surface area ranged from 308.50mm^2 to 406.66mm^2 and seed volume between 362.74mm^3 to 542.01mm^3. The following polynomial regression models were developed to these effects;

$$V = -0.0064M^2 + 25.062M + 169.72 \quad (R^2 = 0.9519) \quad 22.$$

$$A_S = -0.0831M^2 + 15.528M + 193.75 \quad (R^2 = 0.9510) \quad 23.$$

From the above observations, seed volume and surface area increased polynomially as moisture content increased. This is dissimilar to the results of some researchers like Seifi and Alarmadani (2010) who suggested a linear increase of seed volume and seed surface area as moisture content of corn increased. Zareiforoush *et al.* (2009) and Kibar *et al.* (2010) posited a linear increase of these properties for paddy rice.

3.4 Equivalent Diameter

The equivalent diameter was seen to exhibit a polynomial increase as moisture content increased as shown in Fig 3. This is due to the fact that the seed dimensions increased when the seed (kernel) absorbed more moisture because more matter is then added to the seed, hence there is an expansion in size. Seifi and Alimardani (2010) reported a linear response for corn. Zeifouroush *et al.* (2009) reported a linear response too for paddy grain. Equation (24) gives the regression model to this effect,

$$D_e = -0.0048M^2 + 0.3479M + 8.6254 \qquad (R^2 = 0.9472) \qquad 24.$$

Asoegwu *et al.* (2011) reported linear relationship of equivalent diameter of African breadfruit seed with increasing moisture content.

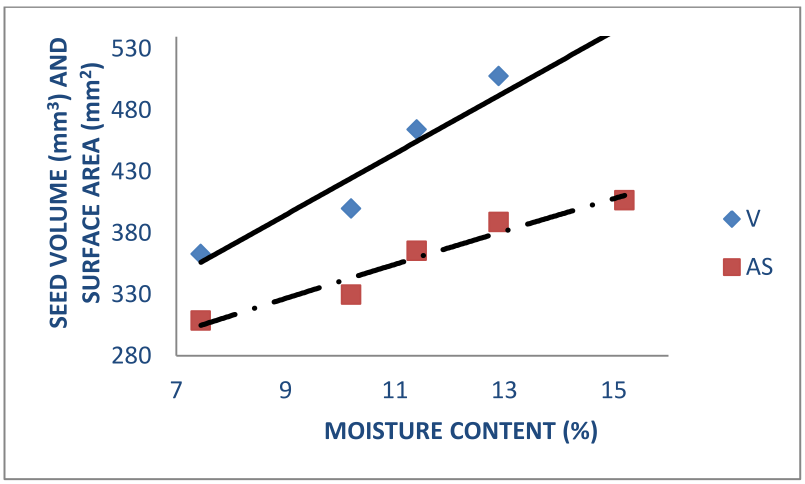

Fig 2.Effect of moisture content on seed volume and surface area

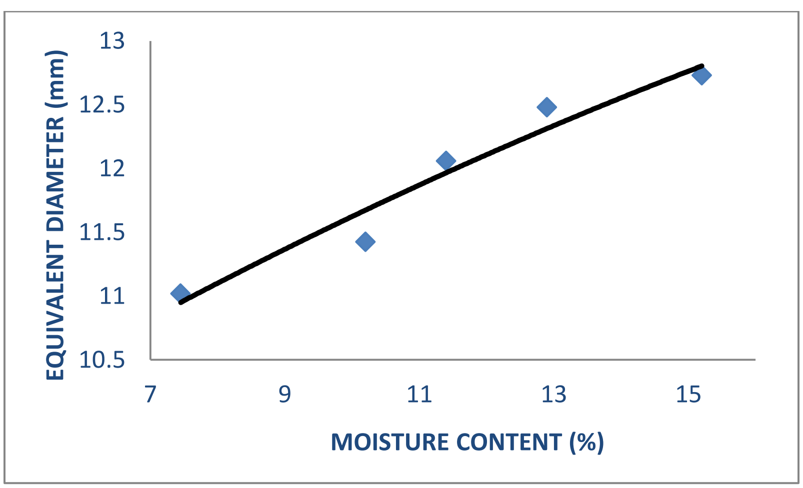

Fig 3. Effect of moisture content on equivalent diameter

3.5 Aspect Ratio and Sphericity

There was a gradual polynomial decrease of seed sphericity as moisture content increased as shown in Fig 4. This indicates that the seed is a little bit close to being a sphere as the principal dimensions of the seed increased with respect to moisture content. On the other hand, aspect ratio showed a third degree polynomially increasing trend. The following regression models were developed to these effects;

$A_r = -0.0003M^3 + 0.0118M^2 - 0.1282M + 1.2028$ ($R^2 = 0.9103$) 25.
$\Phi = 0.0003M^2 – 0.0086M + 0.7585$ ($R^2 = 0.9278$) 26.

Seifi andAlimardani (2010) suggested a linear response for the aspect ratio and sphericity of corn. Subukola and Onwuka (2011) and Zareiforoush *et al.* (2009) suggested a linear behaviour too for the sphericity of *Parkia fillicoidea* specie of locust bean and paddy grain respectively. Similar trends have been reported by Olajide and Ade-Omowaye (1999) for locust bean seed and Asoegwu *et al.* (2006) for African oil bean seed. Sánchez-Mendoza *et al*. (2008) reported a quadratic (polynomial) regression model for the effect of moisture on the sphericity of roselle seeds, while Asoegwu *et al.* (2011) suggested a power model for African breadfruit seeds.

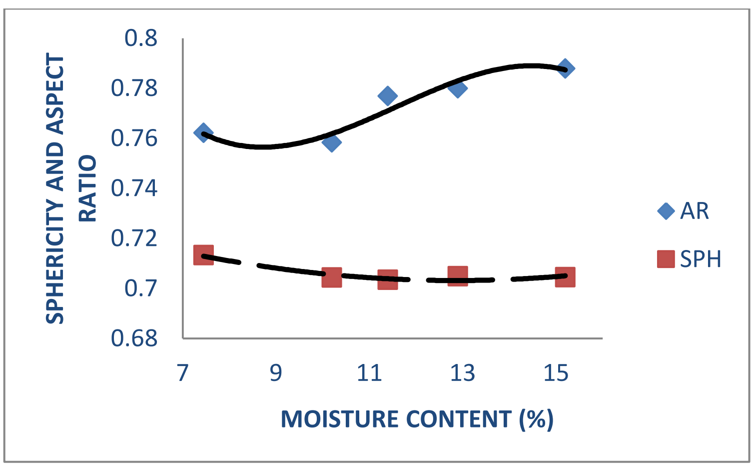

Fig. 4 Effect of moisture content on aspect ratio and seed sphericity

3.6 Density

From Fig. 5, bulk density increased polynomially from 0.4510g/m^3 to 5420g/m^3 and true density showed a third degree polynomial increase from 0.795g/m^{3}to 1.400g/m^3. A linear behaviour was suggested by Amin *et al*. (2004) for both the bulk and true densities of lentil seeds with respect to moisture content variance. Asoiru and Ani (2011) suggested an average safe storage density of yam bean to be 1.01779g/cm^3 and 1.0036g/cm^3 respectively for true and bulk densities. Nimkar and Chattopadhyay (2001) posited a linear increase in density of 807kg/m^3 to 708kg/m^3 (bulk density) and 1363kg/m^3 to1292kg/m^3 (true density) for green gram.

Equations (27) and (28) are regression models developed to these effects;
$\varrho_b = - 0.0001M^2 + 0.016M + 0.3353$ ($R^2 = 0.9175$) 27.
$\varrho_t = - 0.0082M^3 + 0.2872M^2 – 3.1368M + 11.632$ ($R^2 = 0.9748$) 28.

3.7 Porosity

The porosity of the seeds exhibited an increasing third degree polynomial trendline with respect to increase in moisture content as seen in Fig 6. This is because less pore spaces are created as the seeds absorb more moisture. The porosity varied from 41.10% to 61.32% as moisture content increases. Nimkar and Chattopadhyay (2001) suggested a linear increasing response of this parameter for green gram. Kingly, *et al.* (2006), Subukola and Onwuka (2011) and Tavakoli *et al*. (2009) suggested a decrease in porosity of pomegranate seeds, *Parkiafillicoidea*specie of locust bean and barley grains respectively with increasing moisture content.

Equation (29) is the regression model developed to this effect.

$$\varepsilon = -0.1942M^3 + 6.8146M^2 - 74.083M + 295.2 \quad (R^2 = 0.987) \qquad 29.$$

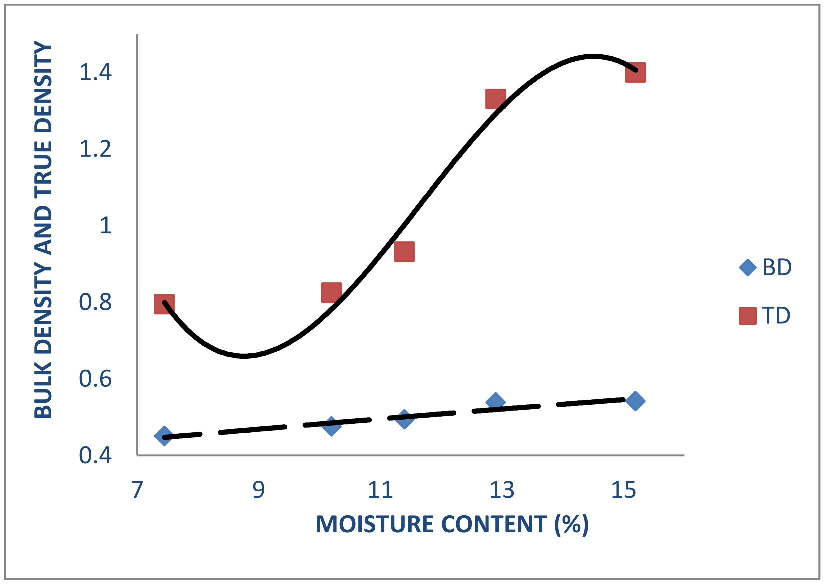

Fig. 5 Effect of moisture content on bulk density and true density

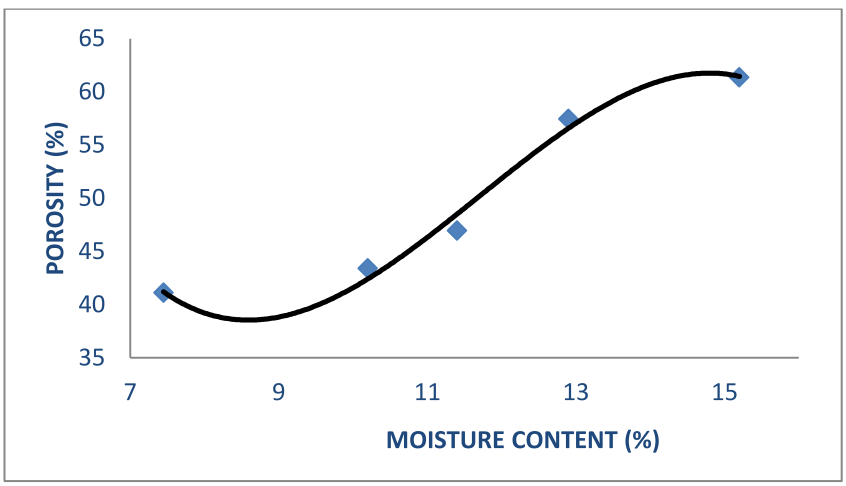

Fig. 6 Effect of moisture content on porosity

3.8 Static Coefficient of Friction

The static coefficients of friction of friction on the three different surfaces and at five different moisture content levels are shown in Fig 7. It can be observed that the static coefficient of friction for all the structural surfaces tested in the experiment had a polynomial increase as moisture content increases, with plywood having the highest coefficient followed by mild steel and lastly aluminum. This is due to the fact that the seeds become stickier as moisture content increases, leading to more resistance to relative motion between seeds and the surface. This increase in resistance therefore leads to an increase in the coefficient of static friction. It was also observed that the coefficient of static friction also varied with surfaces, this was as a result of the dependency of frictional properties and mechanical behavior of a material on the microstructure of the material.

Structural material grains shape and their crystallographic orientation are two features of microstructure that affect friction on this material. Due to the difference in crystallographic orientation of the grains which creates a difference in the surface texture, the material grains of the two surfaces prevent one surface from sliding freely on the other. The rougher the grains, the more the surfaces interlock, resulting in more resistance to relative motion between them which equally leads to increase in the coefficient of static friction. The material grains of plywood are rougher than those of mild steel and aluminum. Hence, the reason for the high coefficient of static friction with plywood. Therefore, the power demand of processing machines involving friction increases with increase in moisture content and also with increase in coefficient of static friction. This implies that in plywood constructed machines, higher power will be required than in similar machine constructed with aluminum. Appendix V gives the experimental values generated to this effect.

Asoiru and Ani (2011) posited linear increase for average values of coefficient of static friction from aluminum to asbestos to plywood at a safe moisture content for African yam bean. Oje and Ugbor (1991) also suggested a linear increase for oil bean seeds using galvanized steel, plywood, stainless steel, aluminum and mild steel with a simultaneous increase in moisture content and equally posited that plywood gave highest values. Kingly *et al*. (2006) posited a linear increase for pomegranate seeds for various structural surfaces with plywood giving the highest values.

The following are regression models developed to this effect;

$$\mu_{PLW} = 0.0004M^2 + 0.044M + 0.1763 \qquad (R^2 = 0.9902) \qquad 30.$$
$$\mu_{MS} = 0.002M^2 + 0.0069M + 0.2846 \qquad (R^2 = 0.9931) \qquad 31.$$
$$\mu_{AL} = 0.0015M^2 + 0.0113M + 0.1892 \qquad (R^2 = 0.9973) \qquad 32$$

3.9 Angle of Repose

Fig 8 shows the angle of repose at five different moisture contents and it was observed that the angle of repose had a third degree polynomial variation with increase in moisture content. The reason being that the higher the moisture content, the higher the cohesion between the seeds. In terms of flowability, the seeds are heavier and the inertia to move is increased. This increase in resistance to flow prevents seeds from sliding on each other, thereby increasing the angle of repose of the seeds. Appendix VI shows the experimental values generated to this effect.

Nimkar and Chattopadhyay (2001) , Subukola and Onwuka (2011), Tavakoli *et al.* (2009) and Zareiforoush *et al.* (2009) all suggested a linear increase too for green gram seeds, *Parkia fillicoidea* specie of locust bean, barley grains and paddy grains respectively.The following regression model was developed to this effect;

$$\Theta_R = -0.1366M^3 + 4.7214M^2 - 50.226M + 189.64 \qquad (R^2 = 0.9993) \qquad 33.$$

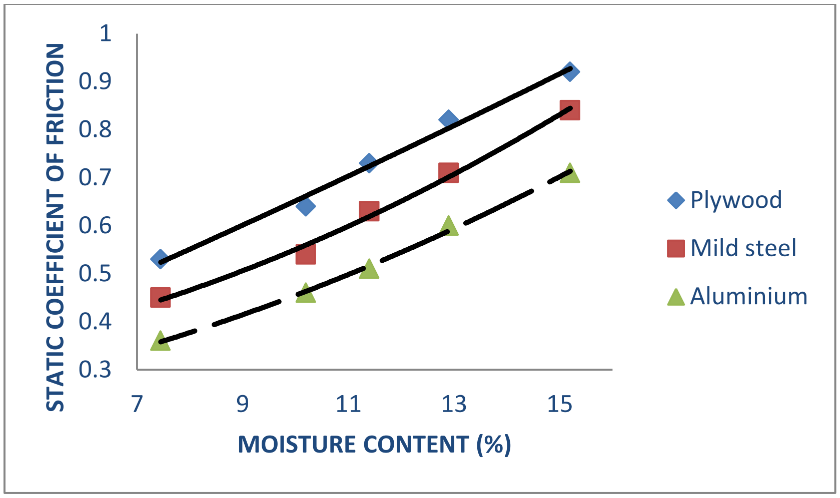

Fig. 7 Effect of moisture content on static coefficient of friction

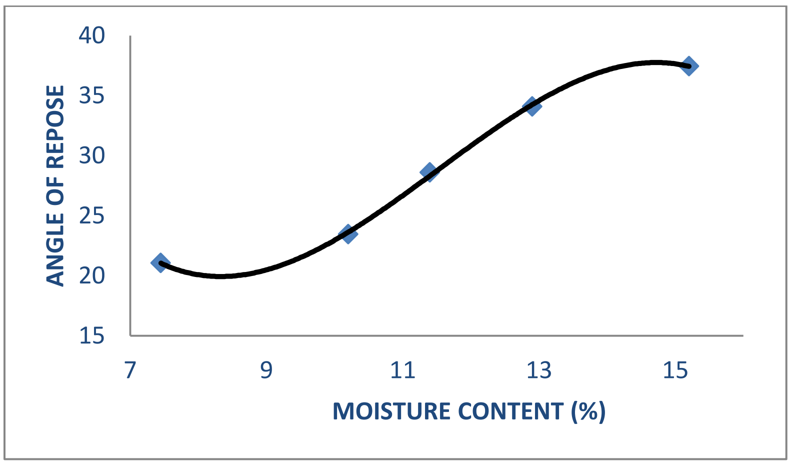

Fig 8 Effect of moisture content on angle of repose

4. CONCLUSIONS AND RECOMMENDATION

All properties studied were found to have a linear or polynomial response (second order or third) to moisture content increase within the moisture content range studied. The average dimensions; major, intermediate and minor and equivalent diameters increased from 15.09 to 17.56mm, 11.50 to 13.84mm, 7.19 to 7.79mm, and 11.02 to 12.73mm respectively as moisture content increased from 7.45% to 15.2% (dry basis). The seed volume and the seed surface area of *Parkia biglobosa* increased from 362.74mm^3 to 542.01mm^3 and 308.50mm^2 to 406.66mm^2 within the range of moisture content tested. Bulk density and true density increased from 0.45g/m^3 to 0.54g/m^3, and 0.80g/m^3 to 1.40g/m^3 respectively with increasing the moisture content range tested. Aspect ratio, sphericity and porosity of *Parkia biglobosa* varied with increase in the tested moisture content range from 0.76 to 0.79; 0.713 to 0.704 and 0.41 to 0.61 respectively. Angle of repose increased from 21.05^0 to 37.45^0 while static coefficient of friction increased from 0.53 to 0.92 (plywood), 0.45 to 0.84 (mild steel) and 0.36 to 0.71 (aluminum) as moisture content increased from 7.45 to 15.2% (dry basis). All resultant values generated in this research were statistically analysed using Microsoft office excel 2010, hence developing the regression models of the effects of moisture on all the properties studied.

REFERENCES

Ajav, E. A. and J. O. Ojediran 2006. Some physical and aerodynamic properties of three Nigeria cereal crops as related to their cleaning. ASABE Meeting Presentation. Paper Number 066006: 1 – 13.

Alibi, D. A. 1991. Parkiabiglobosa: An endangered species. In proceeding on Lost Crop of Nigeria; Implications for food Security (J.A. Okojie and D.U.U. Okali, eds.) pp. 265 – 283, University of Agriculture, Abeokuta, Nigeria.

Al-Mahasneh, A.M. and T.M. Rababah. 2007. Effect of moisture content on some physical properties of green wheat. *Journal of Food Engineering* 79: 1467–1473.

Amin, M. N., M. A. Hossain and K. C. Roy 2004. Effects of moisture content on some physical properties of lentil seeds. *Journal of Food Engineering* 65: 83 – 87.

ASAE standards 46th Edition 1999. Moisture measurement-unground grain and seeds. St. Joseph, Mich. ASAE.

Asoegwu, S. N., S. O. Ohanyere, O. P. Kanu and C. N. Iwueke 2006. Physical properties of African Oil Bean Seed (*Pentaclethra macrophylla*). *Agricultural Engineering International: the CIGR Ejournal.* Vol V11.

Asoegwu, S. N., G.U. Iroakazi, L.A.S. Agbetoye & A.S. Ogunlowo 2011. Some Handling and Frictional Properties of African Breadfruit Seeds as a function of Moisture Content *PROC.* NIAE 32nd p. 639 – 653

Asoiru, F. U. and Ani, A. O. 2011. Determination of some physical properties of African Yam Beans. *The Pacific Journal of Science and Tech.* 12(1): 374 – 380.

Aviara, N. A., M. I. Gwandzang and M. A. Haque 1999. Physical Properties of Guna Seed. *Journal of Agric Engineering Research* 73(2): 105 – 111.

Aydin, C. 2002. Physical Properties of Hazel nuts. *Biosystem Engineering* 82.297 – 303.

Baryeh, E. A. 2001, Physical properties of Bambara groundnuts. *Journal of Food Engineering* 47:321 – 326.

Baryeh, E.A., 2002. Physical properties of millet. *Journal of Food Engineering* 51: 39–46.

Baryeh, E.A. and B.K. Mangope, 2002. Some physical properties of QP-38 variety pigeon pea. *Journal of Food Engineering* 56: 59-65.

Desphande, S. O., S. Bal and T. P. Ojha 1993. Physical Properties of Soybean. *Journal of Agric. Engineering Research*, 66: 1 – 8.

Ghasemi Varnamkhasti, M., H. Mobli, A. Jafari, S. Rafiee, M. Heidary Soltanabadi, and K. Kheiralipour. 2007.Some Engineering Properties of Paddy (var. *Sazandegi*). *International Journal of Agriculture and Biology* 5:763-766.

Gumble, L. O. and C. Maina. 1990. Friction coefficient of cereal seeds on various surfaces. *Agricultural Mechanization in Asia, Africa and Latin America* 21(4): 61–64.

Gupta, R.K. and S. K. Das 1997. Physical properties of sunflower seeds. *Journal of Agricultural Engineering Research*, 66: 1 – 8.

Isik, E. 2007. Some physical and mechanical properties of round red lentil grains. Applied Engineering in Engineering (ASABE) 23(4): 503 – 508.

Joshi, D. C., S. k. Das and R. K. Mukherjee 1993. Physical properties of pumpkin seeds. *Journal of Agric. Engineering Research* 54: 219 – 229.

Karimi, M., K. Kheiralipour, A. Tabatabaeefar, G. M. Khoubakht, M. Naderi and K. Heidarbeigi. 2009. The effect of moisture content on physical properties of wheat. *Pakistan Journal of Nutrition* 8(1): 90 – 95.

Kingly, A. R. P., D. B. Singh, M. R. Manikantan and R. K. Jain 2006. Moisture-dependent physical properties of dried pomegranate seeds (Anardana). *Journal of Food Engineering* 75: 492 – 496.

Kibar, H., T. Öztürk and B. Esen. 2010. The effect of moisture content on physical and mechanical properties of rice (*Oryza sativa L.*). *Spanish Journal of Agricultural Research* 8(3): 741-749. Available online at www.inia.es/sjar ISSN: 1695-971-X eISSN: 2171-9292

Masoumi, A. A. and L. Tabil. 2003. Physical properties of chickpea (C. arietinum) cultivars. ASAE Paper No. 036058. St. Joseph, Mich.: ASAE.

Mohsenin, N. N. 1986. Physical Properties of Plant and Animal Materials, 2nd ed. *Gordon and Breach Science Publishers*, New York.

Molenda, M. and J. Horabik. 2005. Characterization of mechanical properties of particulate solids for storage and handling. Institute of Agrophysics. Polish Academy of Science. Lublin.

Moshsenin, N. N. 1970. Physical Properties of Plant and Animal Materials. Gordon and Breach Publishers, New York. 734p.

Mpotokwane, S. M., E. Gasitlhatlhelwe, A. Sebaka and V. A. Jideani. 2008. Physical properties of Bambara groundnuts from Botswana. *Journal of Food Engineering* 89:93 -98.

Nelson, S. O. 2002. Dimensional and density data for seeds or cereal grain and other crops. *Transactions of of the American Society of Agric. Engineers* 45(1): 165 – 170.

Nimkar, P.M. and P. K. Chattopadhyay 2000. Some physical properties of green gram. *Journal of Agric. Engineering Research* 80: 183 – 189.

Odunfa, S. A. and E. Y. Adwuyi 1985. Optimization of process conditions for the fermentation of African locust bean (Parkiabiglobosa): Effect of time, temperature and humidity. Chem. microbial. Technol. Lebensn 9: 6 – 10.

Ogunjimi, L. A., N. A. Aviara and O. A. Aregbesola 2002. Some engineering properties of loclust bean seed. *Journal of Food Engineering* 55: 95 – 99.

Oje, K. 1993. Locust bean pods and seeds: some physical properties relevant to dehulling and seed processing. *Journal of Food Science Technology* 30: 253 – 255.

Oje, K. and E. C. Ugbor 1991. Some physical properties of oil bean seeds. *Journal of Agricultural Engineering Research* 50: 305 – 313.

Oladele, F. A., M. O. Fawole and R. B. Bhat 1985. Leaf anatomy of Parkiaclappertoniana Keay (Mimosaceae). *Korean Journal of Botany*. 28(1): 21 – 28.

Olajide J.O., Ade-Omowaye B.I.O., 1999. Some physical properties of locust bean seed. *Journal of Agric. Engineering Research*. 74, 213-215.

Omobuwayo, T. O., E. A. Akande and L. A. Sanni 1999. Selected physical, mechanical and aerodynamic properties of African bread fruit (Treculiaafricana) seeda. *Journal of Food Engineering.* 40: 241 – 246.

Omobuwajo, T. O., L. A Sanni and Y. A. Balami. 2000a. Physical properties of sorrel (*Hibiscus sabdariffa*) seeds. *Journal of Food Engineering* 45(1): 37–41.

Omobuwajo, T. O., O. R. Omobuwajo and L. A. Sanni. 2003. Physical properties of calabash nutmeg (*Monodora myristica*) seeds. *Journal of Food Engineering* 57: 375–381.

Oni, K. C. 1990. Shelling machine related properties for African Locust Bean fruit. Journal of American Society of Agriculture Engineers: 572 – 576.

Owoyale, J. A., M. Shok and T. Olagbemiro 1986. Some chemical constituents of the fruit of *Parkia clappertoniana* as a potential raw materials. Presented at the 2nd annual conference of Biotechnology Society of Nigeria, University of Ilorin, Nigeria. 16 – 19 May.

Sahay, K. M. and K. K. Singh. 1994. *Unit Operations in Agricultural Processing*. 1st Edition. Vikas Publishing House Pvt. Ltd., New Delhi India.

Sánchez-Mendoza, J., A. Domínguez-López, S. Navarro-Galindo and J. A. López-Sandoval. 2008. Some physical properties of Roselle (*Hibiscus sabdariffa* L) seeds as a function of moisture content. *Journal of Food Engineering* 87: 391 - 397.

Seifi, M. R. and R. Alimardani 2010. The moisture content effect of some physical and mechanical properties of corn. *Journal of Agric. Science,* Canadian Centre of Science and Education 2(4): 125 – 134.

Singh K. K. and Goswami, T. K. 1996. Physical properties of cumin seed. *Journal of Agric. Engineering Research* 64: 93- 98.

Subukola, O. P. and Onwuka, V. I. 2011. Effects of moisture content on some physical properties of locust bean seed (Parkiafillicoidea). *Journal of Food Process Engineering Research* 34: 1947 – 1961.

Suthar, S. H. and S. K. Das 1996. Some physical properties of Karingda {Citrulluslanatus (thrumb) Mansf} seeds. *Journal of Agricultural Engineering Research,* 65(1): 15 – 22.

Tavakoli, M., H. Tavakoli, A. Rajabipour, H. Ahmedi, S. M. T. Gharib-zahedi 2009. Moisture-department physical properties of barley grains. *International Journal of Agric. And Biological Engineering* 2(4): 84 – 91.

Wang, B., D. Li, L. Wang, Z. Huang, L. Zhang, X. D. Chen, and Z. Mao. 2007. Effect of moisture content on the physical properties of fibered flaxseed. *International Journal of Food Engineering* Vol. 3 Issue 5 Article 1 (1 – 13).

Zareiforoush, H., M. H. Komarizadeh and M.R. Alizadeh 2009. Effect of moisture content on some physical properties of paddy grains. Journal of Appiled Sciences, Engineering and technology 1(13): 132 – 139.

ENERGETIC ANALYSIS OF CLAY OVEN USED FOR BREAD BAKING

R. Akinoso[1], A. K Aremu[2] and A. R. Ismaila[3]
[1]Department of Food Technology, Faculty of Technology, University of Ibadan, Nigeria.
[2]Department of Agricultural and Environmental Engineering, Faculty of Technology, University of Ibadan, Nigeria.
E-mail: akinoso2002@yahoo.com

ABSTRACT

Food processing including baking consumes a lot of energy thereby increasing cost of production. Therefore, energy and exergy distribution patterns in clay oven were determined, and computer software to evaluate the energy was developed. Ten clay oven bakeries were used for the study. Sizes, shapes, thicknesses and sources of energy were recorded and temperature taken at an interval of 30min for 7hrs. Energy, exergy and energy losses of the ovens were computed using standard equations. Software was developed using Visual Basic programming language and the performance was evaluated. The ovens were of dome shape, the sizes ranged between 27.40m^2 and 36m^2 and the thickness ranged from 0.19m to 1.11m. Mass of fossil fuel (dry wood) used ranged between 244kg and 270kg as the source of energy. Peak mean temperature of 451 ± 5.6^{o}C was achieved after 180min of heating un-loaded oven. At this temperature, the mean energy, exergy and energy loss recorded were 184.85 ± 8.78MJ, 169.33 ± 7.65MJ and 3.31 ± 1.25MJ respectively. Loading with bread dough reduced the temperature to 153^{o}C after 1hr. The mean energy, exergy ranged between 24.85 ± 0.14MJ and 184.85 ± 8.78MJ and from 15.9 ± 1.86MJ to 169.33 ± 7.65MJ respectively. The mean energy loss ranged between 0.44 ± 0.14MJ and 3.32 ± 1.25MJ. The mean total energy loss was 26.3MJ out of which the door contributed about 26.2MJ (99.5%) of the heat loss. Validation of the software indicated that less than 0.5% marginal error was recorded. The computer software developed served as a useful tool for estimating energy distribution pattern in clay oven.

KEYWORDS: Clay oven, bread baking, energy analysis, computer simulation

1. INTRODUCTION

Bread is a fermented confectionary product produced mainly from wheat flour, water, yeast and salt by a series of process involving mixing, kneading, proofing, shaping and baking . Other ingredients are sugar, milk or fat, which improve the quality of bread. Bread factory at small-scale level produce larger proportion of bread consumed in Nigeria. Baking is a major unit operation in bread making and it has been reported by to consume about 75% of total energy input (Akinoso and Ganiu, 2011). Majority of these bakers adopt clay oven, which uses wood as source of fuel. Clay oven is a thermally insulated chamber used for the heating, baking and drying of food substances. It utilizes high energy in the form of heat. The technology behind clay oven is that it absorbs heat from the fire and then radiates the absorbed heat. The heat absorbed by the wall of the oven flow from region of higher temperature to the region of lower temperature. The heat source is built either within the oven itself (a black or Roman oven) or in a firebox that vents into the oven (a white oven); smoke is vented through the front of the oven, either directly to the outside or through a chimney immediately above the oven door. The oven comes in different sizes and forms, depending on its usage, either commercial or subsistence, although, both use the same technology.

Energy and foods are concern of developing countries, because chains of food production consume a lot of energy (Wang, 2009). Energy efficiency is a fundamental element towards a sustainable food and energy development. Therefore, improvement on energy generation, estimation and conservation is important for development of industries. Although some studies have been conducted that explore the multifaceted sources and uses of energy in agriculture at the farm level, there are however currently few studies on energy use for further downstream in the food chain especially in food processing, packaging, storage, and distribution (Ziesemer, 2007). Few of the processing factories have little precise idea of the energy consumption of different production areas and in the absence of detailed internal monitoring, the energy efficiencies of different operations is also usually unknown (Jekayinfa and Olajide, 2007). Research reports on energy consumption and conservation patterns in Nigeria include rice processing (Ezeike, 1981), beverage industry (Akinbami *et al.*, 2001), and palm kernel oil processing (Jekayinfa and Bamgboye, 2004). Energy expenditure on sugar processing (Abubakar et al., 2010), bread baking (Akinoso and Ganiu, 2011) and *gari* (Akinoso and Kasali, 2012) have been reported.

The use of energy as a measure for understanding and improving the efficiencies of energy systems can be misleading and confusing (Marc et al., 2009). Therefore, it is important to understand the concept and component of energy for proper analysis. This must be made through the energy quantity as well as the quality. Exergy, which is based on the second law of thermodynamic analyses energy on quantity as well as the quality. It identifies the magnitudes and the locations of real energy losses, in order to improve the existing systems, processes or components (Ganapathy et al., 2009). It also can be used to assess and improve the efficiencies of energy systems, and can help better understand the losses in energy systems by providing more useful and meaningful information than energy provides. Exergy analysis is a methodology that uses the conservation of energy principle (embodied in the first law of thermodynamics) together with non-conservation of entropy principle (embodied in the second law) for the analysis, design and improvement of energy and other systems (Marc et al., 2009). The exergy method is useful for improving the energy efficiency, for it quantifies the locations, types and magnitudes of wastes and losses. This analysis identifies the margin available to design more efficient energy systems by reducing inefficiencies. Operations of food processing equipments require energy and inefficient energy utilization hike cost of production, and clay is one the major mineral deposit in Nigeria (RMRDC, 1990; Omowumi, 2001).

The objective of this study was to analyze energy and exergy distribution patterns in clay oven used for bread baking.

2. MATERIAL AND METHODS

2.1 Parametric Data

Shapes, thickness, size, quantity of wood used in baking and temperature gradient at 30 minutes interval for 7 hours of ten clay ovens use for bread baking in Ibadan Nigeria were measured. Capacity of the ovens for bread baking was also recorded.

2.2 Energy Analysis

Heat generated, heat loss, energy and exergy efficiencies of the clay ovens were calculated using standard equations (Equations 1 to 8).

$$Q = mC_p(T_1 - T_0) \qquad (1)$$

$$E_{xi} = Q(1 - \frac{T_0}{T_1}) \qquad (2)$$

$$Q_L = \frac{kA}{x}(T_1 - T_0) \qquad (3)$$

$$Q_c = \frac{A}{A_T} * Q_w \qquad (4)$$

$$Q_{TL} = (Q_L) + (Q_c) \qquad (5)$$

$$q = Q_G - Q_{TL} \qquad (6)$$

$$Energy\ efficiency = \frac{enegy\ output}{exergy\ input} \qquad (7)$$

$$Exergy\ efficiency = \frac{exegy\ output}{exergy\ input} \qquad (8)$$

Where Q = quantity of energy generated (MJ); E_{xi} = exergy input (MJ); T_o = reference temperature (ambient); T_1 = highest temperature (°C); m = weight of firewood (kg); C_p= specific heat capacity of wood (kJ/kg k); Q_L = Quantity of heat loss by conduction (kJ); K = Thermal Conductivity of the clay (W/mk); X = Thickness of the Clay oven (m); A = Dimensional area of the oven (m^2); Q_c = quantity of heat loss by convection (MJ); Q_w = Total heat generated by wood (MJ/kg); h = convective heat transfer coefficient ($W/m^{2o}C$); A = area (m^2); A_T = Total area of clay oven (m^2); Q_{TL}= total heat loss (MJ); q = Effective heat; Q_G = heat generated; Q_{TL} = Total Heat loss

2.3 Software Development

The software package was developed using Visual Basic. Data obtained from energy analysis was used as a platform on which the event programme was structured. Highlighted programme algorithm was used.

1. Start program.
2. Select type of computation to perform. Either 'Exergy' computation or 'Mass of wood' computation.
3. Input variables C, To, K, T, Tf, Tw, A', A'',A'''.
4. Compute wall surface area excluding door, A'=A'-A'''
5. Compute total, T'=A'+A''+A'''
6. If selection type="Exergy" then input M else input E then goto 13
7. Compute total energy, Etotal=MC(T-To)
8. Compute energy loss (wall), Ew=(KA'(T-To)/Tw), energy loss(floor), Ef=(KA''(T-To)/Tf), energy loss(door), Ed=(A'''/T')E
9. Computer total energy loss, Eloss=Ew+Ef+Ed
10. Compute effective energy, Eeff=Etotal-Eloss
11. Compute exergy, E=Eeff(1-(To/T))
12. Display E and goto 17
13. Compute effective energy=(E-T)/(T-To)
14. Compute Etotal=(Eeff+Ew+Ef)/(1-(A'''/T'))
15. Compute M=Etotal/(C(T-To))
16. Display M
17. Display Ew, Ef, Ed, Eloss, Etotal, Eeff
18. End program.

3. RESULTS AND DISCUSSION

3.1 Parametric Data of Clay Oven

Each oven was used to bake bread dough produced from 300 kg wheat flour. The result obtained for the ten clay ovens A - J showed that they were of dome shape, with oven A to H having a circular-like shape floor and oven I and J, a rectangular shape floor. The areas of the wall showed that oven A, B and I have the same value of 22.1m^2, for oven C, D, E, F, G, H, and J the corresponding areas are 22.4m^2, 26.8m^2, 25.1m^2, 26.2m^2, 20.4m^2, 20.3m^2 and 23.5m^2 respectively. Ovens A and B have the same floor area of 9.60m^2, likewise oven D and J with value 9.10m^2 and oven H and I with value 9.00m^2. Oven C, E, F and G floor areas were 8.20m^2, 10.90m^2, 8.00m^2 and 7.00m^2 respectively. The value of door areas showed that 0.44m^2 was recorded for oven C and D, 0.40m^2 was recorded for F and G, and 0.68m^2, 0.64m^2, 1.20m^2, 0.50m^2, 0.48m^2, 0.42m^2 for oven A, B, E, H, I and J respectively. Thickness of wall oven A, B, E, F, I and J have the same value of 0.2m, oven C and D recorded 0.19m and oven G with a value of 0.22m. Floor heights of oven E and H have the same value of 0.90m, oven F and I with value 0.95m and 0.60m, 0.50m, 0.45m, 0.85m, 1.11m, and 0.48m for oven A, B, C, D, G, and J respectively.

3.2 Source of Heat Energy

Dry wood was used to heat the ovens. Recorded masses of dry wood used for baking 300kg of wheat flour dough to bread showed that oven A and B consumed 265kg of dry wood, oven E and F consumed 260kg of dry wood, and for oven C, D, G, H, I, and J, the values of dry wood consumed were 268kg, 262kg, 250kg, 240kg, 270kg and 244kg respectively. The lowest mass of dry wood was 244kg and the highest mass was 270kg.

3.3 Temperature Distribution

The result of heat energy generated from the dry wood showed that energy increases steadily with duration (Figure 1). As expected, oven temperatures increased with heating period. From ambient temperature of 30±2^{o}C, temperature of the oven chambers rose to 120^{o}C in the first 30 min. of heating for all the ovens except oven F and G which recorded temperatures of 130^{o}C, and oven A with 110^{o}C. Loading with bread dough reduced the temperature to 153^{o}C after 1hr. The peak heat energy generated was achieved after 180min of heating un-loaded ovens and the peak temperature ranged between 440^{o}C and 460^{o}C. Oven B recorded the highest temperature of 460 ^{o}C, clay oven G recorded the lowest temperature of 440^{o}C in 180min (Table 1).

3.4 Heat Loss

Three media of heat loss to the environment were noticed. Heat was lost through the walls, floor and door of the oven. In the first 3hrs, it was observed that heat loss in the clay oven increased steadily up to a peak value before decrease. Peak heat energy loss value recorded for door were 3.97MJ, 3.82MJ, 4.24MJ, 2.26MJ, 6.07MJ, 3.06MJ, 2.01MJ, 2.47MJ, 2.97MJ, and 2.22MJ for oven A, B, C, D, E, F, G, H, I and J ovens respectively. The peak energy loss through the wall of ovens A, B, C, D, E, F, G, H, I and J respectively were 12337.50J, 11602.50J, 11878.75J, 12526.32J, 14810.53J, 13365.75J, 13427.50J, 9736.36J, 11165J, 11740.63J. While floor energy lost were 1990.63J, 1680.00J, 2054.40J, 2266.67J, 1124.12J, 1289.83J, 863.16J, 662.16J, 1045J, 1006.58J for A, B, C, D, E, F, G, H, I and J ovens. The highest heat loss was observed at the door of the clay ovens, this was associated to opening of door during heating and construction of the door with mild steel of high thermal conductivity of about 48.5W/mK..

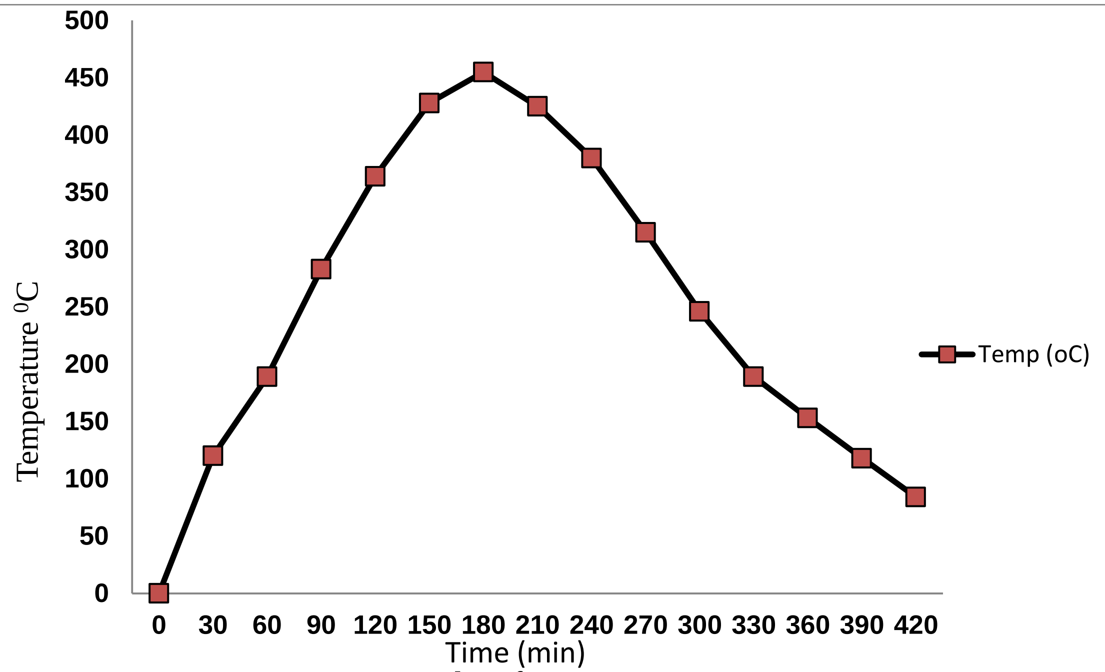

Figure 1. Plot of temperature against time

Table 1. Heating temperatures of the ovens during baking

Time (min)	**Oven A °C**	**Oven B °C**	**Oven C °C**	**Oven D °C**	**Oven E °C**	**Oven F °C**	**Oven G °C**	**Oven H °C**	**Oven I °C**	**Oven J °C**
0	30	30	32	30	30	29	30	30	32	30
30	120	110	120	120	120	121	130	120	130	120
60	190	185	188	190	185	200	200	185	178	189
90	290	250	290	290	280	280	280	280	290	300
120	380	320	350	380	380	360	375	360	345	360
150	440	400	420	440	440	440	425	400	400	430
180	450	450	460	455	450	455	440	450	445	455
210	415	430	435	425	420	420	410	420	450	435
240	370	390	395	380	360	380	360	360	420	380
270	300	340	305	340	300	330	290	300	340	305
300	240	270	235	250	240	300	225	240	280	235
330	182	240	150	200	180	170	180	180	230	180
360	155	185	120	155	150	155	155	150	150	152
390	120	130	100	130	110	125	120	120	105	120
420	90	90	85	90	90	80	85	90	80	89

3.5 Thermal Efficiency of the Ovens

Each oven was used to bake bread dough produced from 300 kg wheat flour. Actual energy utilized for bread baking increased progressively with time in the entire clay oven up to a peak point before it began to decline (Figure 2). The peak time recorded for clay oven A – J was 180min and the corresponding percentage values are 91.37%, 91.20%, 91.35%, 92.20% 92.14% 90.60% 92.10% 91.98% 91.25% 91.98% respectively (Table 2). High efficiency might be associated with low thermal conductivity of clay as reported by (Folaranmi, 2009). The least efficiency (58.99% to 65.85%) were recorded after 420min of heating. At 300min, percentage of actual energy utilized across the clay ovens for baking were recorded which ranged from 84.67% to 87.41%. It also showed the ability of clay oven to hold heat as reported by (Forno, 2012) that thermal mass and insulation are the two primary characteristics that describe an oven's ability to absorb and hold heat, and make it useful for cooking. The thermal conductivity of clay, which is the property of a material that indicates its ability to conduct heat, is mostly controlled by water content and other properties (Kromer and Mörtel 1988). It ranges between 0.25 to 2.0 W/mK.

The small difference in the efficiencies is because the specific chemical exergy of firewood is slightly greater than its specific base enthalpy. The lower value for exergy efficiency shows that even if some energy is associated with the firewood, this part of energy becomes less available in reality. Exergy efficiency is a measure of how near a process approaches ideality and a measure of how near energy transfer approaches ideal transfer.

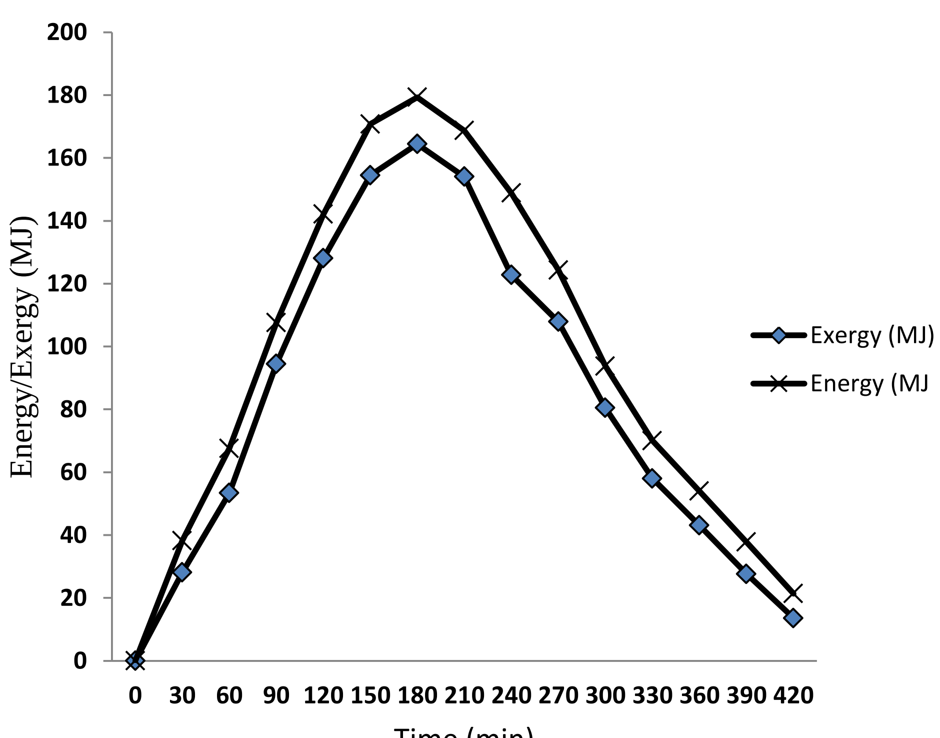

Figure 2. Plot of energy and exergy against time

Table 2. Energy efficiencies of the ovens during baking

Time (min)	Oven A %	Oven B %	Oven C %	Oven D %	Oven E %	Oven F %	Oven G %	Oven H %	Oven I %	Oven J %
0	-	-	-	-	-	-	-	-	-	-
30	74.04	71.19	71.88	73.35	74.09	73.57	76.03	73.92	74.11	73.86
60	83.13	82.02	81.33	82.36	82.76	82.74	82.74	82.57	80.64	82.84
90	88.51	86.15	87.20	87.68	88.20	86.74	88.25	88.00	87.47	90.27
120	90.93	88.72	89.05	90.08	90.98	88.97	90.93	90.34	89.20	91.60
150	91.99	90.55	90.55	91.13	92.05	90.39	91.86	91.16	90.45	91.98
180	92.14	91.37	91.20	91.35	92.20	90.60	92.10	91.98	91.25	91.98
210	91.58	91.06	90.80	90.90	91.72	90.08	91.60	91.52	91.32	91.68
240	90.72	90.36	90.07	90.08	90.55	89.38	90.60	90.34	90.82	90.70
270	88.85	89.26	87.73	89.17	88.90	88.26	88.61	88.70	89.06	88.79
300	86.38	87.02	84.67	86.07	86.43	87.41	85.66	86.24	87.08	85.90
330	82.45	85.66	77.10	83.13	82.32	80.26	82.36	82.13	84.64	82.06
360	79.61	82.02	71.88	78.87	79.02	78.66	79.71	78.84	77.34	79.04
390	74.04	75.30	66.65	75.23	71.84	74.32	74.13	73.92	68.35	73.86
420	65.81	65.26	61.11	65.20	65.85	61.69	63.95	65.70	58.99	65.28

3.6 Software Application

The data collected from different oven was used to validate the software. The result showed that less than 0.5% marginal error was recorded. The exergy software calculator is a screen-oriented programme that can be used to estimate energy distribution pattern obtainable from a known mass of firewood in clay oven with respect to its dimension. Figure 4 show the flowchart on how the programme was run to achieve results. Figure 3 show the graphical user interface used to execute the events programme respectively. The graphical user interface is the platform by which input variables data were captured into the text boxes provided for the user before the computer system could run. The graphical user interface was divided into six sections. The first section has an option button showing exergy and mass of wood depending on the subject of interest; the buttons that correspond will be click. The second section is the input variable section mass of firewood, specific heat capacity of firewood, thermal conductivity of clay, temperature of oven, thickness of the oven wall, thickness of the floor, ambient temperature and lastly radius of oven. The third section only has surface area of clay oven pre-determined or radius and height of the clay oven chamber. The fourth section also has pre-determined floor area or length and breadth of the floor input. The fifth section command button evaluates the data and generates result of energy, energy losses and exergy into section 6. Exergy calculation was carried out by clicking on the exergy option at the top of the interface in Figure 3 and all the input variable are captured in the text boxes provided. Calculation was done by clicking on the "calculate" button at lower left end of the interface. This quantifies the exergy from firewood in the clay oven and can be in the reverse order to calculate the mass of wood for a known quantity of exergy.

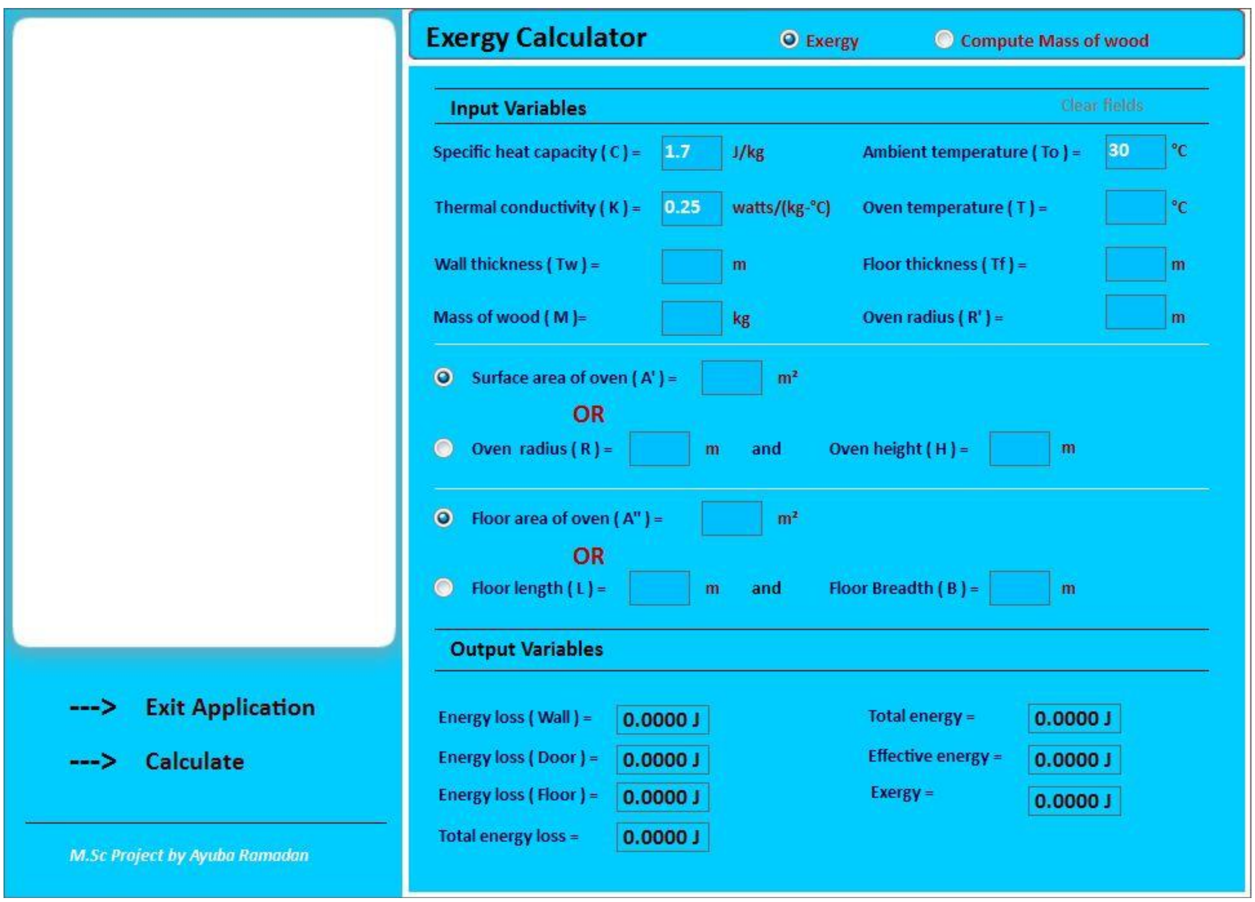

Figure 3. Graphical user interface for exergy calculator

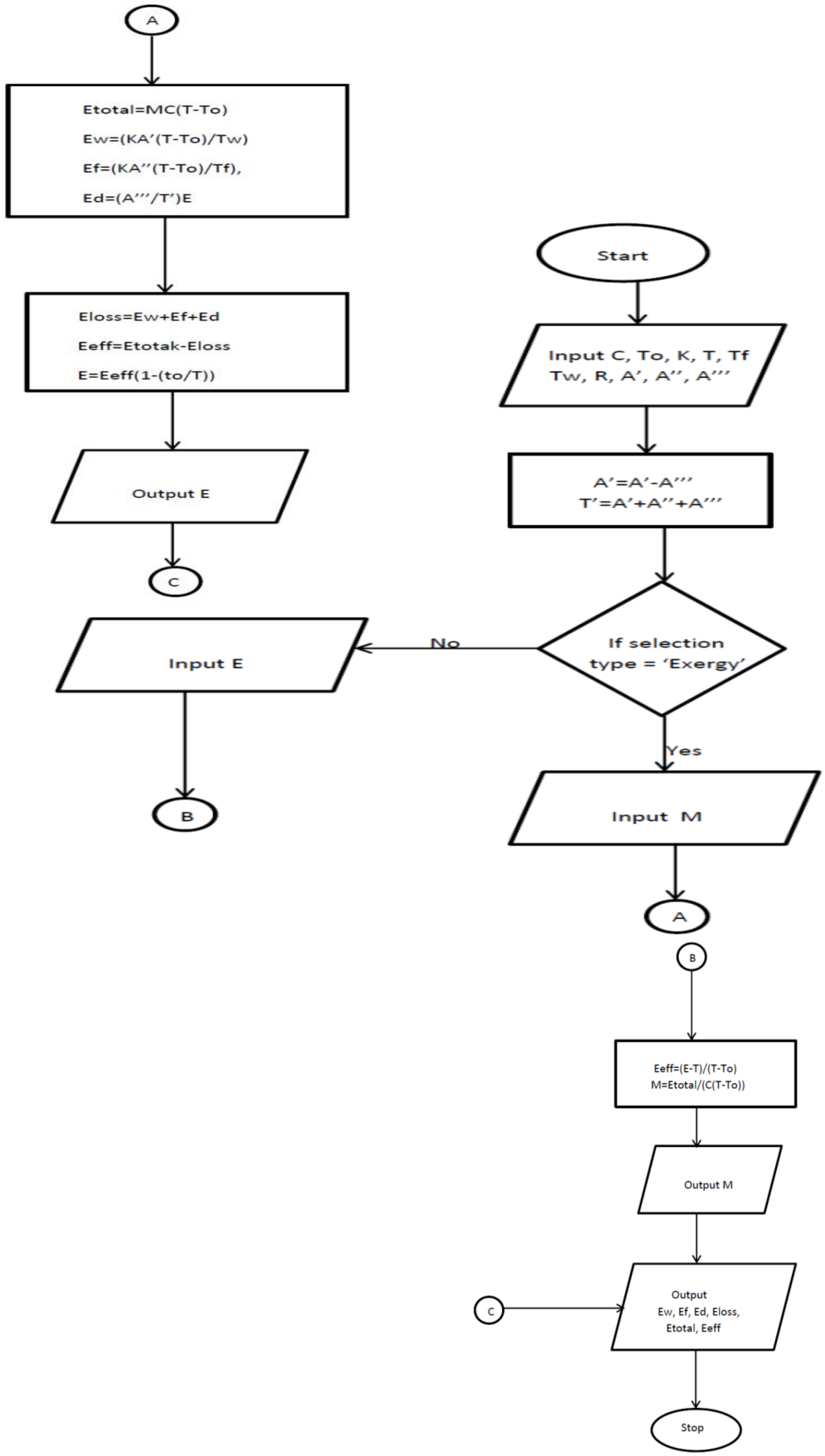

Figure 4. Flow chart of exergy estimation process

4. CONCLUSION

Based on the research carried out, it was concluded clay oven has high heat retention properties. Using the investigated clay ovens to bake dough produced from 300 kg wheat flour, peak energy, exergy and temperature respectively were 184.8MJ, 169.3MJ and 451^{o}C and were attained at 180 minutes heating duration using 258.4 kg of firewood as energy source. Energetic and exergetic efficiency of clay oven were 74.7% and 72% respectively. The developed computer software is a useful tool for estimating energy distribution pattern in clay oven. It saves time with high level of accuracy.

REFERENCES

Abubakar, M. S., Umar, B., and Ahmad, D. 2010. Energy use atterns in sugar production: a case study of savannah sugar company, Numan, Adamawa State, Nigeria. Journal of Applied Science Research 6: 377-382.

Akinbami, J. F. K., Ilori, M. O., Adeniyi, A. A. and Sanni, S A. 2001. Improving efficiency of energy use in Nigeria's industrial sector: a case study of a beverage plant. Nigeria Journal of Engineering Management 2:1-8.

Akinoso, R and Ganiyu, I. A. 2011. Estimation of energy requirements in small-scale bread making. LAUTECH Journal of Engineering and Technology 6: 81-85.

Akinoso, R and Kasali, W. O. 2012. Energy Expended in Processing *Gari*- Cassava (*Manihot esculenta* Crantz) Flakes - using three Levels of Mechanization. Pakistan Journal of Scientific and Industrial Research Series B Biological Sciences 55: 114 – 116.

Ezeike, G. O. I. 1981. Energy consumption in rice processing operation in Nigeria: selected case studies. Journal of Agricultural Mechanization in Asia, Africa, Latin America 18: 33-40.

Folaranmi, 2009. Effect of Additives on the Thermal Conductivity of Clay. Leonardo Journal of Sciences ISSN 1583-0233

Forno B. The History of Brick Ovens.

Ganapathy, T, Alagumurthi, 1, N, Gakkhar1, R. P and Murugesan, K. 2009. Exergy analysis of operating lignite fired thermal power plant. Department of Mechanical & Industrial Engineering, Indian Institute of Technology, Roorkee, India.

Jekayinfa, S. O., and Bamgboye, A. I. 2004. Energy requirements for palm kernel oil processing operations. Nutrition Food Science, 34:166-173.

Jekayinfa, S. O. and Olajide, J. O. 2007. Analysis of energy usage in the production of three selected cassava- based foods in Nigeria. Journal of Food Engineering 82: 322-329.

Kromer, K. and Mortel, H. 1988. Refinement and enrichment of clay and kaolin raw materials. Proceeding of the Final Contraction Meeting on Clay-based Materials for the Ceramic Industry. 39-40

Marc, A. R and Cornelia, A. B. 2009. Using Exergy to understand and improve the efficiency of electrical power technologies. Faculty of Engineering and Applied Science, University of Ontario Institute of Technology, Canada

Omowumi, O. J. 2001.Characterization of some Nigerian clays as refractory materials for furnace lining. Nigerian Journal of Engineering Management, 2: 9-13.

RMRDC 1990. Raw Material Research and Development Council, Research Report,

Wang, L. J. 2009. Energy efficiency and management in food processing facilities. CRC Press Taylor & Francis Group, LLC, Boca Raton, FL, USA.

Ziesemer, J. 2007. Energy use in organic food systems. Natural Resources Management and Environment Department, Food and Agricultural Organization of the United Nations, Rome.

DETERMINATION OF SOME MECHANICAL AND THERMAL PROPERTIES OF COCONUT (*COCOS NUCIFERA L.*) UNDER VARYING MOISTURE CONTENT

F. U. Asoiro and K. I. Onah
Department of Agricultural and Bioresources Engineering, University of Nigeria, Nsukka, Nigeria
Email: felixasoiro@yahoo.com

ABSTRACT

Some mechanical and thermal properties of coconut (cocos nucifera l.) were determined under varying moisture content ranges (37%, 49% and 55% db). It was discovered that at moisture content of 37%, 49% and 55% d.b mean thermal heat conductivity were 4089×10^{-3}W/m^{0}C, 32132×10^{-3} W/m^{0}C and 1.59×10^{-3} W/m^{o}C respectively. Thermal heat resistivity were 2445.5^{0}C-m/w, 3112.076 ^{0}C-m/w and 627 ^{0}C-m/w respectively. Thermal heat diffusivity for the different moisture content levels were 2.57×10^{-7}m^2/s, 2.508×10^{-7}m^2/s and 2.356×10^{-7}m^2/s respectively. Specific heat capacity were found to be 6.36 J/g^{0}C, 4.997 J/g^{0}C and 26.539 6 J/g^{0}C respectively. The bioyield strength, rupture strength and compressive strength at 37% db were 31175, 57254.2 and 61211.03N/m^2 respectively. At 49% db moisture content, bioyield strength, rupture strength and compressive strength were 24925.22, 46734 and 50598.22N/m^2 respectively while at 55% db, bioyield strength, rupture strength and compressive strength were 22066.59, 35834.63 and 34896.88N/m^2 respectively. It is obvious that thermal conductivities, thermal diffusivities and specific heats of coconut were found to increase with increase in moisture content. Also, as moisture content increased, mechanical strength decreased.

KEYWORDS: Coconut, specific heat capacity, thermal heat conductivity, bio-yield strength, rupture strength, compressive strength

1. INTRODUCTION

Coconut (cocos nucifera) is a native of South America and carried west ward across the Pacific in prehistoric times. Its original home must be sought in some sheltered valley of the Equatorial Andes. All the other members of the Cocoineae (except *Elaeis guinensis*) are American. However, it has been opined that despite the presence of botanically related genera on the plains, plateaus and highlands of continental south America, the home of the coconut is often said to be unknown. Its mode of dispersal is thought to have evolved on the coastal beaches of ant hills and islands of the Indian Ocean and western pacific.

Cocos nucifera trees have a smooth, columnar, light grey-brown trunk, with a mean diameter of 30-40 cm at breast height, and topped with a terminal crown of leaves. Tall selections may attain a height of 24-30 m. Dwarf selections also exist. The trunk is slender and slightly swollen at the base, usually erect but may be leaning or curved. The leaves are pinnate, feather shaped, 4-7m long and 1-1.5 m wide at the broadest part. The leaves stalk 1-2 cm in length and thorn less. The inflorescence consists of female and male axillaries flowers. Flowers are small, light yellow, in clusters that emerge from canoe-shaped sheaths among the leaves. The male flowers are small and more numerous. Female flowers are fewer and occasionally completely absent with larger, spherical structures, about 25 mm in diameter. Fruits (Figure 1) are roughly ovoid, up to 5 cm long and 3 cm wide, composed of a thick, fibrous husk surrounding a somewhat spherical nut with a hard, brittle, hairy shell. The nut is 2-2.5 cm in diameter and 3-4 cm long. Three sunken holes of softer tissue, called (eyes) are at one end of the nut. Inside the shell is a thin, white, fleshy layer (meat). The interior of the nut is hollow but partially filled with a watery liquid known as (coconut milk). The meat is soft and jellylike when immature but becomes firm with maturity. Coconut milk is abundant in unripe fruit but is gradually absorbed as ripening proceeds. The fruits are green at first; turning brownish as they mature while yellow varieties go from yellow to brown.

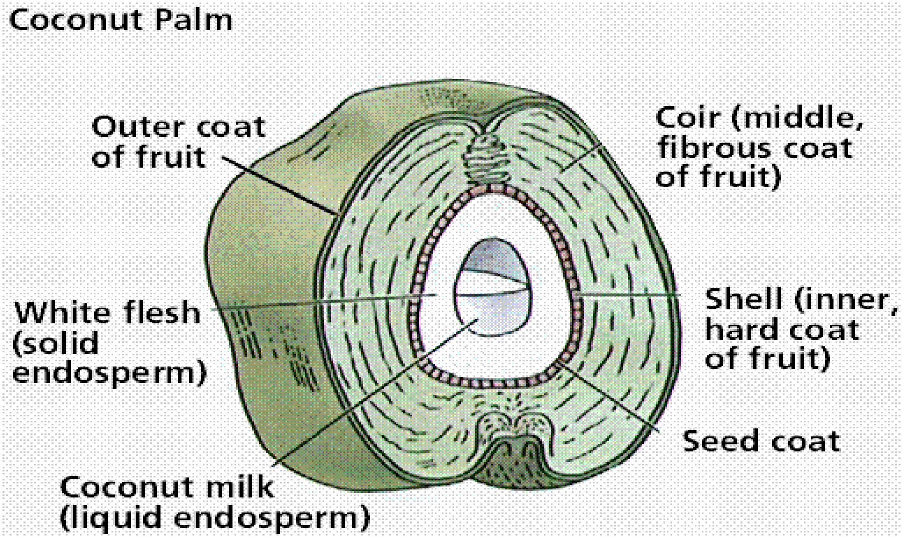

Figure 1. A longitudinal disection of coconut fruit

The composition of coconut varies with the varieties and maturity. The major constituents are coir, mesocarp, copra, and water with composition of 35%, 12%, 28% and 25% respectively. Percentage composition of the shell and husk are shown in Tables 1 and 2.

Table 1. Composition of coconut shell

Content	**Percentage (%)**
Water	8.0
Ash	0.6
Extractives	4.2
Lignin	29.4
Cellulose	26.6
Pentasans	27.7
Uronic anhydrides	3.5
Exthoxyl(zienel)	5.6
Nitrogen	0.11

Table 2. Percentage composition of coconut husk

	Fiber		
	Old Nut (%)	Young Nut (%)	Very Young Nut (%)
Water soluble substances	26	29	38. 50
Pectin, others soluble in boiling water	14. 25	14. 85	15. 25
Hemicelluloses	8.5	8.15	9. 00
Lignin	29. 33	31. 64	20. 13
	23. 87	19. 26	14. 39

Coconut has vast social, economic, cultural and medicinal values and it is widely consumed in the entire country and beyond. It is served as a highly priced special delicacy to entertain guests and visitors during burials, marriages, festival and ceremonies among the Igbos in some south eastern part of Nigeria. It has different names by the various countries and ethnic groups across the world. It is known as coconut in English. The Igbos in Nigeria refer to it as aki-oyibo/oba. It is known as klapperboom by the Dutch. In French it is known as coco, noix de coco, cocotier, cocoyer, coq au lait. The German refer to it as kokospalme, kokosnusspalme. In Indonesian it is known as kelapa. For the Italians it is called cocco while the Spanish know it as cocotero. Despite the huge economic and agricultural potential of this nut, very little information is available in literature on the mechanical properties of the fruit.

Coconut fruits can be processed into other food units. Part of the post harvest operation in the processing of coconut fruit involves cracking of the shell and subsequently heat treatment. In other to design, fabricate and develop systems, devices and controls for value addition, drying, transportation, conveying, storage, processing etc. knowledge of thermal and and mechanical properties of coconut at varying moisture content is required.

The moisture content of agricultural materials greatly affects various mechanical and thermal properties. Therefore, mechanical and thermal properties data at different moisture contents can be directly used to design/select planting, harvesting, processing, handling and storage equipment, like cleaners, graders, dryers, mills, conveyors, etc.(Kachru *et al*., 1994). Aviara *et al*. (1999) noted that the moisture dependent characteristics of thermal properties have effect on the adjustment and performance of agricultural product processing machines. They further noted that the optimum performance of machines could be achieved at a specific range of moisture contents. It has been reported that the knowledge of thermal properties and their dependence on the moisture content are useful for the design and development of methods and equipment (Oje, 1993; Visvanathan *et al*., 1996). Moisture content also has a great influence in threshing, separation, cleaning and grading operations.

Data on the thermal and mechanical properties of various nuts under varying moisture content are widely available, but relatively few data are available for coconut. Therefore, the present study was conducted to quantify the changes in mechanical and thermal properties of coconut as a result of changes in moisture contents levels (37 %, 49 % and 55 % dry basis).

2. MATERIALS AND METHODS

2.1 Sample Source

About 40 matured coconut heads were harvested from a coconut tree at Ogbodu-Aba in Udenu Local Government Area of Enugu State, Nigeria. Samples were weighed in a weighing balance, soaking in distilled water, kept in a polythene bag for five days for moisture to redistribute across the nuts, oven dried to required moisture content and conditioned in a refrigerator. Thereafter the thermal properties were analyzed at the National Centre for Energy Research and Development, University of Nigeria, Nsukka (NCERD) while the mechanical properties were determined at the Civil Engineering Laboratory of the same university.

2.2 Determination of Moisture Content of Coconut

The moisture content of the coconut seed were determined by AOAC method. An empty dish was dried in an oven at 105°C for 72 hours and transferred to a desiccator to cool and weighed. About 1 sample of the coconut was weighed in the dish and placed in the oven, dried for 72 hours at 105°C. After drying, the dish partially covered with lid and transferred to the desiccator to cool and reweighed. The loss in weight expressed as a percentage of the initial weight, was taken as the moisture content of the sample. The moisture content was calculated using equation 1.

$$MC_{wb} = \frac{(W_i - W_f)}{W_i} \times 100 \qquad (1)$$

Where, MC_{wb} is moisture content (%) wet basis; W_i is initial weight of sample (g) and W_f is final oven-dried weight of sample (g)

2.3 Mechanical Properties

Some mechanical properties of coconut such as, compressive strength, deformation at rupture and bio-yield strength were evaluated using 4 samples of the nut. Four samples of the nut were also tested for each of the diameter. This was done by means of a UK- made Universal Testing Machine.

2.3.1 Determination of Bio-yield Strength of Coconut

The bio-yield force is the force at which the sample begins to fail. This is the force at which the material yields. Further application of force beyond the bio-yield force ruptures the sample.

2.3.2 Determination of Compressive Strength of Coconut

Compressive strength was calculated as the rupture force divided by the deformation. Compressive strength, H (N/mm) is the ratio of rupture force and deformation at rupture point. It was calculated using equation 2

$$H = \frac{F_R}{R_{DR}} \quad (2)$$

2.3.3 Determination of Deformation at Rupture of Coconut

Deformation at rupture point, R_{DR} (mm) is the deformation at loading direction. It is measured in (mm).

2.4 Thermal Properties

2.4.1 Determination of Heat Capacity of Coconut

The method of mixtures has been the most common technique reported in the literature for measuring the heat capacity of agricultural and food materials due to its simplicity and accuracy. (Singh and Goswani 2000; Aviara and Haque 2001; NouriJangi et al. 2011; Deshpande et al. 1996.). This method was used for the determination of heat capacity of coconut at varied moisture levels. It involves the use of a lagged calorimeter, a digital thermometer to measure change in temperature with other heat determinant apparatus. The lagged calorimeter was calibrated using various temperatures ranging from 30^{o}C - 75^{o}C. The calibration of calorimeter is necessary to minimize experimental error. The calorimeter was calibrated by pouring a certain quantity of cold water into it. The temperature of the cold water was allowed to stabilize at a given temperature before a measured quantity of hot water was added to it. The equilibrium temperature of the mixture of hot and cold water was recorded. The respective quantities of hot and cold water were adjusted until a final temperature of the mixture that was close to the room temperature was obtained. The energy balance equation for the calibration of the calorimeter is given in equation 3 (Aviara and Haque 2001; Deshpande et al 1996; Razavi and Taghizadeh, 2007).

$$C_c = \frac{\left[M_{cw}C_w(T_h - T_e - M_{cw}C_w)\right]}{T_e - T_c} \quad (3)$$

Where, C_c is heat capacity of calorimeter (KJ/^{o}C); M_{cw} is mass of cold water (Kg); T_h is temperature of hot water (^{o}C); T_e is equilibrium temperature (^{o}C); C_w is specific heat of water (KJ/Kg^{o}C) and T_c is temperature of cold water (^{o}C)

The calibration was replicated five times and the quantities of hot and cold water adjusted to achieve final temperatures. The average value of the specific heat of calorimeter was noted.

The heat capacity of coconut was determined by dropping a sample of known weight, temperature (within a range of 25 – 30^{o}C) and a given moisture content into the calorimeter containing water with known weight and temperature. The mixture was stirred continuously using a copper stirrer. The temperature was recorded at an interval of 60s using aK-type thermocouple digital thermometer. At equilibrium, the final or equilibrium temperature was noted and the specific heat of the coconut was calculated using equation 3 (Aviara and Haque, 2001).

$$C_s = \left\{ \frac{(C_c + M_h C_w)[T_h - (T_e + tr^1)]}{M_s[(T_e + tr^1) - T_s]} \right\} \quad (4)$$

Where, C_s is specific heat of coconut (KJ/Kg^{o}C); C_c is heat capacity of calorimeter (KJ/^{o}C); M_h is mass of hot water (Kg); C_w is specific heat of water (KJ/Kg^{o}C); T_h is temperature of hot water (^{o}C); T_e is equilibrium temperature (^{o}C); M_s is mass of seed (Kg); T_s is temperature of coconut (^{o}C); tr^1 account for the heat of hydration and heat of exchange with the surroundings; and r^1 is the rate of temperature rise of the mixture after equilibrium was reached.

At each moisture level, the experiment was replicated four times and the average values of the specific heat reported.

2.4.2 Determination of Thermal Conductivity of Coconut

The thermal conductivity was determined employing the method described by Aviara and Haque, (2001) and Mohsenin, (1980) using a guarded hot-plate apparatus with steady-state heat flow method. Figure 2 shows the transfer of heat through surfaces with different temperature.

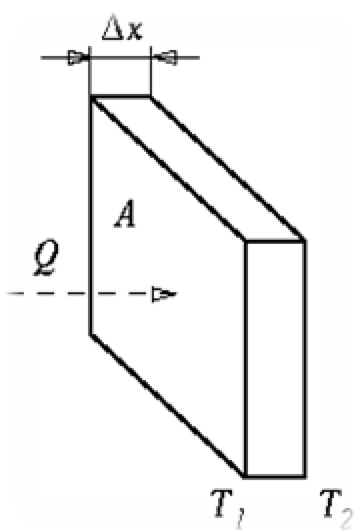

Figure 2. Heat transfer process through surfaces with different temperature
Source: Mohsenin, 1980.

The thermal conductivity method used for the work consisted of an upper (hot) plate and a lower (cold) plate, all made of mild steel. The upper plate was 90 mm in diameter and 30 mm thick. It was surrounded by a guard ring of 120 mm diameter and 13 mm thickness. The gap between them was filled with fiber glass at both the top of the plate and the sides to a thickness of 10 mm. The lower plate had a diameter of 90mm and a thickness of 9 mm. It was surrounded by a wooden guard ring of 125 mm diameter and 14 mm thickness, from which it will be separated by fiber glass to a thickness of 14 mm. The upper plate was heated electrically and this was controlled using a variable voltage regulator. Measurements of current and voltage were made using a multi-meter. The temperature of the plates was measured with 0.2-mm K-type thermocouples and digital thermometer at the heat source and heat sink respectively. The heat flux of the thermal conductivity apparatus was obtained using samples of known thermal conductivity, which was also used to calibrate the equipment. The thermal conductivity of coconut was computed from the temperature changes and heat flux obtained for known thermal conductivity using a sample at specified moisture content which was cut into a regular shape. The heat source was adjusted to maintain a temperature range of 61 – 64^{o}C. At the equilibrium condition or steady state condition, the temperature difference was recorded and used in calculating the thermal conductivity of the sample from equation 5.

$$K = \frac{Q(X_2 - X_1)}{A(T_2 - T_1)} \quad (5)$$

Where, K is thermal conductivity (W/m^{o}C); Q is rate of heat transfer (W/s); X_2 is longer distance (m); X_1 is shorter distance (m); A is area (m^2); T_1 is inside hotter temperature (^{o}C) and T_2 is outside cooler temperature (^{o}C).

The experiment was replicated four times for each of the moisture levels and the average calculated as the thermal conductivity.

2.4.3 Determination of Thermal Diffusivity of Coconut

Two methods could be used for the determination of thermal diffusivity of coconut. They are: The mathematical method and experimental method**.** Mathematical method involves direct calculation of thermal diffusivity using thermal conductivity, specific heat and density data. This is the simplest method and has been used by many researchers for thermal diffusivity estimation of peanut, kernel, shell. (Bitra et al., 2010). This method was used for the determination of thermal diffusivity of coconut as it gave a more robust result. This was computed using equation 6 as reported by Fadele, (2010).

$$\beta = \frac{K}{D_b C_s} \quad (6)$$

Where, β is thermal diffusivity (m^2/s); K is thermal heat conductivity (W/m^{o}C); D_b is bulk density (Kg/m^3) and C_s is specific heat (KJ/Kg^{o}C).

This was computed for the three moisture content levels.

2.4.4 Determination of Thermal Resistivity of Coconut

Thermal resistivity was computed using equation 7

$$R_T = S\left[\frac{Q}{4\pi}\right]^{-1} \quad (7)$$

$$Q = I^2 r \quad (8)$$

Where, Q is the heat input per unit length, I is current (Amp), r is the resistance of the nichrome wire per unit length (Ω/cm) and S indicates the slope of the straight line portion of the temperature θ versus log (time) plot

3. RESULTS AND DISCUSSION

3.1 Mechanical Properties

Some mechanical properties of coconut under varying moisture content is presented in Table 3.

Table 3. Some mechanical properties of coconut (cocos nucifera) with varying moisture content

Property	Moisture Content (%) d.b		
	37%	**49%**	**55%**
Bio-yield force (N)	1300	1000	877.5
Bio-yield strength (N/m^2)	31175	24925.22	22066.56
Rupture force (N)	2387.5	1875	1425
Rupture strength (N/m^2)	57254.2	46734	35834.63
Compressive force (N)	2552.5	2030	1387.5
Compressive strength (N/m^2)	61211.03	50598.2	34896.88
Diameter (m)	115.25	0.113	0.11
Length (m)	27.75	0.0027	0.0027

The bio-yield force was highest at 37%db of moisture content with a value of 1300N and lowest at 55% with a value of 877.5N. It has a value of 1000N at 49% db of moisture content. The rupture strength of coconut is 57254.2N/m^2, 46734N/m^2 and 35834.63 N/m^2 at moisture content levels of 37, 49 and 55%db respectively. The compressive strength of coconut is highest at 37%db (61211.03N/m^2) and lowest at 55%db (34896.88N/m^2). From Table 3, it is clear that mechanical property values of coconut decreased with increase in moisture content.

3.2 Thermal Properties

Some thermal property values of coconut (*cocos nucifera*) is shown in Table 4.

Table 4. Some thermal properties of coconut (*cocos nucifera*) with varying moisture content

Property	Moisture Content (%) d.b		
	37%	**49%**	**55%**
Thermal conductivity (W/m^{o}C)	4.089×10^{-3}	3.2132×10^{-3}	1.59
Thermal resistivity (^{o}C-m/W)	2445.5	3112.076	627.2
Thermal diffusivity (m^2/s)	2.57×10^{-7}	2.508×10^{-7}	2.356×10^{-7}
Thermal heat capacity (J/g^{o}C)	6.36	4.997	26.537

The thermal conductivity values of coconut increased with increase in moisture content. The thermal diffusivity decreased with increase in moisture content from 37% to 55% db. The thermal conductivity of coconut was 4.089×10^{-3}W/m^{o}C at 37%, 3.2132×10^{-3}W/m^{o}C at 49% and 1.59×10^{-3}W/m^{o}C at 55% db of moisture content. The thermal diffusivity of coconut at 37%, 49% and 55% db were 2.57×10^{-7} m^2/s, 2.508×10^{-7} m^2/s and 2.356×10^{-7} m^2/s respectively. The thermal resistivity of coconut was 2445.5^{o}C-m/W at 37% db, 3112.076 ^{o}C-m/W at 49% db and 627.2 ^{o}C-m/W at 55% db. The thermal heat capacity values decreased from 6.36 J/g^{o}C to 4.997 J/g^{o}C as moisture content increased from 37% to 49% db. It then increased from 4.997 to 26.537 J/g^{o}C as moisture content rose from 49% to 55%db.

4. CONCLUSIONS AND RECOMMENDATIONS

Moisture content greatly affects the thermal properties of coconut fruit. The thermal conductivity decreased as moisture content rose from 37% db to 49% db and later increased as moisture content rose again to 55% db. Similar trend was observed with values for thermal heat capacity. However, thermal resistivity showed a reversed trend. As moisture content increased from 37% to 49%, thermal resistivity values increased from 2445.5 ^{o}C-m/W to 3112.08 ^{o}C-m/W and later decreased to the value of 627.2 ^{o}C-m/W Thermal diffusivity decreased as moisture content increased from 37 to 55%db. As moisture content increased, mechanical strength decreased

It is recommended that other mechanical properties should be tested for any further future work. Mechanical and thermal properties of more than one variety of coconut, under varying moisture content should be investigated and results compared. This work was restricted to only 37 to 55% levels of moisture. More levels of moisture content should be investigated and its behavior ascertained.

REFERENCES

Aviara, N. A., and M. A. Haque. 2001. Moisture dependence of thermal properties of shea nut kernel. *J. Food Eng.* 47(2): 109-113.

Aviara, N.A ., M. I Gwandzang and M. A. Haque. 1999. Physical properties of guna seeds. *Journal of Agricultural Engineering Research,* 73, 105-111.

Bitra, V. S. P., S. Banu, P. Ramakrishna, G. Narender, and A. R. Womak. 2010. Moisture-dependent thermal properties of peanut pods, kernels, and shells. *Biosystems Eng.* 106(4): 503-512.

Desphande, S. D., S. Bal, and T. P. Ojha. 1996. Bulk thermal conductivity and diffusivity of soybean. *J. Food Proc. and Preserv*. 20(3): 177-189.

Fadele, O.K. 2010. Determination of Some Engineering Properties of Doum Palm Fruit (*Hyphaenethebaica*).Unpublished MSc. Thesis. University of Ibadan.

Kachru, R. P., R. K Gupta, and A. Alam. 1994. *Physico–Chemical Constituents and Engineering Properties of Food Crops*. Jodhpur, India: Scientific Publishers.

Mohsenin N.N., 1980**.** Thermal Properties of Food and Agricultural Materials. Gordon and Breach Press, New York, USA.

NouriJangi A, Mortazavi1 SA, Tavakoli M, Ghanbari H, Tavakolipour A, Haghayegh GH. 2011. Comparison of mechanical and thermal properties between two varieties of barley (*Hordeumvulgare* L.) grains. Aust. J. Agric. Eng. 2(5):132-139.

Oje, K. 1993. Locust bean pods and seeds. Some Physical Properties relevance to dehulling and seed processing. *Journal of Food Science and Technology*. 30(4): 233-255.

Razavi, SMA and Taghizadeh, M. 2007. The specific heat of pistachio nuts as affected by moisture content, temperature, and variety. J Food Eng. 79:158–167.

Singh S.S and Goswani T.K. 2000. Thermal properties of cumin seed. J Food Eng.45: 181-187.

Visvanathan, R., P. T. Palanisamy., L. Gothandapani and V .V. Sreenarayanan. 1996. Physical properties of neem nut. *Journal of Agricultural Engineering Research*, 63, 19-36.

EFFECT OF MOISTURE CONTENT ON AERODYNAMIC PROPERTIES OF CORN SEED (ZEA MAYS)

F. U. Asoiro and J. C. Chidebelu
Department of Agricultural and Bioresources Engineering, University of Nigeria, Nsukka, Nigeria
Email: felixasoiro@yahoo.com

ABSTRACT

Knowledge of the aerodynamic properties of agricultural materials is needed in equipment design for operations such as cleaning, separation and pneumatic conveying in loading/unloading operations of corn seeds into/from silos. While considerable information is available on seed grains, little is known about the aerodynamic behavior of corn seed (*Zea mays* L.). In this research, aerodynamic properties of corn seed at different moisture level were determined. It was observed that moisture content has great effect on seeds aerodynamic properties. The results showed that the terminal velocity of the corn seeds increased linearly from 10.65 to 12.15m/s as the moisture rose from 4 to 40% (d.b) at four levels of moisture content. The results also showed initial decrease in drag coefficient from 0.61 to 0.52 at 4 and 12% moisture content respectively, and thereafter increases from 0.53 to 0.63 at 16 to 40% moisture content respectively, due to the variation in the shape of the seeds as observed on the process. The experiment showed that seed drag coefficient is independent of seed weight, but depends mainly on the shapes of the seed. It was also observed that the seed drag force increased linearly from 1.57 to 2.85 N as the moisture increased from 4 to 40% (d.b). Linear regression model equations for aerodynamic properties and moisture content of seeds were determined from the graph of moisture against aerodynamic properties using excel. The analysis of variance (ANOVA) performed showed a great significant difference in aerodynamic properties at different level of moisture content of the seeds.

KEYWORDS: Maize, Corn, Moisture content, Aerodynamic properties, Terminal velocity, Drag force, Drag coefficient

1. INTRODUCTION

The word *corn* has many different meanings depending on what country you are in. Corn in the United States is also called maize or Indian corn. In some countries, corn means the leading crop grown in a certain district. Corn in England means wheat; in Scotland and Ireland, it refers to oats. Corn mentioned in the Bible probably refers to wheat or barley. It has been established that Mesoamerican region, now Mexico and Central America is the center of origin for Zea mays (Ozkan et al. 2005). According to Bar Yosef (1998), the domestication of maize began at least 6000 years ago, occurring independently in regions of the south-western United States, Mexico, and Central America. The Portuguese introduced maize to Southeast-Asia from the America in the 16th century. The maize was introduced into Spain after the return of Columbus from America and from Spain it went to France, Italy and Turkey. In India, Portuguese introduced maize during the seventeenth century. From India it went to China and later it was introduced in Philippines and the East Indies. Corn is now a major staple food grown in virtually every parts of the world including USA, China, Brazil, Argentina, Mexico, South Africa, Rumania, Yugoslavia, India and West Africa as well as Nigeria (Borojevic and Borojevic, 2005).

Corn has huge economic, nutritional and medicinal importance. Several millions of households, communities and industries rely on corn for their daily diet, survival and raw materials. Maize could be processed into bread, noodles, poultry feeds and other value added products as well as feedstock for biodiesel production. Corn is a storehouse of nutrients essential for human diet. Corn provides nearly 55% of carbohydrate and 20% of the food calories. It contains carbohydrate 78.10%, protein 14.70%, fat 2.10%, minerals 2.10%, indigestible cellulose material called dietary flour and considerable proportions of vitamins (thiamine and vitamin-B) and minerals (zinc, iron). Corn is also a good source of traces minerals like selenium and magnesium, nutrients essential to good health. By nature, con has several medicinal virtues. Starch and gluten in corn provide heat and energy. The outer bran provides the much-needed roughage which cures widespread prevalence of constipation and other digestive disturbances and nutritional disorders, indigestion and aids easy movement of the bowel. Corn can also help to build and repair muscular tissues and can be used for cure of some heart diseases. It has proven effective in handling diseases such as coeliac disease, schizophrenia, gluten ataxia, migraines, acute psychoses, and a range of neurological illnesses. corn also provide protection against ischaemic, disease of the colon, called diverticulum, appendicitis, obesity, diabetes as well as autoimmune diseases such as rheumatoid arthritis which may be more prevalent in coeliac patients and relatives.

Knowledge of aerodynamic properties of grain such as terminal velocity, drag force and drag coefficient are important design criteria for modern harvesters, grain cleaners, pneumatic conveyors and other equipment. It also helps in agro based industries where proper separation of grains from their foreign materials with less or no grain loss is vital. Such design criteria are be based on the aerodynamic characteristics of the grain (Mohsenin, 1970). Nigeria imports large quantity of high quality/ high grade grains annually to meet the growing demand both for consumption and industrial purposes, despite the fact that it is a major producer of maize. The reason for the massive importation as observed is likely due the inferior quality of the locally produced maize occasioned by improper cleaning and poor post harvest operation. In addition, there is lack of local machines for cleaning and separation of contaminants from the products. Importation of these machines is not a viable option as they quit expensive and often times in adaptable to the local maize varieties. The possibility of aerodynamically separating seed from chaff was studied by Uhl and Lamp (1966). Hawk et al (1966) determined the aerodynamic properties of several different kinds of grain in a horizontal wind tunnel. The terminal velocity of alfalfa seed as a function of size has also been reported. Aerodynamic properties has also been used in separating the whole kernel of beans from the broken ones.

The moisture content of agricultural materials greatly affects aerodynamic properties of grains. Despite the huge medicinal, economic importance and the high consumption rate of corn seed and its potential as a good source of foreign earnings for Nigeria if properly winnowed, the traditional method of post harvest processing, provides a poor-quality product. This limits it utilization both locally and internationally. In Nigeria, there is scarcely any large-scale cleaning, winnowing and processing machine. Many small-scale producers carry out these operations manually. Many researchers have worked on the effect of moisture content on aerodynamic properties of various grains, very little information is available for corn seeds.

The broad objective of this work is to determine the effect of moisture content on the aerodynamic properties of corn seed. The specific objectives are to determine the aerodynamic properties of corn seed, to determine the moisture content of corn seeds at various levels and to analyze the results using statistical tools such as SPSS and excel packages.

2. MATERIALS AND METHODS

2.1 Sample Collection and Preparation

The corn seeds samples (Figure 1) used were selected from Corn, Zea Mays L. varieties hybrid single cross (SC 10) planted in the Department of Agricultural Extension Farm, University of Nigeria, Nsukka. The seeds were cleaned manually to remove all foreign materials and immature seeds.

Figure 1. Samples of corn seeds

The initial moisture content of the samples was measured as 9.8% (d.b.). The density of the corn seed samples was also determined by the fluid (Toluene) displacement method (Mohsenin, 1970) as 1267.02 kg/m^3 with three replications. The volume of the seed was calculated from its mass and density. The dimensions (Figure 2) were measured and were used in computing the projected area of the corn seed samples.

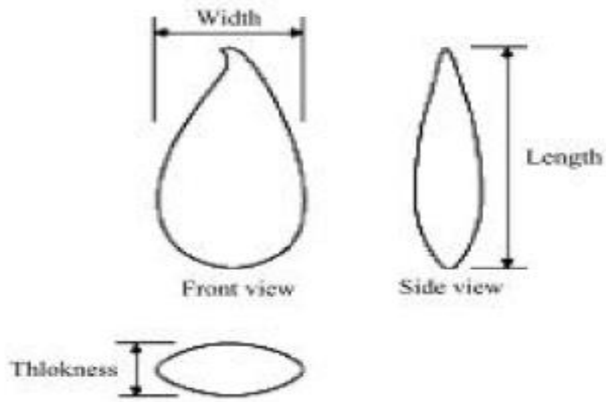

Figure 2. Dimensions of corn seeds

2.2 Determination of Moisture Content of Corn Seeds

The initial moisture contents of the seeds were determined using ASAE 1998 standard. The 500g of the sample was divided into 5 parts. The desired moisture contents were obtained by adding distilled water calculated using equation (1). The samples were quickly transferred to separate high density polyethylene bags and sealed tightly and labeled. The samples were kept at 5^{o}C in a refrigerator for a week to enable the moisture to be distributed uniformly throughout each sample. This rewetting technique to attain the desired moisture content in seeds and grains has frequently been used (Coskun *et al*., 2005; Garnayak *et al*., 2008; Sacilink *et al*., 2002). Before use, the samples were kept in a dessicator (Glaswerk Wertheim, Model 471, Size 1172, Germany) Every weighing and recording was done using electronic balance (Yamato, model HB 3000, Japan) reading to 0.01g.

$$Q = \frac{A(b-a)}{(100-b)} \qquad (1)$$

Where, A is initial mass of the sample (g); a is the initial moisture content of the sample (% dry basis); b is the final (desired) moisture content of sample (% dry basis) and Q is the mass of distilled water to be added (g).

2.3 Determination of Aerodynamic Properties of Corn Seeds

2.3.1 Determination of Terminal Velocity of the Corn Seeds

The terminal velocity of corn seed was determined by the slight modification of that developed by Adejumo et al. (2009) and Babatunde and Olowinbi (2000). The terminal velocity was determined using cylindrical air column with fluid (Glycerol) in a glass measuring cylinder as shown in Figure 3.

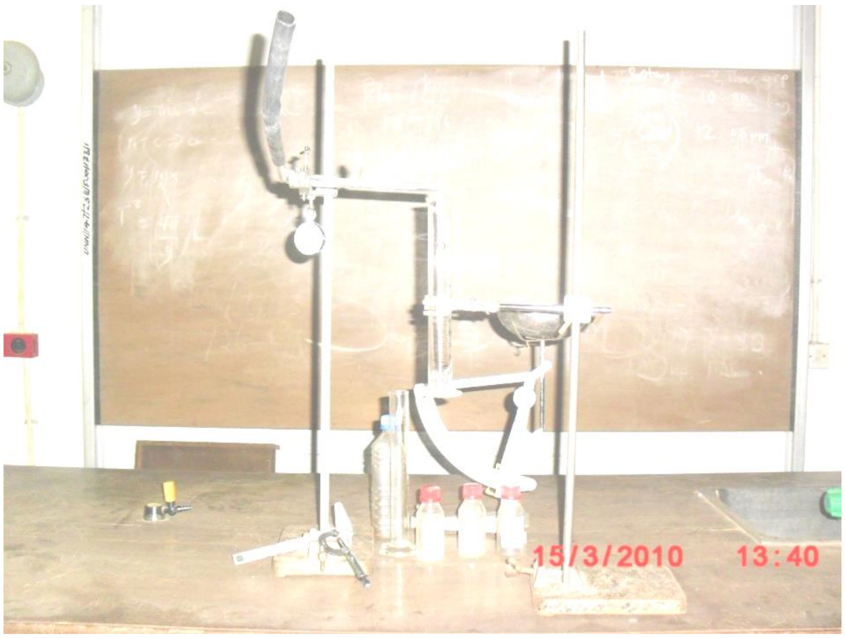

Figure 3. Set up for the measurement of terminal velocity

The terminal velocity of the seeds at different moisture content (4-40%) was determined by placing the seeds in the outlet of the cylindrical air column and forced air into the cylindrical air column through air tube connected to the cylindrical air column which then dropped the seed into a glass measuring cylinder filled with glycerol oil. As the seeds was accelerating in the fluid, it was observed at a certain point that the seeds initial velocity ceased and at that point the seed assumed uniform velocity. The initial high velocity of the seed in the viscous fluid was opposed by viscous fluid force of the fluid which equals the viscous drag force and downward force of the seed. On the other hand, as the seed accelerate, the speed increases and so does the viscous force of the fluid until a point is reached were the viscous drag force equals to the downward force. At this stage, the terminal velocity is reached and time is taken for the displacement (i.e. from the initial high velocity to where the velocity ceased and move with uniform velocity) of the fluid. The measured time and displacement is used to calculate the terminal velocity of the seeds at different moisture content using equation (2)

$$V_t = \frac{Displacement(m)}{Time(\sec)} \qquad (2)$$

2.3.2 Determination of the Drag Force of the Corn Seeds

The drag force is a resistive force, opposing the motion of the corn. The most familiar form of drag force is made up of friction forces, which act parallel to the object's surface, plus pressure forces, which act in a direction perpendicular to the object's surface. For a solid object moving through a fluid, the drag is the component of the net aerodynamic or hydrodynamic force acting in the direction of the movement. The component perpendicular to this direction is considered lift. Therefore drag acts to oppose the motion of the object. The drag force can be computed using equation (3)

$$F_d = \frac{C_d \ell_a A_p V_t^2}{2} = C_r V_t^2 \quad (3)$$

The projected area of the corn seed can be calculated using equation (4)

$$A_p = \frac{\pi L W}{4} \quad (4)$$

Where, F_d is the drag force (N); C_d is drag coefficient (dimensionless); ℓ_a is air density (1.25, kg/m^3); A_p particle area projected to air (m^2); V_t is terminal velocity (m/s); C_r is resistance coefficient (kg/m); L is length of the corn seed and W is width of the corn seed.

2.3.3 Determination of the Drag Coefficient of the Corn Seeds

Among aerodynamic properties, the drag coefficient (commonly denoted is a dimensionless quantity that is used to quantify the drag or resistance of an object in a fluid environment such as air or water. It is used in the drag equation, where a lower drag coefficient indicates the object will have less aerodynamic or hydrodynamic drag. The drag coefficient is always associated with a particular surface area. It is computed with equation (5)

$$C_d = \frac{2F_d}{V_t^2 \ell_a A_p} \quad (5)$$

Where, all the parameters and units are as defined earlier.

2.4 Statistical Analyses

Data was analyzed statistically using SPSS and simple Excel packages. Analysis of Variance (ANOVA) was performed to determine the significance of the treatment and interaction effects. When analysis of variance was significant at the *5%* probability level, treatments were separated by Duncan's New Multiple Range Tests at the 5% level of probability. Simple Excel was used to plot the graph of Moisture Content (%db) of the corn seeds at various level against the aerodynamic properties of seeds to obtain graphical and linear representation of moisture effect on aerodynamic properties of the seeds.

3. RESULTS AND DISCUSSIONS

Table 1 presents the mean values of the terminal velocity, drag coefficient and drag force of corn seeds at various moisture content (% db).

Table 1. Mean values of aerodynamic properties of corn seeds

Moisture Content (%) d.b	Mean Terminal Velocity(m/s)	Mean Drag Coefficient (C_d)	Mean Drag Force (N)
4	10.65	0.61	1.57
8	10.77	0.55	1.68
12	11.14	0.52	1.77
16	11.36	0.53	1.88
20	11.46	0.57	1.98
24	11.65	0.54	2.08
28	11.69	0.57	2.25
32	11.77	0.58	2.45
36	12.04	0.64	2.71
40	12.15	0.63	2.85

3.1 Aerodynamic Properties of Corn Seeds

3.1.1 Terminal Velocity

It was observed that moisture content significantly affected terminal velocity. By increasing moisture content from 4 to 40%, the terminal velocity increased linearly from 10.65 to 12.15m/s. This result was the same as found by other researchers for some other agricultural materials (Tabak and Wolf, 1998; Gupta and Das, 1997; Suthar and Das, 1996 and Carman, 1996). Figure 4 shows the effect of corn moisture content on terminal velocity. The reason for the increase in terminal velocity with moisture content could be because of the increase in the mass of an individual seed per unit frontal area presented to the airflow. The relationship between moisture content and terminal velocity produced a linear equation with a very high coefficient of determination, R^2 of 0.966.

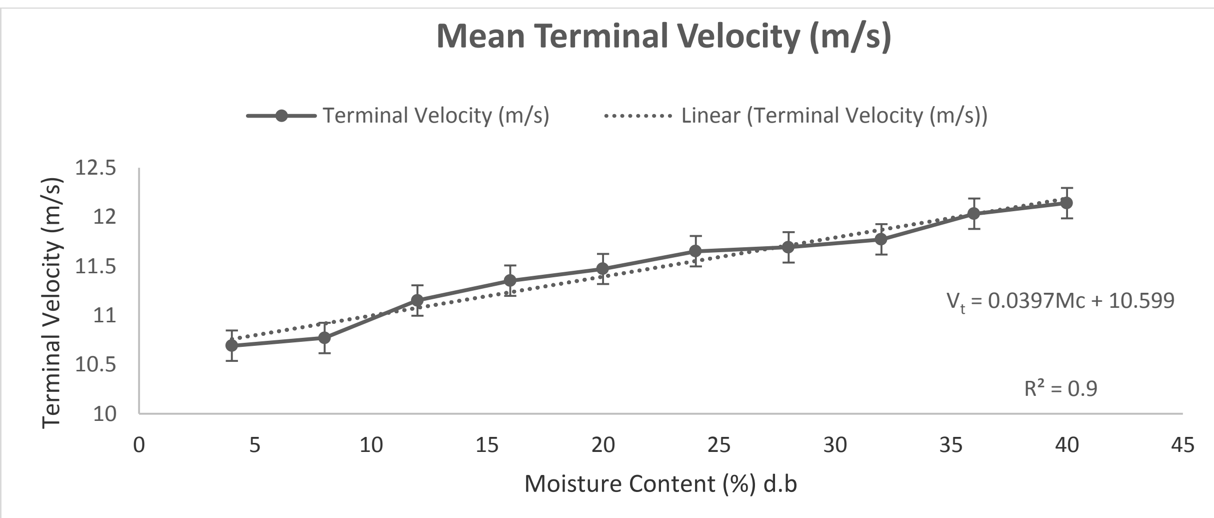

Figure 4. Terminal velocity (m/s) as affected by moisture content (%db)

3.1.2 Drag Force

Drag force is the force acting opposite to the relative motion of the seed moving with respect to a surrounding fluid. Drag force increased linearly from 1.57 to 2.85N as moisture content vary from 4 to 40%db at an intervals of 4. From Table 5, it is clear that moisture has great effect on seeds drag force. Increase in the acceleration of seeds in the fluid leads to increase in the drag force of the fluid. And this increase in acceleration of seeds in the fluid is caused by increase in the moisture content of the seeds. The relationship is a linear curve with a very high coefficient of determination, R^2 (0.9743).

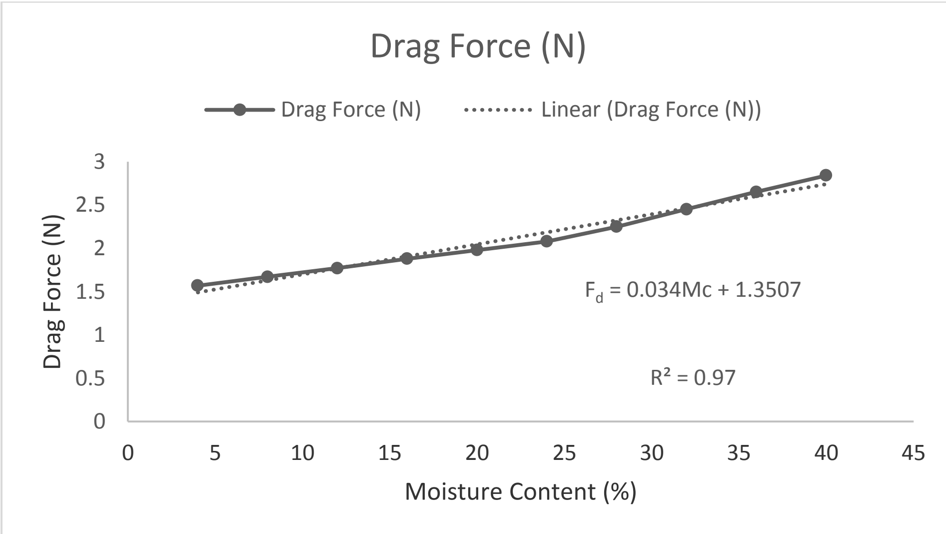

Figure 5. Effect of moisture content on drag force

3.1.3 Drag Coefficient

Drag coefficient for the seeds initially decreased from 0.61 to 0.52 as the moisture increases from 4 to 12% (Figure 6), and thereafter rose from 0.53 to 0.57 as the moisture increased from 16 to 20% (d.b). Drag coefficient value increased from 0.57 to 0.64 between moisture content of 28 and 36. It was 0.63 at 40 %db. This increase and decrease of drag coefficient of the grain at different moisture level is mainly due to the changes in the shape of the seeds, it was also observed that seed drag coefficient is independent of seed mass. Drag coefficient against moisture content also gave a linear curve.

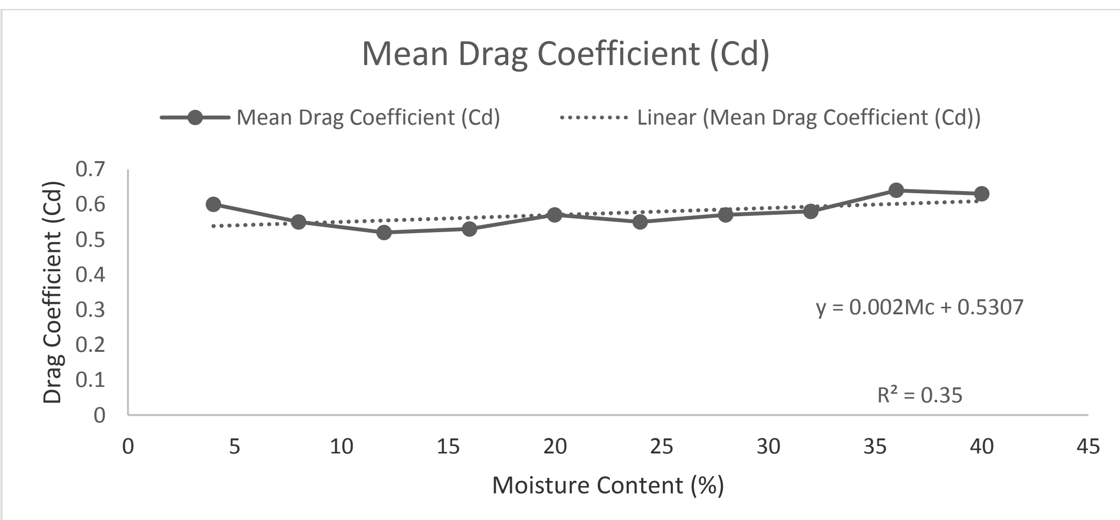

Figure 6. Drag coefficient as affected by moisture content (%db)

3.2 Statistical Analysis Results

The analysis of variance (ANOVA) performed showed a great significant difference (at 5% probability levels) in the terminal velocity, drag force and drag coefficient at different level of moisture content of the seeds. All these are shown in Tables 2 – 4.

Table 2. Difference among means of terminal velocity of the corn seed at ten moisture levels

Terminal Velocity (m/s)

Duncan

Moisture content (d.b)	N	Subset for alpha = 0.05				
		1	2	3	4	5
4.0	3	10.6500				
8.0	3	10.7667				
12.0	3		11.1400			
16.0	3			11.3633		
20.0	3			11.4633		
24.0	3				11.6500	
28.0	3				11.6933	
32.0	3				11.7700	
36.0	3					12.0467
40.0	3					12.1467
Sig.		.060	1.000	.103	.065	.103

Means for groups in homogeneous subsets are displayed.
a. Uses Harmonic Mean Sample Size = 3.000.

Table 3. Difference among the means of drag force of the corn seeds at ten moisture levels

Drag Force (N)

Duncan

Moisture content db	N	Subset for alpha = 0.05									
		1	2	3	4	5	6	7	8	9	10
4.0	3	1.5733									
8.0	3		1.6800								
12.0	3			1.7733							
16.0	3				1.8767						
20.0	3					1.9800					
24.0	3						2.0800				
28.0	3							2.2533			
32.0	3								2.4533		
36.0	3									2.7167	
40.0	3										2.8500
Sig.		1.000	1.000	1.000	1.000	1.000	1.000	1.000	1.000	1.000	1.000

Means for groups in homogeneous subsets are displayed.
a. Uses Harmonic Mean Sample Size = 3.000.

Table 4. Difference among the means of drag coefficient of corn seed at ten moisture levels

Drag Coefficient Cd

Duncan

Moisture contentdb	N	Subset for alpha = 0.05				
		1	2	3	4	5
12.0	3	.5200				
16.0	3	.5200				
24.0	3	.5433	.5433			
8.0	3		.5500			
28.0	3		.5667	.5667		
20.0	3		.5667	.5667		
32.0	3			.5800		
4.0	3				.6100	
40.0	3				.6333	.6333

36.0	3					.6467
Sig.		.099	.109	.338	.084	.311

Means for groups in homogeneous subsets are displayed.
a. Uses Harmonic Mean Sample Size = 3.000.

4. CONCLUSIONS AND RECOMMENDATIONS

A preliminary study to characterize the aerodynamic properties of corn seed at varying moisture content was investigated. Terminal velocity and drag force increased with increase in moisture content. It was also observed that drag coefficient decreased to some point and increased there after as the seeds moisture content increased. The terminal velocity, drag force and drag coefficient all gave linear curve with moisture content.

It has been observed that the reason why most Nigerians prefer imported grains such as maize to the locally produced ones is due to improper cleaning and separation of impurities from the grains. And this problem can only be solved by applying the knowledge of aerodynamic properties of grains at varying moisture content in cleaning, winnowing, separating operations in our local agro-base industries.

REFERENCE

Adejumo, A.O. , Ajav, E.A. and Igbeka, J.C. 2009. Effect of moisture content on some frictional and aerodynamic properties of Okra (Abelmosus Esculentus l. moench varieties. Proceedings of the 3rd West Africa Society of Agricultural Engineering and the 9th Nigerian Institution of Agricultural Engineers (A division of the Nigerian Society of Engineers). Held at the Obafemi Awolowo University, Ile Ife. Pp. 249-255.

ASAE 1998. Moisture Measurement – Unground seeds S352.2. American Society of Agricultural Engineers, 2950 Niles Road, St. Joseph MI 49085-9659, Michigan, USA.

Babatunde, O.O and Olowinbi, M.M. 2000. Experimental study of cleaning drying crop products using forced air stream in a vertical tunnel. Proceedings of the Nigerian Institution of Agricultural Engineers (A division of the Nigerian Society of Engineers), 22:103-107.

Bar-Yosef, O. 1998. The Natufian Culture in the Levant, Threshold to the Origins of Agriculture. *Evolutionary Anthropology* 6(5):159-77.

Borojevic, K. and K. Borojevic. 2005. The Transfer and History of "Reduced Height Genes" (Rht) in Wheat from Japan to Europe. *Journal of Heredity* 96(4):455-9.

Carman, K. 1996. Some physical properties of lentil seeds. Journal of Agricultural Engineering Research 63:87-92.

Coskun, M. B., I. Yalcin and C. Ozarslan. 2005. Physical properties of sweet corn seed (Zea Mays Saccharata Strut). Journal of Food Engineering 74:523-528.

Garnayak, D.K., R.C. Pradhan, S.N. Naik and N. Bhatnagar. 2008. Moisture-dependent physical properties of Jatropha seed (Jatropha Carcas L.). Industries Crop and Products 27:123-129.

Gupta, R.K. and S.K. Das. 1997. Physical properties of sunflower seeds. Journal of Agricultural Engineering Research 66:1-8.

Hawk, A. L., D. B. Brook, and J. J. Cassidy. 1966. Aerodynamic characteristics of selected farm grains. Trans. ASAE 9:48- 51.

Mohsenin, N.N. 1970. The Properties of Plant and Animal Materials. New York: Gordon and Breach.

Ozkan, H., A. Brandolini, C. Pozzi, S. Effgen, J. Wunder and F. Salamini. 2005. A reconsideration of the domestication geography of tetraploidwheats. *Theoretical and Applied Genetics* 110:1052-60.

Saclink, K., R. Ozturk and R. kesikin 2002. Some physical properties of hemp seeds. Biosystem Engineering. (86)2:191-198.

Suthar, S.H. and S.K. Das. 1996. Some physical properties of karingda seeds. Journal of Agricultural Engineering Research. 65:15-22.

Tabak, S. and D. Wolf. 1998. Aerodynamic properties of cotton seeds. Journal of Agricultural Engineering Research 70:257-265.

Uhl, J. B. and B. J. Lamp. 1966. Pneumatic separation of grain and straw mixtures. Transactions of the ASAE 9(2): 244-246.

DEVELOPMENT OF MATLAB ALGORITHM FOR THE CASAGRANDE MODEL FOR ANALYSIS OF PRE-CONSOLIDATION AND PRE-COMPRESSION STRESS IN SOILS

F. O. Temitope and A. A. Ebenezer
Department of Agricultural and Environmental Engineering,
Federal University of Technology, Akure Ondo State, Nigeria.
Email: ayo.ajayi@gmail.com

ABSTRACT

Pre-consolidation/Pre-compression stress is a soil mechanical stability criterion, which is often used to determine the maximum external loads an undisturbed soil and structures can withstand without irreversible deformation. The most acceptable and widely use method of estimating pre-consolidation stress in the soil is the method developed by casagrande in 1936. In this method, determining pre-consolidation stress require accurate location of the point of maximum curvature on the soil compression curve which involves a lot of subjective perception or interpretation. In order to prevent such subjective interpretation in the determination of the point of maximum curvature, Mathematical model for determining the pre-consolidation stress was developed. The algorithm was implemented in MATLAB, thereby creating room to proper visualization of the graphical interface. The model was validated with data from Nigeria and Brazil. The results were compared with those generated with the previous EXCEL representation of the model by Dias Junior. The result showed a strong correlation with coefficient of determination $r^2 = 1$. The study contributes to a non-subjective way of estimating soil pre-consolidation/pre-compression stress from uni-axial experiment data, thereby assisting in prevention of soil compaction and consequent degradation.

KEYWORDS: Soil compaction, pre-consolidation stress, pre-compression stress, casagrande model, MATLAB

1. INTRODUCTION

The term ‘soil’ is used variedly depending on circumstances or profession. In soil science, soils are viewed as medium for plant growth, so the focus is on the organic rich part of the soil horizon (usually the topsoil), while the sediments below the weathered zone is referred to as the parent material. Moreover, soil scientists classify soils based on their physical, chemical, and biological properties which can be observed and measured. On the other hand, engineers use the soil as foundation to support structures and embankments and therefore define soil as any material that can be excavated with a shovel (no heavy equipment). They classify it based on the particle size, distribution, and the plasticity of the material. These classification criteria relate more to the behaviour of soils under the application of load, and this necessitate the need to determine the strength of the soil mass arising from its being subjected to varying degree of load.

In mechanised agriculture, the soil as a medium of cultivation is constantly subjected to loading in preparation for cultivation, during phyto-sanitary management and at harvest of cultivated crops. Thus the strength of the soil must be understood to ensure sustainable use.The strength of a soil determines its ability to support load; the factor which is strongly influenced by the amount of moisture present in the soil. Therefore, the intensive use of the soil without moisture control could lead to structural degradation in the soil (Pedrotti and Dias Junior, 1996). For example, soil compaction result when traffic of agricultural machines during a cropping season is not managed with reference moisture levels.

Soil compaction has been identified as one of the leading problem causing soil degradation (Barnes et al., 1971; Gupta et al., 1985; Larson et al., 1989 Canillas and Salokhe, 2002). Compaction restrict root penetration due to the insufficient root turgor pressure to overcome the mechanical resistance of the soil (Gysi, 2001), increases the bulk density and soil strength (Taylor, 1971; Lebert et al., 1989), decrease the total porosity and thereby limiting nutrient uptake, water infiltration and redistribution and, seedling emergence. The consequences of all these are decreased yields, increased erosion and power requirement for tillage.

In areas with intense rainfall, soil compaction had been recorded due to tillage and harvest operation carried out when the soil surface is wetter than optimal for wheel traffic (Silva et al., 1986, Dias Junior, 1997), in pasture, due to the excessive trampling of the cattle (Kondo and Dias Junior, 1999) and in forest areas due to the traffic during harvest operations and wood transport under inadequate soil water conditions (Dias Junior et al., 1999; Dias Junior, 2000).

However, soil compaction which is a major and about the most popular form of structural degradation can be avoided, if an early detection and monitoring process is established (Dias Junior, 1994; Dias Junior and Pierce, 1995; Ajayi et al., 2013). Among several methods that have been proposed, the use of soil compression curve has stand the test of time. The soil compression curve delineates the behaviour of soil into zones of Elastic deformation (secondary compression curve) and the zones of plastic deformation (virgin compression curve). The pre-consolidation/pre-compression pressure is widely agreed as the point that separates the two on a compression curve (Dias Junior and Pierce, 1995; Horn et al., 1995). In defining the pre-consolidation pressure point on a soil compression curve, it is necessary to establish the optimum point of curvature on the curve. Determining this has been a subject of intense interest in soil mechanics and soil physics study, resulting in the development of graphical mean of estimation. However, the graphical determination is been burdened by a lot of subjectivity, thus Casagrande 1936, develop a method of determining pre-compression pressure from the soil compression curve.

The pre-consolidation pressure/ pre-compression stress (σ_p) is an indication of soil strength or maximum previously applied stress sustained by a soil. It defines the limit of elastic deformation in the soil compression curves (Holtz and Kovacs, 1981, Dias Junior and Pierce, 1995; Defossez and Richard, 2002), and may be used as a quantitative indicator of soil structure sustainability. Thus, in agriculture, application of stress greater than the pre-compression stress should be avoided. The change in pre-compression stress σ_p as a function of moisture content is important for root growth and also essential for determining the load support capacity of the soil.

Considering its importance to soil management, the determination of pre-consolidation pressure should be made less subjective, therefore the elimination of this in the location of the point of maximum curvature necessitate the development of a computer model to accurately determine the pre-consolidation pressure emanating from the casagrande model on the soil compression curve.

Therefore, the study is aimed at: (a) developing an algorithm that solves the Casagrande equation, (b) develop a graphical interface for the visualisation and interpretation of Casagrande model solution and apply the developed model to dataset of stress versus strain from four different soil samples collected from Brazil and Nigeria, comparing the result with those estimated from Excel spreadsheet representation of the model.

2. METHODOLOGY

2.1 Modelling Process for Pre-compression Determination

The principles of mathematical modelling and computer simulation is based on the idea that if the goal of the particular problem can be quantified, it may be possible to express it mathematically so that it may be possible to device a computational skill or method that will yield a solution to the problem. Modelling process used in this project is broken into 5 steps as outlined below:

2.1.1 Problem Definition

In order to build a model of a system to represent something else, or develop a model through a mathematical expression, it is necessary to first list out the factors to be considered and identify the goal to be achieved. In many cases the physical situation must be analysed and how some variable parameters affect or influence the model to be developed must be recognised and applied to the simplified form.

In this study, the major concern is to eliminate the subjective interpretation of the turning point or point of maximum curvature on the soil compression curve to accurately determine the soil pre-compression stress. The turning point is estimated from the casagrande model, which this work intends to represent in well-defined and structured algorithm.

2.1.2 Data Collection/Analysis

The dataset used for the implementation of the model were obtained from uniaxial compression test experiment on soils samples collected at the B-Horizon in locations in Brazil (Lavras, Uberladia and Rio Gran de Sul) and a location in Nigeria (Ire Ekiti). The dataset of the samples collected are shown in Tables 1 – 4:

Table 1: First Data Used for Validating the Model (Lavras)

Pressure (kPa)	Reading (pol^{-4})	Reading (cm)	Delta H (cm)	Delta E	Void Index	Height (cm)	Volume dm^3	ρ_b kg dm^{-3}
					1.3550	2.5100	0.0797	1.1253
25	70	0.0178	0.0178	0.0167	1.3383	2.4922	0.0792	1.1333
50	282	0.0716	0.0538	0.0505	1.2878	2.4384	0.0775	1.1583
100	647	0.1643	0.0927	0.0870	1.2008	2.3457	0.0745	1.2041
200	1112	0.2824	0.1181	0.1108	1.0900	2.2276	0.0708	1.2680
400	1612	0.4094	0.1270	0.1192	0.9708	2.1006	0.0667	1.3446
800	2095	0.5321	0.1227	0.1151	0.8557	1.9779	0.0628	1.4280
1600	2495	0.6337	0.1016	0.0953	0.7604	1.8763	0.0596	1.5054

Table 2: Second Data Used for Validating the model (Uberladia)

Pressure (kPa)	Reading (pol^{-4})	Reading (cm)	DeltaH (cm)	DeltaE	Void Index	Height (cm)	Volume dm^3	ρ_b kg dm^{-3}
					1.3259	2.5000	0.0794	1.1393
25	102	0.0259	0.0259	0.0241	1.3018	2.4741	0.0786	1.1513
50	179	0.0455	0.0196	0.0182	1.2836	2.4545	0.0780	1.1605
100	270	0.0686	0.0231	0.0215	1.2621	2.4314	0.0772	1.1715
200	370	0.0940	0.0254	0.0236	1.2385	2.4060	0.0764	1.1839
400	546	0.1387	0.0447	0.0416	1.1969	2.3613	0.0750	1.2063
800	887	0.2253	0.0866	0.0806	1.1163	2.2747	0.0723	1.2522
1600	1289	0.3274	0.1021	0.0950	1.0213	2.1726	0.0690	1.3110

Table 3: Third Data Used for Validating the model (Rio Gran de Sul)

Pressure (kPa)	Reading (pol^{-4})	Reading (cm)	DeltaH (cm)	DeltaE	Void Index	Height (cm)	Volume dm^3	ρ_b kg dm^{-3}
					1.4687	2.5500	0.0810	1.0734
25	20	0.0051	0.0051	0.0049	1.4638	2.5449	0.0808	1.0756
50	58	0.0147	0.0097	0.0093	1.4545	2.5353	0.0805	1.0797
100	166	0.0422	0.0274	0.0266	1.4279	2.5078	0.0797	1.0915
200	355	0.0902	0.0480	0.0465	1.3814	2.4598	0.0781	1.1128
400	611	0.1552	0.0650	0.0630	1.3185	2.3948	0.0761	1.1430
800	947	0.2405	0.0853	0.0826	1.2358	2.3095	0.0734	1.1852
1600	1420	0.3607	0.1201	0.1163	1.1195	2.1893	0.0696	1.2503

Table: 4 Fourth Data Used for Validating the model (Ire)

Pressure (kPa)	Reading (pol^{-4})	Reading (cm)	DeltaH (cm)	Delta E	Void Index	Height (cm)	Volume dm^3	ρ_b kg dm^{-3}
					1.3728	2.5200	0.0801	1.1168
25	5	0.0013	0.0013	0.0012	1.3716	2.5187	0.0800	1.1174
50	20	0.0051	0.0038	0.0036	1.3680	2.5149	0.0799	1.1191
100	74	0.0188	0.0137	0.0129	1.3551	2.5012	0.0795	1.1252
200	195	0.0495	0.0307	0.0289	1.3262	2.4705	0.0785	1.1392
400	415	0.1054	0.0559	0.0526	1.2736	2.4146	0.0767	1.1656
800	762	0.1935	0.0881	0.0830	1.1906	2.3265	0.0739	1.2097
1600	1248	0.3170	0.1234	0.1162	1.0743	2.2030	0.0700	1.2775

2.1.3 Model Formulation

At this stage of the model development, each factor (stress and bulk density) is given a sense of value by assigning a variable. The main objective of model formulation is to eliminate error of locating the point of maximum curvature or to make it as small as possible and then develop a computer model to represent the model formulation.

In order to eliminate this error, computational skill was adopted to develop a MATLAB algorithm for the casagrande model. The parameters used in developing the computer model are; stress and bulk density. The stress and bulk density therefore generate the finite divided difference of the curve (FD), second derivative (SD), Virgin Compression Line (VL) and the regression lines (RL).

(i) Virgin Compression Model

The model is used to estimate the deformations that could occur when pressure greater than the pre-compression stress is applied to the soil. This model takes the general form illustrated in equation (3). It is necessary to first calculate the finite difference (FD) and second derivative (SD).

The equation of the finite difference (FD) and second derivative (SD) (with x_i corresponding to the logarithm of the applied stress interval and y_i corresponding to void ratio or dry bulk density intervals) are as illustrated below:

$$FD_j = \frac{y_{i+1} - y_i}{x_{i+1} - x_i} \quad \text{-- (1)}$$

$$SD_j = FD_{j+1} - FD_j \quad \text{-- (2)}$$

j = 0, 1, 2, 3, 4, ----,
i = 0, 1, 2, 3, 4, ----.

where,
FD = Finite divided difference of the curve; SD = Second derivative; i = Number of stress and bulk density values used; j = Number of times to iterate

The Virgin Compression Line (VCL) representing the plastic region on the soil compression curve can be found from the formula below:

$$VCL = \frac{y_{final} - y_{final-1}}{x_{final} - x_{final-1}}\left(x_{i+1} - x_{final-1}\right) + y_{final-1} \quad \text{-------------------------------- (3)}$$

(ii) Regression/Recompression Model
This model describes the region in which the soil will undergo a recoverable deformation. The model takes the general form illustrated in equation (4) and (5) below:

$$\rho_b reg(1) = \frac{y_{i+1} - y_i}{x_{i+1} - x_i}\left(x_{i+1} - x_i\right) + y_i \quad \text{-- (4)}$$

$$\rho_b reg(2) = c + x_{i+1}(slope) \quad \text{--- (5)}$$

where,
x_1 and y_1 = The data pair where second derivative (SD) value is minimum
$\rho_b$reg(1) = The first regression line that passes through the first two data point.
$\rho_b$reg(2) = Regression line fitted to the first four data points
C = The intercept of the linear regression line for the first four data point on y-axis
Slope = The gradient of the linear regression line for the first four data point of bulk density (y_1, y_2, y_3, y_4) and Log of stress (x_1, x_2, x_3, x_4), taken the form $y = a + bx$ (linear model).

The point of interception between $\rho_b$reg(1) , $\rho_b$reg(2) and virgin compression line correspond the soil pre-compression stress.

(iii) Soil Management Model
The soil management model refers to the soil pre-compression stress model that may be used to estimate the maximum pressure that can be applied to the soil in order to avoid structure degradation. The model takes general form illustrated in equation (7) and (10) including its corresponding bulk density model in equation (8) and (11).

$$Log(\sigma_p 1) = \frac{FD_{min}(-x_2)) + y_2 - y_{final} - FD_{max}(-y_{final}))}{FD_{max} - FD_{min}} \qquad (6)$$

$$\sigma_p 1 = Anti\log(Log\sigma_p 1) \qquad (7)$$

$$\rho_{b1} = FD_{\min}((\sigma_p 1 - (x_2)) + y_2 \quad (8)$$

$$Log(\sigma_p 2) = \frac{c + ((FD_{\max})(x_{final})) - y_{final}}{FD_{\max} - slope} \quad (9)$$

$$\sigma_P 2 = Anti\log((Log(\sigma_p 1)) \quad (10)$$

$$\rho_{b2} = c + slope(\log(\sigma_p 2)) \quad (11)$$

where,

σ_{p1} = Pre-compression stress when suction (i.e the removal of water and air from the soil by the application of load) is less than 100kpa

σ_{p2} = Pre-compression stress when suction is greater than 100kpa. Parameters such as intercept (c), slope, FD_{min}, FD_{max}, are the same as described in equation (1), (2) and (5).

2.1.4 Model Solution/Analysis

A solution of the model was attempted using the appropriate computational skill or method. The solution to the problem was designed from Graphical User Interface Development Environment (GUIDE) with the programme of the model written and implemented in M-file of MATLAB.

2.2 The MATLAB

MATLAB® is a high-performance language for technical computing. It integrates computation, visualization, and programming in an easy-to-use environment where problems and solutions are expressed in familiar mathematical notation. Typical uses include:

i) Mathematics and computation
ii) Algorithm development
iii) Modeling, simulation, and prototyping
iv) Data analysis, exploration, and visualization
v) Scientific and engineering graphics
vi) Application development, including graphical user interface building MATLAB in an interactive system whose basic data element is an array that does not require dimensioning. This allows the MATLAB to solve many technical computing problems, especially iterating values.

It should therefore be noted that in this paper work a lot of values were iterated which actuate the need of using MATLAB software. The programme and the codes generated were saved and run in an M-file

2.3 M-file

To take advantage of MATLAB's full capabilities in this project, a long sequence of statement was constructed. This was done by writing the commands in a file and calling it from within MATLAB. Such files are called "m-files" because they must have the file name extension ".m". This extension is required in order for these files to be interpreted by MATLAB.

2.4 The Program Designing

The stress and the bulk density data (with the mass of solid, diameter of ring used in determining the bulk density during experiment considered) were input into the computer programme by importing an EXCEL spreadsheet to generate the finite divided difference, Second derivative, virgin compression line (VCL) and the regression values. This is only possible whenever the stress and bulk density are selected, this can be applicable to many data as possible. The results of the iterated values that produces the casagrande graphical interface were arranged in an array in the Graphical User Interphase (GUI) of the MATLAB including the output values of the pre-compression/pre-consolidation stress. The algorithm and flow chart designed for the programme following the step by step of eliminating the subjective interpretation of the point of maximum curvature is as described in Figure 1.

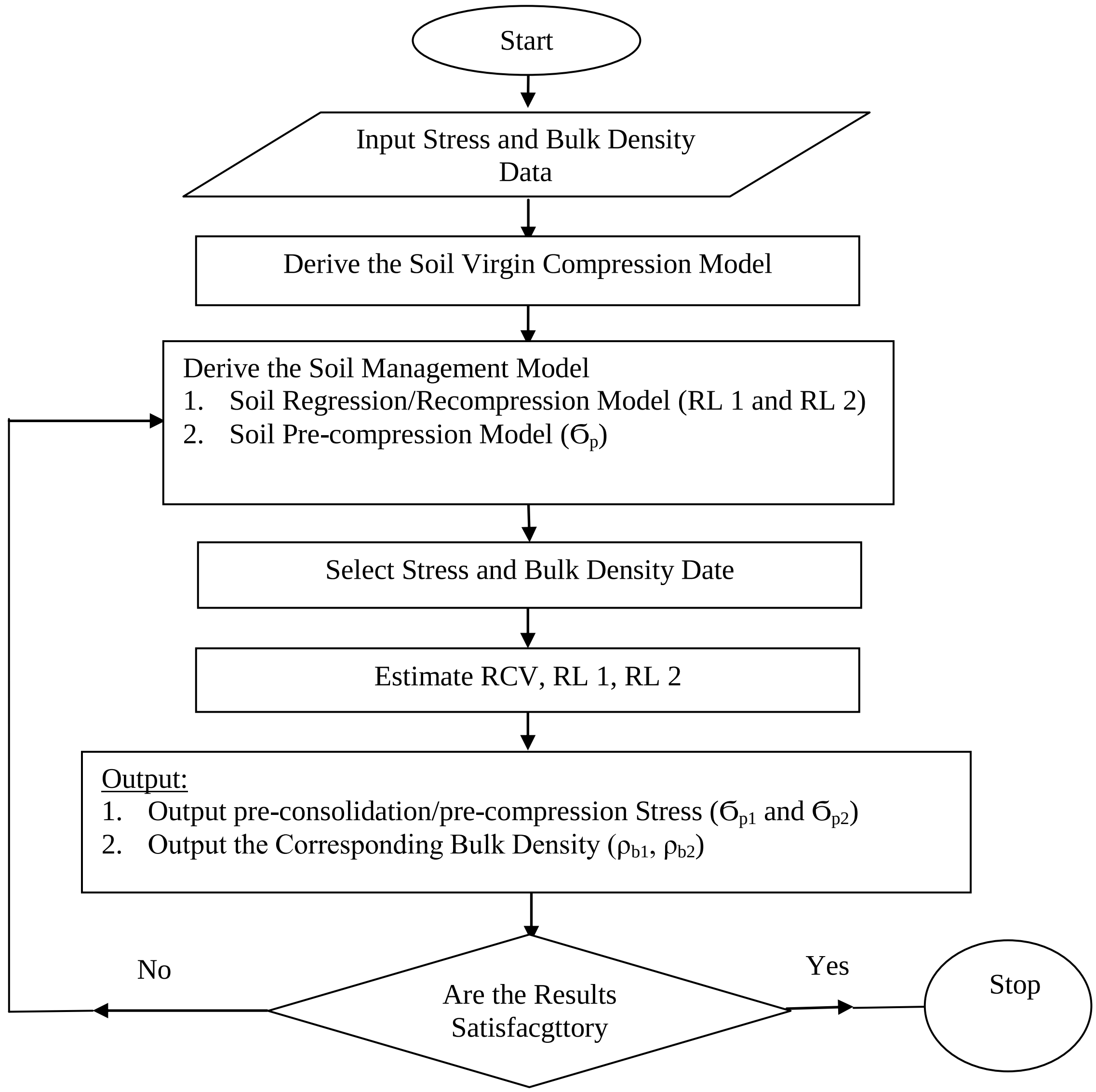

Figure 1: The Program Flow Chart for the Casagrande Model

3. RESULTS AND DISCUSSION

After the program for the model had been test run, it was validated with sample collected from Nigeria (Oye Ekiti) and Brazil (Lavras, Uberladia and Rio Gron resul,) at the B-Horizon .The model was tested before usage by using data from the uni-axial comprexibility test. The results were compared with a previous EXCEL representation of the model by Dias Junior, 1994. The results with its corresponding graphical representation for the Lavras sample collected at the B-Horizon is as illustrated in Table 5 – 8 and the graphical interface is as shown in Figure 2 – 5.

Table 5: Computer model result for the Lavras Set of Data for Validating the model

Stress	Log(Stress)	Bulk Density	RCV	RL(1)	RL(2)
25	1.3979	1.1333	1.0410	1.1333	1.1234
50	1.6990	1.1583	1.1184	1.1583	1.1684
100	2.0000	1.2041	1.1958	1.1833	1.2134
200	2.3010	1.2680	1.2732	1.2083	1.2584
400	2.6021	1.3446	1.3506	1.2333	1.3034
800	2.9031	1.4280	1.4280	1.2583	1.3484
1600	3.2041	1.5054	1.5054	1.2833	1.3934

$Ϭ_{p1}$ = 84.7597 $x_1 = 1.92819$

$Ϭ_{p2}$ = 145.7670 $x_2 = 2.16366$

Bulk density (1) = 1.17734 Bulk density (2) = 1.23788

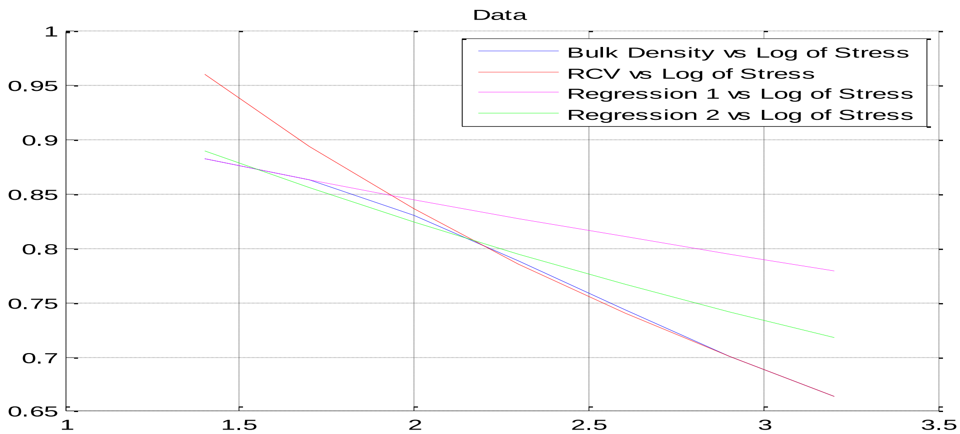

Figure 2: Graphical Interface for Estimating Pre-compression Stress for the Lavras Set of Data

Table 6: Computer model result for the Uberladia Set of Data for Validating the model

Stress	Log(Stress)	Bulk Density	RCV	RL(1)	RL(2)
25	1.3979	1.1513	0.9579	1.1513	1.1505
50	1.6990	1.1605	1.0168	1.1605	1.1613
100	2.0000	1.1715	1.0756	1.1696	1.1722
200	2.3010	1.1839	1.1345	1.1788	1.1831
400	2.6021	1.2063	1.1933	1.1880	1.1940
800	2.9031	1.2522	1.2522	1.1972	1.2048
1600	3.2041	1.3110	1.3110	1.2063	1.2157

$Ϭ_{p1} = 371.12$ $x_1 = 2.56951$

$Ϭ_{p2} = 403.541$ $x_2 = 2.60589$

Bulk density (1) = 1.18698 Bulk density (2) = 1.19409

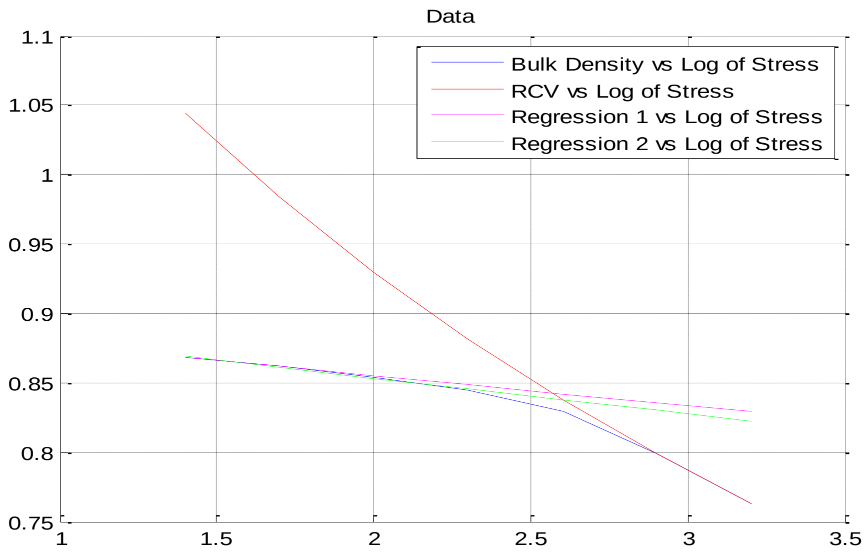

Figure 3: Graphical Interface for Estimating Pre-compression Stress for the Uberladia Set of Data

Table 7: Computer model result for the Rio Gron Resul Set of data for validating the Model

Stress	Log(Stress)	Bulk density	RCV	RL(1)	RL(2)
25	1.3979	1.0756	0.8708	1.0756	1.0714
50	1.6990	1.0797	0.9386	1.0797	1.0837
100	2.0000	1.0915	1.0064	1.0838	1.0961
200	2.3010	1.1128	1.0742	1.0879	1.1084
400	2.6021	1.1430	1.1419	1.0920	1.1207
800	2.9031	1.1852	1.2097	1.0961	1.1331
1600	3.2041	1.2503	1.2775	1.1002	1.1454

Ϭp1 = 290.125 $x_1 = 2.46258$
Ϭp2 = 402.857 $x_2 = 2.60515$

Bulk density (1) = 1.09006 Bulk density (2) = 1.12086

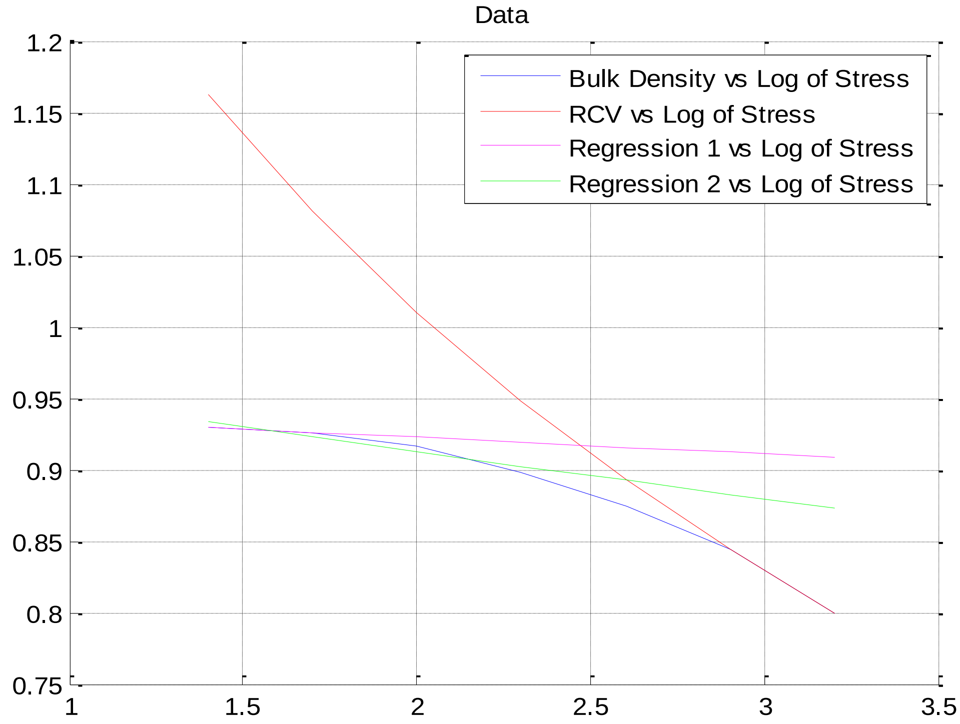

Figure 4: Graphical Interface for Estimating Pre-compression Stress for Rio Gron Resul Set of Data

Table 8: Computer Model Result for the Ire Set of Data for Validating the Model

Stress	Log(Stress)	Bulk density	RCV	RL(1)	RL(2)
25	1.3979	1.1174	0.8708	1.1174	1.1145
50	1.6990	1.1191	0.9386	1.1191	1.1216
100	2.0000	1.1252	1.0064	1.1208	1.1288
200	2.3010	1.1392	1.0742	1.1225	1.1360
400	2.6021	1.1656	1.1419	1.1242	1.1431
800	2.9031	1.2097	1.2097	1.1258	1.1503
1600	3.2041	1.2775	1.2775	1.1275	1.1575

$\sigma p1 = 331.912$ $x_1 = 2.52102$

$\sigma p2 = 405.428$ $x_2 = 2.60791$

Bulk density (1) = 1.12369 Bulk density (2) = 1.1426

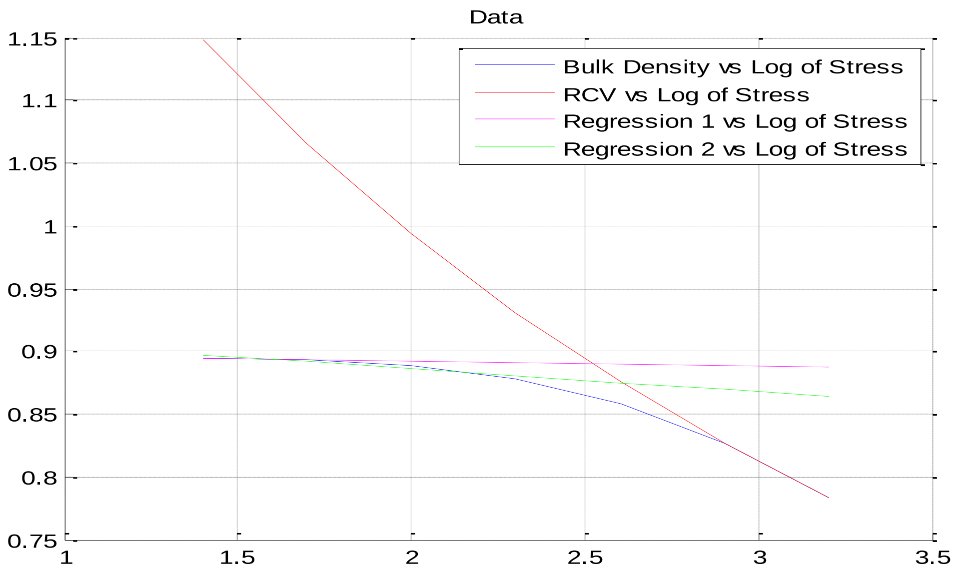

Figure 5: Graphical Interface for Estimating Pre-compression Stress for the Ire set of data

The model implemented using the MATLAB software produced the results in Table and Figure 2 - 5 by using some available data from uni-axial compressibility test collected in Nigeria (Ire) and Brazil (Lavras, Uberladia and Rio Gron resul) at the B-Horizon. The graphical interface for the visualisation and interpretation of the casagrande model for the data collected are as described in Figure 2 - 5. The figures show stress versus bulk density in which the stress/loads applied to the soil are at the interval of 25, 50, 100, 200, 400, and 800. Figure 2 - 5 describe the graphical representation of the casagrande model, consisting of the soil Virgin Compression Line (VCL) or Re-compression virgin (RCV) that describe the region of plastic or permanent deformation and the regression lines (RL1 and RL2) representing the zone or region of recoverable/elastic deformation. The point of interception of RCV and RL1 correspond to the pre-consolidation stress (P_1) while the point of interception of RCV and RL2 correspond the soil pre-consolidation stress (P_2) as shown in figure 3.1-3.4. The soil pre-consolidation stress separates the two zones on soil compression curve.

Table 9 and Figure 6 - 7 below show that pre-consolidation stress output from MATLAB strongly correlate with the previous Excel representation of the model by Dias Junior 1994. This implies that the prediction from the MATLAB was accurate.

Table 9: Comparison of Pre-consolidation Stress (P_1 and P_2) Estimated from MATLAB and EXCEL Representation of the Model

S/N	EXCEL RESULT		MATLAB OUTPUT	
	P_1(kpa)	P_2(kpa)	P_1(kpa)	P_2(kpa)
1	84.5294	145.0957	84.7597	145.7670
2	371.1197	403.5412	371.12	403.541
3	290.1248	402.8570	290.125	402.857
4	331.9118	405.4283	331.912	405.428

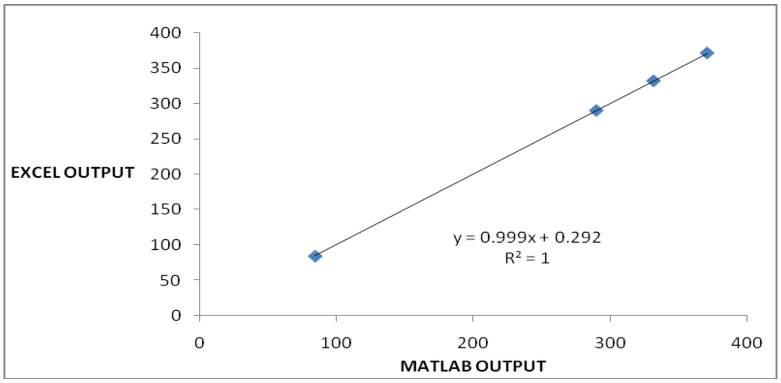

Figure 6: The Relationship of Pre-compression Stress (P_1) Result Estimated from Excel and the Output from MATLAB

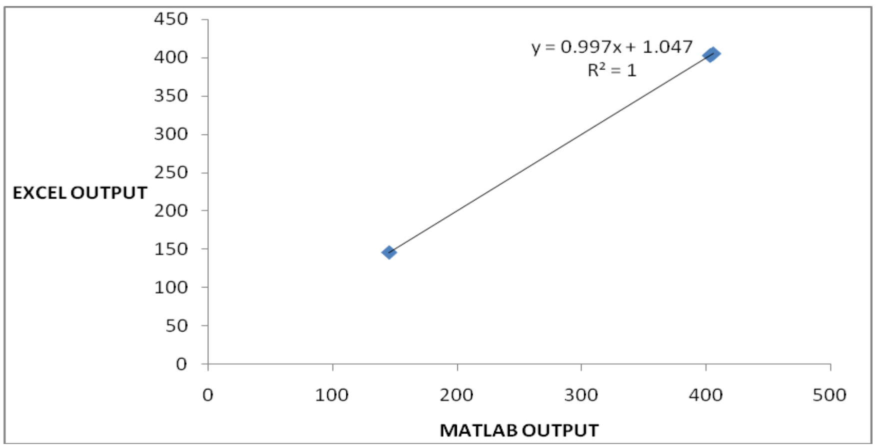

Figure 7: The Relationship of Pre-compression Stress (P_2) Result Estimated from Excel and the Output from MATLAB

4. CONCLUSION

This study presents a MATLAB algorithm for determining the soil pre-consolidation stress by eliminating the subjective interpretation of the point of maximum curvature on the soil compression curve, the model was validated with seven inputs of soil bulk density and stress i.e the applied load).

The model evaluation was carried out by comparing the computer model result with the previous EXCEL representation of the model by Dias Junior 1994, the comparison of MATLAB output with the EXCEL representation of the Model shows a strong degree of correlation of r^2=1, therefore showing that the MATLAB output is accurate. Based on the MATLAB algorithm developed for the Casagrande model using the MATLAB software, it can be concluded that the subjective interpretation of the point of maximum curvature or minimum radius of curvature was eliminated. In addition the soil pre-compression stress was accurately determined. This fact was established based on the fact that the predicted results of the model match/agree with EXCEL representation of the model.

REFERENCES

Alawaji H.A, 2001. Shear induced collapse settlement of arid soils

Assalay.A.M, Jefferson.I, Ragers.C.D.F, Smalley.I.J, 1997. Fragipan formation in loess soils: development of the Bryant hydroconsolidation hypothesis.

Assouline. S, 2002. Modelling soil compaction under uniaxial compression.

Badawy S I.F, Hussain M.A, 2004. Effect of starting material particle size on its agglomeration iour in high shear wet granulation

Canillas, E. C. and Salokhe, V. M., 2002. A decision support system for compaction assessment in agricultural soils. Soil Till. Res. 65, 221-230.

Constantini E.A.C, Damiani. D, 2004. Clay minerals and the development of quarternary soils in central italy.

Dias Junior, M. S., 1994. Compression of three soils under long-term tillage and wheel traffic. Ph.D Thesis, Michigan State University.

Dias Junior, M. S., 2000. Compactação do solo. In R.F. Novais; V.H. Alvarez V and C.E.G.R. Schaefer (Editors). Topics in Soil Science. Soc. Bras. Ci. Solo. pp. 55-94.

Dias Junior, M. S., 2002a. Compactação do solo. Relatório de Pesquisa. Aracruz Celulose S.A. 72pp.

Dias Junior, M. S., 2002b. Avaliação de impactos de sistemas de colheita nas características físicas dos solos. Relatório de Pesquisa. Celulose Nipo- Brasileira S.A.113 pp.

Dias Junior, M.S. 2000. Compactação do solo. Relatório Técnico. 46p.

Dias Junior, M.S., Ferreira, M.M., Fonseca, S., Silva, A.R., Ferreira, D.F., 1999.

Avaliação quantitativa da sustentabilidade estrutural dos solos em sistemas florestais na região de Aracruz – ES. R. Árv., 23, 371-380.

Dias Junior, M. S. and Miranda, E.E.V., 2000. Comportamento da curva de compactação de cinco solos da região de Lavras (MG). Ci. Agrot. 24, 337- 346.

Dias Junior, M. S. and Pierce, F.J., 1995. A simple procedure for estimating preconsolidation pressure from soil compression curves. Soil Tech., 8, 139 Dijkstra T.A, Smalley I.J, Rogers C.D.F, 1995. Particle packing in loess deposits and the problem of structure collapse and hydroconsolidation

Donkor, N.T.; Gedir, J.V.; Hudson, R.J.; Bork, E.W.; Chanasky, D.S. and Naeth, M.A. (2001): Impact of grazing systems on soil compaction and pasture production in Alberta. Canadian J. of Soil Science, 2001

Greenwood, K.L. and Mc Kenzie, B.M. (2001): Grazing effects on soil physical properties and the consequences for pastures: a review. Austr. J. of experimental Agriculture, 2001, 41 1231-1250

Gupta, S.C.; Hadas, A.; Voorhees, W.B.; Wolf, D.; Larson, W.E. and Schneider,E.C., 1985. Development of quids for estimating the ease of compaction of world soils. Bet Dagan, Israel. Research Report, Binational Agric. Res. Development, University of Minnesota, 178 pp.

Gysi, M., 2001. Compaction of a Eutric Cambisol under heavy wheel traffic in Switzerland: Field data and a critical state soil mechanics model approach. Soil Till. Res. 61, 133-142.

Hartge, K. H., R. Horn 1991. Einführung in die Bodenphysik. Stuttgart, Ferdinand Enke Verlag. 303 S.

Horn, R. 2001. Die verformung von Böden – Ursachen und Folgen für eine nachhaltige

Horn R., Domzal H., Slowinska-Jurkiewicz A., C. Van Ouwerkerk 1995. Soil compaction processes and their effects on the structure of arable soils and the environment, Soil & Tillage Research 35 (1995): 23-36Kanton Zürich (1995). Kantonaler Richtplan. Kantonsratsbeschluss

Lesturgez Gregory, Daniel Tessier, Elliane Huard, Hartmann.C, and Poss.R, 2004. Collapsing and traffic load: the formation of dense layer in a sandy soil.

Miller H, Djerbib Y, Jefferson I.F and Smalley I.J, 1998. Modelling the Collapse of Metastable Loess Soils

Semmel H., R. Horn 1994. Spannungen und Spannungsverteilungen in Ackerböden aufgrund von Befahrungen - Überlegungen zur Druckfortpflanzung und der mechanischen

Belastbarkeit von Böden. Landbauforschung Völkenrode *147*, Mitt. d. Bundesforsch. anst. f. Landwirtsch. Braunschweig-Völkenrode (FAL):41-76

Zhang, H.Q. and Horn, R. 1996: Einfluss der Beweidung auf die physikalischen Eigenschaften einer Salzmarsch im Deichvorland (I): diegesättigte Wasserleitfähigkeit und das Bodengefüge. Z. f. Kulturtechnik und Landentwicklung, 1996, 37, 24-31

EFFECTS OF FRYING PARAMETERS ON SOME PHYSICAL PROPERTIES OF FRIED SWEET POTATO (*IPOMEA BATATAS*)

A. O. Oladejo and M. O. Victor
Department of Agricultural and Food Engineering, University of Uyo, Uyo, Nigeria.
Corresponding author: ayobamioladejo@uniuyo.edu.ng

ABSTRACT

The effects of frying parameters (temperature; 130-170^{o}C and time; 2-10 mins) on moisture content, oil content, bulk density and breaking force of fried sweet potato were determined using response surface methodology (RSM). Sweet potato tubers sliced into a uniform thickness (3.0 mm) were fried with sunflower oil using a commercial deep fat fryer. The results from the research showed that frying time had significant ($p<0.05$) effect on moisture content and bulk density. Also, the interaction of temperature and frying time showed significant effect ($p<0.1$) on bulk density. The quadratic term of time had significant ($p<0.1$) effect on the oil content, while the quadratic term of temperature had significant ($p<0.05$) effect on the breaking force of the sweet potato chip. The results further showed that increase in frying temperature and time led to decrease in moisture content, bulk density and breaking force. While increase in frying temperature and time brought about increase in oil content. The optimization developed from this work showed that frying temperature of 145^{o}C and frying time of 6 min would produce sweet potato of high quality in terms of low breaking force, bulk density, moisture and oil content.

KEYWORDS: Sweet potato, frying, moisture content, oil content, bulk density, breaking force.

1. INTRODUCTION

Sweet potato (*Ipomoea batatas)* is a perennial herbaceous dicotyledonous species of the morning glory family Convolvulaceae that is cropped as an annual in many countries (Oates, 2003). Most of the world production is concentrated in 15 countries which account for almost 97% of total world output (Scott, 1992). China is the largest producer of sweet potato in the world (FAO, 2010; Oates, 2003; Jiang et al., 1995). It is the fifth most important crop in the developing countries after rice, wheat, maize and cassava (Oates, 2003). Sanni et al. 2009 stated that Nigeria has the highest production of sweet potato in Africa with 24%, followed by Uganda (23%), Tanzania (8%) and Madagascar (5%) and the rest of the Africa having 29%. Sweet potato (*Ipomea batatas*) is a high-energy crop that is also rich in beta carotene, vitamins and dietary fibres. Several varieties of sweet potato contain higher levels of minerals and proteins than other vegetable (Woolfe, 1992). Utilization of sweet potato includes boiled sweet potato eaten with soup, sweet potato fufu, sweet potato starch, sweet potato noodles, sweet potato snacks, chips and sweet potato flour. Mutungamiri et al. (2001) also demonstrated sweet potato can be processed into jam. Other products that can be derived from sweet potato include juice and ketchup. Sweet potatoes are highly perishables and are not normally stored for any length of time (Fasina, 2006).

Frying is the immersion of a food product into a heated edible oil to achieve a good quality in terms of crispiness, flavour, colour and storability (Hubbard and Farkas, 1999). It is a complex process that involves high temperature, removal of moisture from food product, heat and mass transfer, and micro-structural changes both to the surface and body of the chips (Bouchon *et al.,* 2001). Frying is a very turbulent process that involves the movement of small bubbles particles over the boundary layer of the product surface (Farinu and Baik, 2008). During frying, heat is transferred by convection from the surrounding oil to the surface of the food and by conduction within the solid food. The four stages involved in frying are initial heating, surface boiling, falling rate and bubble endpoint (Farkas *et al.*, 1996).

According to Montgomery (2005), Response Surface Methodology (RSM) makes use of mathematical and statistical techniques for the modelling and analyzing of problems in which a response of interest is influenced by several variables with the aim of optimizing this response. Several works have been carried out on the frying of foods (Yamsaengsung and Moreira, 2002; 2002; Taiwo and Baik, 2002; Moyano and Pedreschi, 2006). The objective of this work is to investigate the effects of processing conditions on the physical properties (moisture content, oil content, bulk density and breaking force) of fried sweet potato using response surface methodology.

2. MATERIALS AND METHODS

The sweet potatoes of local variety (shaba) was purchased from a local market in Uyo, Nigeria. Sweet potato of similar sizes was selected for the experiments. The sweet potato tubers were sliced using a manual slicer (Mothers Choice, Ltd, Texas) to obtain a uniform thickness (2.7mm-3.2mm). The prepared samples were rinsed for 1 min in distilled water to loosen material adhering to the surface; the samples were gently blotted out with towel to remove surface water.

2.1 Experimental Design

The experimental design is based on a three-level factorial design for two variable case as developed by Design Expert 9 (www.startease.com). The two independent variables were frying temperature (130-150^{o}C) and frying time (2-10 mins). Each of these independent variables has three levels. These levels were based on recommendations in literature and trial experiments. The total number of experiments carried out was 13 including five (5) replicates as shown in Table 1.

2.2 The Frying Process

The experiments were performed using a deep fat fryer (MC-DR1030, 3L, Master Chef, China). The deep fat fryer consists of a heating element and a basket. The frying process began by heating oil to the desired temperature, followed by loading the electric fryer with the 12 slices of sweet potatoes per sampling time, using oil-product ratio of 6:1 as recommended by (AOCS Press, 1995). Each experiment was carried out and analyzed according to the experimental design (Table1). After the frying procedure of each batch, the electric fryer was turned off, the basket was lifted out of the oil, and was left to drain oil from fried food. The fried food products were left to cool for 5 minutes, after which they were taken for further analysis.

2.3 Determination of Moisture Content

Moisture content was determined using the Oven dryer (Genlab thermal, MINO/50, Cheshore). Two slices of the sample were weighed and placed in a moisture dish. The sample was heated at 105^{0}C in the oven dryer to constant mass, the sample was cooled at room temperature for 5minutes inside the desiccators and weighed. The amount of weight loss is the moisture contents expressed on wet basis and calculated using formula:

$$\text{Weight loss} = \frac{(initial\ weight\ of\ sample - final\ weight\ of\ sample)}{Initial\ weight\ of\ sample} X\ 100\% \ldots\ldots\ldots\ldots\ldots\ldots\ldots\ldots\ldots\ldots (1)$$

Table1: Experimental Design and Data for Fried Sweet Potato

Run	Temperature A	Time B	Moisture content	Oil content	Breaking force	Bulk density
	^{0}C	Min	%	%	N	g/cm3
1	170	2	15.73	9.53	0.026	0.688
2	150	6	26.05	16.52	0.03	1.042
3	150	6	12.5	13.65	0.02	0.805
4	150	10	2.87	10.7	0.025	0.547

5	150	6	3.46	6.23	0.02	1.115
6	150	2	21.9	2.91	0.03	1.063
7	150	6	6.94	10.74	0.026	0.869
8	130	2	41.1	13.15	0.043	1.1926
9	130	10	9.05	8.54	0.03	0.598
10	170	10	2.98	8.91	0.02	0.684
11	130	6	15.37	16.97	0.05	0.857
12	170	6	12.3	12.47	0.05	0.882
13	150	6	4.01	15.5	0.02	0.684

2.4 Determination of Oil Content.

This was done using Soxhlet extraction with petroleum ether gravimetrically (AOAC, 1995), available in the food engineering laboratory. The oil content was expressed as:

Oil content = $\frac{weight\ of\ oil}{weight\ of\ sample} X100\% \ldots\ldots\ldots\ldots\ldots\ldots\ldots\ldots\ldots\ldots (2)$

2.5 Determination of Bulk Density

Bulk density was determined by the procedure and formula as described by Irtwange and Igbeka, (2002). Twelve samples put inside the beaker were weighed using the electronic balance. The beaker was weighed separately and the weight was subtracted from the initial weight (samples + beaker) to obtain weight of sample. The inner diameter (radius) r and height h of the beaker were measured to calculate the volume V=$\pi r^2 h$. The bulk density was then calculated using:

$$\rho = \frac{W}{V} \ldots\ldots\ldots\ldots\ldots\ldots\ldots\ldots\ldots\ldots (3)$$

Where ρ is the bulk density g/cm^3, W is the weight of sample (g) and V is the volume of sample (Cm^3).

2.6 Determination of Breaking Force (Crispness)

The texture of the fried sweet potatoes was analysed using the Rig apparatus, the constant force N exerted by the apparatus per unit length is 1.0 N/m, samples were inserted into the cracking space and the height was read from the metre rule, the knobs were adjusted to crack the sample, the point where the sample cracks (i.e. gives the crack sound) was also read from the metre rule, the difference was multiplied by the force exerted by the Rig apparatus, the calculated value was recorded as the breaking force for the sample. It is calculated using formula;

Breaking force (N) = (Initial Height – Final Height) × Constant force *N/m*………………………… (4)

2.7 Statistical Analysis

The experiment process was repeated in triplicates for each experiment and the mean values recorded as obtained data. The experimental data obtained were subjected to ANOVA and regression analysis by the statistical software, Design Expert 9 (Stat Ease. Inc, Minneapolis, MN). A second order polynomial equation was used to express the responses as follows:

$$Y = \beta_0 + \sum_{i=1}^{2} \beta_i X_i + \sum_{j=0}^{2} \beta_{ii} x_{i^2} + \sum_{i=1}^{1} \sum_{j=i+1}^{2} \beta_{ij} X_i X_j \quad \ldots\ldots(5)$$

Where Y is the response, β_0 is the constant coefficient, β_i is the linear coefficient, β_{ii} is the quadratic coefficient. β_{ij} an interaction coefficient and X_i and X_j are the coded values of the independent variables.

3. RESULTS AND DISCUSSION

Table 1 shows the experimental data for fried sweet potato and Table 2 shows the ANOVA and coefficient estimates of the responses.

3.1 Effect of Temperature and Time on Moisture Content

As shown in table 2, frying time had significant ($p<0.05$) effect on the moisture content of the fried sweet potato, while the other terms showed no significant effect on the moisture content. However, it is shown in table 2 that the coefficient estimates of linear terms of temperature and time had a negative effect on the moisture content while the coefficient estimates of quadratic terms of temperature and time and interaction of temperature and time had a positive effect on the moisture content. Figure 1 shows the response surface plot for moisture content where moisture content decreased as frying temperature and time increased.

Table 2: Result of ANOVA and Estimated Coefficient of the Responses

Response	Intercept	A	B	AB	A^2	B^2
Moisture content	10.3731	-5.75167	-10.6383*	4.825	4.00914	2.55914
p-value		0.1078	0.0113*	0.2472	0.4123	0.5953
oil content	12.3852	-1.29167	0.426667	0.9975	2.6919	-5.2231**
p-value		0.4480	0.7983	0.6279	0.2932	0.0633**
Breaking force	0.0265862	-0.0045	-0.004	0.00175	0.014948*	0.007551
p-value		0.2606	0.3127	0.7091	0.0282*	0.2062
Bulk density	0.900359	-0.0656	-0.185767*	0.14765**	-0.0242552	0.088755
p-value		0.3192	0.0189*	0.0894**	0.7957	0.3578

A = temperature, B = time
*****$p<0.05$
******$p< 0.1$

Higher frying temperature and longer time would result in a product with lower moisture content because during frying there is transfer of heat from the oil to the surface of the product by convection and then from the surface to the center of the product by conduction. This causes an increase in temperature until the boiling temperature is attained and water starts evaporating (Moreira et al., 1999). This shows that at higher frying time and temperature there is decrease in moisture content and vice versa. These results are in agreement with those reported by Krokida *et al.*, (2000); Mariscal and Bouchon, (2008).
The model equation for moisture content is given as:

Moisture content (%) = +355.02142 - 3.65631 *Temperature-13.62581 *Time +0.060312 *Temperature * Time +0.010023 * Temperature^2+0.15995* Time^2……………………….. (6)

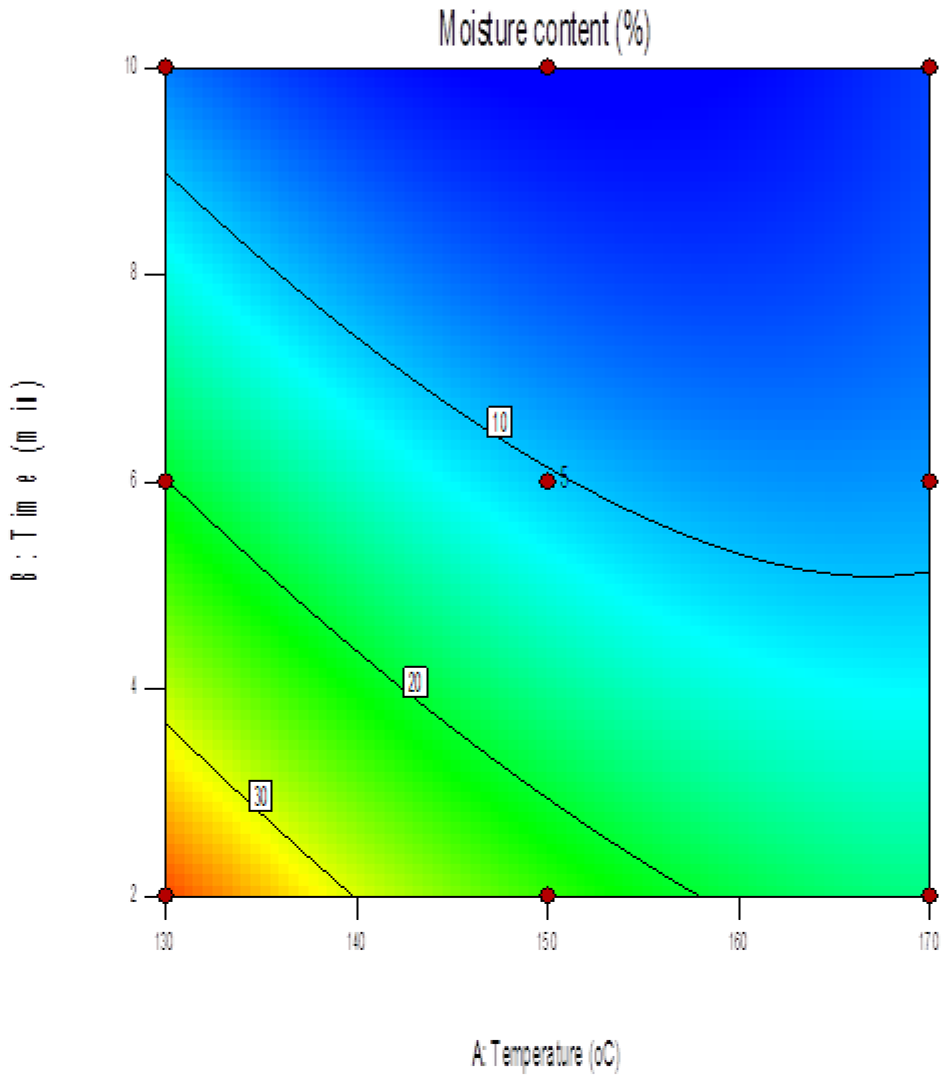

Figure 1: Response surface (Contour) plot for moisture content

3.2 Effect of Frying Temperature and Time on Oil Content

Table 2 shows that only the quadratic term of time had significant ($p<0.1$) effect on oil content while the other terms had no significant ($p>0.1$) effect on oil content. However, the coefficient estimate of linear term of temperature and quadratic term of time had a negative effect on the oil content, while the other terms had a positive effect on the oil content. Oil adsorption is an important aspect in the area of deep fat frying which has been examined by several researchers. Studies show that most of the oil penetrates the product during cooling when the product is removed from the fryer (Moreira et al., 1997; Ufheil & Escher, 1996; Moreira & Barrufat, 1998). At lower temperatures we have higher oil content and at higher temperatures we have lower oil content. Figure 2 shows that the oil content increased as the frying temperature and time increased (Krokida et al., 2000). It has been confirmed that there is a relationship between the moisture content and oil content of fried foods. During frying, moisture leaves the sweet potato through the capillaries inside sweet potato tuber.

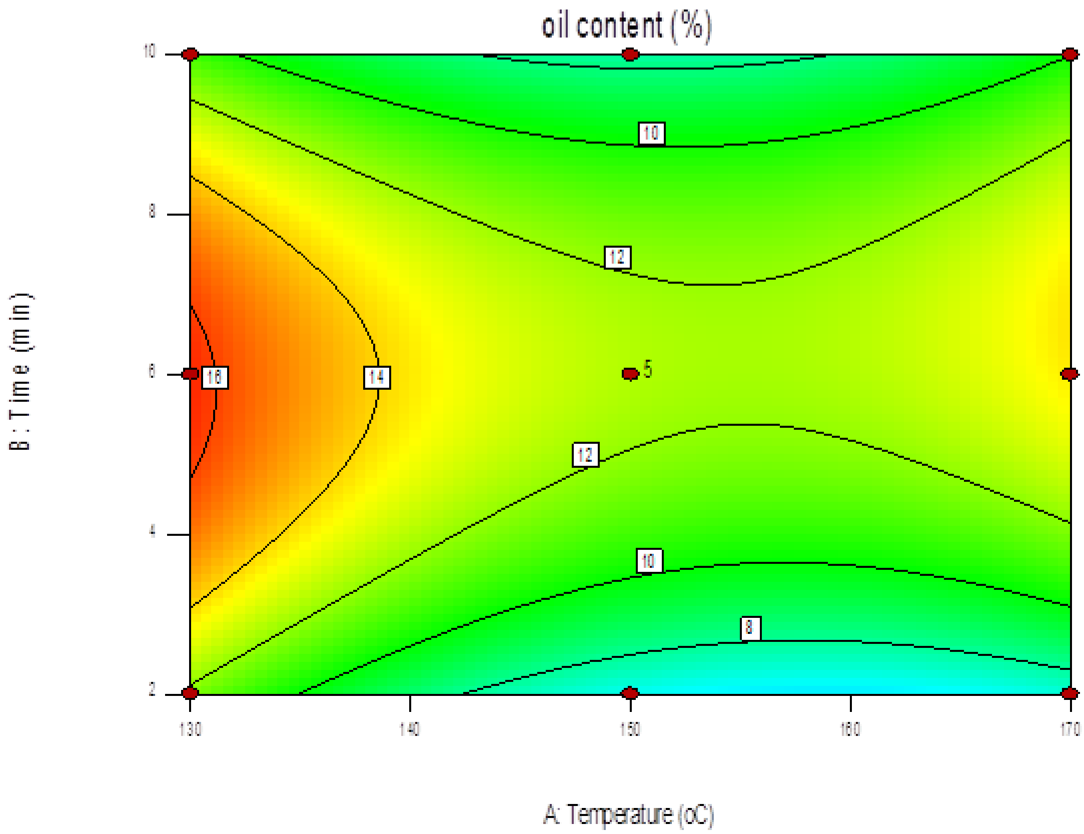

Figure 2: Response surface (contour) plot for oil content.

The oil goes in to occupy the space left by the moisture in the sample. In other words, as the moisture content decreases the oil content increases (Rima-Brncic *et al*., 2004).
The model equation for oil content is given as:

Oil content (%) =+172.32175-2.15832* Temperature+2.15368* Time +0.012469 *Temperature*Time +6.72974E-003* Temperature^2-0.32644* Time^2…………………… (7)

3.3 Effects of Frying Temperature and Time on Bulk Density

It is observed in table 2 that frying time had significant ($p<0.05$) effect on the bulk density of the fried sweet potato. The interaction of temperature and time also had significant ($p<0.1$) effect on the bulk density of the sweet potato. The coefficient estimates of linear terms of temperature and time and quadratic term of temperature had negative effects on bulk density while the other terms had positive effect on bulk density. Figure 3 shows the response surface plot as affected by temperature and time. This result indicates that increase in frying temperature and frying time brought about decrease in bulk density. The decrease in bulk density was as a result of water vaporization, air pore development and oil uptake (Krokida *et al.,* 2000).

The model equation for bulk density is given as:

Bulk density (g/cm^3) = +1.76802+3.83763E-003* Temperature-0.25672* Time+1.84563E-003* Temperature * Time-6.06379E-005* Temperature^2-5.54720E-003* Time^2……………… (8)

3.4 Effect of Frying Temperature and Time on Breaking Force (Crispiness)

Table 2 shows that only the quadratic term of temperature had significant ($p<0.05$) effect on the breaking force of fried sweet potato. The coefficient estimate of linear terms of temperature and time had negative effects on the breaking force while the quadratic and interaction terms of temperature and time had positive effects on the breaking force. Figure 4 shows the response surface plot as affected by temperature and time.

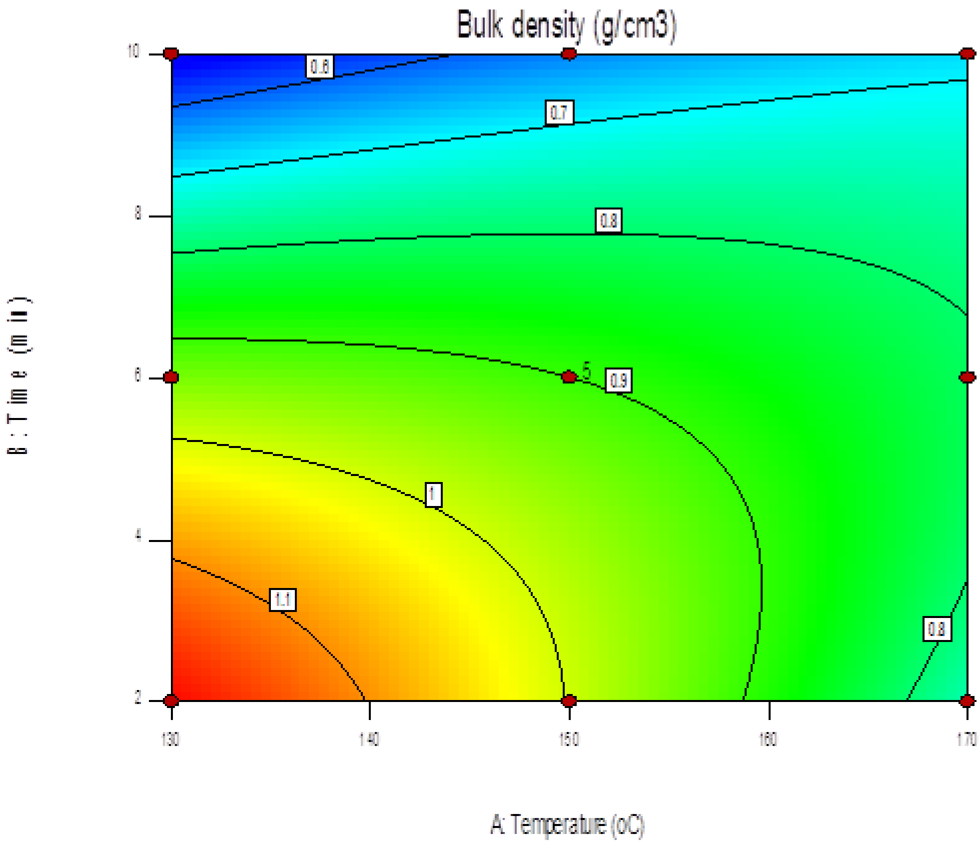

Figure 3: Response surface (contour) plot for bulk density.

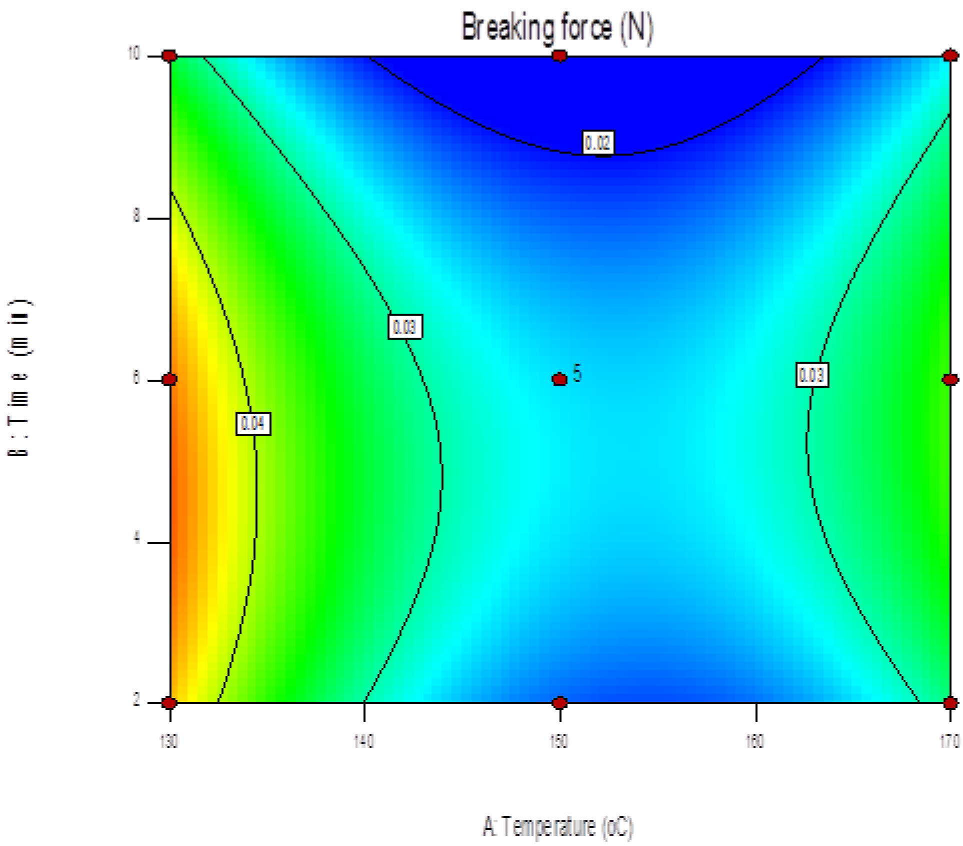

Figure 4: Response surface (contour) plot for breaking force.

The result indicates that breaking force

The result indicates that breaking force decreased as frying time and temperature increased. This is a desirable quality in fried sweet potato because lower breaking force corresponds to higher crispness (Shyu and Hwang, 2001). This is due to decrease in moisture contents as a result of increase in frying temperature.

The model equation for breaking force is given as:

Breaking force (N) = +0.90987-0.011567* Temperature+1. 38254E-003* Time+2.18750E-005* Temperature * Time+3.73707E-005* Temperature^2-4.71983E-004* Time^2……………… (9)

3.5 Optimization of Frying Processes of Sweet Potato

Response Surface Methodology (RSM) was used to generate the optimized values of the frying process variables (temperature and time) based on minimized moisture content, oil content, bulk density and breaking force. Therefore, the optimized values are 145^{o}C and 6 min for temperature and time, respectively. The implication of this is that to produce the fried sweet potato of good quality, the frying temperature should be set at 145^{o}C for frying time of 6 min.

4. CONCLUSION

The various effects of the frying process (temperature and time) had been investigated on the independent variables (moisture content, oil Content, bulk density and breaking force). Frying time was found to have significant effect on the responses in most cases. Response surface methodology had been employed in this work to evaluate and optimize the frying process of sweet potato. The optimized values (temperature of 145°C and time of 6 min) were adequate to produce high quality sweet potato chips.

REFERENCES

AOAC.1995. Official methods of analysis, 5th ed., Association of Official Analytical Chemists. Washington, US.

AOCS 1995. Official methods and recommended practices of the American Oil Chemists Society (4th ed.). Washington DC: The American Oil Chemists Society.

Bouchon, P., Hollins, P., Person, M., Pyle, D. L. and Tobin, M.J. 2001. Oil distribution in fried potatoes monitored by infrared microspectroscopy. Journal of Food Science, 66 (7): 918–923.

FAO. 2010. Food and Agriculture Organization of the United Nations. http://www.fao.org.

Farinu A, And Baik O.D, 2008. Convective mass transfer coefficients in finite element simulations of deep fat frying of sweet potato. J. Food Engineering,89(2):187-194.

Farkas, B. E., Singh, R. P., and Rumsey, T.R. 1996. Modeling heat and mass transfer in immersion frying. I, Model development, J. Food Engineering, 29:211-226.

Fasina, O.O. 2006. Thermodynamic properties of sweet potato. J. Food Engineering (75) 149-155.

Hubbard L J, Farkas B. E 2000.Influence of oil temperature on convective heat transfer during immersion frying. J. Food Engineering, **51 (3)** 98-108.

Irtwange, S. V. And Igbeka, J. C.2002. Some physical properties of two Africa yam bean (S*phenostylis stenocarpa*) accessions and their interactions with moisture content. J. Applied Engineering in Agriculture. 18(5):567-576.

Jiang, X., Jianjun, .H and Wang, .Y. 1995. Sweet potato processing and product research and development at the Sichuan Academy of Agricultural Sciences. Cheng Du, P.R.China.pp. 124 – 126.

Krokida M.K., Oreopoulou, .V and Maroulis, Z.B.. 2000 Water loss and oil uptake as a function of frying time.J.Food Engineering 44, 39-46.

Mariscal, M and Bouchon, P. 2008. Comparison between atmospheric and vacuum frying of apple slices. Food Chemistry, 107: 1561-1569.

Montgomery, D. C. 2005. Design and Analysis of Experiments, 6th ed. Hoboken, NJ: John Willey, US.

Moreira, R. G., and Barrufet, M. A. 1998. A new approach to describe oil absorption in fried foods: a simulation study. Journal of Food Engineering, 35, 1-22.

Moreira, R. G., Sun, X., and Chen, Y. 1997. Factors affecting oil uptake in tortilla chips in deep fat frying. Journal of Food Engineering, 31, 485±498.

Moreira, R., Castell-Perez, M. E., and Barrufet, M. A.1999. Deep-fat Frying: fundamentals and applications. Aspen Publishers, Inc. Maryland, US.

Moyano P, Pedreschi F. 2006. Kinetics of oil uptake during frying of potato slices: Effect of pretreatments. LWT 39, 285-291.

Mutungamiri, A., Zingoni, C and Rukuni, T. 2001. Evaluation of sweet potato varieties and pectin from fruit source for acceptability of jam. African Crop Science Conference Proceedings, 5. 503-506.

Oates, .C. 2003. sweet potato – Asia in: Select markets for taro, yams and sweet potatoes. Compiled by Grant Vining. RIPDC. Pp. 3.

Rima-Brncic S, Lelas V, Rade D, and Simundic B 2004. Decreasing of oil absorption in potato strips during deep fat frying. J.Food Engineering, 64:237-241.

Sanni, .L.O., Adebowale, A.A., Idowu, .M.A., Sawi, M.K., Kamara, Olayiwola, I.O., Egunlety, .M., Dipeolu, A., Aiyelagbe, I.O.O and Fomba.S. 2009. West African Foods from Root and Tuber crops [A brief review]. Jedidah. Nigeria, pp.19, 20.

Scott, G.J. (1992) Transforming traditional food crops: product development for roots and tubers. In: Scott, G.J. Wiersema, S and Ferguson, P.I. Eds. Product Development for Root and Tuber Crops. Volume 1. Asia. Proceedings of the International Workshop April 22-May 1, 1991, ViSCA, Baybay, Leyte, Philippines. CIP, Lima, Peru, pp 3-20.

Shyu, S. and Hwang, L. 2001. Effects of processing conditions on the quality of vacuum fried apples. Food Research International, 34: 133-142.

Taiwo, K. A. and Baik, O. D. 2007. Effects of pre-treatments on the shrinkage and textural properties of fried sweet potatoes. Lebensmittel-Wissenschaft und Technologie, 40, 661–668.
Ufheil G and Escher F. 1996. Dynamics of oil uptake during deep-fat frying of potato slices. Lebensm-Wiss Technol 29(7):640–4.
Woolfe J.A. 1992. Sweet potato: an untapped food resource. Cambridge University Press, Cambridge, UK.
Yamsaengsung, R., and Moreira R. G 2002. Modelling the transport phenomena and structural changes during deep fat frying. Part 2: Model solution &Validation. J. Food Engineering, 53,11-25.

DEVELOPMENT OF AN INDIRECT FORCED CONVECTION SOLAR DRYER FOR CASSAVA CHIPS

A. F. Alonge and N. I. Jackson
Department of Agricultural and Food Engineering, University of Uyo, Uyo, Nigeria
Email: akindelealonge@uniuyo.edu.ng, jnsuhoridem@yahoo.com

ABSTRACT

Solar drying has been widely applied as a preservative measure for agricultural/food materials, as a system which combines cost-effectiveness (coupled with other advantages) with efficiency. This work presents the design, construction and preliminary testing of an indirect forced convection solar dryer. The system was constructed using locally available materials at a total cost of ₦40,550. The calculated collector area is 0.32 m^2, fan ratings is 20 CFM; 24 VDC; 1.4 A. Photovoltaic Panel rating is 15 W, while battery rating is 24 VDC. It was tested under no load (for temperature variations) and load (for temperature, relative humidity and moisture content variations) conditions. The equipment was used to dry cassava *(Manihot spp)* chips in order to study the effect of the enhanced airflow on the drying rate of the product. The drying test was carried out in two replications. The duration of each test was 0800hr to 1800hr. At no load maximum temperatures of 60℃ and 48℃ were obtained in the collector unit and drying cabinet respectively on 04/05/2014 when the ambient temperature was 35℃. Under load condition maximum temperatures of 57.5℃ and 50℃ were obtained in the collector unit and drying cabinet respectively on 10/05/2014 when the ambient temperature was 36.4℃. During second replication the relative humidity in the drying cabinet varied from 58% to 78% while the ambient relative humidity varied from 70% to 90%. In a day with maximum ambient temperature of 6.4℃, the dryer efficiency was calculated as 53.2% , the dryer capacity was 116.3g/hr and drying time of cassava chips in the forced convection solar dryer was 10 hours, as opposed to 2-3 days drying of crops in natural convection solar dryers as reviewed in this work.

KEYWORDS: Design, preliminary testing, forced convection, indirect, solar dryer, cassava chips

1. INTRODUCTION

In food processing, drying can be defined as a Unit operation which involves the removal of moisture from an agricultural/food material until the moisture content is in equilibrium with the surrounding air. Drying serves as a preservative measure, as it helps to lower the moisture content and water activity of the produce, thereby inhibiting the growth of microorganisms (Alonge and Adeboye, 2012). Alonge and Adeboye (2012) stated that preserving dried food by removing enough moisture from the food can prevent decay and spoilage. Drying is essential as it facilitates crop handling by reducing weight and improving resistance to attacks by some pests and insects (Yohanna and Umogbai, 2010). The drying process involves simultaneous heat and mass transfer. Successful drying depends on enough heat to draw moisture without cooking the food, dry air to absorb the released moisture and adequate air circulation to carry off the moisture. The key is to remove moisture as quickly as possible at a temperature that does not seriously affect the flavour, texture and colour of the food (Alonge and Adeboye, 2012). Drying must therefore occur at a temperature that is not too high, to prevent surface hardening (at very low humidity) and not too low, to prevent growth of microorganisms before the product is dried. In the nutshell, the drying air must be constantly monitored by velocity, temperature and humidity to ensure quick and effective drying that does not alter the aesthetic and nutritional quality of the product (Mabrouk, 2012). The agro-processors and food industries employ several methods in product drying. Sanni *et al.* (2012) lists the commonly employed drying systems as Open sun drying, Cabinet dryers, Flash dryers, Solar cabinet Dryers, Rotary dryers and a combination of Solar and Indirect heating of the drying room, which can be described as a hybrid drying system.

Solar drying could be employed in the drying of cassava chips instead of open air and uncontrolled sun-drying or electrical/ mechanical drying. Open air drying comes with its attendant problems as product is unprotected from rain, wind-borne dirt and dust, infestation by insects, rodents and other animals. Also products may be seriously degraded to the extent that sometimes become market valueless and inedible, with the attendant adverse economic effects on domestic and international markets (Ogheneruona and Jusuf, 2011). The disadvantage of electrical/mechanical drying borders on the high cost and limited availability. Solar drying is effective in that it is economical, readily available and also avoids the problems associated with open air drying.

When drying a crop like cassava which is known to possess a high spoilage rate, conversion of the raw product into dried form must take place in an efficient, cost-effective system capable of completely drying the product within one day. This is particularly necessitated by the fact that if the product is subjected to intermittent drying, bacterial organisms could germinate and grow, and cause spoilage overnight. For cost effectiveness and other advantages, solar drying is the best choice. However, conventional solar dryers, most of which operate by natural convection are not satisfactory at achieving complete drying within one day. Cassava products are said to be ‘‘completely dry’’ when the moisture content is reduced from the initial value of 67-75%Wb to an acceptable limit of 14%Wb (Ogheneruona and Jusuf, 2011). To achieve this, forced airflow, generally termed ‘Forced Convection’ drying needs to be investigated. Forced convection drying here involves incorporating a fan in the design to give the hot air delivery needed for complete drying of the material within one day. This is the opposite of natural convection drying which depends on density differentials to move heated air. Further since the system is solar equipment, the source of power must also be solar. A photovoltaic ‘voltage generator’ needs then be incorporated into the design to generate the voltage needed to power the fan. Finally, Ogheneruona and Jusuf (2011) stated that the optimal drying temperature for cassava products is 52°C. Regulation of drying temperature within the optimum would be impossible with a direct solar dryer, thus an indirect solar dryer is what is required here.

Photovoltaic technology involves the direct conversion of sunlight into electrical energy, using solar panels or arrays. The advantages of this source of energy is that it is an inherently clean source of energy, produces no noise , smoke, acid rain, water pollutants, CO_2 or nuclear waste because it relies on the power of the sun for its fuel (Anon., (2012). The history of photovoltaic technology goes back to the year 1839, when Becquerel discovered the Photovoltaic effect. A semiconductor age began about 100 years later. After Shockeley had developed a model for PN junction, Bell Laboratories produced the first solar cell in 1954; with 5% efficiency (Quaschning, 2011). When light shines on a PV cell, it may be reflected, absorbed, or refracted. The absorbed light generates electricity if it possesses a ‘threshold energy’ needed to release electrons (Anon., 2013).

The objective of this work was to develop a forced convection dryer for crops.

2. MATERIALS AND METHODS

2.1 Design Concept/Consideration

An indirect forced convection solar dryer was designed and fabricated using low-cost materials. The effectiveness of the forced convection drying was measured by subjecting the dryer to test using cassava chips. The size of the dryer was fixed based on investigations using the design capacity. The following were considered for the design of the indirect forced convection solar dryer as adapted from Alonge and Oniya (2012), Ogheneruona and Jusuf (2011) and Babagana et al (2012).

2.1.1 Technical Design Considerations

The technical design considerations for the dryer include the following: The mass of cassava chips to be dried (taken as 2kg); the initial and final moisture contents of the cassava; the daily sunshine hours for the selection of total drying time; amount of moisture to be removed from the 2kg of wet product to bring the moisture content to a safe level in the drying time; the mass and volumetric flow rate of air (kg/hr; m^3/hr) needed for complete drying over the drying time (to be supplied by the fan i.e., for fan selection); the daily solar radiation to determine the energy received by the dryer per hour and hence determine; the area of the flat plate collector , (considering also; the average ambient temperature for Uyo meteorological area; the transmittance of the transparent glass cover; the absorptivity of the collector material; and the useful energy gain of the system); the Brake Horsepower (BHP) of the fan for rating of photovoltaic module (PV module selection); the watt-peak of photovoltaic which will supply the needed BHP; The dimensions of the drying chamber (to handle the design 2kg of cassava chips), and of the solar heater that will accommodate the fan size and the solar collector (of area designed); and the angle of inclination of the solar collector to the horizontal for optimum efficiency.

2.1.2 Sanitary Design Considerations

For ease of cleaning, the food contact surfaces (trays) are made of tin-coated wire meshes. Also the trays are removable to ease dislodging of any accumulated dirt. The non-food contact surface (wood) is covered with grey Formica and sealed with Porte sealant to prevent absorption of water and entry of insects and flies. The fan air inlet and outlet air vent are covered with fine nets to prevent the entry of tiny bodies, such as insects and flies.

2.1.3 Economic Considerations

For the lowest possible cost, the dryer is constructed with locally available materials. The plywood is thick enough to eliminate any need for additional insulation. The capacity of the photovoltaic is selected to supply just the needed power to the fan. The fan is also selected to supply just the needed air flow rate.

2.2 Design Analysis

The design is divided into two areas typical of food engineering design: solar cassava chips drying process design and solar cassava chips drying equipment design.

2.2.1 Process Design

- **Basis:** Process type: Batch; Weight of feed: 2kg Cassava Chips; Initial moisture content : 72% $^{w}/_{w}$ (wet basis); Final moisture content : 14% $^{w}/_{w}$ (wet basis); Ambient air temperature: 32°C for Uyo meteorological area (Augustine and Nnabuchi, 2010); Dryer temperature : 52°C
- **Material Balances:** The quantum of moisture to be removed to reduce the product moisture content to the safe level was determined using the material balance equation:

Total Material Balance (TMB): Total Input = Total output

$$F + H_a = V + D \qquad 3a$$

Where; F = Weight of wet cassava chips, $^{kg}/_{batch}$; D = Weight of dried cassava chips, $^{kg}/_{batch}$; H_a = Weight of heated air, $^{kg}/_{batch}$ and V = Weight of exhaust air saturated with water vapour, $^{kg}/_{batch}$.

- **Desired Drying Rate:** This was determined using:

$$R_d = {}^{Q}/_{t} \qquad 3b$$

Where; R_d is the desired drying rate; Q is mass of moisture removed and t is required drying time.

- **Energy Balances:** The mass flowrate of air required to achieve the desired drying rate was determined using the overall energy balance equation:

- **Total Energy Input = Total Energy Output**
  Energy in Raw cassava chips + Energy in heated air = Energy in Dry cassava Chips + Energy in Water vapour

$$F\,({}^{kg}/_{batch})\,C_{pf}\,{}^{kJ}/_{kg°C}\,(52-t_d)°C + H_a\,({}^{kg}/_{batch})\,C_{pa}\,{}^{kJ}/_{kg°C}\,(52-t_d)°C$$

$$= D\,({}^{kg}/_{batch})\,C_{pp}\,{}^{kJ}/_{kg°C}\,(52-t_d)\,°C + Q\,({}^{kg}/_{batch})\,\{\Delta h_{lv} + \Delta h_{vv}\}\,{}^{kJ}/_{kg} \quad 3(c)$$

Where: $Q\,{}^{kg}/_{batch}$ = Mass of moisture to be removed = $1.35\,{}^{kg}/_{batch}$; $C_{pf}\,{}^{kg}/_{batch}$ = Specific heat capacity of wet chip;

$C_{pa}\,{}^{kJ}/_{kg°C}$ = Specific heat capacity of air; $C_{pp}\,{}^{kJ}/_{kg°C}$ = Specific heat capacity of dried chips; $\Delta\,h_{vv}\,{}^{kJ}/_{kg}$ = Enthalpy of vaporisation of vapour and $\Delta h_{lv}\,{}^{kJ}/_{kg}$ = Enthalpy of liquid.

- **Volumetric Flow rate of Air Required**

$$V_a = \frac{H_a\,{}^{kg}/_{hr}}{\rho(air)\,{}^{kg}/_{m^3}} \quad 3\,(g)$$

Where, $\rho(air) =$ Density of air at 52°C (325K) and atmospheric pressure and H_a is mass flowrate of air.

2.2.2 Equipment Design

The equipment design involved the following: Fan selection, Photovoltaic panel selection, solar air heater design and drying cabinet design.

- **Fan Selection:** The fan type considered for the design was vane axial fan for technical reasons**.** The volumetric flow rate of the fan as calculated is $10cfm$; but for the purpose of selection an *overdesign factor* of 2 was introduced. The duct Static pressure was estimated as $0.0249KPa$. These data were used to select the correct fan for the job from NIDEC fan catalogue.
- **PV Panel Selection:** For size considerations, a photovoltaic panel of ratings 12VDC; 15W was selected to be used with a 24VDC Deep Cycle Battery already charged to full capacity. This supplies a voltage of 24VDC across the fan terminals for maximum capacity.
- **Solar Air Heater Design:**
- The **area of the flat plate solar collector** was determined using equations 3c and 3d given by (Mumah, 1995)

$$\boldsymbol{Q_u = H_a C_{pa}(T_2 - T_1)} \quad \textbf{3c}$$

$$\boldsymbol{Q_u = A_C[T\alpha I_T - U_L(T_{pm} - T_a)]} \quad \textbf{3d}$$

Where: H_a is Mass flow rate of air, T_1;T_2 are ambient and dryer temperature respectively; I_T = Total incident solar radiation on the collector cover $KJ/_{hr.m^2}$; $\boldsymbol{T\alpha}$ = Effective transmittance-absorptance product of the collector; $\boldsymbol{A_C}$ = Collector area, m^2; $\boldsymbol{U_L}$ = Collector overall heat loss coefficient, $KJ/_{hr.Km^2}$; $\boldsymbol{T_{pm}}$= Mean temperature of the collector absorber plate; and $\boldsymbol{T_a}$ = Outdoor or ambient air temperature.

- **Inclination of the Collector** $\emptyset$: The angle of inclination of the collector was fixed based on the latitude of Uyo given by Augustine and Nnabuchi (2010) as 5.06°
- **Other parameters** such as the collector and cabinet dimensions were fixed using simple geometry.

2.3 Equipment Construction and Performance Testing

The equipment was constructed at the Faculty of Engineering Workshop, University of Uyo, Nigeria. Testing of the dryer took place at the vicinity of Food Engineering Laboratory, University of Uyo, Nigeria.

2.3.1 Temperature and Relative Humidity Measurements

The equipment was subjected to temperature tests at no load (4th May 2014) and at loaded condition (5th May 2014 and 9th May 2014).Tests were run from 0600hrs to 1700hrs each day. A Digital thermometer was placed outside to read ambient temperature. Another Digital thermometer was inserted into the drying chamber to read temperature of the cabinet while a mercury-in-glass thermometer was inserted into the solar air heater to read the temperature of the heated air. Also two Wet-and-dry bulb thermometers (psychrometers) were placed each at the inside and outside to obtain Wet and dry bulb temperatures utilized in estimating the relative humidity of the drying cabinet and ambient air respectively, using standard CIBB'S Psychrometric chart.

2.3.2 Drying Tests/Moisture Content Determination

The equipment was tested with cassava chips. The Cassava roots was washed, peeled, washed and sliced into chips of standard sizes (3-5mm) in diameter, using a manual slicer. The sliced chips was then blanched at 70℃ for 2minutes to deactivate the enzymes and microorganisms present. 1kg of blanched cassava chips was placed in each tray and loaded into the dryer. The equipment was allowed to start up for 1hr and the fan put on for the equipment to run under forced convection. The drying experiment was conducted in two replications.

Each drying experiment started with the determination of initial moisture content. Samples were taken and analysed for moisture content using the AOAC Standard, involving oven dry method. Weight measurements were carried out using the weighing balance. The moisture contents were determined using the following equation (Alonge and Oniya, 2012).

$$\text{MC (wet basis)} = {(w_2 - w_3)}/{(w_2 - w_1)} \qquad 3(j)$$

Where; w_1 = weight of empty crucible; w_2= weight of crucible + sample before oven drying; w_3 = weight of crucible + sample after drying

2.2.3 Efficiency and operational Capacity of the Dryer

The efficiency of the convective solar dryer was calculated using Equation 3(k) (Mumar, 1995).

$$E = {}^{M_W L_V}\!\Big/ (I_T A_C + E_f) \qquad 3k$$

Where, E = current dryer efficiency, % ; M_W= evaporated moisture mass of the product, kg ; L_V= specific latent heat of water vaporization, kJ/kg; I_T= solar radiation energy per collecting area, kJ/m^2; A_C= collector area,m^2 ; E_f = fan energy, kJ

- The operational capacity of the dryer was calculated using equation 3(l)

$$M_W/t_s \qquad 3(l)$$

Where, t_s = time in hours

2.4 Design Features and Construction Details

The Solar Powered air dryer is an innovative technology based on a combination of Solar Thermal and Photovoltaic Technologies. The main parts of the equipment can be divided into three; the Drying abinet, the Solar Air Heater, and the Voltage generator. The drying cabinet has dimensions $900 \times 540 \times 525\ millimeters$ and is fitted with two high strength wire gauze trays of dimension $490 \times 475\ millimeters$; the wire gauze is supported with wood rod. The distance between the trays is $250\ millimeters$. The inside of the dryer is painted black to enhance the absorption and radiation of heat; the effect of which prevents the loss of heat by conduction through the wood. At the front of the cabinet is an access door fitted with a handle for easy opening and closing. The door is specially designed to fit when closed to reduce heat losses. Figure 1 shows the front features of drying cabinet.

Fig. 1: The Dryer Showing the Drying Cabinet.

At the top left hand side of the drying cabinet is an exhaust air vent of diameter $54\ millimeters$ as revealed by the isometric picture of Figure 2. The air vent and fan air inlet are covered with a fine mesh to keep out insects and pests while allowing easy passage of air out of the dryer and into the dryer respectively. Figure 2 also shows the drying cabinet trays in an exploded position with the dried cassava chips.


Figure 2: Internal Features Showing the Dried Cassava Chips.

The solar air heater comprises a flat plate solar collector of area (0.32m^2(690 X 460 millimetres) made from black-painted aluminium. The collector is placed at angle 5.06^{0}C for maximum energy absorption and encased in a wooden box covered with silicate glass of 2.5 millimetres in thickness for green-house effect. Axial to the collector length is a dc axial flow fan, 200 millimetres in diameter. Figure 3a shows the external features of the solar air heater. The circular opening is the fan air inlet; the transparent silicate glass reveals the heat absorber inside.


Plate 3a: Pictorial View Showing the Solar Air Heater and PV

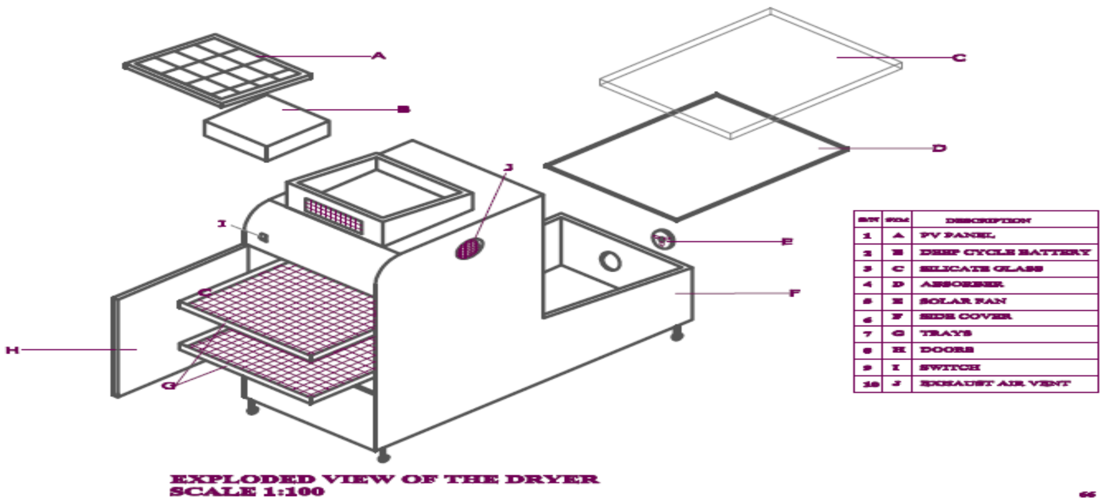

Fig. 3b. Exploded view of the dryer scale 1.100

The Voltage generator comprises a Photovoltaic panel, a horizontally placed deep-cycle battery, and an enclosure with an opening to aerate the battery, as well as wiring. The Photovoltaic panel is connected to the battery which is in turn connected to a breaker (switch) and to the dc fan. The Switch is placed in front of the drying cabinet. Fig. 3b also reveals the solar voltage generator at the top of the drying cabinet. The solar panel is fixed at the top at an angle of 5.06℃.

The body of the dryer is made of plywood of thickness 1.5 centimetrs. The bottom cover of the dryer is made of plywood of the same thickness. The external surface of the dryer is covered with grey Formica for durability and aesthetic reasons. The equipment is mounted on movable casters to allow rolling movement of the equipment. The equipment is designed for Uyo meteorological area and is located North-South during solar drying.

2.5 Working Principles of the Equipment

The Cassava *(Manihot spp)* chips are placed in the perforated wire gauze trays (which are removable), perforations allowing for the rising of heated air through the two trays. Heated air enters the drying chamber from the solar air heater via an opening between the cabinet and the solar air heater. As the heated air rises, the product is dried by transfer of heat from the air to the product and transfer of moisture (mass) from the product to the activated air. The exhaust air mixed with water vapour leaves the cabinet through the exhaust air vent. The heat delivered to the drying cabinet is generated by a solar heat collector made of black-painted aluminium and placed in the solar air heater. The dc axial flow solar fan blows air across the collector to be heated and delivered into the drying cabinet. The fan sucks in air through a specially designed opening equal in diameter to the fan. Power delivery into the dc fan is controlled using the on/off switch located on the drying chamber.

The solar photovoltaic panel generates the voltage, through the photoelectric effect, which in combination with the current flow constitutes the power supply to the dc fan. The Solar panel also charges a deep cycle battery which serves as a backup, ensuring a supply of 24Vdc across the fan terminals. Both solar panel and Solar air heater are inclined in the posterior direction at 5.06℃ and aligned due South for maximum solar energy utilization.

3. RESULTS AND DISCUSSION

3.1 Temperature Variations with Time

The drying equipment was tested under no load and load conditions. Figure 4 shows a typical of ambient, collector and solar drying cabinet air temperatures. From the result obtained under no load test, it is clear that the temperature of the solar collector air is the highest, followed by the cabinet temperature. At an ambient temperature of 35℃, the temperature in the drying cabinet reached its peak for the day at 45℃ while the collector temperature reached its peak for the day at 60℃. One striking observation here is that despite the forced air delivery of the fan, the temperature in the collector area was always higher than the temperature of the drying chamber. It is also safe to candidly state here that the design temperature (52℃.) was exceeded at the collector area on this typically sunny day, but the maximum temperature in the drying chamber was 45℃.

Fig. 5 shows the ambient, collector and drying cabinet temperatures for the first drying replication. The figure shows that even at low ambient temperatures the temperatures in the cabinet and collector are higher, although the difference is not significant. However at very low ambient temperatures, the fan tends to cool the system and the collector and cabinet temperatures continued to fall as observed between 1400h and 1700h.

Fig. 6 shows the variation with time of the ambient, collector and drying cabinet air temperatures, under load (during the second replication). The figure shows that as the ambient temperature increases, both the collector and cabinet temperatures also increase rapidly in such a way that the temperature of the cabinet and collector are always higher than the ambient temperature. The day was a typical sunny day.

3.2 Variation of Relative Humidity with Time

The relative humidity variations for ambient and drying cabinet air are shown in Figure 7. The curve shows that at all time intervals and temperatures, the relative Humidity within the dryer is lower than the relative humidity outside the dryer. This lower Relative humidity in the drying chamber accounts for the ease of mass transfer of moisture from the product to the air. The Graph also shows a rapid increase in drying chamber air relative humidity between 2pm and 5pm.

3.3 Variation of Moisture Content with Time

Fig. 8 shows the variation of moisture content of the cassava chips with time (first replication). Relating the figure to Figure 5 (showing the variation of temperature with time), it can be seen that there was no significant drop in moisture content of the product due to the poor weather conditions (low ambient and dryer temperatures). At the end of the one-day drying period, the product still contained 57% moisture on wet basis. The insignificant moisture loss must also have been due to high air humidity occasioned by the rain. The first replication could not continue the next day as the product was already deteriorated.

Fig. 9 is a drying curve (graphical representation of the variation of moisture content of the cassava chips with time) during the second replication. The moisture content of the product reduced slowly during the early hours of the day, but very rapidly between the hours of 3pm to 5pm, reaching a final moisture content of 14% wet basis at 6pm. Relating the figure to Figure 6, (showing the variation of temperature with time during the same (second) replication), the high moisture reduction rate compared to the first replication occurred due to the relatively high ambient and dryer temperatures. Also, relating this curve to Figure 7 (showing the variations of relative humidity with temperature), it can be seen that the increased moisture loss from the product between 2pm and 5pm caused the relative humidity in the drying chamber to rise rapidly. The results obtained during this second drying test is very close to the design objective; the difference being that while the design calculations was aimed at achieving complete drying (reduction of moisture content to 14% on wet basis) in 9hrs (8:00am to 5:00pm), the drying process achieved the safe moisture content of 14% wet basis in 10hrs (8:00am to 6:00pm).

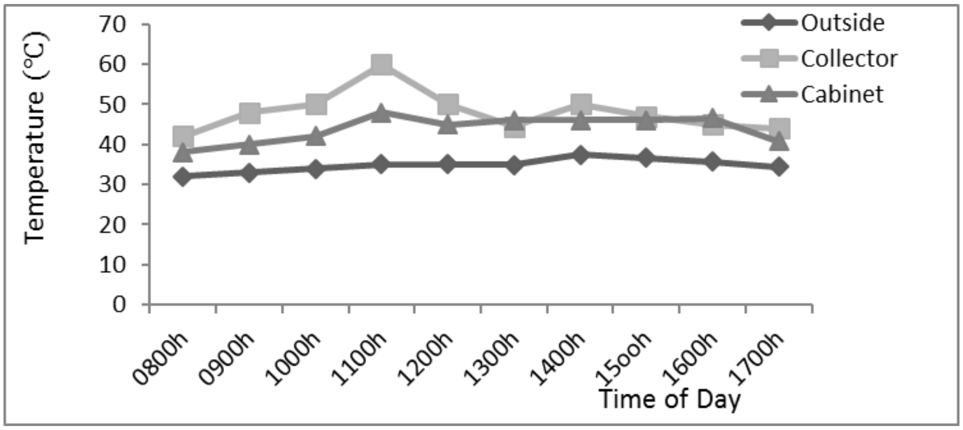

Fig 4: Variation of Temperature with time (no load)

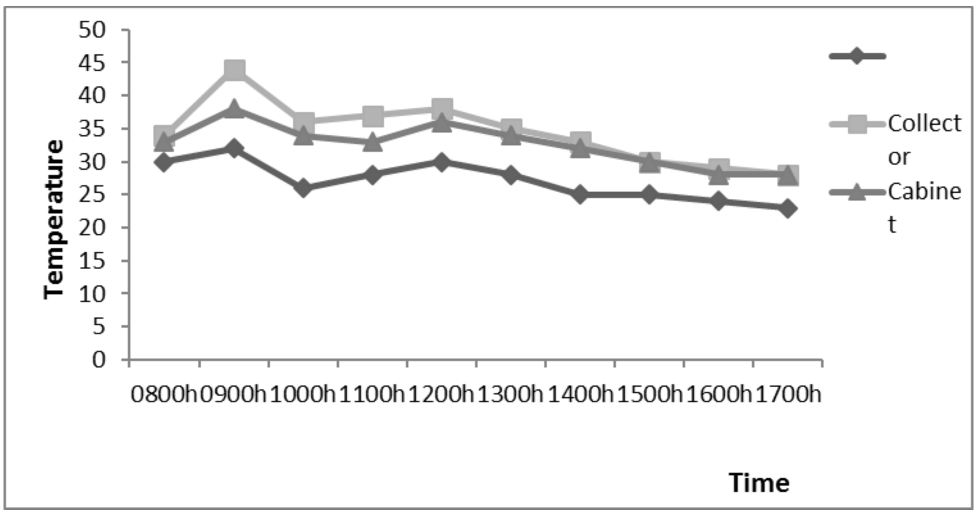

Fig. 5. Variation of Temperature with Time (Under Load; First Replication)

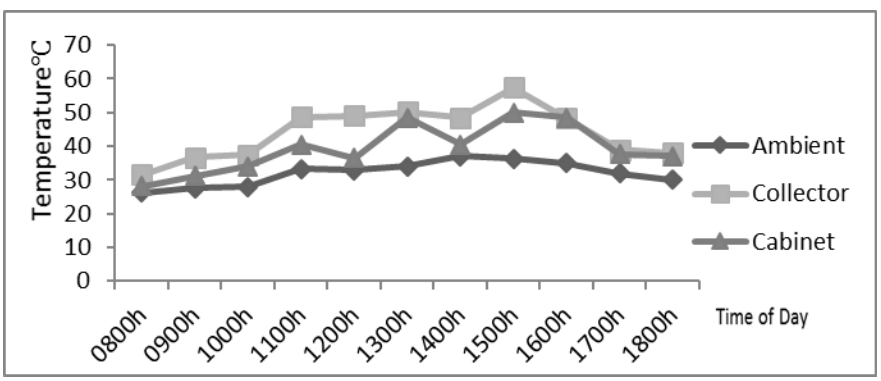

Fig 6. Variation of Temperature against Time (Under Load; Second Replication)

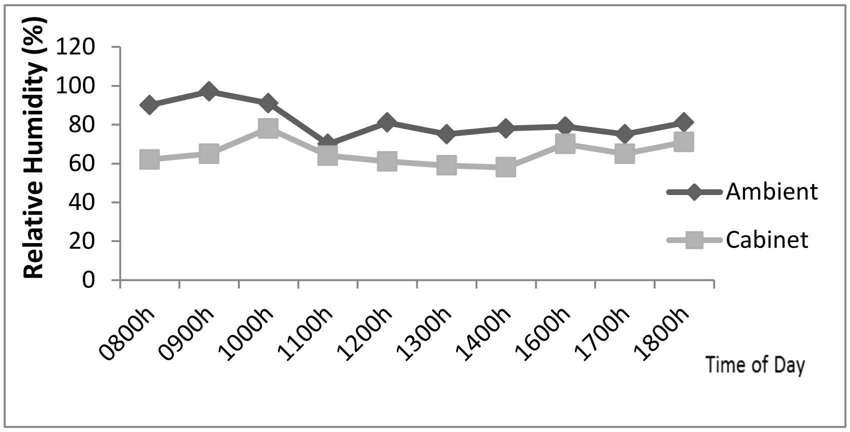

Fig 7. Variations of Relative Humidity with Time (Second Replication)

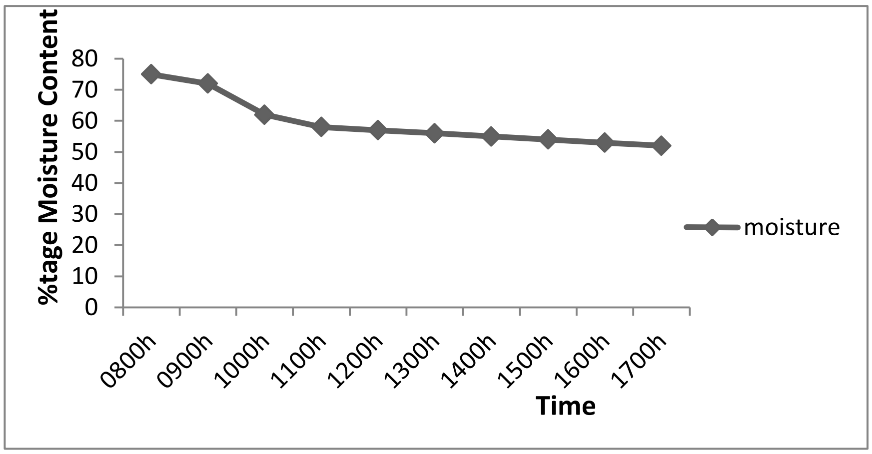

Fig 8. Variation of Moisture Content with Time (First Replication)

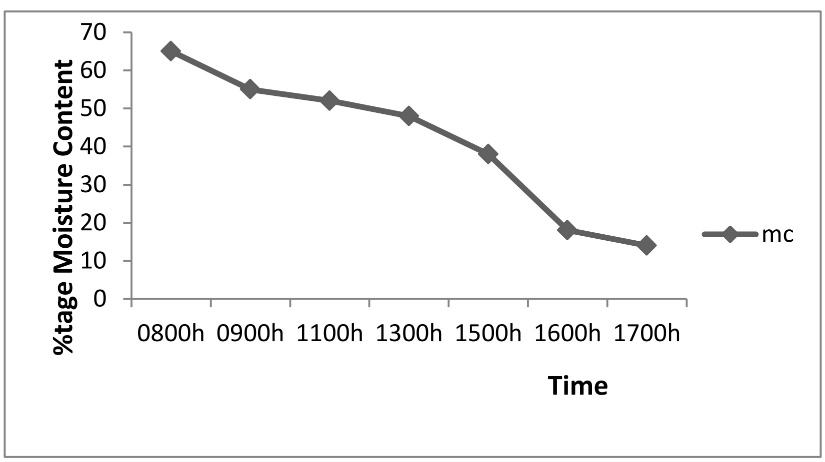

Fig 9. Variation of Moisture Content with Time (Second Replication)

4. CONCLUSIONS AND RECOMMENDATIONS

The essential steps of the engineering design method as well as the heuristics of intelligent designs were followed in design, construction, and performance evaluation of the Indirect Forced Convection Dryer for Cassava Chips. The results obtained fall within regions of acceptability. From the results it could be concluded that:

(i) Forced convection solar dryers can generate temperature significantly higher than the ambient temperatures, provided the intensity of sunlight is sufficient;

(ii) In cases of insufficient intensity of solar radiation, occasioned by poor weather conditions experienced in a rainy season, the fan tends to cool the system, and the collector and drying chamber temperature falls with time;
(iii) As a result of (i) above, the drying rate of product in forced convection solar dryers is significantly high at good ambient conditions;
(iv) As a result of (ii) above, the rate of drying of product in forced convection solar dryers is unimaginably poor at very poor weather conditions and very low solar intensity.
(v) The dryer achieved significant reduction in the relative humidity of air and this accounts for the high drying rate obtained during the second drying replication.
(vi) In a normal day (with high solar insolation), it is possible to dry cassava chips in the forced convection solar dryer to a safe moisture content in just $10 sunshine\ hours$ compared to the 2-3 days product drying obtainable in natural convection drying as reviewed in section 2.7.

REFERENCES

Alonge A. F. and Adeboye O. A. 2012. Drying Rates of Some Fruits and Vegetables with Passive Solar Dryers. *International Journal of Agricultural and Biological Engineering* 5(4): 6.

Alonge and Oniya . 2012. An Indirect Passive Solar Dryer for Drying. Advanced Material Research 36(7) 517-524.

Yohanna, J. K. and Umogbai, V. I. 2010. Solar Energy Potential and Utilization in Nigeria Agriculture. Journal of Environmental Issues in Agriculture in Developing Countries. Vol. 2 No. 2&3. Pp45-47.

Mabrouk, S., Hatem O. and Abdelkader M. 2012. System Design, Mathematical Modelling and Simulation of Process Drying in a Solar-gas Convective Tunnel Dryer. International Journal of Scientific and Engineering Research Vol. 3 No. 5. Pp1-2.

Sanni, L. O., Onadipe-Phorbee, O. and Alenkhe, E. B. 2012. Low Cost Sustainable Cassava Drying Technologies in West Africa. IITA/CFC-WA Project Report pp28.

Ogheneruona D. and Jusuf M. 2011. Design and Fabrication of a Direct Natural Convection Solar Dryer for Tapioca. *http://lejpt.academicdirect.org/A18/095_104.html* . Accessed 03/03/2013

Anonymous. 2012. Photovoltaic Technology. *http://mhattwr,tripod.com/thesis/photovoltaic_technology.html#pvtech*. Accessed: 12/05/2013.

Quaschning, V. 2011. Photovoltaic Systems; Technology Fundamentals. www.volker-quaschning.de/articles/f ; Accessed 10/05/2013

Anonymous. 2013. Solar Electric Photovoltaic Modules. *http//www.solardirect.com/pv/lighting.htm*. Accessed 12/05/2013

Ayensu A. 2011. Thermal Convection and Moisture-diffusion in Thin-layer Fixed-bed Solar Drying. *Quarterly Science Vision* Vol. 9 No. 1-2 & 3-4. Pp 46-47.

Bukola O. B. and Ayoola P. O. 2008. Performance Evaluation of a Mixed-mode Solar Dryer. *AU. J.T* 11(4) 225-231

Babagana G., Silas K., and Mustafa B. G. 2012. Design and Construction of Forced/Natural Convection Solar Vegetable Dryer with Heat Storage. *ARPN Journal of Engineering and Applied Sciences*. Vol.7 No.10. pp 5-6.

Mumar, S. N. 1995. Sizing and Performance Evaluation of a Flat Plate Collector for a Solar Absorption Refrigeration System. *Nigerian Journal of Solar Energy*. Vol. 13.pp.67-75

DEVELOPMENT OF A TIGERNUT SEEDS CLEANING AND SORTING MACHINE

A. A. Balami[1], M. Birma[2] and S. M. Dauda[1]
[1]Department of Agricultural & Bioresources Engineering,
Federal University of Technology, Minna, Nigeria.
Email: aabalami@futminna.edu.ng
[2]Department of Agricultural Engineering, Federal Polytechnic, Nassarawa, Nigeria.

ABSTRACT

This study is about the development of a machine for cleaning and sorting of tiger nut seeds. Some selected physical properties of the tiger nut seeds such as size and shape, volume and density, surface area, weight, spherecity, coefficient of friction, angle of repose, as well as terminal velocity were also determined and used in the design of the machine. The average values obtained from the physical properties at 17 % moisture content are: surface area (206.12 mm^2), geometric mean diameter (7.29 mm), spherecity (74.39 %), coefficient of friction (0.26) and angle of repose (25.40°) and terminal velocity of 17.60 mm/s of the tiger nut seed at moisture content of 17 % (wb). Based on the properties of the seed, a cleaning and sorting machine was developed that cleans and sorts the crop into size groups 12, 8, and 6 mm diameter. The machine was evaluated using the brown type tiger nut. The results of the ANOVA indicate that the sorting differs significantly with the three sieve diameters. The analysis also shows that the machine performed better at 12 mm diameter sieve compared to the other two sieve diameters**.** The developed machine has a throughput capacity and cleaning efficiency of 1.1 kg/min and 94.7 % respectively as against the manual cleaning of 0.22 kg/min and 18.94 % respectively.

KEYWORDS*:* Cleaning and sorting, coefficient of friction, drudgery, spherecity, tiger nut seed.

1. INTRODUCTION

Tiger nut seed (*Cyperus esculantus*) produced by a grass like plant which is ranked among the oldest cultivated plants in Ancient Egypt. It is commonly known as Chufa in Spain, Attadwe in Burkina Faso and Zulu nuts in South Africa while in Nigeria, it is known as “Aya” in Hausa, “Ofio” in Yoruba, and “Akiausa” in Igbo. It is considered a monocot and usually found in three varieties; black, brown and yellow (Fernando, 2011). It does not require heavy rainfall or high humidity it only requires a rainfall of about 50 - 100 mm and with a temperature of about 22^{o}C and relative humidity of about 50 %. It is usually planted during April and May and usually harvested in November or December.

Tiger nut is one of the cash crops which has not been given due recognition and patronage possibly because of lack of knowledge about its nutritional benefits. According to Mordi *et al.* (2010); Addy and Eleshola,(1984), it is a known plant food that is common in West Africa especially Northern Nigeria, where they are cultivated for snacks only and recently is used for kunu (a beverage drink). It is one of the best nutritional crops that can be used to augment the diet of humans (Afenu, 2008). Tiger nut has a fairly good essential amino acids composition similar to olive oil and castor seeds and is a potential oil crop for the production of bio-diesel. It is also used in medicine and perfume production. The yellow variety of tiger nut contains low fats and has less anti-nutritional factors especially polyphenols (Temple *et al.*, 1990; Devries and Feuker, 1999; Okafor *et al.*, 2003).

Despite the huge economic importance of tiger nut crop, its potentials are yet to be fully harnessed. This is because of lack of processing facilities where the crops are mostly produced. The sequence of post-harvest operations of tiger nuts by the manual method consists of washing, drying, sorting and bagging. Post-harvest processing is still manually done particularly the sorting which is the most tedious.

Though mechanical sorting of agricultural crop according to size, shape and colour has been reported (Pasikatan and Dowell, 2002; Hannah, 2011; Risse *et al.,* 1991; Blankenship and Woodall, 1997;

Suszkwi, 2001), these machines are expensive and sophisticated to the peasant tiger nut farmers. Hence, the need for the design, construction and evaluation of a vibrating table sorting machine for tiger nuts becomes paramount in reducing the drudgery of manual sorting by the peasant farmers.

The objective of this work was to develop a tigernut seeds cleaning and sorting machine.

2. MATERIALS AND METHODS

2.1 Design Consideration and Material Selection

The materials used for the construction of the machine were chosen on the basis of their availability, suitability, economy and viability in service among other considerations (ASAE, 2003; Gupta and Das, 1997; Sahay and Singh, 1994; Mohsenin, 1986; Khurmi and Gupta, 2007). Each component was designed following standard engineering principles (Birma, 2012).

2.2 Equipment description

The developed tiger nut sorting and cleaning machine (Fig. 1) basically consists of two major units (cleaning and sorting) which is operated by a 1hp electric motor. A blower was incorporated to facilitate easy and proper cleaning and separation of the nuts from foreign materials. As the tiger nut seeds are fed into the cleaning unit through the feeding hopper, air is blown by the fan which blows off lighter and damaged seeds, while the vibrating deck does the sorting according to sizes.

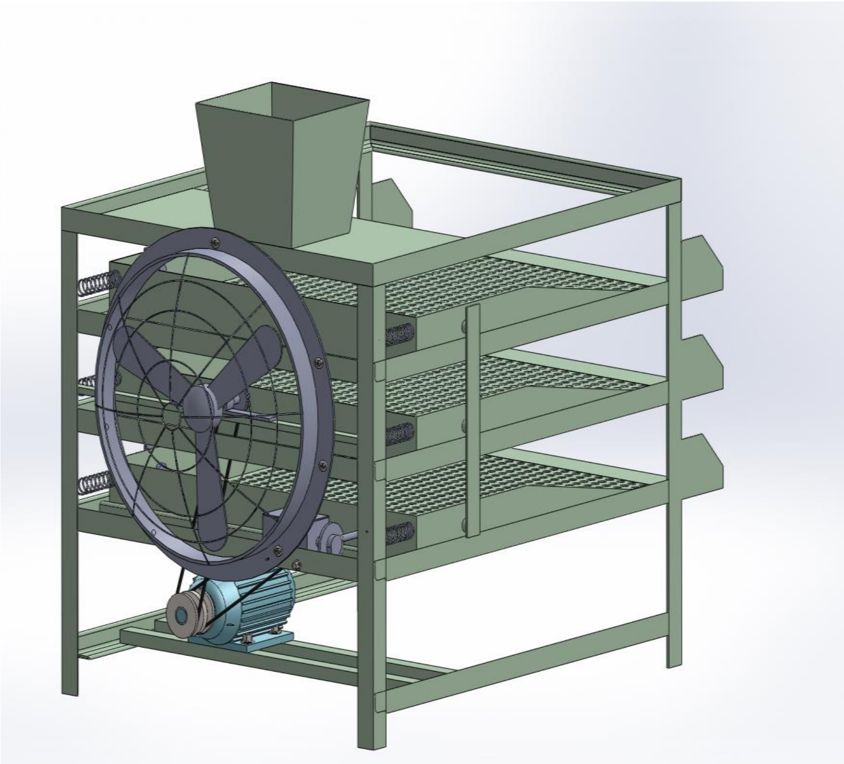

Fig. 1: The Tiger Nut Cleaning and Sorting Machine

2.3 Cam Design

The determining factors for a cam of minimum size are the maximum pressure angle, the least radius of curvature and the cam shaft diameter. The pressure angle was determined using equation 1 adopted from Rothbart (1962).

$$\tan\gamma = \frac{57.3V_{cf}h}{R_n\beta} \quad (1)$$

Where:

$\tan\gamma$ = tangent of pressure angle, in degrees; V_{cf} = velocity coefficient at any point, (mm/sec); h = total displacement of follower, (mm); R_n = Radius at the reference point on the pitch curve, (mm); β = angular displacement of cam for displacement h, (radians).

2.4 The Least Radius of Curvature

The least radius of curvature was determined from the expression given in equation (2).

The least radius of curvature: $R_C = R_A \dfrac{\sin\Delta\theta}{\sin\alpha}$ (2)

Where: R_A = Maximum radius of the pitch curve, (mm)

2.5 Cam Shaft Design

The diameter of the camshaft is governed by the maximum shear theory (Khurmi and Gupta, 2007) which was determined using equation 3.

The diameter of the camshaft.

$$d_c^{\,3} = \frac{16T_e}{\pi T_{\max}} \quad (3)$$

Where: T_e = Equivalent twisting moment, (Nm); T_{max} = Maximum Shear stress, (N/mm^2)
Similarly, the cam velocity was determined using equation 4.

$$V_c = V_{cf}h\left(\frac{6N}{\beta}\right) \quad (4)$$

Where:

V_c = Cam velocity, mm/sec; V_{cf} = velocity coefficient at any point, (mm/sec); h = total displacement of follower, (mm); N = speed of camshaft (rpm); β = angular displacement of cam for displacement h, (radians)

2.6 Pulley Diameter

The ratio of the pulley for the electric motor to that of the cleaning shaft was calculated in equation 5 (Spott 1988).

$$N_1d_1 = N_2d_2 \quad (5)$$

Where: N_1 = Speed of the driving pulley, rpm; N_2 = Speed of the cleaning shaft, rpm; d_1 = Diameter of the driving pulley, mm; d_2 = Diameter of the driving pulley, mm

2.7 Tensions on Belts

The tensions on the belt were determined using Equations 6 and 7 as given by Khurmi and Gupta (2007).

$$\frac{T_1}{T_2} = e^{\mu\theta_1} \quad (6)$$

$$P = (T_1 - T_2)V \quad (7)$$

Where: T_1 = tension of belt on tight side in (N); T_2 = tension of belt on slack side (N); μ = mean coefficient of friction of tiger nut; θ_1 = angle of contact between motor pulley and belt in radian; v = velocity of belt m/s; P = power from electric motor.

2.8 Power Required to Operate the Machine

The power required to operate the machine was calculated using equation 8.

$$P_o = T_c\omega \ (Nm) \quad (8)$$

Where:
P_o = Power in Kw, T_c = torque on camshaft (Nm), ω = angular speed of cam (rad/s).

2.9 Hopper Design

The volume of the hopper was determined using equation 9 (Tim, 2009).

$$V_{hp} = \frac{1}{3}(A_1 + A_2 + \sqrt{A_1.A_2})h_p \quad (9)$$

Where:
V_{hp} = volume of hopper, m^3, A_1, A_2 = Areas of top and bottom base of the hopper m^2,
h_p = depth of hopper, mm

2.10 Cleaning Unit Design

The housing diameter and blower width were determined using equations 10 and 11 (Sahay and Singh 1994).

$$D_{bh} = 1.5D_b \quad (10)$$

$$C_{bh} = 1.25W_{bh} + 0.1D_b \quad (11)$$

Where:
D_{bh} = diameter of blower housing in (m); D_b = diameter of the blade in (m);
C_{bh} = width of the blower housing in (m); W_{bh} = blade width in (m);

2.11 Blower Shaft Design

The diameter of the blower shaft (d_s) was determined using equation 12 (Khurmi and Gupta, 2007).

$$d_s = \left(\frac{16M_t}{2\pi S_s}\right)^{0.333} \quad (12)$$

Where: d_s = expected diameter of shaft (mm), M_t = total weight acting on the shaft (N),
S_S = permissible shear stress of shaft (mild steel) = $115x10^6$ N/m^2

The peripheral velocity of the belt (V_{pb}) was obtained using equation 13.

$$V_{pb} = \frac{\pi d_1 N_1}{60} \quad (13)$$

Where: V_{pb} = peripheral velocity of motor pulley in m/s, N_1= speed of the blower pulley, d_1 = diameter of the pulley of motor (given by manufacturer = 0.15 m).

2.12 Belt Length

The belt length was determined using equation 14 (Khurmi and Gupta 2007).

$$L_{bt} = \frac{\pi}{2}(d_1 - d_2) + 2C + \left(\frac{d_1 - d_2}{4C}\right)^2 \quad (14)$$

Where: $C = 2d_1$ = center distance in (m);
d_1, d_2 = diameters of electric motor and blower pulley, mm.

2.13 Angle of Contact of Belt on Electric Motor Pulley

The angle of contact between the belt and electric motor pulley was determined using equation 15.

$$\theta_1 = 180 - \sin^{-1}\frac{d_1 - d_2}{2C} \quad (15)$$

$$\theta_2 = 180 + \sin^{-1}\frac{d_1 - d_2}{2C} \quad (16)$$

Where:
θ_1 = angle of contact between belt and motor pulley (degree), θ_2 = angle of contact between belt and machine pulley (degree), C = center distance between pulley (0.634 m), d_1 = diameter of driven pulley (0.15 m), d_2 = diameter of driving pulley (0.3m).

2.14 Blower Housing Design

The tangential velocity of centrifugal fan (V_{tc}) was determined using equation 17 (Sitkei 1986).

$$V_{tc} = \omega r \quad (17)$$

Where: $\omega = \frac{2\pi N}{60}$ = angular speed, (rad/s); r = radius of cylinder surface (m)

2.15 Sieve Selection

The basic factor taken into consideration in the design of the sieves is the diameter of the tiger nut seeds, using the three principal dimensions of tiger nut seed (12, 8 and 6 mm).

2.16 Performance Evaluation

The brown type tiger nut seeds, weighing 75 kg were obtained from a local market in Minna, Nigeria. The moisture content of the nuts was determined using the oven dry method (ASAE, 2003). The tiger nut seeds at 17 % moisture contents (wb) were divided into (5, 10, 15, 20 and 25 kg) and fed into the machine for cleaning and sorting. The quantity of the seeds collected at the ends of each of the sieve out lets (12; 8; 6 mm diameters) were recorded and the cleaning efficiency (%) and throughput capacity (kg/h) of the sieves were determined using the equations 18 and 19 (Donahue *et al.*, 1999).

Cleaning efficiency (%) = $\frac{S_1 x100}{S_1 + S_2}$ (18)

Where: S_1 = total mass of clean and unclean nut (kg), T_m = time of cleaning (h), S_2 = mass of damaged seed, leaves etc. (kg),

The throughput capacity (kg/h) = $\frac{S_1}{T_M}$ (19)

The machine was tested based on the performance of the three sieves having 12, 8 and 6 mm diameters respectively.

3. RESULTS AND DISCUSSION

3.1 Physical and Aerodynamic Properties of the Tiger Nut Seed

The physical and aerodynamic properties of tiger nut seed are presented in Table 1.

Table 1: Physical and Aerodynamic Properties of tiger nut seed

S/No.	Properties		Value
1	Mass of one piece of tiger nut seed (M)		4.3 x 10^{-4}, g
2	Diameter of tiger nut	Major	9.01 mm
		Intermediate	6.80 mm
		Minor	5.26 mm
3	Density (ρ) of tiger nut seed		1.4x10-9 g/m^3
4	Volume (Vm) of tiger nuts seed		0.6x10^{-6} mm
5	Moisture content of tiger nut seed		17 % (wb)
6	Coefficient of friction (μ)		0.26
7	Angle of repose of tiger nut seed		25.4°
8	Spherecity of tiger nut seed		74.39
9	Surface area of tiger nut seed		206.12 mm
10	Specific gravity of tiger nut seed		9.3 g
11	Terminal velocity of tiger nut seed		17.60 mm/s^2

The technical characteristics of the machine are presented in Table 2.

Table 2: Technical characteristics of the machine

S/No.	Technical characteristics	Values
1	Power required to operate machine	3,2 kW (electric motor of 5 hp ≈ 3.73 kW)
2	Diameter of blower shaft	24 mm
3	Peripheral velocity of belt	1.89 m/s
4	Belt length	1.92 m
5	Sieve sizes	12, 8 and 6 mm
6	Angle of inclination of sieves	15°, 20° and 25°
7	Cam velocity	0.10243 m/s
8	Pressure angles	$\gamma_1 = 86.87$ $\gamma_{60} = 86.87$ $\gamma_{119} = 86.87$

9	Diameter of camshaft	20 mm
10	Centre distance	0.6 m
11	Cleaning efficiency, %	94.7 %
12	Machine throughput	1.1 kg/min.
13	Manual throughput	0.22 kg/min.

The results of the performance test are presented in Table 3.

Table 3: Results of the Performance Test

		Output Quantity (kg)			
No. of test run	Input quantity (kg)	Sieve 1	Sieve 2	Sieve 3	Time (min.)
1	5	2.4	1.6	0.8	2
2	10	6	2	1.6	4
3	15	8	4	2	6
4	20	10	6	4	8
5	25	14	8	2	10
6	30	20	4	6	14
7	35	24	6	4	18
8	40	20	10	8	26
9	45	18	20	6	40
10	50	24	20	4	46

The analysis of variance (ANOVA) at 5 % probability level is given in Table 4.

Table 4: Two-Way ANOVA of Sieve Sizes (1, 2, 3) against Input Quantity

				F Values	
Source of Variation	Degree of Freedom	Some of Square	Mean of Square	$F_{Cal.}$	F_{Table}
Input Quantity(kg)	2	612.04	306.021	12.34**	0.00
Time	9	597.7	66.411	2.68**	0.036
Error	18	446.41	24.801		
Total	29	1656.15			

**= highly significant at 5% level

3.2 Discussion of results

The three principle mean dimensions of tiger nut seed measured were 9.01, 6.80 and 5.26 mm for the major, intermediate and minor diameters respectively while the geometric mean diameter was 7.29 mm at the 17 % moisture content (w.b) which fall within the range given by Abano and Amoah (2011) for other grains and seed. The mean value of the spherecity of tiger nuts was found to be 74.39. This result shows that tiger nut seed are spherical and means it can roll freely (Baryeh, 2001). Also the average value of the surface area of tiger nut seed at that 17 % (wb) moisture was found to be 206.12 mm^2. This value is also close to that obtained by Baryeh (2001). The mean volume, density and the weight of 1000 tiger nut seeds were found to be 0.000006 m^3, 1.4 x 10-9 kg/m^3 and 429.63 g respectively (Table 2). It can also be observed that the mean values of the angle of repose of tiger nut seed for wood (20.5°), glass (17.5°) and metal (14.4°) while the mean coefficient of friction for the three different materials used which were 0.37, 0.32 and 0.26 respectively. This conformed to the findings of Dutta *et al.* (1988); Joshi *et al.* (1993); Singh and Goswani, (1996); Baryeh (2001, 2002) that used similar technologies for other grains and seed. The terminal velocity of the tiger nut seed nut at 17 % moisture content (w.b) is 25.40° (Table 2). This result also agrees with that of Abano and Amoah (2011). These parameters are important in designing agricultural machinery. From Table 3 it can be seen that sieve one (12 mm diameter) performed better compared to the other two sieve diameters (8 and 6 mm diameters). The analysis of variance (ANOVA) (Table 4) shows that calculated $F_{Cal.}$ of 12.34 for 2 and 2.68 for 9 degrees of freedom is greater than $F_{Tab.}$ of 0.036 at same degree of freedom and at 5 % level of significance which means that the alternative hypothesis that there is a significant difference in the performance of the three sieves is accepted.

The cleaning efficiency obtained was 94.7% (Table 3). The capacity of the machine was 1.1kg/min as compared to manual capacity of 0.22kg/min.

4. CONCLUSION

The physical and aerodynamic properties of the brown type tiger nut seed which is spherical in shape including size, volume and density, surface area, specific gravity, weight, coefficient of friction, angle of repose and terminal velocity were determined at 17 % moisture content. The machine was evaluated using 75 kg of the brown type tiger nut at 17 % moisture content (wb). The throughput capacity of the machine and the manual operating rate of sorting tiger nut seeds were 1.1 kg/minutes and 0.22 kg/minutes respectively. The machine was found to have about 94.7 % sorting efficiency. The developed machine could reduce the drudgery associated in manual sorting and saves about 76 % operating time.

REFERENCE

Abano, A., and Amoah, B. 2011. Physical properties of yellow variety of tiger nut (cyperus esculentus L.): *Journal of Agricultural Engineering Research;* 72*: 175-180.*

Addy, E.O., and Eleshola, E. 1984. Nutrient value of a mixture of tiger nut tuber cyperus esculentus L. and Baobab Adansonia digitatal: *Journal Science food Agriculture,* 35:437 - 440.

Afenu, S. 2008Production of Tiger nut Beverage. HND Dissertation, Cape Coast Polytechnic. Cape Coast, Ghana 1:4 - 36.

ASAE, 2003. *ASAE Standards S319.3* (33 ed.). St. Joseph, Michigan, USA: American Society of Agricultural Engineers.

Baryeh, E.A. 2001. Physical properties of bambara groundnut. *Journal. Food Engineering.* 47: 321 — 326.

Baryeh, E.A. 2002. Physical properties of millet: *Journal Food Engineering,* 51: 30-96.

Birma, M 2012. Development of a Vibrating Table Sorting Machine for Tiger Nuts. Unpublished M. Eng. Thesis, Federal University of Technology, Minna, Nigeria. pp.35.

Blankenship, P., Woodall, M. 1997. A triple deck parallel belt screen for farmers stock peanuts: Retrieved October 20 2012. *From the U.S. Department of Agriculture Agricultural research services Tektran http://www.nal.usda.gov/ttic.*

Devries and T. Feuker, 1999. Chufa (cyperus esculentus): A weedy Cultivar or cultivated weed? *Economic Botany*, 45: 27—37.

Dutta, S.K., V.K. Nema and R.K. Bhardwaj, 1988. Physical properties of grain: *Journal. Agricultural. Engineering Research*, 39: 259-268.

Donahue, D. W., Bushway, A. A., Moore, K. E., Lagasse, B.J. 1999. Evaluation of current Winnowing system, for Maine wild Blue Berries: Retrieved October 20, 2012, from the American society of Agricultural Engineers Technical Library Website: http://asae. Fry multi. Com/.

Fernando, B., 2011. Magazine Esporta, Health and fitness: Retrieved from http://www. Tiger nut.com. On the 20th April, 2011.

Gupta, R.K. and S.K. Das 1998. Friction Coefficient of sun flower seeds and kernel on various structural Surface. *Journal of Agricultural Engineering Research,* 72: 175 - 180.

Hannah, H. 2011. UVM Crop and Soil program: University of Vermont extension at uvm.edu. Retrieved October, 20 2012.

Joshi, D.C., Das, S.D. and Mukherjee, R. K. 1993. Physical properties of pumpkin seeds: *Journal Agricultural Engineering Research*, 54: 219-229.

Khurmi, R. S. and Gupta, J. K. 2007. Machine Design: Revised. Edition: Eurasia Publishing House (PVT.), LTD. Ram Nagar. New Delhi- 110055S.

Mohsenin, N. N. 1986. *Physical properties of plant and Animal materials: structure, physical characteristics and mechanical properties*: 1st Edition, Gordon and Breach Science Publishers, New York, USA.

Mordi,J. I., Ozumba, A. U., Elemo, G.N. and Olatunji, O. 2010. Physicochemical and Sensory Evaluation of Nigerian Tigernut Extrac Beverage: *Bioscience Research Communications.* 0795-8072/2010; vol.22, No. 4, august 31, 2010[2010 klobex Academic publishers.http://www.klobex.org/brc.

Okafor, J.N.C., Mordi, J.I., Ozumba, U.U., Solomon, H.M., and Olatunji, O. 2003. Preliminary studies on the characterization of contaminants in tiger nut (yellow variety): *Proceeding of the 27th Annual Nigerian Institute of Food Science and Technology (NIFST) Conference,* 13-17 October. Pp: 210—211.

Pasikatan, M., and Dowell, E. 2002. Evaluation of a high-speed colour Sorter for segregation of Red and White Wheat: Retrieved October 20 2012, from the U. S. Department of Agriculture,Agriculture research service Tektran service, http://www.nal.usda.gov.

Pearson, T.and Doster, M. 1999. Automated Sorting for pistachio defects by machine vision: Retrieved October 20 2012, from the US. Department of Agriculture, Agriculture research service Tektran service web site www.nal.usda.gov.

Risse, J.H., Misra, M. K., Knapp, A.D., and Bern, C.J. 1991. Conditioning shriveled soy bean seed part I variation in physical properties: *Transaction of the ASAE,* 31(2): 481 - 486.

Rothbart, H. A. 1962. Cam-Design Dynamics and Accuracy: John wiley & sons, inc.

Sahay, K. M., and Singh, K. K. 1994. Unit Operation in Agricultural Processing: Vikas Publishing House, New Delhi.

Singh, K.K. and T.K. Goswani, 1996. Physical properties of cumin seed: *Journal. Agricultural. Engineering. Research.* 64:93 - 98.

Sitkei, H.K. 1986. Design of Transmission Elements: John Willy & Sons.Inc.

Spott, M.F. 1988. *Design of Machine Element*. 6th Editon: Prentice- Hall of India. New Delhi.

Suszkwi J. 2001. Combine attachment offers on the fly peanut cleaning: Retrived 20 October 2012, from the U.S. Department of Agriculture, Agriculture Research service web site. http://www. Ars.usda.gov/is/pr/2001/010919. html.

Sara, M. 2011. Discovery Health Magazine No. 52, Retrieved from http://www.TigernutandHealth.com. On the 20th May 2011.

Tim, F. 2009. *Modern tools for hopper design*: Freeman technology at www.freeman technology.Company.UK. Retrieved, May 20th 2011.

Temple, V. T., Ojobe, T.O., and Kapu, M. M. 1990. Chemical analysis of tiger nut (cyperus esculentus). *Journal, Science Food and Agriculture.* 50,261-263.

DEVELOPMENT OF A DIRECT ACTIVE SOLAR DRYER AND ITS USE IN DRYING CHESTER LEAVES (*HEINSIA CRINITA*)

A. F. Alonge[1] and U. S. Uduak[2]
Department of Agricultural and Food Engineering, University of Uyo,
Uyo, Akwa Ibom State, Nigeria
[1]Email: akindelealonge@uniuyo.edu.ng

ABSTRACT

A direct active solar dryer was designed and fabricated to dry Chester leaves (*Heinsia Crinita*) within one day but with features that will enhance its efficiency such as fans, battery, photovoltaic module, storage unit. Thus, it achieved solar drying utilizing forced convection to enhance the drying operation. Temperatures of the dryer were monitored on hourly basis while the moisture content analysis was done on a two (2) hourly basis. Test results showed that under no – load conditions, the dryer achieved a maximum temperature of 68.7°C under sunshine. *Heinsia Crinita* weighing 1000 g of initial moisture content of 66.4% (w.b) was reduced to a final moisture content of 11.5% (w.b) under eight (8) hours. The Vitamin C content of *Heinsia Crinita* leaves was also determined by Redox titration at the beginning and end of the drying operation. The Vitamin C content of the solar dried leaves was compared with that of Sun dried leaves. Vitamin C was found to decrease as the Drying took place from 14.3 mg/100 g to 6.23 mg/100 g at the end of the solar drying whereas the Vitamin C content was found to be 2.67 mg/100 g at the end of sun-drying. Solar drying preserved color to a great extent as compared to sun dried leaves. There was also significant reduction in drying time as compared to sun drying. Equipment tests showed that there was a significant retention of product quality at least when compared to sundrying. The dryer performed satisfactorily and is recommended to be used in drying other high moisture crops to achieve product stability.

KEYWORDS: Direct active, *heinsia crinita*, solar dryer, sun drying, vitamin C.

1. INTRODUCTION

Drying of vegetables have achieved so much attention because farmers grow vegetables which have to be sold in the market immediately after harvesting, when the production is high, the farmers have to sell the products at very low prices, thereby incurring great economic losses (Babagana *et al,* 2012).

Chester Leaves (*Heinsia Crinita)* popularly known locally as Atama in Efik and Tonoposho in Yoruba is also an edible green vegetable especially found in the Southern part of Nigeria. It is also used for various purposes such as making of soup, leaf extract used in the treatment of skin rashes, treatment of umbilical hernia and other medicinal purposes (Alobi *et al*, 2012). However, freshly picked leaves of *Heinsia Crinita* cannot store for a long time as it will begin to decay. This is due to its high moisture content of 67.8% (Udousoro and Ekanem, 2013). In order to prevent this, the leaves are processed to more stable forms but still suitable for intended use. It has been reported that processed forms of the leaves are exported for various medicinal applications and also for foreign hotels offering intercontinental dishes. One major way of achieving product stability for *Heinsia Crinita* leaves is by reducing its moisture content. This process is even carried out locally by sun drying (Abo *et al*, 2011).

An important strategy for achieving product stability for *Heinsia Crinita* is by drying. Drying is the removal of water from a product through the application of some energy source which can be in the form of direct solar energy or energy from burning fuel or electrical heating (Alonge, 1997). The main purpose of drying in preserving foods is to remove moisture, so that the water activity of the dried product is low enough (e.g a_w <0.6) to stop spoilage and the growth of pathogenic microorganisms and to reduce other deterioration processes [Ajav and Fakayode, 2011]. Generally, it has been accepted that safe moisture levels for vegetables and fruits are within the range of 7% - 15% and temperature ranges of 35^0C to 63^0C are quite recommended for drying vegetables and fruits.

Admittedly, drying *Heinsia Crinita* could be done naturally as in open air sun drying, drying in chimneys or other means of drying. But with these drying methods are associated problems such as low product quality, questionable product safety, reduced market value, vulnerability to natural elements such as rain, insects, rodents or other animals, wasted time among others. In view of these, there is need to develop a system that can significantly minimize these problems. Solar dryers have been found to be an effective means to reduce associated problems that comes with achieving product stability. It is essential to mention that solar dryers are very economical and efficient, one reason for such owing to its availability and low cost implication. Solar drying is a process of using solar energy to heat air/or the products so as to achieve drying of agricultural products (Ajay *et al*, 2009).

Babagana *et al* (2012) designed and constructed a forced/ natural convection solar vegetable dryer with heat storage. Using this system, it was found out that the drying time of tomato, onion, pepper and spinach were greatly reduced as compared to open sun drying. Alonge and Adeboye (2012) evaluated the drying rates of some fruits vegetables with passive solar dryers. The passive solar dryers which were direct and indirect types were tested with pepper, okro and vegetables. The crops dried faster with the direct passive solar dryer than with the indirect passive solar dryer.

Alonge and Eke (2011) developed and evaluated a medium scale direct mode passive solar Tomato dryer. The dryer achieved over 50% in drying time when compared with the time taken in open sun drying. Moisture of tomato sample was reduced from 93.5% wet basis to 4.5% wet basis within 58 hours while the open sun drying took 124 hours. The problem is to design a solar drying system that will be able to dry *Heinsia Crinita* leaves to acceptable moisture levels preferably 12% or less required to obtain product stability under a period of one day .It is important that the products be dried under one day as intermittent drying could lead to spoilage due to bacterial infestation. Besides, if the product stays for too long in the drying unit, quality deterioration will occur.

Hence, to achieve drying in one day, the solar drying unit will be a forced convection dryer since natural convection dryers may not achieve desired drying within one day. Also, since mass production of the products for increased commercialization is of essence, drying has to take place faster, hence the need for an active solar dryer. The means used in achieving forced convection in the system will be through a fan which will be powered by a photovoltaic module which also charges a battery to supplement power for the fans. To further complement the fan, the solar dryer will incorporate a heat storage unit which will serve as a supplement during off sunshine hours.

The aim of this project is to design, construct, and test a direct active solar dryer with storage unit for *Heinsia Crinita* leaves which will achieve drying under a period of one day and also find out the effect of direct active solar drying on Ascorbic acid (Vitamin C) content of the leaves as compared to conventional sun drying. The results of No – load dryer test, Loaded dryer performance test, Solar drying test, Sun drying test as well as Ascorbic Acid determination are discussed.

2. MATERIALS AND METHODS

2.1 Materials

Fresh *Heinsia Crinita* were obtained from a local market in Uyo, Akwa Ibom State, Nigeria. It was directly transported to the drying site. The moisture content was determined using AOAC (2000) methods and the initial moisture contents for both first and second replications were 69.4% and 66.4% wet basis respectively.

2.2 Direct Active Solar Dryer

A sectional view of the Direct Active Solar Dryer is shown in Fig.1 while Fig.2 shows the actual picture of the dryer. The Dryer was designed designed and built in the Department of Agricultural and Food Engineering, University of Uyo. Features of the dryer include: solar collector, storage unit, photovoltaic module, battery, axial flow inlet and outlet fans, mesh tray, drying chamber, glass cover, switch.

The design of the dryer was based on the following considerations:

i. Meteorological Data collection.
ii. Amount of moisture to be removed from a given quantity of wet crop to bring it to safe storage level in a specific time.
iii. Physical features of the dryer
iv. Dryer area and dimension
v. Amount of heat stored in storage unit
vi. Fan capacity
vii. To reduce heat loss due to convection and radiation.
viii. Construction materials.
ix. Quantity of air needed for drying.

Sanitary considerations as well as Economic considerations were made in the course of constructing the dryer.

Basically, the equipment is a structure with frames made of wood. It has a short frame at the front which contains the suction inlet fan and a tall frame at the back which contains the door and the exhaust fan. The side frames constitute the length of the dryer and attached to one side of it are the battery ports and photovoltaic attachment. It incorporates a glass cover at the top for the greenhouse effect and thus the heat needed for drying operation. The dryer has a storage unit which is underneath the absorber plate at the bottom of the dryer. It is designed to absorb heat during sunshine hours and release the stored heat during off sunshine hours . The dryer is painted grey on the outside to prevent heat loss. The equipment has no external insulation as the thickness of the frame material is considered to provide reasonable insulation.

The solar drying equipment works on the principle of forced convection. The dryer has a suction inlet fan which delivers ambient air over the absorber plate, thereby causing convective heat transfer to take place from the absorber plate to the air. The heated air then rises and in the process comes in contact with the product on the mesh trays. There is convective heat transfer to the product resulting in the vaporization of water in the product. Thus, it is a simultaneous heat and mass transfer process. The mass (water) is then transferred to the hot dry air thereby causing it to be humid. At this point, the exhaust fan at the outlet exhausts the humid air to the environment.

The glass cover at the top also provides heat via the greenhouse effect. This heat is also absorbed by the collector and also used for the drying process. Thus, the principle of forced convection delivers more heated air to speed up the drying process and also exhausts more humid air to enhance the drying process. Moreover, as the name of the equipment implies, the products in the dryer are directly exposed to the sun during drying operation. This further enhances the drying operation. The Technical Specifications for major items of the Dryer is presented in Table 1.

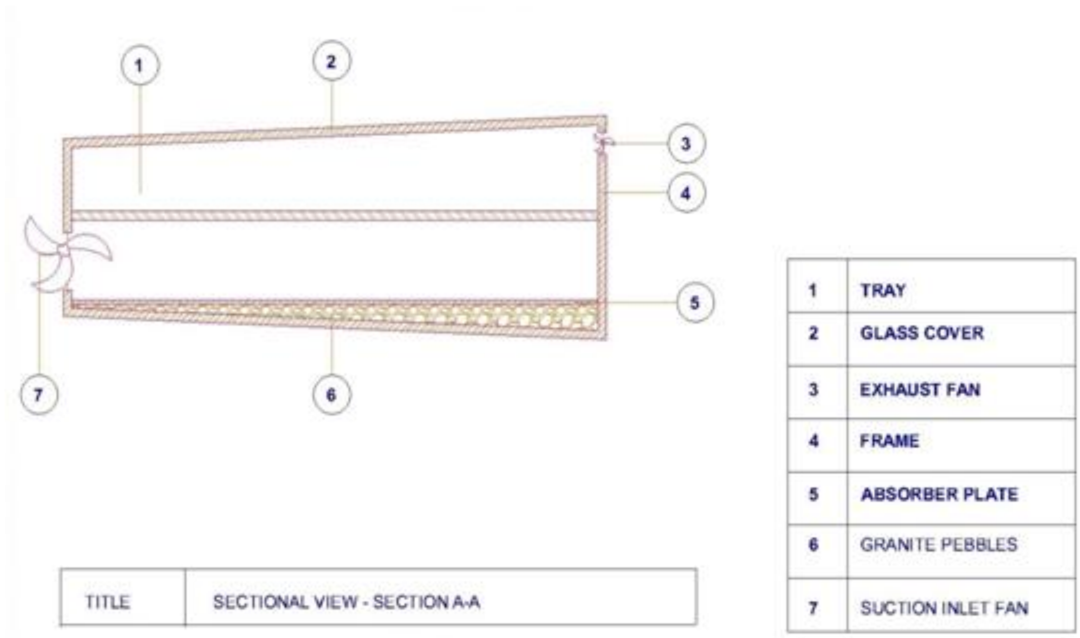

Figure 1. Sectional View of the Director Solar Dryer

Figure 2. Front View of Dryer

Some of the important design calculations made were as follows:

a) Design Basis: 1kg of *Heinsia Crinita* leaves

b) Amount of water to be removed from products

$$M_W = M_P(M_i - M_f) / (100 - M_f) \qquad (1)$$

Where M_W = amount of water to be removed (kg)

M_p = mass of product (kg)

M_i = initial moisture content (%)

M_f = final moisture content (%)

c) Average drying rate

$$\mathbf{d_r = {}^{m_r}/_{t_d}} \qquad (2)$$

Where M_r = amount of moisture removed (kg)

t_d = drying time(hrs)

d) Mass of air required for evaporation

This shall be gotten from the energy equation for the evaporation of water.

$$M_W L_V = m_a C_p (T_1 - T_2) \qquad (3)$$

Where M_W = mass of water (kg)

L_V = latent heat of vaporization (kJ/kg)

m_a = mass of air (kg)

C_p = specific heat capacity of air (kJ/kg°C)

T_1 = final temperature (expected dryer temperature) (^{0}C)

T_2 = initial temperature (ambient temperature) (°C)

e) Collector useful thermal energy gain

$$Q = \left[C_P W_P (T_C - T_A) + \quad L_V \left(MC_i W_P - MC_f (W_P - MC_i W_P)\right)\right] \qquad (4)$$

Where Q = collector useful thermal energy gain (kJ)

C_p = specific heat capacity of product (kJ/kg°C)

T_c = collector temperature (°C)

T_a = ambient temperature (°C)

L_v = latent heat of evaporation (kJ/kg)

MC_i = initial moisture content (%)

Wp = weight of product (kg)

MC_f = final moisture content (%)

f) Mass/Volume flowrate of air

$$m_{a1} = {}^{M_a}/_{t_d} \qquad (5)$$

Where $m_{a1} = mass\ flowrate\ of\ air$

$$v_a = {}^{m_{a1}}/_{\rho} \qquad (6)$$

Where $v_a = volume\ flowrate\ (m^3/hr)$
$\rho = density\ of\ air\ (kg/m^3)$

g) Area of Collector: Neglecting heat losses, the rate of heat absorption by a solar collector can be estimated as:

$$Q/A = (\tau\alpha I_0) \qquad (7)$$

Where Q = heat absorbed by solar collector (kJ)

A = area of solar collector (m^2)

$\tau\alpha$ = transmittance - absorptivity index of collector

I_0 = incident solar radiation (W/m^2)

Table 1: Technical Specification of Major Components in the Dryer.

Item	Specification
External dryer dimensions	1.29m(length) × 0.51m(width) × 0.52(height of long frame) × 0.37m(height of short frame).
Area of solar collector	0.6m^2
Fans	Inlet fan: axial flow, 10cfm, 12VDC Outlet fan: axial flow, 5cfm, 12VDC
Photovoltaic module	Crystalline carbon, 15WP, 17VMP
Battery	18V, < 5.1A initial current
Heat storage material	Black Granite
Temperature range of dryer	58°C - 63°C

2.3 Experimental Methods

2.3.1 No – Load Dryer Test

As the name implies, this was done with no product inside the dryer for eleven hours. The values for the following parameters were recorded on an hourly basis: time, collector temperature, cabinet temperature, outlet temperature, ambient temperature.

2.3.2 Drying Tests

This was carried out with two replications each for the *Heinsia Crinita*. The leaves (1kg) were loaded onto the drying tray and then placed inside the dryer. The door of the dryer was shut, then the switch was switched on for the drying process to begin. The parameters used to characterize the drying tests include: collector temperature, ambient temperature, cabinet temperature, outlet temperature which were used to derive the dryer performance curves under each loaded test.

Moisture content analysis in triplicates for both replicates was done on a two (2) hourly basis for the crop dried. For sun drying, 1kg of *Heinsia Crinita* leaves were spread out in the sun on a clean suface and away from contaminating influences.

2.3.3 Vitamin C Determination

Vitamin C concentration in *Heinsia Crinita* was determined by Redox Titration as reported by the Outreach College of Science, University of Cantebury. This method determines the vitamin C concentration in a solution by Redox titration using iodine. As the iodine is added during the titration, the ascorbic acid is oxidised to dehydroascorbic acid, while the iodine is reduced to iodide ions. The determination was carried out for fresh, solar dried and sun dried *Heinsia Crinita* leaves. The determination was divided into:

a) Sample Preparation: 100g of sample was cut into small pieces and grinded in a mortar and pestle. 10ml of distilled water was added several times while grinding the sample, each time decanting off the liquid extract into a 100ml volumetric flask. Thereafter, the ground vegetable pulp was strained through a cheese cloth, rinsing the pulp with a few 10ml portions of water and collecting all filtrate and washings in the volumetric flask. The extracted solution was made up to 100ml with distilled water.

b) Titration

i) 20ml aliquot of the sample solution was pipetted into into a 250ml conical flask and 150ml of distilled water and 1ml of starch indicator solution was added.

ii) The sample was titrated with a $0.005 molL^{-1}$ iodine solution. The endpoint of the titration was identified as the first permanent trace of a dark blue-black colour due to the starch-iodine complex.

iii) The titration was repeated two more times with further aliquots of sample solution until concordant results were obtained.

3. RESULTS AND DISCUSSION

3.1 Result of No – Load Dryer Test

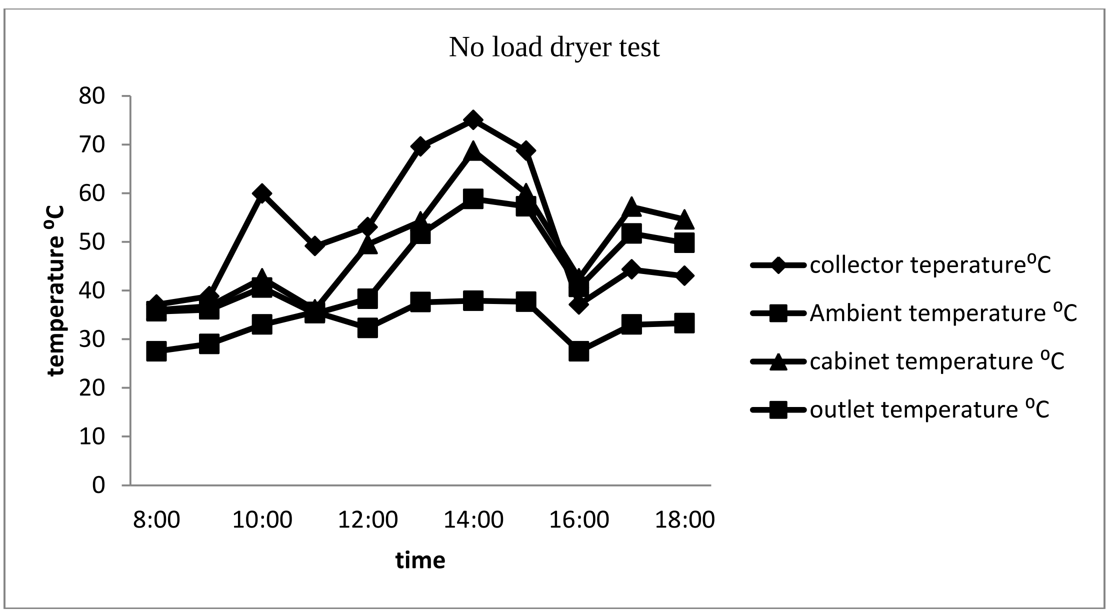

Figure 3: Curves of Collector, Ambient, Cabinet and Outlet Temperatures versus drying Time at No - Load

The result from Figure 3 showed a steady increase in temperature as the solar insolation increased. The collector reached the greatest temperature at 75℃ during the day at 14:00 hours. However, due to the fluctuations in weather conditions, the collector surface experienced a series of temperature drops. The collector temperature started decreasing as the day went by and as the solar insolation decreased. The collector minimum temperature was 37.1℃.

The ambient temperature oscillated about the mean temperature for Uyo metropolis - 32℃. It reached its peak of 37.9℃ at 14:00 hours. The minimum ambient temperature for that day was 27.5℃ at 8:00 hours.

The cabinet temperature steadily increased as the insolation increased. It reached a peak of 68.7℃ at 14:00 hours. It had a minimum temperature of 36℃ at 8:00 hours.

As the graph above clearly shows, the temperature at the outlet closely followed the cabinet temperature but differed only with some minor differences in temperature. However, it generally takes the shape of the cabinet temperature. Thus, it can be inferred that at no – load, the dryer achieved its objective drying temperature of 59℃ for which it was designed for and even exceeded it by 9.7℃. However, it should be noted that the dryer was tested during the rainy season when solar insolation is highly unstable. But, even with that, the dryer showed good results and has a better potential if tested during the dry season.

3.2 Loaded Dryer Performance Curve for *Heinsia Crinita* Leaves (1st and 2nd Replications)

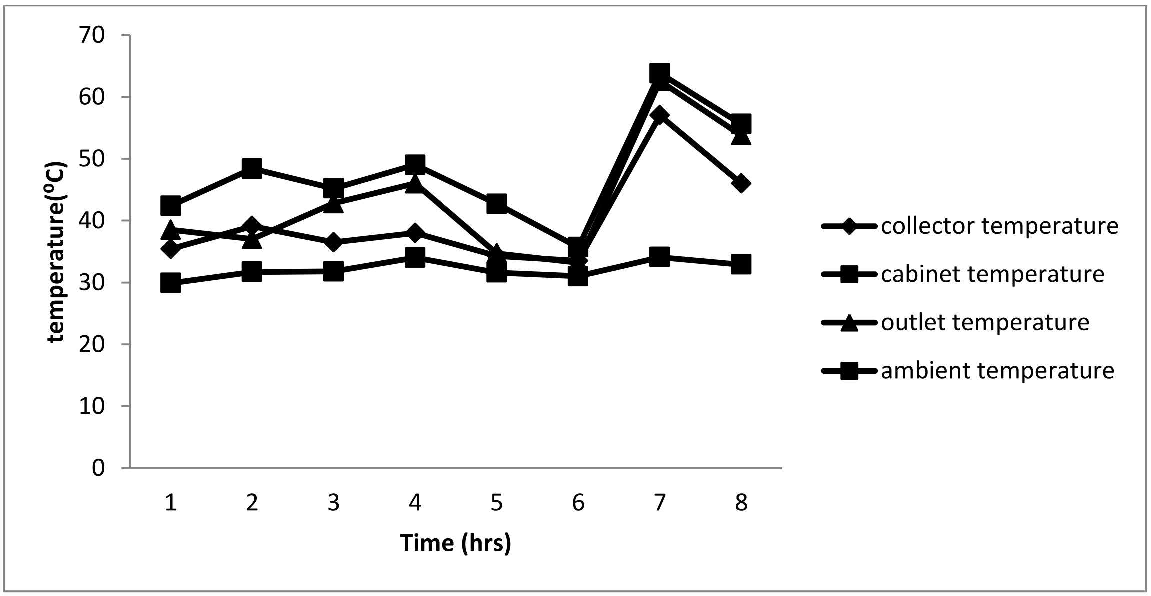

Figure 4: Curves of collector, Ambient, Cabinet and outlet Temperatures versus Drying time for Dryer Loaded with *Heinsia Crinita* – 1st Replication

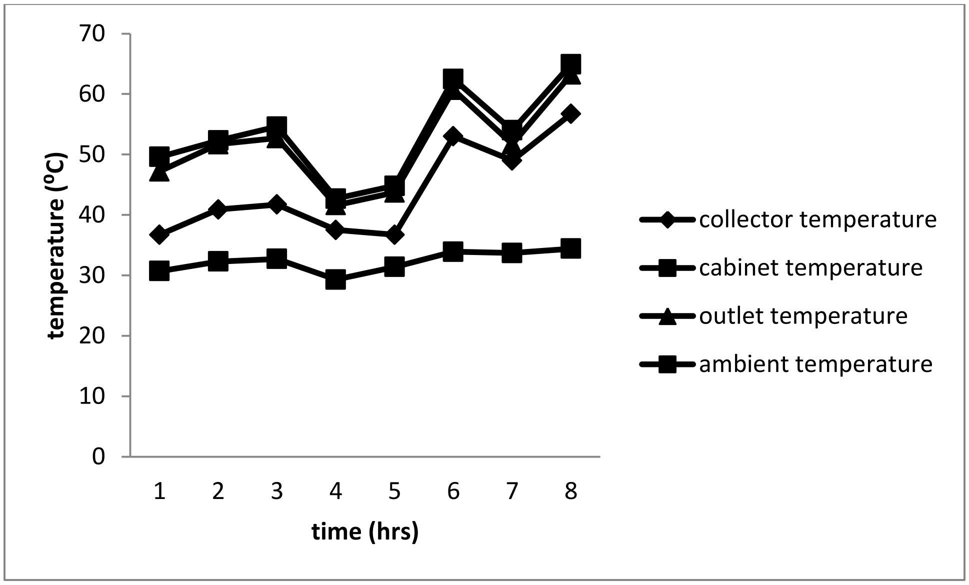

Figure 5. Curves of Collector, ambient, Cabinet and Outlet Temperatures versus Drying Time for Dryer Loaded with *Heinsia Crinita* – 2ne Replication

Both graphs (Figs. 4 & 5) show difference in performance mainly due to the weather patterns on the days of the first and second replication. The graph for the first replication showed wide fluctuations in the collector, cabinet and outlet temperatures. However, the graph for the second replication showed better results as the collector, cabinet, outlet and ambient temperatures followed a regular pattern of steady increase and drops.

3.3 Drying Curve for *Heinsia Crinita* (1st And 2nd Replication)

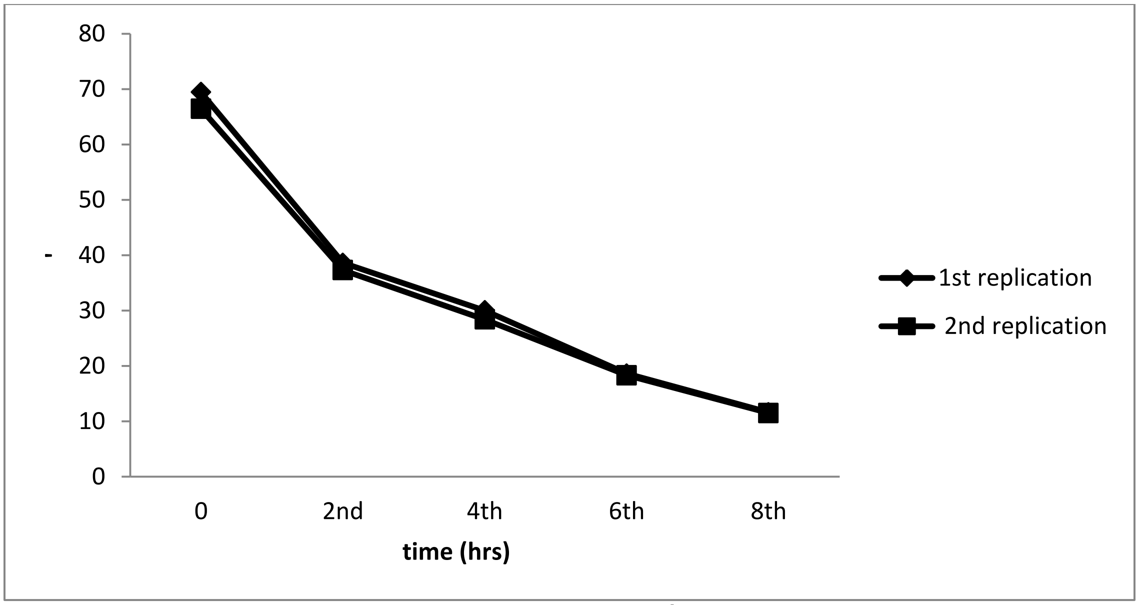

Figure 6. Drying Curves for *Heinsia Crinita* **-** (1st and 2nd Replications)

As seen from the graph (Figure 6), the drying curves for both the first and second replications seem to coincide with each other except at some points where the curves are seen as two distinct curves. This shows that the drying of *Heinsia Crinita* for both replications follow the same pattern. The first replication drying curve shows that there was a steady decrease in moisture content from its initial moisture content of 69.4% until the end of the drying time at which a moisture content of 11.6% was achieved.

The curve for the second replication showed a decrease in moisture content from its initial moisture content of 66.4% till a final moisture content of 11.5% was achieved at the end of the drying period. Both replications showed a good result and agrees with the objective of the design which is to reduce the moisture content of the leaves to a safe level of 12% moisture content.

3.4 Result of Sun Drying Test

It took more than one day to achieve product stability for Sun dried samples as compared to solar dried samples which took eight (8) hours. Sun dried samples also showed the least colour retention as compared to the solar dried leaves which preserved colour significantly.

3.5 Result of Vitamin C Determination

The Ascorbic acid (Vitamin C) content of the fresh *Heinsia Crinita* was 14.3mg/100g and the Ascorbic acid (Vitamin C) content of the Solar dried leaves was 6.23mg/100g while the Ascorbic acid (Vitamin C) content of the Sun dried *Heinsia Crinita* was 2.67mg/100g.

The results show that the vitamin C content the leaves decreased as the drying operation took place. Sun dried *Heinsia Crinita* especially showed a marked reduction in Vitamin C content. This declination is due to the fact that ascorbic acid is destroyed by heat and atmospheric oxygen. Thus, it can be concluded that the drying operation reduced the vitamin C content of the *Heinsia Crinita* leaves markedly.

4. CONCLUSIONS

The design and fabrication of a direct active solar dryer was done for drying *Heinsia Crinita* under a period of one (1) day. The performance of the dryer under test conditions showed that it is technically and economically feasible and easy to operate and maintain. This was especially because of the enhanced air flowrates inside the dryer. Evaluation of the test results have clearly shown that the direct active solar dryer performed satisfactorily and reduced drying time considerably when compared to sun drying for the same kind of crop. Results conclusively showed that Solar Drying preserved certain quality attributes of the leaves such as Vitamin C and colour. Thus it can be seen that considerable reduction in drying time for the leaves will result in economies of scale for mass production of the dried leaves.

REFERENCES

Abo, K. A., Lawal, I. O. And Ogunkanmi, A. 2011. Evaluation of extracts of *Triclisia Suboardata* Oliv and *Heinsia Crinita* for antimicrobial activity against some Clinical bacterial isolates and fungi. African Journal of Pharmacy and Pharmacology. 5(2), 125-131.

Ajav, E. A And Fakayode, O.A. 2011. Design and Construction of an Electric Dryer for some Tropical perishable Crops. Proceedings of 32nd Annual conference of Nigerian Institution of Agricultural Engineers (NIAE). 32, 452- 464.

Ajay, C.,Orsunil K. S. and Deepak D. P. 2009. Design of Solar Dryer with Turbo ventilator and Fireplace. Online at www .solarfood.org. Accessed on 29/5/2013.

Alobi, N. O., Ikpeme, E. M., Okoi, A. I., Etim, K.D. And Eja, M. E. 2012. Phytochemical and Nutritional profile of *L. African, H. Crinita* and *G. Latifolium.* New York Science Journal. 5(3). 45-48.

Alonge, A. F. 1997. A Natural Convection Solar Crop Dryer. Proceedings of 19th Annual Conference of the Nigerian Society of Agricultural Engineers (NSAE). 19, 211-214.

Alonge, A. F and Adeboye, O. A 2012. Drying Rate of some Fruits and Vegetables with Passive Solar Dryers. International Journal of Agricultural and Biological Engineering. 5(4) 83 – 90.

Alonge, A. F. and Eke, A. B 201. Development and Evaluation of a medium Scale Direct mode Passive Solar Tomato Dryers. Department of Agricultural and Food Engineering University of Uyo/Department of Agricultural and Bioresource Engineering, University of Agriculture, Umudike, Nigeria.

AOAC. 2000. Official Methods of Analysis, 17th Ed., Association of Official Analytical Chemists, Maryland, VA.

Babagana, G, Silas K, and Mustafa, B. G. 2012. Design and Construction of Forced/Natural convection Solar Vegetable dryer with Heat Storage, Asian Research Publishing Network (ARPN) Journal of Engineering and Applied science . 7(10), 1213 – 1217.

Outreach College of Science, University of Canterbury, Private Bag 4800, Christchurch, New Zealand. Determination of Vitamin C. concentration by Titration. Online at www.outreach.cantebury.ac.nz. Accessed on 28/5/2014.

Udousoro, I and Ekanem, P. 2013. Assessment of Proximate Composition of twelve edible Vegetables in Nigeria. International Journal of Modern chemistry. 4(2), 79- 89.

EFFECT OF INOCULUM TO SUBSTRATE RATIO ON BIOGAS PRODUCTION FROM SHEEP PAUNCH MANURE DIGESTED IN BATCH BIODIGESTERS

A. A. Lawal, A. U. Dzivama and M. K. Wasinda
Department of Agricultural and Environmental Resources Engineering
Faculty of Engineering, University of Maiduguri, Maiduguri, Borno State, Nigeria.
Corresponding author; Email: abulawal2010@yahoo.com

ABSTRACT

In this study sheep paunch manure (SPM) was anaerobically digested under mesophilic condition to determine its biogas potential. Three inoculums to substrate (I/S) ratios 1.3, 1.9 and 3.8 were digested in biodigesters labeled R1, R2 and R3 respectively to determine the effect of substrate concentration on biogas yield. Results showed that I/S ratio had significant effect on biogas production rate and accumulation. Biogas production rate increased to their peak in the order of R3 (0.30526 Nm^3/kgVSd), R2 (0.15308 Nm^3/kgVSd) and R1 (0.11009 Nm^3/kgVSd) on day 5 and decreased to zero on day 27, 29 and 31 of the digestion period respectively. Biogas production accumulation increased from 0.57195 to 1.46784 Nm^3/kgVS as I/S ratio increased from 1.3 to 3.8. Linear and exponential regression equations were used to simulate biogas production rate while biogas production accumulation was simulated using first order kinetic and modified Gompertz equations. Coefficient of determination (R^2) of linear regression equation of biogas production rate ranged from 0.707 to 0.797 while exponential regression equation had R^2 values that ranged from 0.7718 to 0.9929 showing better simulation. R^2 of first order kinetic equation ranged from 0.9769 to 0.9827 while R^2 for modified Gompertz ranged from 0.9965 to 0.999. Thus modified Gompertz equation showed better simulation of biogas production accumulation.

KEYWORDS: Manure, anaerobic digestion, I/S ratio, biogas production rate and accumulation, simulation.

1. INTRODUCTION

Biomass is one of the renewable sources of bioenergy capable of significant contribution to the global future energy supply (WEC, 2004). Bioenergy generated from diverse sources provides local energy needs, reduce dependence on fossil fuel and help mitigates greenhouse gas effect. The main concerns limiting bioenergy utilization are relative inefficiency and cost of conversion technologies. However, anaerobic digestion of residue/waste materials from agricultural crops, animal rising and agro-processing industries could be of simple, efficient and low cost technology.

Anaerobic digestion occurs when organic material is converted biologically in the absence of oxygen to gaseous product called biogas (Angelidaki, 2002). Studies on anaerobic digestion process of several organic residues/wastes have led to the understanding of their inherent conversion potentials and kinetics that resulted to design, development and process control and optimization of biodigesters. But to fully utilize biogas potentials from biomass materials, biogas production behavior and potentials of more organic residue/waste materials need to be determined.

Researches to determine biogas potential of several substrates have been conducted for similar purpose. Buswell and Mueller (1952), Baserga (1998) and Raposo et al. (2011) proposed empirical relationship that utilizes the elemental or organic chemical compositions of biomass to estimate its theoretical maximum biogas yield. Researchers (Chynoweth et al., 1993; Hansen et al., 2004; Wymyslowski et al., 2010; Feng et al., 2013; Monch-Tegeder et al., 2013; Zhang et al., 2013) have investigated the biochemical methane potential of several substrates and co-substrates using batch method. They determined physicochemical compositions of substrate and developed anaerobic assay for biogas production. The effects of operating parameters on biogas potential have been investigated. Researchers (Chynoweth et al., 1993; Labatut et al., 2008; Feng et al., 2013; Kheiredine et al., 2014) investigated the influence of inoculums to substrate ratio by varying the amount of substrate added to inoculums. The effect of temperature and pH were also investigated (Hashimoto et al., 1981). Simulation studies on biogas production accumulation and conversion kinetics of several substrates have been conducted (Raghunathan et al., 2008; Yusuf et al., 2011; Adiga et al., 2012; Feng et al., 2013) and results showed that different substrates have different potential and conversion kinetics.

The objectives of this study were to evaluate the effect of inoculums to substrate ration on biogas production of sheep paunch manure (SPM) under mesophilic condition and to simulate the biogas production rates and accumulation.

2. MATERIALS AND METHOD

2.1 Sample Collection, Conditioning and Characterization

2.1.1 Inoculums

For the purpose of this study cow dung was used as inoculum. Sample of fresh cow dung, 2 kg, were collected at the animal farm University of Maiduguri, Nigeria and taken to Agricultural and Environmental Resources laboratory of same institution for experiment. In order to adapt the inoculums to mesophilic condition, cow dung were diluted in distilled water to 10% dry matter (DM) and transferred into a 4 liter glass bottle. The headspace of the 4 liter glass bottle was flushed with a gas mixture of 80% N_2 and 20% CO_2 and closed with a thick rubber septum which was held tight by a resin. The inoculums solution was then incubated in a water bath at 35 ± 1^oC. During incubation, the inoculums solution was degassed completely by allowing gas build-up in the headspace to escape via a valve controlled tube.

2.1.2 Substrate

Approximately 2 kg of fresh SPM was collected at animal slaughter house, Maiduguri. Sample collected was stored over ice and delivered to the laboratory for experiment and analysis. Sub-sample of SPM was collected and diluted to 15%, 10% and 5% (DM) and transferred separately into 2 liter glass bottles and stored at 5^oC.

2.1.3 Nutrient medium

A nutrient medium containing the following groups of nutrients and vitamins was prepared:

a. Nacl, $Mgcl_2.6H_2O$, $Cacl.2H_2O$
b. $Fecl_2.4H_2O$, $Zncl_2$, $Mncl_2.4H_2O$, $(NH_4)_6Mo_7O_{24}$
c. Folic acid and ridoflavin

Stock solutions were prepared by dissolving specific quantities (g) of the nutrients from a group in 1 liter distilled water. 10, 1 and 1 ml of a, b and c stock solutions were then added to 988 ml distilled water to obtain the nutrient medium used for the experiment.

2.2 Physicochemical Composition Analysis

Fresh samples of the inoculums and SPM were analyzed for total solids (TS) and volatile solids (VS) contents according to the standard method of American Public Health Association (APHA, 1992). The method involved TS determination by oven drying sample at 95^oC until weight was constant and subsequent oven drying TS for 1 hour at approximately 550^oC to determine proportion of matter lost in the dried sample. To determine the carbohydrate, crude protein, crude fat, crude fiber and ash content, SPM sample was analyzed at Soil Science Laboratory, University of Maiduguri.

2.3 Batch Digestion Test

Biogas unit

The biogas unit consisted of the following equipment:

- A unit comprises of 200 ml glass bottle and a thick rubber septum with a flexible rubber tube fixed on the rubber septum through an opening was used as biodigester.
- A thermostatically controlled water bath with a plastic rack used for agitating and keeping biodigesters in place.
- A 100 and 10 ml plastic syringe and gas pressure gauge.
- 80% N_2 and 20% CO_2 gas mixture.

2.4 Experimental Procedure

In this experiment 60 ml of the degassed inoculums (10% DM) was collected after shaking using 100 ml plastic syringe and transferred into a biodigester unit. 1 ml of nutrient medium and 30 ml of a SPM substrate solution were collected and added to the biodigester unit containing inoculums. This procedure was carried out in 3 biodigesters labeled R1, R2 and R3 containing inoculum to substrate ratios of 1.3, 1.9 and 3.8 respectively and control (biodigester containing only inoculums). Biodigesters were flushed with 80% N_2 and 20% CO_2 gas mixture and transferred into water bath preset at 35 ± 1^oC. The entire biodigester unit was agitated twice a day. Biogas produced was measured using gas pressure gauge twice daily at the initial stage and once daily toward the final stage of the process until no more biogas was produced. After every measurement of biogas accumulation over time biogas was allowed to escape in order to avoid pressure build up that would exceed pressure gauge capacity. This experiment was repeated 3 times and average was reported as biogas production.

2.5 Simulation of Biogas Production Rate and Accumulation

Biogas production rate of SPM was simulated using linear and exponential plots. Equation 1 was used for linear simulation with the assumption that biogas production rate increased linearly to its peak and then decreased linearly to zero. Exponential equation (equation 2) also was used to simulate the increasing and decreasing of stages biogas production rate under the assumption that production rate increased exponentially to peak and then decreased exponentially.

$$B_l = a_l + b_l \times t \qquad (1)$$

$$B_e = a_e + b_e \times \exp(c_e t) \qquad (2)$$

B_l and B_e are biogas production rates for linear and exponential estimation ($Nm^3/kgVSd$) at time (day), t is the time (day) of digestion period, a_l is intercept ($Nm^3/kgVSd$) and b_l is slope ($Nm^3/kgVSd^2$), a_e and b_e are constants ($Nm^3/kgVSd$) and c_e is constant (d^{-1}) and is negative for decreasing stage. Finally biogas production accumulation was simulated using the first order kinetic and modified Gompertz equations:

$$B_f = B_{Of}\,(1 - \exp(-k \times t)) \qquad (3)$$

$$B_G = B_{OG} \times \exp\{-\exp[(\mu_m \times e/a_G)(\lambda - t) + 1]\} \qquad (4)$$

where B_f and B_G are biogas production accumulation for first order kinetic and modified Gompertz equations respectively at time (day), B_{Of} and B_{OG} are maximum biogas production for first order kinetic and modified Gompertz equations ($Nm^3/kgVS$), k is first order kinetic constant, μ_m is maximum biogas production rate ($Nm^3/kgVSd$), λ duration of lag phase and e is equal to 2.718282.

2.6 Statistical Analysis

Simple descriptive statistical analysis was used to report averages and standard deviations of experimental data. ANOVA test was used to detect if there was significant difference on biogas production rate and accumulation due to the effect of I/S ratios. Statistix version 9 software was used to determine equation parameters while Microsoft excel was used to plot graphs.

3. RESULTS AND DISCUSSION

3.1 Characteristics of SPM and Inoculums

The physicochemical composition of SPM and inoculums determined are presented in Table 1. The ash content of SPM was 4.3% which resulted to a high VS/TS ratio of 93.7% indicates that SPM could be a suitable substrate for anaerobic digestion. The pH level of SPM was within anaerobic digestion range.

Table 1: Physicochemical Compositions of SPM and Inoculum

	Moisture content (%)	Total solids% (w.b)	Volatile solids% (w.b)	VS/TS ratio	pH	Carbo hydrate % (TS)	Crude protein % (TS)	Crude fat% (TS)	Crude fiber % (TS)	Ash% (TS)
SPM	82.4(2.43)	17.4(1.76)	16.3(2.44)	0.937	7.8 (0.518)	36 (2.91)	9.5 (0.97)	1.1(0.44)	46 (1.85)	4.3(0.84)
Inoculum	24.04 (3.13)	75.9(3.51)	67.6 (4.67)	0.89	ND	ND	ND	ND	ND	ND

3.2 Biogas Production Rate and Accumulation

Experimental result showed no biogas produced from controlled biodigester over the digestion period. Figure 1 (a) and (b) presents SPM biogas production rate and accumulation plots. Results showed that it took biodigesters R1, R2 and R3 31, 29 and 27 days to complete digestion respectively. It appeared that as I/S ratio increased from digestion period decreased and biogas production rate increased from. It can be observed from Figure 1 (a) that the biogas production rate curves of all biodigesters exhibited similar pattern over the entire digestion period where R3 biodigester exhibited maximum biogas production rates followed by R2 and R1 biodigesters respectively. The peak (maximum) biogas production rate occurred on the 5th day for all biodigesters in the order of R3 (0.30526 $Nm^3/kgVSd$), R2 (0.15308 $Nm^3/kgVSd$) and R1 (0.11009 $Nm^3/kgVSd$). It is apparent that I/S ratio had significant effect ($p<0.0372$) on biogas production rate. Total accumulated biogas produced was found to be in the order of 1.46784, 0.88177 and 0.57195 $Nm^3/kgVS$ in R3, R2 and R1 biodigesters respectively. Raghunathan et al., (2008) reported closely similar biogas production accumulation values (1.1 to 0.382 $Nm^3/kg\ VS$). Experimental results showed that 80% of maximum biogas production in biodigesters R1, R2 and R3 had accumulated on the 14th, 15th and 14th day of digestion period respectively.

Figure 2(a and b) shows the linear regression line fitted to rising and falling limbs plots of experimental data of biogas production rate in R1, R2 and R3 biodigesters. Equations 5 to 10 present the linear relationship between biogas production rates and digestion period:

$R1_{A,}$ $B_l = 0.019t - 0.005$, $R^2 = 0.784$ (5)

$R2_{A}$, $B_l = 0.025t - 0.014$, $R^2 = 0.731$ (6)

$R3_{A}$ $B_l = 0.051t - 0.034$, $R^2 = 0.707$ (7)

$R1_{D}$ $B_l = 0.001t - 0.035$, $R^2\ 0.757$ (8)

$R2_{D}$ $B_l = 0.002t - 0.066$, $R^2 = 0.797$ (9)

$R3_{D}$ $B_l = 0.004t - 0.115$, $R^2 = 0.766$ (10)

where B_l is linear estimation of biogas production rate ($Nm^3/kgVSd$), subscripts A and D represent rising and falling limbs, and t is time (day). The coefficient of determination of falling limbs showed better linear simulation than rising limbs except in R1 biodigester. The exponential regression line simulating biogas production rate for both limbs are presented in Figure 3(a and b). The following equations (equations 11-16) expressed the exponential relationship between biogas production rates and digestion period:

$R1_A$, $B_e = 0.00533+0.00491\exp(0.6144t)$, $R^2 = 0.9065$ (11)
$R2_A$, $B_e = 0.0118+0.00087\exp(1.0175t)$, $R^2 = 0.9822$ (12)
$R3_A$, $B_e = 0.0154+0.00236\exp(0.9642t)$, $R^2 = 0.9749$ (13)
$R1_D$, $B_e = -0.0733+0.1111\exp(-0.0146t)$, $R^2 = 0.9929$ (14)
$R2_D$, $B_e = 0.0236-1.14\times10^{-7}\exp(-220.52t)$, $R^2 = 0.9075$ (15)
$R3_D$, $B_e = 0.0362-7.8\times10^{-8}\exp(-107.82t)$, $R^2 = 0.7718$ (16)

where B_e is exponential estimation of biogas production rate ($Nm^3/kgVSd$). R^2 of exponential equation of biogas production rates ranged from 0.7718 to 0.9929, where rising limbs showed better simulation than falling limbs except R1 biodigester. Exponential regression appeared to show better simulation of biogas production rates than linear regression except for falling limb of R3 biodigester.

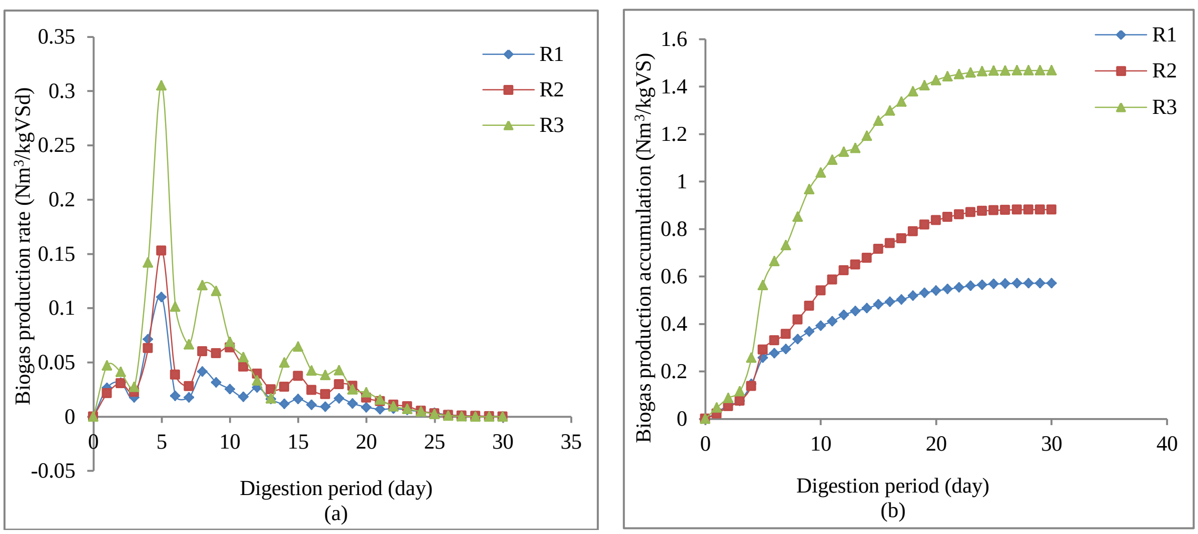

Figure 1. Biogas production rate (a) and accumulation (b) in R1, R2 and R3biodigesters.

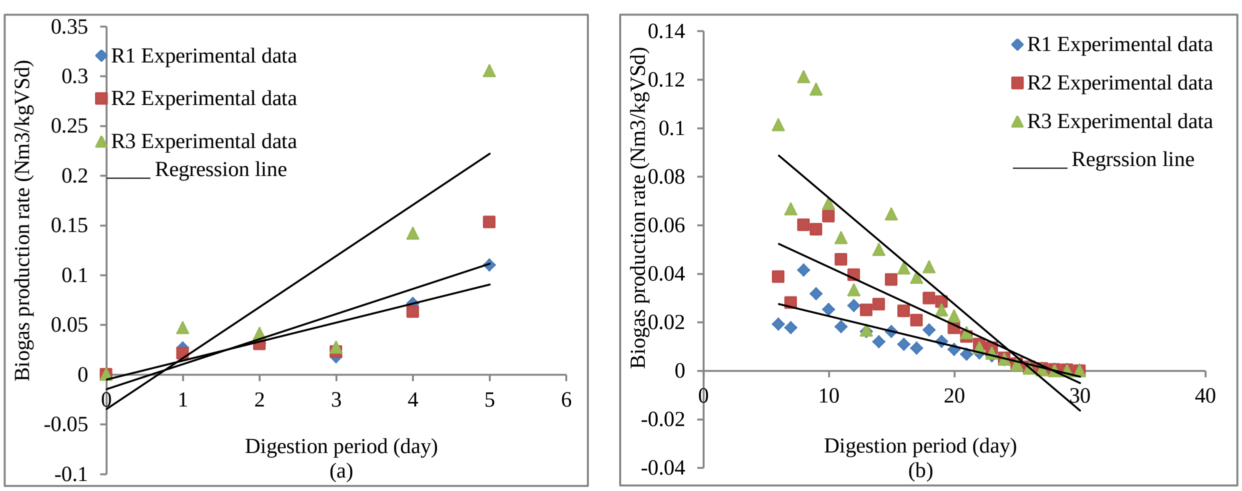

Figure 2. Linear plots of biogas production rates of rising (a) and falling (b) limb in R1, R2 and R3 biodigesters.

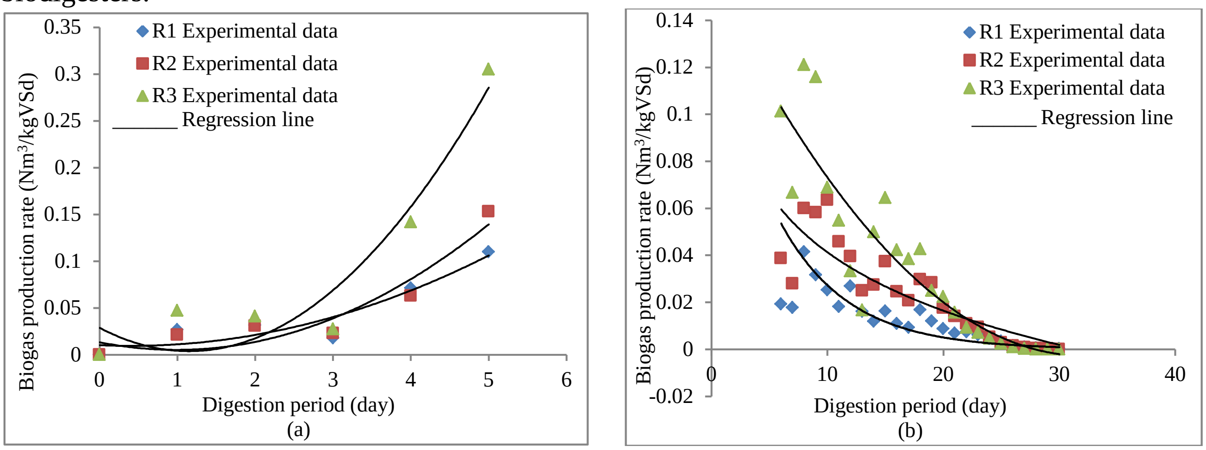

Figure 3. Exponential plots of biogas production rates of rising (a) and falling (b) limb in R1, R2 and R3 biodigesters.

The first order kinetic and modified Gompertz plots of biogas production accumulation are presented in Figure 4 (a and b). The first order kinetic constants (k) were found to be in the order R1 (0.0926), R3 (0.0858) and R2 (0.0649), while estimated biogas potential increased as I/S ratio decreased (Equations 17 to 19). In modified Gompertz equation, R3 biodigester had the maximum biogas production rate (μ_m) followed by R2 and R1 respectively (Equations 20 to 22). Simulation results of SPM Biogas production accumulation showed that modified Gompertz equation had better R^2 that ranged from 0.9965 to 0.999 than R^2 for first order kinetic equation which ranged from 0.9769 to 0.9827.

R1 $B_f = 0.6308(1-\exp(-0.0926t))$, $R^2 = 0.9827$ (17)
R2 $B_f = 1.0985(1-\exp(-0.0649t))$, $R^2 = 0.9812$ (18)
R3 $B_f = 1.6796(1-\exp(-0.0858t))$, $R^2 = 0.9769$ (19)
R1 $B_G = 0.5677\exp\{-\exp[(0.0434e/0.5677)(0.4-t)+1]\}$, $R^2 = 0.999$ (20)
R2 $B_G = 0.8965\exp\{-\exp[(0.0631e/0.8965)(1.4-t)+1]\}$, $R^2 = 0.999$ (21)
R3 $B_G = 1.4639\exp\{-\exp[(0.1257e/1.4639)(1.4-t)+1]\}$, $R^2 = 0.9965$ (22)

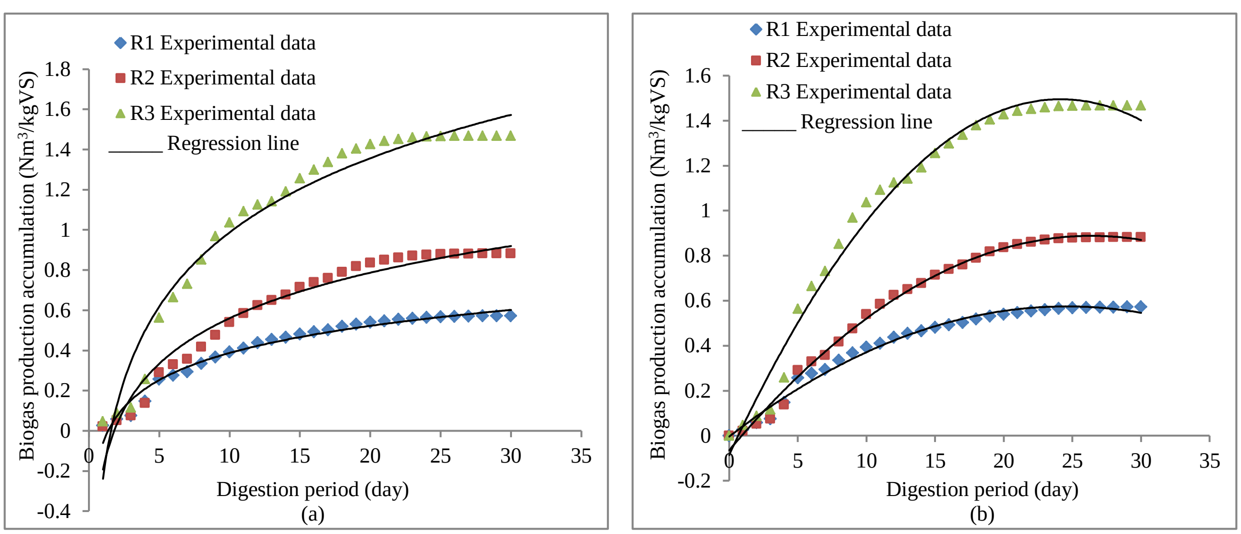

Figure 4. Biogas production as attested by digestion period

4. CONCLUSION

The following conclusions follow, from the study:

SPM had high VS/TS ratio; Biogas production rate and accumulation increased with I/S ratio from 1.3 to 3.8; Exponential plot generally simulated biogas production rate better than linear plot; Modified Gompertz plot had better simulation than first order kinetic plot for biogas production accumulation.

REFERENCES

Adiga, S., Ramya, R., Shankar, B. B., Jagadish, H. P., & Geetha, C. R. 2012. Kinetics of anaerobic digestion of water hyacinth, poultry litter, cow manure and primary sludge: A comparative study. *International Conference on Biotechnology and Environment Management. 42*, pp. 73-78. Singapore: IACSIT press.

Angelidaki, I. 2002. Anaerobic biodegradability of macropolutants. *Harmonisation of anaerobic biodegradation, activity and inhibition assays* (pp. 13-29). Lago d'Orta: European Commission.

APHA. 1992. *Standard Methods for the Examination of Water and Wastewater.* Washington, DC: American Public Health Association.

Buswell, A. M., & Mueller, H. F. 1952. Mechanism of methane fermentation. *Industrial and Engineering Chemistry , 44* (3), 550-552.

Chynoweth, D. P., Turick, C. E., Owen, J. M., & Jerger, D. E. 1993. Biochemical methane potential of biomass and waste feedstocks. *Biomass and Bioenergy , 5* (1), 95-111.

Feng, L., Li, Y., Chen, C., Liu, X., Xiao, X., Ma, X., et al. 2013. Biochemical methane potential (BPM) of vinegar residue and the influence of feed to inoculum ratios on biogas production. *Bioresources , 8* (2), 2487-2498.

Hansen, T. L., Schmidt, J. E., Angelidaki, I., Marca, E., Jansen, J. C., Mosbaek, H., et al. 2004. Method for determination of methane potentials of solid organic waste. *24*, 393-400.

Hashimoto, A. G., Varel, V. H. and Chen, Y. R. 1981. Ultimate methane yiel from beef cattle manure: effect of temperature, ration constituents, antibiotics and manure age. Agricultural wastes, 3:241-256

Kheiredine, B., Derbal, K., & Bencheikh-Lehocine, M. 2014. Effect of inoculum to sustrate ratio on thermophilic anaerobic digestion of the dairy wastewater. *Chemical Engineering Transactions. 37*, pp. 865-870. AIDIC.

Labatut, R. A., & Scott, N. R. 2008. Experimental and Predicted methane yields from the anaerobic co-digestion of animal manure with complex organic substrates. *Proceedings of the American Society of Agricultural and Biological Engineering.* Michigam: St. Joseph, Michigham.

Monch-Tegeder, M., Lemmer, A., Oechsner, H., & Jungbluth, T. 2013. Investigation of the methane potential of horse manure. *Agricultural Enginerring International: CIGR Journal , 15* (2), 161-172.

Raghunathan, C., Velan, M., Velmurugan, B., & Ramanujam, R. A. 2008. Studies on batch kinetics of anaerobi digestion of solid waste (SINEWS) from gelatin industry. *Journal of Enviromental Research and Development , 3* (2), 456-463.

Raposo, F., Fernandez-Cegri, V., De la Rubia, M. A., Borja, R., Beline, F., Cavinato, C., et al. 2011. Biochemical methane potential (BPM) of solid organic substrates: evaluation of anaerobic biodegradability using data from an international interlaboratory study. *Journal of Chemical Technol Biotechnol , 86*, 1088-1098.

WEC. 2004. *Renewable energy projects handbook.* London, UK: World Energy Council.

Wymyslowski, M., Luczak, M., Zawadzka, A., & Imbierowicz, M. 2010. Methane fermentation of poultry slaughterhouse waste. *Polish Journal of Chemical Technology , 12* (3), 15-18.

Yusuf, M. O., Debora, A., & Ogheneruona. 2011. Ambient temperature kinetic assessment of biogas production from co-digestion of horse and cow dung. *Research in Agricultural Engineering , 57* (3), 97-104.

Zhang, T., Liu, L., Song, Z., Ren, G., Feng, Y., Han, X., et al. 2013. Biogas production by co-digestion of goat manure with three crop residues. *PLOS ONE , 8* (6), e66845.

PRODUCTION OF BIODIESEL FROM TGX-1778 SOYBEANS (Glycine max) BY SODIUM HYDROXIDE-CATALYZED TRANSESTERIFICATION

I. Fubara-Manuel, R. B. Jumbo and O. J. Osaghae.
Department of Agricultural and Environmental Engineering,
Rivers State University of Science and Technology, Port Harcourt, Nigeria.
Email: fubara-manuel.isoteim@ust.edu.ng

ABSTRACT

This study investigated the potential of a Nigerian-grown soyabean (TGX-1778) to produce biodiesel. The Soybeans at room temperature, were dehulled, ground to a powdery form, and the oil extracted by Soxhlet extraction method using n-Hexane. 50 ml of the Soybean oil extract and 0.5 g of NaOH were charged into three different reactors labeled A, B, and C, and transesterified in turn with 50, 100, and 150 ml of methanol respectively. Results showed that transesterification with 50, 100, and 150ml of methanol produced biodiesel of densities 0.79, 0.80, and 0.77g/ml respectively, while the corresponding kinematic viscosities at 40^0C were 4.4, 4.6 and 4.1mm^2/s. Other parameters of the biodiesel were refractive index, which ranged from 1.33 to 1.34, pH from 8.5 to 9.6, cloud point (<-32^0C), pour point (-52^0C) and flash point (150^0C). Comparison with the American Society for Testing and Materials (ASTM) D6571 standard indicated that the densities were outside the specified range, while kinematic viscosities were within the acceptable limit. Furthermore, the flash point of the biodiesel produced was higher that the specified minimum level. It was also observed that increasing the methanol quantity from 50 to 150ml, resulted in an increase in biodiesel produced. On the whole, therefore, the oil from the locally grown soybean has a great potential for biodiesel production.

KEYWORDS: Biodiesel, soybean oil, transesterification.

1. INTRODUCTION

The world is in a feverish pitch to replace fossil fuel with renewable fuel because of the continuous depletion of the world's petroleum reserves, global warming, and other environmental concerns. Biodiesel is a clean and renewable fuel, which is considered to be the best substitute for petroleum-based fuel (Singh and Singh, 2010). The use of biofuels was first championed by Rudolf Diesel in the late 1800s when he envisioned vegetable oil as a fuel source for his diesel engine, (Scott, et al., 2009). Although, biodiesel is usually used as a blend with petro-diesel at varying ratios, it can also be used to fuel compression ignition engines alone, (Koc, et al., 2011).

According to the Alternative Fuels Data Center, (2013), soybean oil is one of the major feed stocks for biodiesel production. The use of soybeans for biofuel production is not so new. However, it is now assuming greater importance because of the increasing price of petroleum and more significantly, the emerging concern about global warming that is associated with burning fossil fuels (Gavrilescu, and Chisti, 2005). Biodiesel is a technically acceptable substitute, replacement or blending stock for conventional diesel fuel because it can be used at a 100-percent level (B100) or mixed with diesel fuel in any proportion. However, the most commonly used mixtures are B2 containing 2 percent biodiesel and B20 containing 20 percent biodiesel (Alternative Fuels Data Center, 2013). According to international convention B is used to denote that the fuel is a biodiesel or contains a certain percentage of biodiesel.
Transesterification is a common method for biodiesel production from vegetable oils and animal fats (Abreu, et al., 2003). Although vegetable oils such as soybean oil has been used in the production of biodiesel (Koc, et al. 2011), the potential of the locally available variety of soybeans in Nigeria, (TGX-1778) in the production of biodiesel has not been examined.

The objective of the current study, therefore, was to investigate the potential of the TGX-1778 variety of soybeans in the production of biodiesel by NaOH-catalyzed transesterification with methanol.

2. MATERIALS AND METHODS

2.1 Description of Study Area

The experiment was carried out in the Chemical Analysis Facility of the Department of Chemical/ Petrochemical Engineering, Rivers State University of Science and Technology, Port Harcourt, Nigeria. Port Harcourt is characterized by high humidity (≥80%), and moderately high temperature (25- 30^{0}C), (Fubara-Manuel and Jumbo, 2014). The area is also characterised by heavy rainfall, about 2,400 mm per annum, occurring mostly in the months of June through September. Port Harcourt is located within 4^0 47' 21" N and 6^0 59' 54" E.

2.2 Experimental Procedure

The TGX-1778 variety of soybean seeds were purchased from Premium Seeds Ltd., Zaria, Kaduna State, Nigeria. The soybean seeds were pretreated by cleaning, air drying, and dehulling. The dried seeds were then ground to a powdery form (Figure 1).

Figure 1: Dried and ground TGX-1778 soybean seeds prior to oil extraction.

Approximately 70 g of the ground soybeans was placed in the thimble of the Soxhlet extractor while 250 ml of n-hexane was added to the Soxhlet extractor, and then heated at a regulated temperature of between 60 and 79^{o}C to extract the oil from the soybeans as shown in Figure 2. After the extraction, the mixture of n-Hexane and oil from the Soybeans was then subjected to distillation at a regulated temperature of between 60 and 79^{o}C. This temperature range was chosen because n-Hexane has an optimum boiling point of 78^{o}C. The soybean oil was then recovered and exposed for 72 hours to allow any residual n-Hexane in the mix to evaporate. After the 72 hours, 250 ml of the extracted soybean oil was used to produce the biodiesel by transesterification.

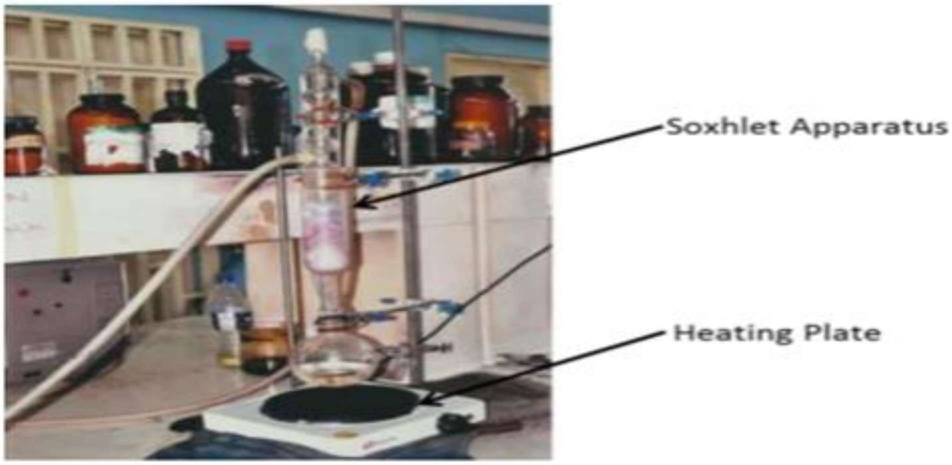

Figure 2: Extraction of oil from powdered TGX-1778 Soybean seeds using Soxhlet apparatus

The soybean oil was divided into 3 aliquots of 50 ml each and placed in reactors labelled A, B, and C. A fixed mass of NaOH and various volumes of methanol were added to each reactor as shown in Table 1.

Table 1: Volumes of methanol and mass of NaOH added to the Soybean oil in each reactor

Starting materials	Reactors		
	A	B	C
Soybean(ml)	50	50	50
Methanol(ml)	50	100	150
Sodium hydroxide(NaOH) (g)	0.5	0.5	0.5

Each mix was then centrifuged and left to settle for 24 hours, after which the mix produced an immiscible mixture of biodiesel and glycerol. The mixture was then decanted to get the biodiesel.

2.3 Determination of Selected Physicochemical Characteristics of the Biodiesel

The parameters determined were density, kinematic viscosity, refractive index and pH. Other parameters were cloud point, pour point, and flash point.

Density was determined manually by weight by weight difference of 10ml volume of the biodiesel in a conical flask, using a weighing balance, while kinematic viscosity was determined with a calibrated capillary viscometer at 40^0C as specified by American Society for Testing and Materials, D445–12, (2004). Refractive index was determined with a refractometer, while pH was determined with a WTW MULTI-340R pH meter as specified by American Public Health Association, (1998).

The methods outlined by American Society for Testing and Materials, D2024–09, (2004) and American Society for Testing and Materials, D97, (2005) were used to determine cloud point and pour point respectively, while flash point was determined by using the Pensky-Martens Closed Cup Tester as specified by American Society for Testing and Materials, D93, (2005).

3. RESULTS AND DISCUSSION

Table 2 shows the physico-chemical characteristics of the biodiesel produced, side by side with American Society for Testing and Materials, D6571, (2008).

Table 2: Physicochemical characteristics of the produced biodiesel

Physico-chemical property	Reactor A	Reactor B	Reactor C	ASTM D6571(2008) Quality Standard
Density (g/ml)	0.79	0.80	0.77	0.86-0.9
Kinematic viscosity @ 40^0C (mm^2/s)	4.4	4.6	4.1	1.9-6.0
Refractive index	1.34	1.34	1.33	-
pH	8.5	9.6	9.0	-
Cloud point (^{0}C)	<-32	<-32	<-32	-
Pour point (^{0}C)	-52	-52	-52	-
Flash point (^{0}C)	150	150	150	130

Reactor A contains 50ml of oil + 50 ml of methanol.
Reactor B contains 50ml of oil + 100ml of methanol.
Reactor C contains 50ml of oil + 150ml of methanol.

From the table, the values of the density obtained range from 0.77 to 0.80 g/ml. These values are slightly outside the range specified by American Society for Testing and Materials (ASTM) D6571, (2008). The values of the kinematic viscosity obtained at 40°C are within the limits specified by American Society for Testing and Materials (ASTM) D6571, (2008). This result also compares well with that of (Koc, et al., 2011), who obtained a kinematic viscosity of 4.66 mm^2/s in his research work. Although American Society for Testing and Materials (ASTM) D6571, (2008), does not have limits for refractive index, the values of the refractive index obtained range from 1.33 to 1.34.

The pH values of 8.5 to 9.6 obtained, showed that the base transesterification reaction was a neutralization reaction but American Society for Testing and Materials (ASTM) D6571, (2008) does not have limits for pH. Cloud point and pour point values were less than -32 and -52 respectively. Also, American Society for Testing and Materials (ASTM) D6571, (2008) does not have limits for cloud point and pour point. The biodiesel obtained in this study was found to have a constant flash point of 150°C, which was above the minimum value specified by American Society for Testing and Materials (ASTM) D6571, (2008). It is worth mentioning that (Koc, et al., 2011) also obtained a flash point of 150°C, as that obtained in this work.

It was observed that the yield of biodiesel increased with the quantity of methanol. Furthermore, Table 2, indicated that parameters such as density, kinematic viscosity, refractive index, and pH were affected by the quantity of methanol used during transesterification. However the variation of the quantity of methanol did not have a well defined trend on the properties. For example, the density of the biodiesel increased with quantity of methanol up to 100 ml before decreasing at 150 ml of methanol. A similar trend was observed for kinematic viscosity. The refractive index remained constant as the quantity of methanol increased up to 100 ml, but decreased as the quantity of methanol increased to 150 ml. Although the pH values almost took the same pattern as those of density and kinematic viscosity, the difference is that the pH value obtained at 50 ml of ethanol was lower than that obtained at 150 ml.

4. CONCLUSION

The TGX-1778 variety of soybeans available in Nigeria has the potential for the production of biodiesel by NaOH-catalyzed transesterification with methanol. The quality of the biodiesel produced from the TGX-1778 variety of soybeans when compared with [13] is acceptable except for density.

REFERENCES

Abreu F.R., Lima D.G., Hamu E. H., Einloft S., Rubim J.C., and Suarez P.A.Z. 2008. New metal catalysts for soybean oil trans-esterification. Journal of the American Oil Chemists Society, 80 (6), 601-604.

Alternative Fuels Data Center (AFDC). 2013. Energy Efficiency and Renewable Energy. A resource of the U.S. Department of Energy’s Clean Cities program, U.S. DoE, WA.

American Public Health Association (APHA). 1998. Standard Methods for the Examination of Water and Wastewater. (20th ed.). 1015 Fifteenth Street, NW Washington, DC 20005 – 2605.

American Society for Testing and Materials (ASTM) D2024–09. 2004. Standard Test Method for Cloud Point of Nonionic Surfactants. ASTM, 100 Barr Harbor Drive, West Conshohocken, PA.

American Society for Testing and Materials (ASTM) D445–12. 2004. Standard Test Method for Kinematic Viscosity of Transparent and Opaque Liquids (and Calculation of Dynamic Viscosity). ASTM, 100 Barr Harbor Drive, West Conshohocken, PA.

American Society for Testing and Materials (ASTM) D6571. 2008. Standard Test Method for Determination of Compression Resistance and Recovery Properties of Highloft Nonwoven Fabric Using Static Force Loading. ASTM, 100 Barr Harbor Drive, West Conshohocken, PA.

American Society for Testing and Materials (ASTM) D93 . 2005. Standard Test Methods for Flash Point by Pensky-Martens Closed Cup Tester. ASTM, 100 Barr Harbor Drive, West Conshohocken, PA.

American Society for Testing and Materials (ASTM) D97. 2005. Standard Test Method for Pour Point of Petroleum Products. ASTM, 100 Barr Harbor Drive, West Conshohocken, PA.

Fubara-Manuel I., and Jumbo R.B. 2014. The effect of septic tank locations on borehole water quality in Port Harcourt,Nigeria. International Journal of Engineering and Technology. 4(5):236-242.

Gavrilescu M. and Chisti Y. 2005. Biotechnology a sustainable alternative for chemical industry. Biotechnol. Advan. 23:417-419.

Koc B., Mudhafer A., and Mohammad F. 2011. Soybeans processing for biodiesel production. In: Soybean: Applications and Technology, N. Tzi-Bun (Ed.), InTech. MYBIODIESEL (2008), Biodiesel Fact Sheet. Available at: www.mybiodiesel.com.2008 .

Scott B., Clements M., Charles G., and Jane I. 2009. Biofuels Impact on Crop and Food Prices: Using an Interactive Spreadsheet . Board of Governors of the Federal Reserve System, International Finance Discussion Papers . 967:1-3.

Singh S. P., and Singh D. 2010. Biodiesel production through the use of different sources and characterization of oils and their esters as the substitute of diesel, a review. Renewable and Sustainable Energy Reviews, 14 (1), 200-216.

BIO-FUEL FOR SUSTAINABLE DEVELOPMENT IN A GROWING ECONOMY

G. U. Asonye, E. C. Abbah and S. N. Asoegwu
Department of Agricultural Engineering, Federal University of Technology, Owerri
Emails: u.asonye@yahoo.com, elochukks@yahoo.co.uk, asosab49@yahoo.com
Corresponding Author's E-mail: u.asonye@yahoo.com

ABSTRACT

Agricultural reform, climate change and energy security have been key drivers in renewed enthusiasm for biofuels. The production of biofuels has also been seen as providing stimulus for the economic revitalization of agriculturally unproductive rural areas both in developing and developed countries. Agriculture is heavily dependent on unsustainable non-renewable energy sources, especially petroleum. Abrupt abandonment of our reliance on these energy sources would be economically catastrophic and equally disruptive, hence the need for reduced reliance on non-renewable energy sources and a substitution of renewable sources to the extent that is economically feasible and sustainable. Sustainability rests on the principle that the needs of the present generation must be met without compromising the ability of future generations to meet their own needs. Therefore, stewarding of both natural and human resources is of prime importance to sustainability. This review surveys many dimensions of biofuel production and its sustainability, which is critical in a growing economy.

KEYWORDS: Bio-fuel, sustainable development, biomass

1. INTRODUCTION

Renewable energy in general and biofuels in particular, has begun to look like an increasingly viable mitigation option for addressing climate change. For rich countries they offer prospects for meeting emission reduction commitments. For low and middle-income countries they offer potential to reduce energy import bills as well as earn precious foreign exchange. The agricultural sector, which will always remain the mainstay of the economy in spite of the discovery of crude oil, is head in the area of energy demand. Energy needed for agricultural production ranges from the energy needed to drive equipment and machinery in and out of the farms to the energy needed in the milking house to that needed to preserve stored products. Fossil fuel have been the major contributors to agricultural energy use.

Liquid biofuels can provide the much needed substitute for fossil fuels used in the agricultural sector of the economy. They can contribute to climate change reduction and other environmental goals, energy security, economic development, and offer opportunities for other profitable ventures. Fossil fuels are the largest contributors of greenhouse gases (GHGs) to the biosphere with associated CO_2 emissions of about 29 Gtonnes [EIA, 2006]; and catastrophic climatic change projections and consequences on nature as well as human systems [IPCC, 2001].

African policy makers believe that developing liquid biofuels can transform Africa's traditional dependence on biomass energy sources, i.e., wood and dung. Biofuels contributes to climate and other environmental goals, energy security, economic development, and offer opportunities for private companies to profit.

There are social and environmental risks associated with biofuels such as cultivation of feedstock, land fertilizer use (Cohen *et al.*, 2008; Coyle 2007; Fargione *et al.*, 2008; Searchinger *et al.*, 2009) but as FAO (2009) points out, there are also considerable advantages for low and middle-income countries to nurture and expand their biofuel industries. Such advantages include infrastructural development, employment opportunities, qualitative and standard social wellbeing. Indeed (IEA Bioenergy, 2008) concludes that these potential drawbacks do not necessarily rule out biofuels as an option, as long as they can be produced in a way that decreases poverty and does not have negative effect on biodiversity. It is projected that the growth in production and consumption of liquid biofuel will continue but their impacts towards meeting the overall energy demands will remain limited (Andrea and Yianna, 2008).

The development of biofuels will bring direct opportunities to developing countries through the creation of jobs from growing raw materials to biofuel manufacture, marketing and use. Furthermore, the production of biofuels by developing countries will help to decrease the dependency on costly fossil fuel [UN-Energy, 2007]. For many developing countries, biofuel production could promote economic development by providing new export opportunity. This paper reviews the positive impacts of biofuels in the sustainable development of a growing economy.

2. WHAT BIOFUELS ARE

Biofuels are combustible materials directly or indirectly derived from biomass, commonly produced from plants, animals and micro-organisms but also from organic wastes. Biofuels may be solid, liquid or gaseous and include all kinds of biomass and derived products used for energetic purposes (Berndes *et al., 2003*). Biofuels are also defined as "fuels that can be produced from agricultural and forest products or the biodegradable portion of industrial and municipal waste" (Andrea and Yianna, 2008). The major sources of energy in rural Africa are biofuels such as wood, sawdust, palm kernel shell, palm fruit fiber, and dung. Liquid biofuels such as ethanol and biodiesel from grains and oil seeds have been used to power engines for transportation since the early 20th century. Biofuels being renewable liquid fuels derived from microorganisms, plant or animal material (biomass) can be used, in their pure form or as part of blends, to fuel transport vehicles as well as to generate heat and power.

Bioethanol, a liquid biofuel is used as a replacement for gasoline and biodiesel in place of diesel. It represents an immense growth area around the world in terms of research, production, development, marketing and use and has an important role to play in displacing the types of fuels the world has used in the past. They are presently mostly used as blends with the existing fuel types in some existing engine designs. Most importantly, it is imperative that developing countries like Nigeria have domestic energy security anchored on biofuels, as more than half of its liquid fuel needs are currently imported and the figure keeps rising. It is crucial that developing countries have their own energy supplies so that they are not dependent upon the supply and pricing dictated by world markets.

3. BIOMASS FOR BIOFUEL

Biofuels are fuels made from biological materials. These renewable fuels viz: biodiesel, biogas and methane, are derived from biological matter. Biofuels are based on ligno-cellulosic material, *i.e.* biomass, which is abundant virtually everywhere around the globe. Biomass can be derived from natural ecosystems (like forests, grassland or aquatic ecosystems), or can also be produced by cultivating bioenergy crops like perennial grasses, oil crops, root crops, grains or wood species. Table 1 shows the world biofuel production from feed stocks essentially agricultural and forestry residues.

Table 1: Theoretical second-generation biofuel potential from ligno-cellulosic residues in 2007

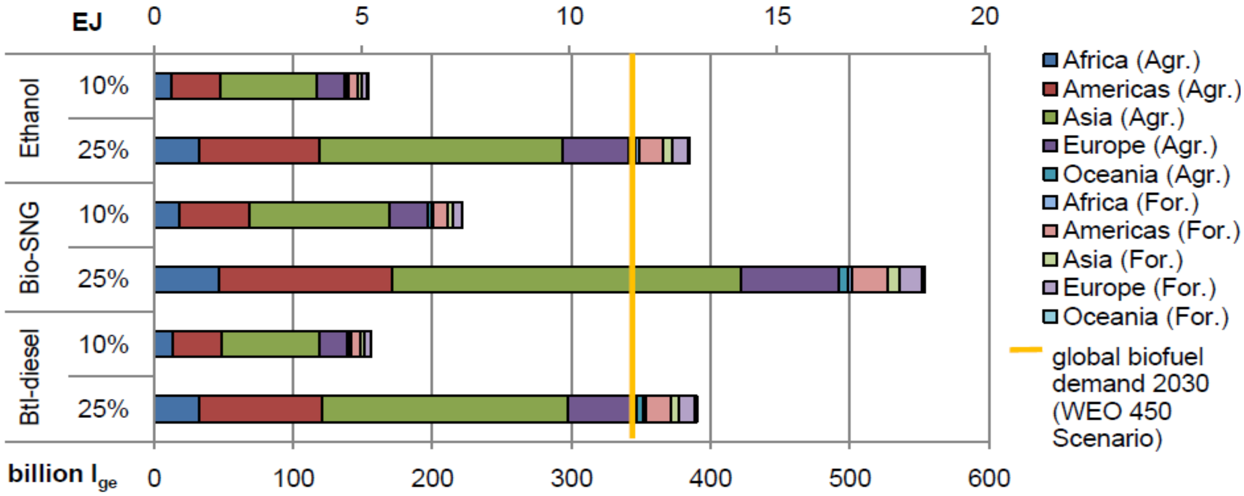

Note: Amounts cannot be summed up. Each bar indicates biofuel yields using all available biomass. 25% and 10% assume respective shares of agricultural and forestry residues to be available for biofuel production. Assumed conversion factors - BTL-diesel: 217 lge/tDM; Ethanol: 214 lge/tDM; Bio-SNG: 307 lge/tDM. Source: IEA based on FAOStat, 2009; FAO, 2003; IFPRI, 2001

In developing countries, over 500 million households still use traditional biomass for cooking and heating. However, already 25 million households cook and light their homes with biogas (displacing kerosene and other cooking fuel); and a growing number of small industries, including agricultural processing, obtain process heat and motive power from small-scale biogas plants. Biomass power contributed about 1% to the total global electric power capacity of 4300 GW in 2006 (REN21 2008).

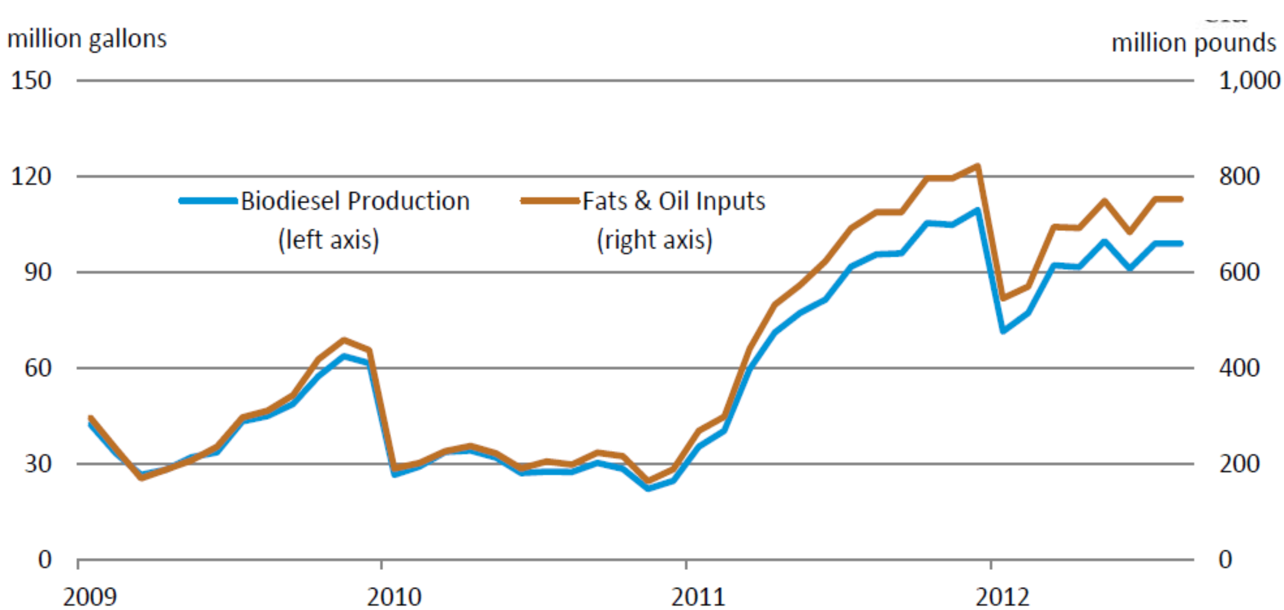

Figure 1: U.S. Biodiesel inputs and production, 2009-12
Source: EIA, Monthly Energy Review, August 2012

4. BIOFUEL IN WORLD ENERGY EQUATION

The world currently uses 86 million barrels of oil per day (BP, Statistical Review of World Energy, 2008) with forecasts that demand for liquid fuels will increase to 118 million barrels by 2030 (International Energy Outlook, 2007). Figure 2 depicts biofuel (ethanol) from 1982-2005. Most of incremental fuel will come from OPEC and specifically from the Middle East. In the last two years, the world's supply of oil has had difficulty keeping up with demand, and prices have skyrocketed to $140 per barrel and more. This has triggered economic hardship, especially among the poorest importing countries. As more and more funds are required to pay for oil products, importing countries find their current account balances eroding and the costs of producing and transporting goods and services increasing. Today, many forecasters predict that while prices will fluctuate, the era of low-cost oil is over and countries must adjust by seeking alternative energy options and strategies.

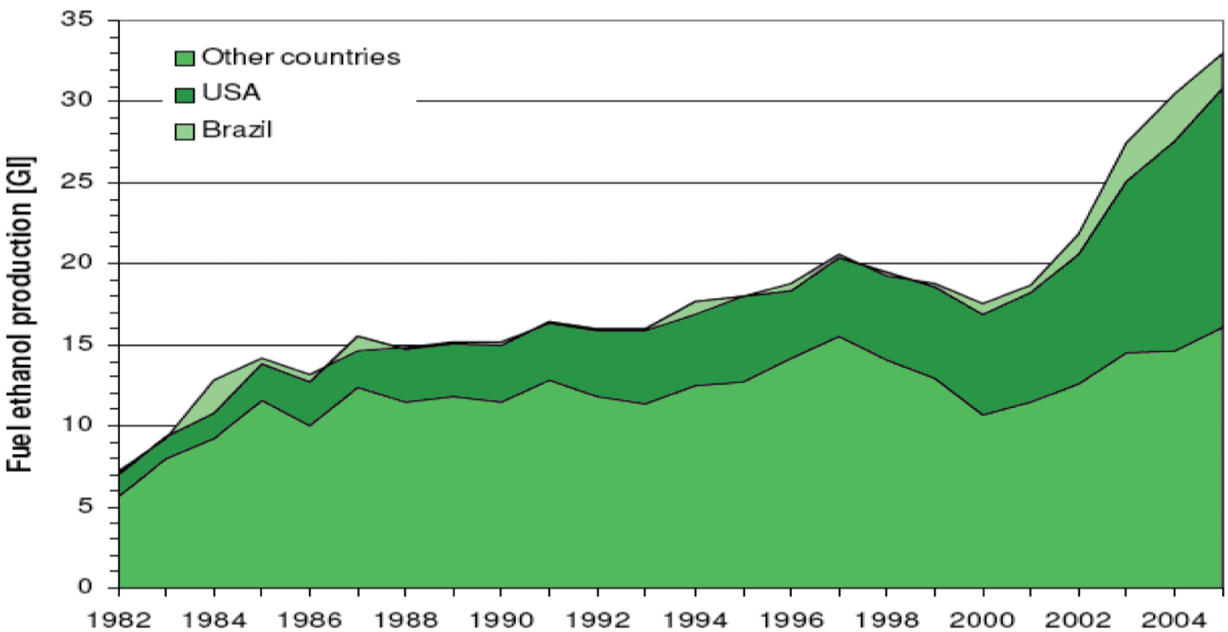

Figure 2: World ethanol production 1982–2005
Source: Walter et al. (2007).

Producing liquid fuels from biomass is one of the only alternatives to petroleum-based fuels. As a result, countries are looking at a menu of biofuel options to reduce their future reliance on petroleum. Since biofuels are likely to be produced in countries outside of OPEC, they may also allow fuel-consuming nations to diversify the sources of their fuels, and hence provide energy security benefits.

5. THE TYPES OF FUEL

5.1 Bio-Diesel

Biodiesel is a renewable and environmentally friendly fuel; made from various feedstock ranging from microalgae, edible oil seeds, non-edible oil seeds, waste vegetable oil, cellulose and the use of enzymes. Biodiesel production is a very modern and technological area for researchers due to the relevance that it is winning every day. It can be used neat, meaning 100-percent biodiesel, or it can be blended with petroleum diesel. Biodiesel is becoming widely available in developed economies and can be substituted for petroleum-based diesel fuel ("petrodiesel") in virtually any standard unmodified diesel engine. Biodiesel offers many advantages over petroleum-based diesel in that:

It is made from domestically produced and renewable agricultural products, mainly vegetable oil or animal fat.

- It is essentially non-toxic and biodegradable.
- It has a high flash point (over 300ºF) and is difficult to light on fire with a match.
- It reduces emissions of many toxic air pollutantslike carbon emissions.
- It functions as an excellent fuel lubricant and performs similarly to low-sulfur diesel with regards to power, torque, and fuel consumption.

Biodiesel offers environmental, economic and national security benefits. The combustion emits fewer regulated and non-regulated pollutants than petrodiesel. Furthermore, biodiesel is biodegradable and its lubricity extends engine life. Biodiesel could benefit farmers and rural communities, depending on ownership of production facilities and the mix and marketability of useful co-products. Also, biodiesel could reduce dependence on foreign oil and corresponding fluctuations in availability and price.

The non-edible vegetable oils such as *Madhuca indica, Jatropha curcas* and *Pongamia pinnata* are found to be suitable for biodiesel production under the experimental conditions (Meher *et al*, 2006; Sent *et al*., 2003). Meher *et al.,* (2006) found that the yield of methyl ester from karanja oil under the optimal condition is 97–98%. Oil content in the Castor bean, Hemp, Neem and Pongame seed is around 50, 35 30 and 40 % respectively.

5.2 Ethanol

This is an alcohol-based fuel derived from crops, usually corn, barley, and wheat. Ethanol can be blended with gasoline in varying concentrations. E85, for example, is a blend of 85 percent ethanol and 15 percent gasoline. Ethanol, or ethyl alcohol, is a high-octane fuel produced from the fermentation of plant sugars. Corn is the primary feedstock for ethanol production in the United States. Ethanol is also produced from other organic sources such as barley, wheat, rice, sorghum, sunflower, potatoes, cassava and molasses. Brazil is the world's largest ethanol producer and exporter, generating 4 billion gallons in 2004 representing 37 percent of the world's total. The United States is second, and is also the second largest ethanol importer. In August 2005, President Bush signed the Energy Policy Act of 2005 (EPAct 2005), which included the Renewable Fuels Standard (RFS) that established the first nationwide baseline for the use of fuels derived from renewable sources. RFS required petroleum refiners to use at least 4 billion gallons of renewable fuel beginning in 2006, increasing incrementally to 7.5 billion gallons per year by 2012.

5.3 Biogas

Biogas is methane produced by the process of anaerobic digestion of organic material by anaerobes (Redman, 2008). It can be produced either from biodegradable waste materials or by the use of energy crops fed into anaerobic digesters to supplement gas yields. The solid byproduct, digestate, can be used as a biofuel or a fertilizer. Biogas can be recovered from mechanical biological treatment waste processing systems.

Note: Landfill gas, a less clean form of biogas, is produced in landfills through naturally occurring anaerobic digestion. If it escapes into the atmosphere, it is a potential greenhouse gas.

6. ADVANTAGES OF BIOFUEL

6.1 Biofuels for Employment Opportunity

The contributions of biofuel in the area of job creation and income generation cannot be overemphasized

1) Biodiesel expands demand for those agricultural products which serve as its feedstock thereby bringing more money into the sector.
2) Farmers cultivating these crops get improved income.
3) The presence of facilities that creates energy from biological sources adds value to the nation's industrial and income base.
4) More jobs and increased personal income in rural communities.
5) Additional and more diversified markets for both starch-based and oilseed-based crops that can help production agriculture be more competitive.

6.2 Biofuel for Climate Change

Recent concern over global climate change has motivated growing interest in all manner of renewable energy sources, biofuels among them. Biofuels have been presented as a potential significant contributor to strategies for reducing net greenhouse gas emissions. When produced and used appropriately, biofuels can deliver lower net greenhouse gas emissions than fuels derived from fossil sources. This is particularly true when considering the amount of greenhouse gasses that synthetic fuels produced from coal or oil shale emits. However, the net greenhouse gas emissions of biofuels vary significantly depending on the feedstock and technologies used in their production and consumption. The overall impact of biofuel development on climate still tied up with differences in carbon stocks and solar reflectance between the biomass crops and the vegetation they replace. It seems virtually certain that biofuels will have a role in national and global strategies to address the dangers of climate change.

6.3 Biofuel for Economic Development

Biofuel production has enjoyed tremendous growth in recent years (Arndt *et al., 2009*). Between 2000 – 2007, global production tripled in volume (Coyle, 2007). In 2007–2008 alone, the share of ethanol in global gasoline increased from 3.8 to 5.5 percent, while the share of biodiesel in diesel increased from 0.9 to 1.5 percent (UNEP, 2009). More countries are setting higher biofuel consumption mandates (for example, 10 percent of transport energy in the European Union member states must come from biofuels by 2020), leading to consensus that the biofuels industry will grow even further. A recent study by the Food and Agriculture Organization of the United Nations (FAO 2009) reveals that only about one-quarter of land in Sub-Saharan Africa with potential for rain fed crop production is currently cultivated. This, together with the widely held perception that African agriculture has considerable scope for raising productivity (Diao *et al.*, 2007), means that biofuel feedstock may not necessarily displace food crops, and even where they do, food production can be maintained on less land through productivity enhancements.

Biofuels and their feedstock could be an important source of export income for developing nations. Participating in the global economy through export activity is a crucial part of the economic development process. In some tropical countries, biofuel production can bring with it "stepping stone" effects such as the extension of transportation networks, as well as job creation. In addition, countries can substitute domestically-produced biofuels for imported oil products, reducing the micro and macro impacts of the sharp escalation in oil prices. Also, biofuels present an opportunity for new entrepreneurial companies and small holders to emerge while simultaneously increasing activities in growing economies. The recent United Nations Report; (Sustainable Bioenergy, A Frame Work for Decision Makers, 2007) examined the implications of Bioenergy on agro-industrial development and job creation. The report found out that "Successful *bioenergy industries have great potential for significant job creation.*" And continues *"because the vast majority of bioenergy employment occurs in farming, transportation and processing, most of these jobs will be created in rural communities where underemployment is a common problem"*

6.4 Bio-Fuel Sustainability for Growing The Economy

Potential sources of bioenergy include agriculture and forest residues, organic waste, and dedicated energy crops grown on agricultural or marginal lands, all of which are major sources of feedstocks for biofuel production. Smeets *etal*., (2007) found that the long-term technical potential of bioenergy could be very large and they estimated that biomass resources could potentially supply up to two times the current global energy demand, without competing with food production. According to the authors, "if a type of agricultural management is applied similar to the best available technology in production of biofuel in undeveloped regions, the world would be capable of producing the demand for biofuel projected by 2050 using only a fraction of the present agriculture land" (Smeets *et al.,* 2007).

According to Ress (1989) "Sustainable development is positive socioeconomic change that does not undermine the ecological and social systems upon which communities and social systems are dependent". In relation to agriculture, sustainability means changing agricultural systems so that farmers are able to produce indefinitely (Rodale, 1988). The importance of sustainability of agricultural production system is becoming a major concern of agricultural researchers and policy makers in both developed and developing countries. Sustainability represents the last step in a long evolution that economic development must consider both in the protection of natural resource and the maintenance of environmental quality (Batie, 1989). Sustainable agriculture for biomass production should be based on approaches that reduce environmental degradation, conserve resources, and provide adequate and dependable farm income through poverty reduction and its associated problems. For the sustainable development of biomass for biofuel, farmers must change their strategies in production, processing and financing of the different biomass production systems. Enhanced biomass production ensures abundant raw materials for biofuels as an alternative source of energy, which in turn enhances the agricultural and other sectors that are indispensable for a sustainable system. Bio-fuels have shown the potential to fit into this category of a sustainable energy source.

Nigeria has pursued with vigor the exploitation of her natural endowment without taking a deep reflection on the challenge of maintaining its sustenance. Given her current international debt issues, it has become increasingly difficult to generate enough resources required for sustainable socioeconomic growth and access to capital to meet her obligations without exerting increased pressure on local resources. It is believed that with development and vigorous pursuit to the biofuel policy in Nigeria, considering its environmental, social and economic benefits, the Nation will scale out of her present economic doldrums.

7. CONCLUSION AND RECOMMENDATIONS

If several sustainability principles are treated seriously, Bio-fuel has tailpipe benefits that hold great promise as a sustainable energy source. Bio-fuels can among several advantages; Capture as much energy efficiency as possible on and off the farm ; reduce production costs and improve energy balance; Convert as much waste as possible into a useable resource, such as converting waste vegetable oil into fuel; Put oil-producing crops and high-quality agricultural lands to their highest and most sustainable use; Raise bioenergy crops that enhance soil and water resources; Create a range of diverse opportunities for biodiesel production in terms of the scale, design and ownership, so farmers and rural communities can share in the economic benefits and ultimately sustain development in a growing economy like Nigeria. Finally, it is important to point out that attaining the goal of sustainable agriculture is the responsibility of all participants in the system, including farmers, laborers, policymakers, researchers, retailers, and consumers who have their own unique contributions to make for a realiazable sustainable economy.

In summary, two major policy and practical changes must occur for biofuels to have a real effect on any country's energy future:

1) A national commitment to energy efficiency in every facet of the nation's life. This may include community redesign, broad changes in food production and delivery systems, greater commitment to mass transit.
2) A massive conversion from gasoline powered automobiles to cleaner-burning automobiles. Capturing energy efficiencies and making the best use of biofuels may be nearly impossible without redirecting current overdependence on fossil fuels, especially for powering our automobiles as is becoming the case in developed economies.

REFERENCES

Andrea, R. and Yianna, L., 2008. *Gender and Equity Issues in Liquid Biofuels Production: Minimizing the Risks to Maximize the Opportunities* (Rome: U.N. Food and Agriculture Organization).

Arndt, C., Benfica, R. Tarp, F. Thurlow, J.and . Uaiene, R. 2009. Biofuels, poverty, and growth: A computable general equilibrium analysis of Mozambique. *Environmental and Development Economics* 15: 81–105. Published online by Cambridge University Press, June 16, 2009

Batie, S. 1989. Sustainable Development: Challenges to the Profession of Agricultural Economics. AJAE 70(5)

Berndes, G. Hoogwijk, M. and Van Den Broek, R. 2003. The contribution of biomass in the world energy.

BP, 2008. *Statistical Review of World Energy*. Available at http://www.bp.com/productlanding.do?categoryId=6929&contentId=7044622, visited June 2008.

Cohen, J., Tirado, C., Aberman, N., and Thompson. B. 2008. *Impact of climate change and bioenergy on climate change*. Washington, D.C., and Rome: International Food Policy Research Institute and Food and Agricultural Organization of the United Nations.

Coyle, 2007. The future of biofuels: A global perspective. *Amber Waves* 5 (5): 24–29. Washington, D.C.: Economic Research Service, U.S. Department of Agriculture.

Diao, X., Hazell, P., Resnick, D., and Thurlow, J. 2007. *The role of agriculture in development: Implications for Sub-Saharan Africa*. IFPRI Research Report 153. Washington, D.C. International Food Policy Research Institute.

EIA., 2006 International carbon dioxide emissions from the consumption of energy, Available from: http://www.eia.doe.gov/pub/international/iealf/tableh1co$_2$.xls; [cited 10.02.09].

EIA,2012.*Monthly Energy Review*, August http://www.eia.gov/totalenergy/data/monthly/query/mer_data_excel.asp?table=T10.04

Energy Policy Act of 2005, Renewable Fuel Standard and Energy Independence and Security Act of 2007, Renewable Fuel Standard

FAO, 2003. United Nations Food and Agriculture Organisation *World Agriculture: Towards 2015/2030. An FAO perspective*, Earthscan Publications Ltd., London.

FAO., 2009. The market and food security implications of the development of biofuel production. Committee on Commodity Problems, 67th session CCP 09/6. Food and Agriculture Organization of the United Nations.

Fargione, J., Hill, J., Tilman, D., S. Polasky, and Hawthorne, P. 2008. Land clearing and the biofuel carbon debt. *Science* 319:1235–1238.

IEA, 2007. *Good Practice Guidelines: Bioenergy Project Development and Biomass Supply*, OECD/IEA, Paris

IEA Bioenergy, 2008. Biofuels for transport – art of a sustainable future? Summary and conclusions from the IEA Bioenergy ExCo61 Workshop. future globalenergy supply: a review of 17 studies. Biomass and Bioenergy 25 (1): 1-28.

IFPR, 2001. International Food Policy Research Institute: *Global food projections to 2020. Emerging Trends and Alternative Futures*, IFPRI, Washington D.C.

International Energy Outlook, 2007. US Energy Information Administration, Available at http://www.eia.doe.gov/oiaf/ieo/oil.html, visited June 2008.

IPCC. 2001. Climate change 2001: impacts, adaptation, and vulnerability. In: A report of working group II of the Intergovernmental Panel on Climatic Change (IPCC). Cambridge.

Redman, G. 2008. The Andersons Centre. "Assessment of on-farm AD in the UK", *National Non-Food Crops Centre*, 2008-06-09. Retrieved on 2009-05-11.

REN21, 2008. Renewables 2007 Global Status Report (Paris: REN21 Secretariat and Washington, DC: Worldwatch Institute). 2008 Deutsche Gesellschaft fur Technische Zusammenarbeit (GTZ) GmbH.

Ress, W. 1989 "Sustainable Development: Myths and Realities" in Environment and Economic Partners for the Future. Conference Proceeding, Winnipeg, Government of Manitoba.

Searchinger, T., Heimlich, R., Houghton, A., Dong, F., Elobeid, A., Fabiosa, J., Tokgoz, S., Hayes, D., and Yu. T., 2009. Use of U.S. croplands for biofuels increases greenhouse gases through emissions from land-use change. *Science* 319: 1238–1240.

Smeets, E., Junginger, M., Faaij, A., Lewandowski, I., Turkenburg, W. 2007. “A Quickscan of Global Bio-Energy Potentials to 2050”, Progress in Energy and Combustion Science 33(1): 56–106

UN Energy, 2007; (United Nations Energy) *Sustainable Bioenergy: A Framework for Decision Makers*,

UN-Energy 2007, Sustainable bioenergy: A Framework for Decision Makers, http://esa.un.org/un-energy/pdf/susdev.Biofuels.FAO.pdf

UNEP 2009. (United Nations Environment Programme). *Towards sustainable production and use of resources: Assessing biofuels*. Nairobi: UNEP.

Walter, A., Rosillo-Calle, F., Dolzan, B., Piacente, E., Borges da Cunha, K. 2007. “Market Evaluation: Fuel Ethanol”, Task 40 Sustainable Bio-energy Trade: Securing Supply and Demand (Deliverable 8), State University of Campinas (Unicamp), Campinas, Brazil.

ENGINEERING PROPERTIES OF TERMITE MOUND BRICKS AS A CONSTRUCTION MATERIAL FOR AGRICULTURAL BUILDINGS

K. A. Adeniran[1], Y. Mijinyawa[2], T. D. Akpenpuun[3] and T. D. Oseni[4]
[1,3,4]Department of Agricultural and Biosystems Engineering, University of Ilorin, Ilorin. Nigeria
kadeniran_2003@yahoo.com[1], akpenpuun.td@unilorin.edu.ng[3], tohebdd@yahoo.com[4]
[2]Department of Agricultural and Environmental Engineering, University of Ibadan, Ibadan.
Email: y.mijiyawa@mail.ui.edu.ng[2]

ABSTRACT

The use of termite mound soil as a construction material and as a replacement for clay in brick production was investigated. This research investigated the physical properties (Moisture Content, Specific Gravity, Dry-bulk Density, Grain Size Analysis), the Atterberg limits (liquid limit (LL), plastic limit (PL) and plasticity index (PI)) and engineering properties of *termitaria* bricks. Mound soil was sourced from two sites (Tanke, Ilorin (A) and Civil Engineering Department, University of Ilorin, Ilorin (B)). The results of the physical properties of mound soil from both sites showed that there was no significant difference in the physical properties. The Atterberg analysis revealed that soil from site A and site B had plasticity index of 40.57 % and 41.07 % respectively. The average compressive strength of 1.70N/mm^2 and 1.52 N/mm^2 was recorded after 14 days of curing for sites A and B respectively. The highest average compressive strength of 2.70 N/mm^2 and 2.50 N/mm^2 was recorded after 28 days of curing for site A and site B respectively. This indicated 58.8 % increment in compressive strength for sites A and 64.50 % increment in compressive strength for site B. These increments in compressive strengths were as a result of the strong bond between the soil particles as a result of a high percentage of clay and silt and the elimination of air and water pockets within the brick formation. As a result, soil samples from both sites are suitable for brick production for agricultural structures such as grain silos and yam barn.

KEYWORD: Termite mound, atterberg limits, compressive strength, properties, plasticity indices

1. INTRODUCTION

Termites are tropical social insects that play an important role of biodegrading fallen and dead wood in the environment. About 2,800 species of termites have been identified. Termites live in nests, which could either be on the earth's surface or below the earth's surface. Nests that are on the earth's surface are also known as Mound (*termitaria*) (Ndaliman, 2006). Nests are structures made from a combination of soil, mud, chewed wood/cellulose, saliva, and faeces and are often located near trees, stumps, wood piles and other cellulosic materials. The nest performs functions such as: protection, housing, air conditioning, control of the CO_2/O_2 balance and water collection. Termites feed on wood and wood products such as books, cardboard, boxes and wooden door and window frames and cabinets (Aguwa, 2009).

Table 1: Chemical Composition of Termite Mound

Composition	Percentages (%)
SiO	58.06
AlO_3	27.72
K_2O	2.59
Fe_2O_3	1.46
TiO_3	0.87
CaO	0.20
MgO	0.36
Na_2O	0.30

Source: Ndaliman, 2006

Termite mounds are a common occurrence in Nigeria but are unwanted on farmlands, most especially in the vicinity of wooden structures. The activities of termites around wooden and agricultural structures is undesirable, as a result, termite mounds in close proximity to these structures must be broken down and properly disposed of in order to prevent recurrence. The objective of this research was to determine the Atterberg limits of mound soil and the engineering properties of termite mound bricks. The aim was to investigate the feasibility of replacing clay with mound soil as well as finding an appropriate method of disposing mound soil.

2. MATERIAL AND METHODS

2.1 Study Area

The study area is Ilorin, Kwara State. Ilorin is located at latitudes 8° 05`N to 10° 05`N and longitudes 2° 50`E to 6° 05` E. The state has an elongated shape covering an area of about 32,500 sq. km. The soils of Ilorin are loamy and clay. The climate in Kwara state is described as tropical. Kwara State experiences an annual rainfall of about 1500 mm, average temperature 33.50 ^{o}C, average relative humidity of 77.50 % and 7.1 hours of sun shines daily (Olanrewaju, 2009).

2.2 Collection of Termite Mound Soil

Termite mound soil used for the study was obtained from two sites in Ilorin South Local Government Area. The collection of the samples from the sites was done using a shovel, pickaxe and polyethylene bags.

2.3 Preparation of Bricks

Wooden forms of dimension (100 × 100 × 100) mm were fabricated. The termite mound soil was sieved using 0.4 mm sieve in order to remove organic debris, which might interfere with bond formation. Fifteen bricks were moulded for each of the soil samples using the forms and tempered properly so as not to have any voids. The forms were lubricated with oil in order to ease demoulding after 24 hours. The bricks were air-dried under a shed to avoid cracking that could have occurred under direct sun drying.

2.4 Determination of Physical Properties

2.4.1 Natural Moisture Content

Equipment used for this test were, moisture cans, gloves, crucibles, electric oven and weighing balance. Oven drying method was used to evaluate the moisture content of soil samples. The moisture content is the basis on which the Atterberg limits of a soil sample are established. The natural moisture content was determined using equation (1) below:

$$\text{Moisture Content, W (\%)} = \frac{Weight\ of\ Water}{Weight\ of\ Oven\ dry\ soil} = \frac{W_1 - W_2}{W_2 - W_3} \qquad 1$$

Where, W_1 = Weight of can and wet soil, g; W_2 = Weight of can and Oven dry soil, g; W_3 = Weight of can, g

2.4.2 Specific Gravity

Equipment used included: Pycnometer, weighing balance, Vacuum pump, Funnel and spoon. The specific gravity was evaluated using the equation (2) stated below:

$$\mathrm{G.S} = \frac{Weight\ of\ oven\ dry\ soil}{Weight\ of\ Water} = \frac{W_2 - W_1}{W_3 - W_2} = \frac{W_2 - W_1}{W_4 - W_1} \qquad 2$$

Where, W_1 = weight of empty bottle; W_2 = weight of empty bottle + dry soil; W_3 = weight of empty bottle + dry soil + water; W_4 = weight of empty bottle + water only

2.4.3 Bulk Density

It is the ratio of the mass of the dry soil to the volume of the soil sample. Equipment used to carry out this experiment were straight edge, weighing balance, moisture can, Measuring cylinder, drying oven and Vernier calliper. The dry-bulk density was evaluated using the equation (3) below:

$$\text{Bulk density}\left(\frac{\mathrm{g}}{\mathrm{cm}^3}\right) = \frac{\text{Weight of Oven dry Soil}}{\text{Total Volume of Soil}} = \frac{\mathrm{W_2 - W_1}}{\mathrm{V}} \qquad 3$$

Where, W_1 = Weight of empty cylinder; W_2 = Weight of empty cylinder + dry soil; V= Volume of Soil = Volume of Cylinder = $\pi r^2 h$; R = radius of cylinder, cm; h = height of soil in cylinder

2.4.4 Sieve Analysis of Mound Soil

Sieve analysis was conducted on the mound soils in the Material Laboratory of Civil Engineering Department, University of Ilorin, Ilorin, Nigeria. The apparatus and materials used were set of sieve (0.15, 0.3, 0.6, 1.18, 2.36, 4.75), weighing balance (accuracy of 0.01 g), brush, mechanical shaker, large pan and timing device.

$$C_U = \frac{D60}{D10} \qquad 4$$

$$C_C = \frac{(D30)^2}{D10 \times D60} \qquad 5$$

Where C_u = coefficient of Uniformity and C_c = Coefficient of Curvature

2.4.5 Atterberg Limits Analysis

Atterberg limits analysis (liquid limit, plastic limit and plasticity index tests) was performed on the fraction of the soil sample that passed through the 0.4 mm sieve based on ASTM D 4318 standard.

Liquid Limit:

Liquid Limit (LL) is the moisture content at which soil begins to behave as a liquid material and begins to flow. Equipment used included: porcelain evaporating dishes, pulverizing apparatus (mortar and pestle), 0.4 mm sieve, Spatula, Weighing balance (accuracy of 0.01 g), Watering bottle, Drying tares, Manually operated Liquid Limit Device(s) and Grooving Tool and Gauge, Oven and Desiccator. The water content in this state is determined using equation above (1), while the Liquid Limit was determined using equation 6 below:

$$\text{Liquid Limit, LL} = \mathrm{W}\left[\frac{N}{25}\right]^{0.12} \qquad 6$$

Geotechnical Engineering Bureau, 2007.

Where, W = moisture content, %; N = Number of blows

Plate 1: Casagrande Liquid Limit Device

Plastic Limit (PL):

Plastic Limit is the moisture content at which soil begins to behave as a plastic material and was determined using equation (2) stated above.

Plasticity Index (PI):

It is a measure of the plasticity of a soil. The plasticity index is the water content level at which soil exhibits plastic properties. It is the difference between the liquid limit and the plastic limit (PI = LL - PL). Soils with a high PI tend to be clayey while those with lower PI tend to be silty and sandy.

3. RESULTS AND DISCUSSION

3.1 Texture and Consistency Limits

The results of the physical properties of the soil samples from the two sites are presented in Table 2 below. Hydraulic conductivity of soil is affected by the size and distribution of soil particles, mineral composition, texture, characteristics of wetting fluid, void ratio and the degree of saturation (Kasali, 2014). Plasticity index recorded for soil samples from sites A and B was 40.57 % and 41.07 % respectively. These values indicate that clay and silt contents are high in both soil samples and this increases the workability of the soil in terms of cohesion. Plasticity index is inversely proportional to voids within the soil. That is, the higher the plasticity index the fewer are voids within the soil structure. Likewise, the higher the plasticity index the lower the hydraulic conductivity (seepage rate) vice-versa. This implies that the rate of moisture absorption by the bricks will be low as a result the bricks are suitable for agricultural structures such as grain silos and yam barns.

Table 2: Physical and Index Properties of Termite Mounds from both Sites

Physical Properties		**Sample A**	**Sample B**
LL Moisture Content		39.70	40.50
PL Moisture Content		16.03	19.80
No. of Blows		30.00	28.00
Liquid Limit, LL, %		26.65	24.03
Plastic Limit, PL, %		16.03	14.26
Plasticity Index, PI = LL – PL, %		40.57	41.07
Specific Gravity		2.55	2.80
Bulk Density, g/cm^3		1.46	1.54
Particles Size Analysis	Coefficient of Uniformity, C_u	8.97	10
	Coefficient of Curvature, C_c	0.67	0.64

AASHTO Classification	A-2-7	A-2-7
USCS Classification	SW-SM	SP-SC

These values indicate that the soil from both sites can be classified as inorganic clays of medium plasticity according to the Casarande Plasticity Chart in Fig. 2 shown below. His classification is based on the Unified Soil Classification System (USCS) following the ASTM 2487 - 00 Standard. This shows that termite mound is workable and capable of carrying considerable loads.

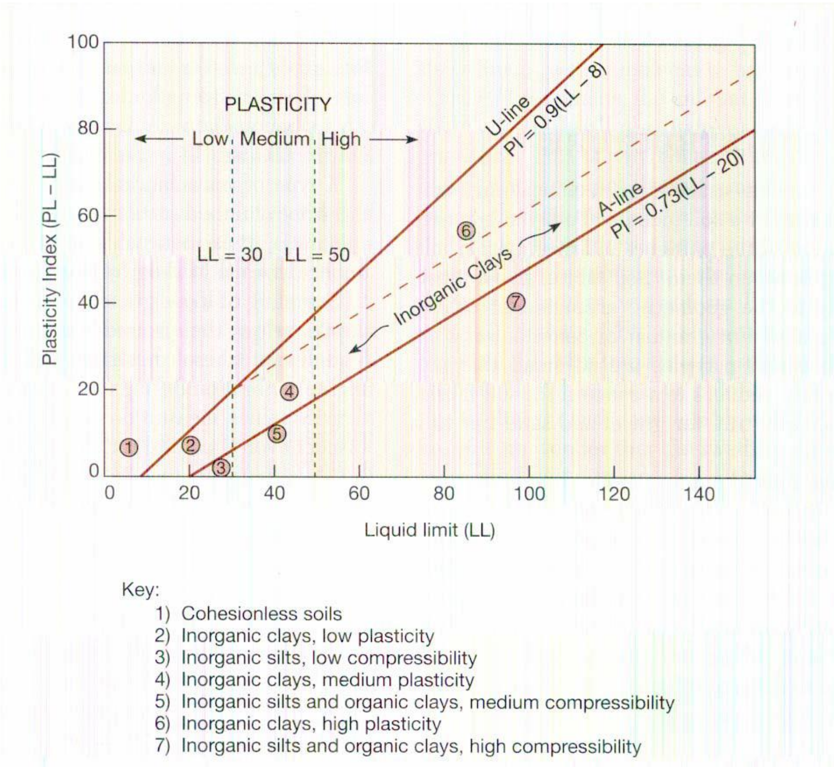

Fig. 1: Casagrande's Plasticity Chart
(**Source:** Geotechnical Engineering Bureau, 2007)

The specific gravity of soil samples from site A was determined to be 2.6, while soil from site B was determined to be 2.8. These values are within the range of the specific gravity of clay (2.79). This implies that mound soil can serve as a replacement for clay soil.

Table 3 below presents the textural and organic properties of the soil samples. It is clear from the table that the clay and silt contents of the samples decrease as the sand content increases.

Table 3: Textural and Organic Properties of Samples

Components, %	**Sample A**	**Sample B**
Organic Carbon	0.51	0.45
Organic Matter	0.87	0.75
Sand	39.52	37.81
Silt	40.00	42.74
Clay	20.48	19.45
Texture (USDAstd)	SL	SL

3.2 Compressive Strength of the Mound Bricks

A total number of thirty bricks of dimension 100 mm x 100 mm x 100 mm were made from the two soil samples; fifteen brick for each soil sample. These specimens were tested by a compression testing machine (Testometric, Model M500-100 AT) after 14, 21, and 28 days curing. At each measurement, the load was applied gradually at the rate of 25 mm/Sec until the specimen failed (Fig. 2, 3). Load at failure divided by area of specimen gives the compressive strength of the mound bricks.


Figure 2: Specimen under Load


Figure 3: Failure at Maximum Load

Tables 4, 5, 6, 7, 8 and 9 below present the respective compressive strength of the mound bricks at their various periods of curing.

Table 4: Compressive Strength of Sample A at 14 Days Curing Age

Replicates	Weight Brick, (g)	Crushing Load, (KN)	Compressive Strength (N/mm^2)
A1	922	17	1.70
A2	956	23	2.30
A3	969	27	2.70
A4	945	20	2.00
A5	938	18	1.80

Table 5: Compressive Strength of Sample A at 21 Days Curing Age

Replicates	Weight Brick (g)	Crushing Load, (KN)	Compressive Strength (N/mm^2)
A6	950	18	1.80
A7	1003	28	2.80
A8	976	24	2.40
A9	990	26	2.60
A10	975	21	2.10

Table 6: Compressive Strength of Sample A at 28 Days Curing Age

Replicates	Weight Brick, (g)	Crushing Load, (KN)	Compressive Strength (N/mm^2)
A11	1017	20	2.00
A12	1040	25	2.50
A13	1062	28	2.80
A14	1085	32	3.20
A15	995	18	1.80

Table 7: Compressive Strength of Sample B at 14 Days Curing Age

Replicates	Weight Brick, (g)	Crushing Load, (KN)	Compressive Strength (N/mm^2)
B1	1044.5	18	1.80
B2	1062	21	2.10
B3	1047	20	2.00
B4	995	10	1.00
B5	1002	12	1.20

Table 8: Compressive Strength of Sample B at 21 Days Curing Age

Replicates	Weight Brick, (g)	Crushing Load, (KN)	Compressive Strength (N/mm^2)
B6	1059	22	2.2
B7	1068	20	2.0
B8	1082	24	2.4
B9	1000	15	1.5
B10	1010	17	1.7

Table 9: Compressive Strength of Sample B at 28 Days Curing Age

Replicates	Weight Brick, (g)	Crushing Load, (KN)	Compressive Strength (N/mm^2)
B11	1061	24	2.40
B12	1083	27	2.70
B13	1112	36	3.60
B14	1101	28	2.80
B15	1009	20	2.00

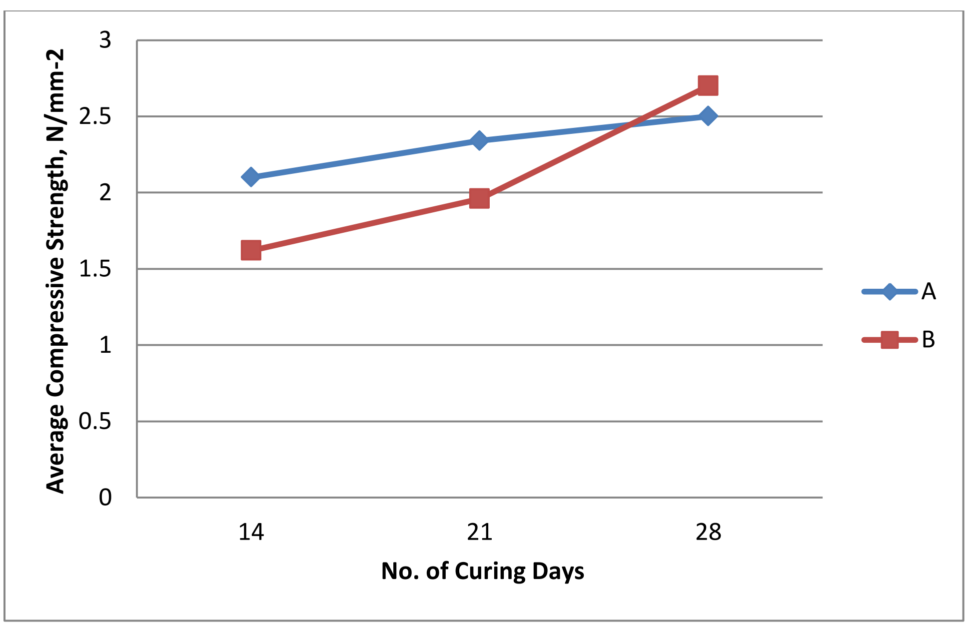

Fig. 4: Average Compressive Strength of Samples

Fig. 4 shows that the compressive strength of all the bricks increased with increasing days of curing. This is expected because as the days of curing increased, the voids within the brick formation continued to reduce due to moisture loss and increased compaction, which eventually leads to loss in weight and increased hardness.

The compressive strength of 2.70 N/mm^2 was recorded as the highest for sample A after 28 days of curing. The values of the compressive strength of the samples were indicative of the stiffness of the bricks and resilience to crack that might lead to seepage and subsequent failure. The high compressive strength could be attributed to the absence of organic content in the mound soil. Ata *et al.*, 2007, observed a decrease in compressive strength of sandcrete blocks as the percentage of laterite content and was increased.

5. CONCLUSION

From the result of the compressive strength, the strength of Sample A increases with an increase in the number of days used in curing while the strength of Sample B increased from 14 days of curing until 28 days of curing. It can thus be concluded that the *termitaria* soils are suitable for agricultural structures.

The Atterberg tests revealed that soils from both sites have 45.74 % and 43.47 % of plasticity indices while the textural and organic properties test revealed that the soil samples had 40 % and 42.75 % of silt and 20.48 % and 19.45 % of clay. These values directly have effects on the plasticity indices of the soils and hydraulic conductivity of the bricks formed. The higher the plasticity indices the lower the hydraulic conductivity which implies low absorption of moisture by the bricks.

From the results, it is recommended that the absorption rate and the shrinkage properties of the mound bricks be investigated.

REFERENCES

Aguwa, J. I. 2009. Study of Compressive Strength of Laterite - Cement Mixes as a Building Material; Austrialian Journal of Technology; 13 (2): 114 – 120.

ASTM D 4318-00. Standard Test Method For Liquid Limit, Plastic Limit and Plasticity Index of Soils. American Society of Testing 100 B Harbour Drive, West Conshohocken, United States. 2005.

Ata, A. Y., Olusola, K. and Olanipekun, A. 2007. A Study of Compressive Strength Characteristics of Laterit Sand Hollow Blocks. Journal of Civil Engineering Dimension; 9 (1): 15 -18.

Geotechnical Engineering Bureau, Geotechnical Test Method: Test Method Liquid Limit, Plastic Limit and Plasticity Index, New York State Department Transportation 2007; 24.

Ndaliman, M. B. 2006. Refractory Properties of Termite Hills Under Varied Proportions of Additives. Leonardo Electronic Journal of Practices and Technologies; 9 (4):161-166.

Olanrewaju, R. M. 2009. Climate and the Growth Cycle of Yam Plant in the Guinea Savannah Ecological Zone of Kwara State, Nigeria. Journal of Meteorological and Climate Science; 5(3): 43-48.

Olusola, E. A. Olanipekun, O. Ata and O. T. Olateju. 2006. Studies on Termite Hill and Lime as Partial Replacement for Cement in Plastering, Building and Environment.; 41(3):302-306.

DEVELOPMENT OF A DIGITAL OPTICAL SENSOR SYSTEM FOR MEASURING SUSPENDED SEDIMENT CONCENTRATION

K. N. Ogbu[1] and C. C. Mbajiorgu[2]
[1]Department of Agricultural and Bioresources Engineering, Nnamdi Azikiwe University, Awka, Nigeria
[2]Eco-Hydrological Systems Research Unit, Department of Agricultural and Bioresources Engineering, University of Nigeria, Nsukka, Nigeria.
Email: knogbu@yahoo.com

ABSTRACT

Streams draining agricultural watersheds are always characterized by high transport of suspended sediment especially during the raining season, and result to water quality and downstream degradation. It has become imperative to continuously monitor sediment discharge so as to develop effective methods of soil and water conservation. This study aimed at developing at developing an optical sensor system for in-situ measurement of suspended sediment concentration in streams. Water samples were collected from Ebonyi River at Obollo-Etiti, Enugu State, Nigeria and used in testing the optical sensor instrument. Suspended sediment concentration readings were obtained using the developed instrument and compared with values obtained using oven-drying method in other to confirm the validity of the instrument. Linear regression equation was obtained with a coefficient of determination of $R^2 = 0.8$, which shows good comparison between the two methods. The developed optical sensor system can be used in-situ for measuring suspended sediment concentration.

KEYWORDS: Optical backscatter sensor, microcontroller, suspended sediment

1. INTRODUCTION

Streams draining intensively-used agricultural watersheds are frequently characterized by high transport of suspended sediment especially during rainfall event (Eder et al., 2010). Sedimentation is a primary and growing environmental, engineering and agricultural issue around the world (Landers et al., 2010). It is also an important index with respect to the mechanics of soil erosion, environmental impact monitoring and reservoir safety capacity (Shi and Zhang, 2012). Loss of aquatic habitats, changes in photosynthesis and visibility, and impacts from contaminants attached to transported sediments are some of the environmental impacts caused by high sedimentation (Wood and Armitage, 1997). The transport of sediment particles in rivers also, has important implications for the management of watersheds, the evaluation of land surface erosion, reservoir sedimentation, ecological habitat quality and coastal sediment budget (IAEA, 2005). Knowledge of sedimentation is also important for the development and management of water resources. High suspended sediment concentration in aquatic ecosystem decreases light penetration into the water column and poses serious threat to aquatic organisms. Therefore, clarity of a natural water body is an indicator of the condition and productivity of that aquatic system. Edwards and Glysson (1999) highlighted some of the practical needs for collecting sediment data which include: (a) For the evaluation of sediment yield with respect to different natural environmental conditions – geology, soils, climate, runoff, topography, ground cover, and watershed size; (b) For the evaluation of sediment yield with respect to different types of landuse; (c) The time distribution of sediment concentration and transport rate in streams; (d) The evaluation of erosion and deposition in channel systems; (d)The amount and particle size characteristics delivered to a water body.

The distribution of suspended sediment in water bodies can be quantified by measuring suspended sediment concentration (Guillen et al., 2000). Manual sediment sampling method by oven-drying is now obsolete, highly time-consuming and cumbersome but however provides a standard for calibrating improved sediment sampling methods. In-situ sensors for measuring suspended sediment concentration have become a suitable practical alternative as it can give high frequency measurements over a long period of time (Vousdoukas et al., 2011). The use of optical sensor systems to monitor suspended sediments in surface water bodies have been widely adopted (Sutherland, 2000). Its advantage includes simple technology, relative low cost of components, ease of deployment and potential high frequency response (Clifford, 1995). Optical backscatter sensors also offer a convenient means of estimating suspended sediment in natural waters (Hatcher et al., 2000).

The objectives of this study are to: develop an optical sensor system for in-situ measurement of suspended sediment concentration in streams and calibrate the new instrument using oven-drying method of estimating suspended sediment concentration.

2. MATERIALS AND METHODS

2.1 Methods of Measuring Suspended Sediment Concentration

Many methods exist for the determination of suspended sediment concentration in streams. Shi and Zhang (2012) however noted that due to different principles, the applicability and precision of each of the method differs considerably. These authors classified the different methods as direct and indirect methods as shown in Table 1.

Table 1: Commonly-Used Measurement Methods for Sediment Concentration

Type	Methods	Limitations	References
Direct methods	Oven-Drying Pycnometer	Sensitive to temperature and salinity content	Abrahams and Atkinson (1993), Zobisch et al. (1996)
Indirect Methods	Capacitance-based	Labour and time consuming	Li et al. (2005), Schlaberg et al. (2006)
	Acoustics	Disturb water flow state; limited scale	Hay and Sheng (1992), Thorne et al.(1993), Huang et al. (1995), Thorne and Hanes (2002)
	Optics	Sensitive to sizes, shapes and distribution of sediment	Vos et al. (2000), Campbell et al. (2005), Orwin and Smart (2005)
	Laser γ-ray	Expensive, in large sizes, harmful radiation	Lei et al. (2002)

Source: Shi and Zhang (2012)

Abrahams et al. (1993) and Zobisch et al. (1996) reported that the traditional oven-drying and pycnometer methods (direct method) for estimating sediment concentration are still widely used even though they are time consuming and labour intensive. The oven-dry method of measuring suspended sediments remains the most direct and accurate but remains inadequate for measuring rapid temporal variations of suspended matter in water bodies (Guillen et al., 2000). These authors also noted that despite its inability to capture temporal variations in the field, this method is considered the best for calibration of other recent methods for determining suspended sediments. Total suspended solids can be determined using:

$$SSC\left(\frac{mg}{L}\right) = \frac{(Residue+Filter)(mg)-Filter\ (mg)}{Sample\ filterd\ (mL)} \times 1000\left(\frac{ML}{L}\right)\ldots\ldots\ldots\ldots\ldots 1$$

Indirect methods for measuring sediment concentration are based on the principles capacitance, acoustics, optics, laser and γ-rays (Shi and Zhang, 2012). The capacitance-based method is sensitive to changes in temperature and salinity in natural water bodies (Li et al., 2005; Schlaberg et al., 2006). Sediment concentration measuring instruments that are based on acoustic principles disturbs the state of streamflow, which results to changes in the stream hydrodynamic properties (Thorne and Hanes, 2002). An optical instrument emits light rays into a sample of water through light emitting diodes (LED) and then measures the reflected light with a photodiode. This reflected light is proportional to the sediment concentration in that water sample (Shi and Zhang, 2012). However, Campbell et al. (2005) stated that such optical

devices need to be calibrated against any direct method before use. Laser and γ-ray based devices have the capability to reduce noises and disturbances from outside, but are usually expensive and large in size (Lei et al., 2002).
Optical instruments have been widely used in the past to monitor suspended sediment and predict the transport of sediment in natural water bodies (Sutherland et al., 2000). Schoellhamer and Wright (2003) reported that the optical backscatter system has been used successfully as a surrogate for suspended sediment concentration in low gradient rivers. Calibrations of optical sensors are important as their measurement depends on sediment particle size, composition, shape and environmental characteristics (Sutherland et al., 2000). Sutherland et al. (2000) also noted that in-situ calibrations of optical sensors are important as it incorporates the effects of sediment quality on the instrument measurement data. Basic designs of optical meters (Omar and Matjafri, 2009) and as shown in Fig. 1 are:

(a) Nephelometer: this is used to directly measure the intensity of light scattered at an angle of 90º from the incident bean on a water sample. The amount of backscattered light is directly proportional to the amount of sediment in the light path. This type of turbidity meter produces higher precision and sensitivity and is normally used for water samples of low turbidity (EPA, 1999). Backscattering technique refers to the measurement if scattered light between 90º – 180º.

(b) Absorptiometer: This is used to measure light intensity after it has passed through the water sample. The transmitted light is measured in relation to initial beam intensity (EPA, 1999).

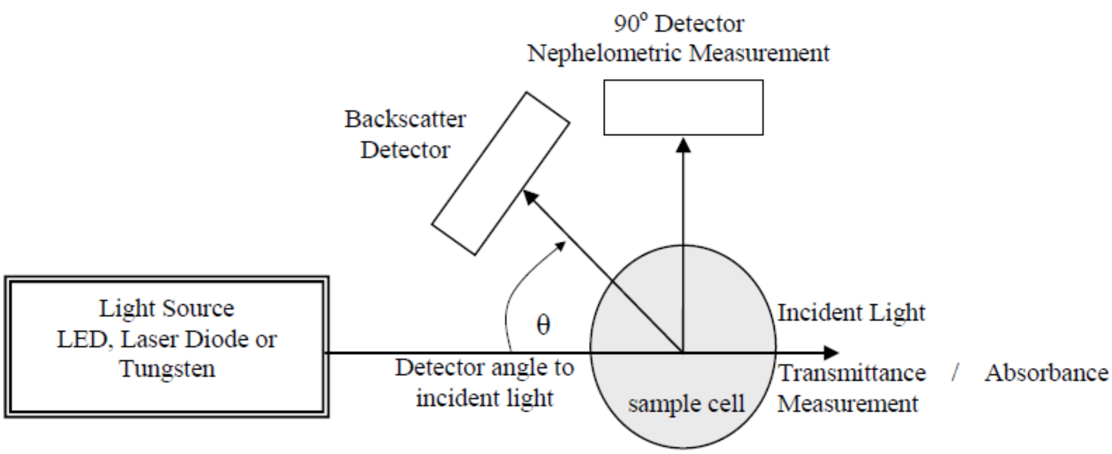

Fig. 1: Turbidity Measuring Techniques

The optical backscatter sensor measures suspended sediment concentration as a result of backscattered light from suspended sediment in water sample. The optical backscatter sensor (OBS) system works on the principle that when it emits infrared light into a water sample, a series of photodiode positioned around the emitter will detect the reelected (backscattered) light (Curtis, 2007). The amount of photocurrent detected by the sensors depends on the illuminated area of the sediment particles and provides an indirect estimate of suspended sediment concentration (Downing, 2006). An important feature of the optical backscatter system sensor is that its signal has a linear relationship with sediment concentration.

2.2 The Measurement System

The materials used for the work are microcontroller, operational amplifier (Op – amp) infrared transmitter, infra-red receiver (light dependent resistor), 7-segment display, transistor amplifier, control switch, connecting wire, resistors, diodes, variable resistors, advance current summer transistors, I.C sockets, capacitors, crystal, LED indicators, 7805 voltage regulator and 9VDC battery cap. The system block diagram and circuit diagram are shown in figure 2 and 3 respectively.

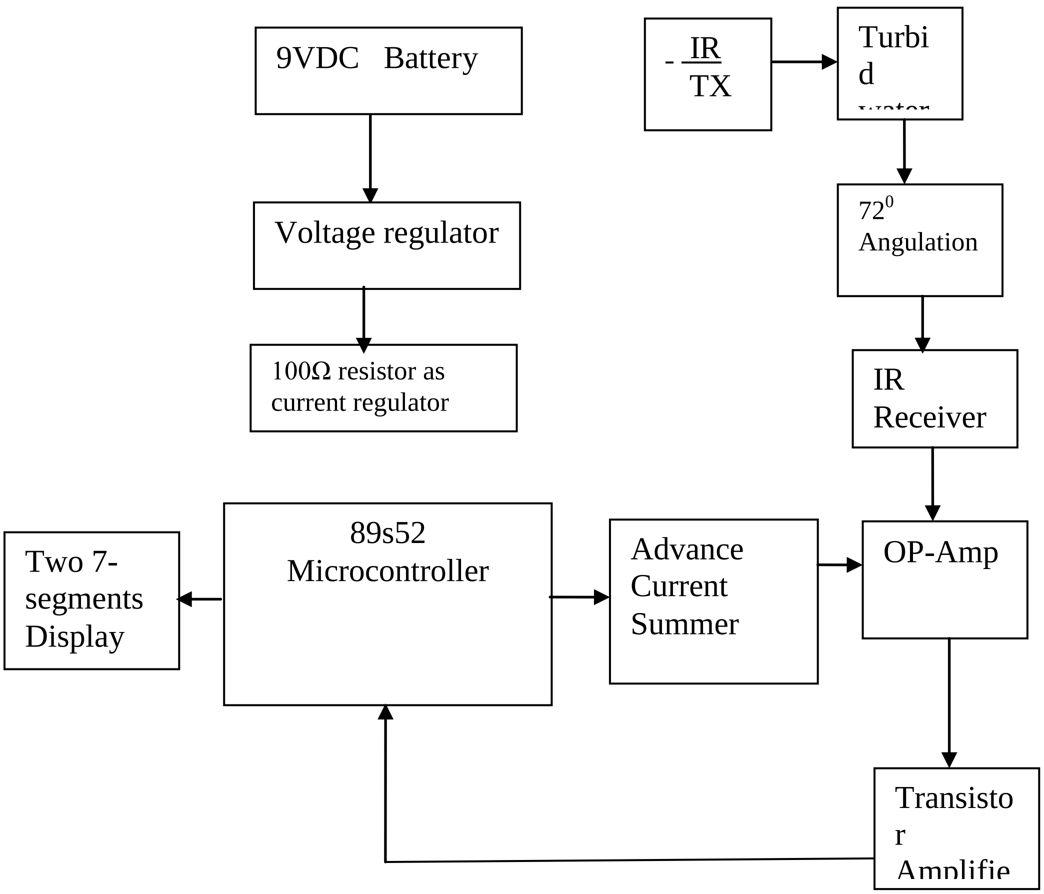

Fig. 2: The System Block Diagram

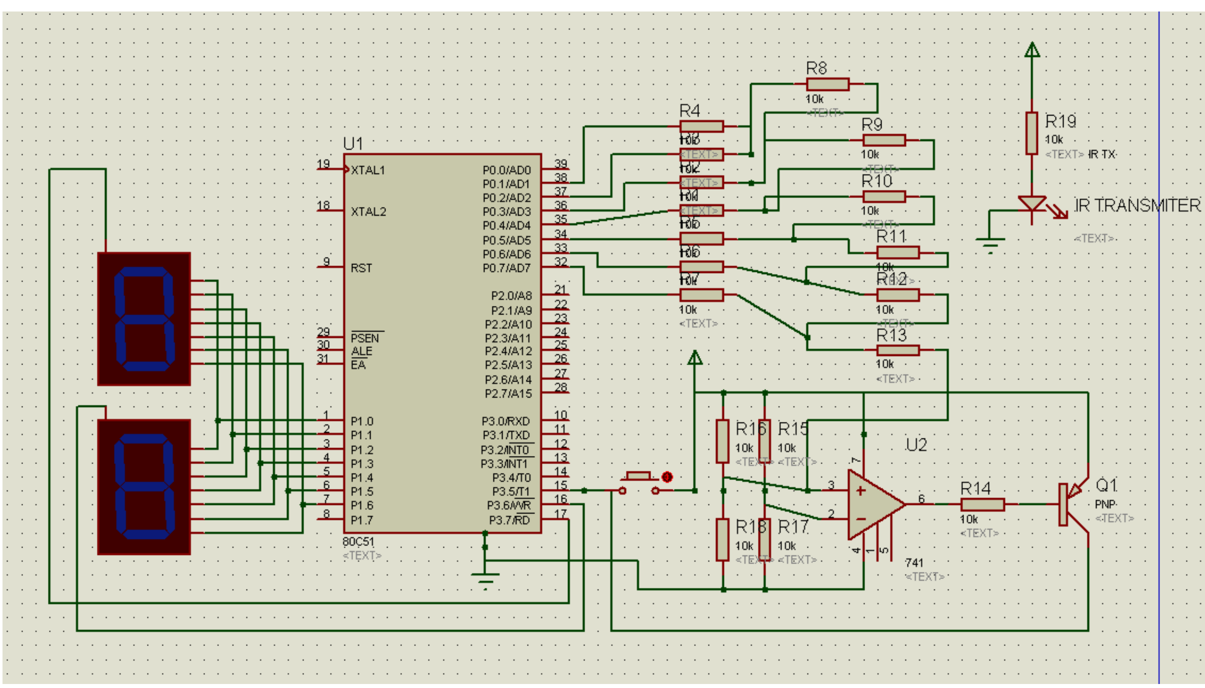

Fig. 3: Circuit Diagram

Microcontroller (MC): This is 89s52 which is an integrated circuit (I.C) of the 8051 family of microcontrollers with 40 pins dual in package (DIP) architecture. It is actually a stand-alone integrated circuit which works like a small computer as indicated by its name. It has a total of four ports for its binary data communication with the external sub-circuits like the infrared receiver, op-amp, 7-segments displays, etc. It has 128 internal general purpose registers address as 00H to 128H or OOH to 7FH (i.e. 00000000B to 01000000B). It has internal microprocessor, Timer 0 and Timer 1, RAMS, ROMs, EEPROM and ALU (Arithmetic and logic unit). The binary/digital input and output to and from the microcontroller ports and its processing of these data, its operations and preferences are controlled by the use of the hex files (i.e. hexa-decimal files) from computer software like ASM, VB.Net, C# (C sharp), JAVA, C, etc. It is not these raw codes/software that we store/burn into the microcontroller using the computer aided programmer but rather, it is a hex (equivalent) file generated from any of raw code/software by our compiler running on our computer system. No matter the programming language used, all of them will give rise to similar hex file for programming our microcontroller (MC). The MC uses an external crystal for stabilizing its clock speed together with two 30μf paper capacitors.

Operational Amplifier (Op-Amp): This is an 8-pin DIP operational amplifier sub-circuit called the 741 Op-Amp. Its major role is to compare the positive and negative voltages and currents at its input pins like pin 2 and 3 as the infra red receiver component (light dependent resistor) is placed between pin 2 and 7 while pin 7 is its V_{cc}/the terminal pin while pin 4 is its GND /ground/negative terminal pin. It can as well amplify the signal input to its pins or amplify the difference between the two signal inputs to its pins. This 741 Integrated Circuit (I.C) is also called a voltage or current comparator since it can compare the degree of positive or negative voltages/currents at its two input pins. Our LDR (serving as our infrared receiver) is connected between pin 2 and 7 of this 741 Op-Amp such that the Op-Amp will be bringing out a negative/low voltage and current output only when the infra red receiver component (light dependent resistor) stop receiving an infrared light (from our infrared transmitter). The light dependent resistor (LDR) serving as our infrared receiver will only stop receiving the infrared light if the water is clear. Our 741 Op-Amp can also stop bringing the needed voltage and current output when the LDR still receives an IR-light (from our IR reflective turbid water) but our microcontroller has counted its binary output (into our advance current summer) balancing/matching our LDR input. It is this high binary count that is being process into outputs being displayed on our two 7-segment display.

Infrared Transmitter: The system has an infrared transmitter sub-circuit. A particular value of resistor was obtained and used to keep our infrared transmitter constantly transmitting infrared light without getting burnt. This stream of infrared light is kept at angle of 78^0 from the infrared receiver (LDR) so that backscattered light (due to presence of sediment in the water) will be detected by the LDR.

Infra-red Receiver and LDR: This optical sensor instrument has an infrared receiver sub-circuit which comprises of the 741 Op-Amp sub-circuitry and it's LDR, resistors, transmitters, diodes, etc. The LDR is used as our infrared receiver as its resistance slightly decreases when it detects the slightly backscattered infrared light by suspended particles in turbid water. The slightest detection of the back scattered infrared light by our LDR will send an appreciable current to our 741 Op-Amp to make it not to give out its usual negative current until our microcontroller counts fast to a level into our advance current summer to meet the LDR matching point in our 741 Op-Amp. At the matching point of the LDR current to our 741 Op-Amp, the Op-Amp will start giving out the expected negative output current which has to be amplified and send to pin 3.5 of our 89s52 microcontroller as a detection of the matching point to enable our microcontroller to quickly process the readings with respect to time before displaying the values on the 7-segment display unit.

Connecting Wire: These are single plastic coated wires of 0.1cm diameter used in connecting our circuit according to its standard block diagram. The connecting wires are also used in connecting the external LDR and infrared transmitter component of our optical sensor system to the Op-Amp circuit which sends its feedback into pin 3.5 of our microcontroller.

Control Switch: This is the 3 by 3 pins soft switch (i.e. 6 pins Dip) that controls the 9V DC battery supply to our circuit via only its two pins out of the six pins. This switch has to be pressed inside to send the current that power on our entire circuit via the 7805 voltage regulator. For the entire system to be switched off, the switch has to be pressed again to bounce out thereby disconnecting its two pins used. An approved standard is for the entire system to be consecutively kept ON via this switch for less than 30 second and rest off for at least one minute for each turbidity reading.

7 – Segment Displays: These are electronic components that are each made from a segmented arrangement of seven light emitting diodes (LED) which are arranged to have common positive terminals of the LED. Each of these two 7-segment displays has the ability to display numbers from 0 to 9 making the two 7-segment combination capable of displaying 00 to 99 as the corresponding decimal equivalent of the digital/binary input received from port 1 of the 89s52 microcontroller. Thus, these corresponding decimal/digital/binary equivalents are also corresponding to the various matching resistances and current between the LDR (that receives our backscattered IR-light) and our advance current summer which both feeds their current output into our 741 Op-Amp integrated circuit.

Transistor Amplifiers: These are small three pins bipolar junction transistors (BJT) which are used to amplify the weak current from the 741 Op-Amp of our infrared Receiver circuit before sending their amplified current to port 3.5 of our 89s52 microcontroller. The two transistors are respectively an NPN and a PNP transistor.

2.3 Testing and Evaluation of the Instrument

The optical sensor instrument was calibrated and tested using water samples collected from Ebonyi River at Obollo-Etiti in Enugu State, Nigeria. Seven water samples were collected separately from the river for analysis. Each of the samples was analyzed for suspended sediment concentration using the optical sensor instrument and also in the laboratory by oven-drying method.

3. EVALUATION RESULTS

The readings obtained for each water sample collected using the two methods are shown in Table 2.

Table 2: Suspended Sediment Concentration Measurements

Sample No.	Instrument Readings(mg/l)	Oven-dry Readings(mg/l)
1	21	20.83
2	0	0.16
3	0	0.22
4	11	11.26
5	7	6.59
6	10	9.91
7	10	10.29

Measurements performed with the optical sensor instrument performed well with that obtained using oven-drying method and are plotted as shown in Figure 4.

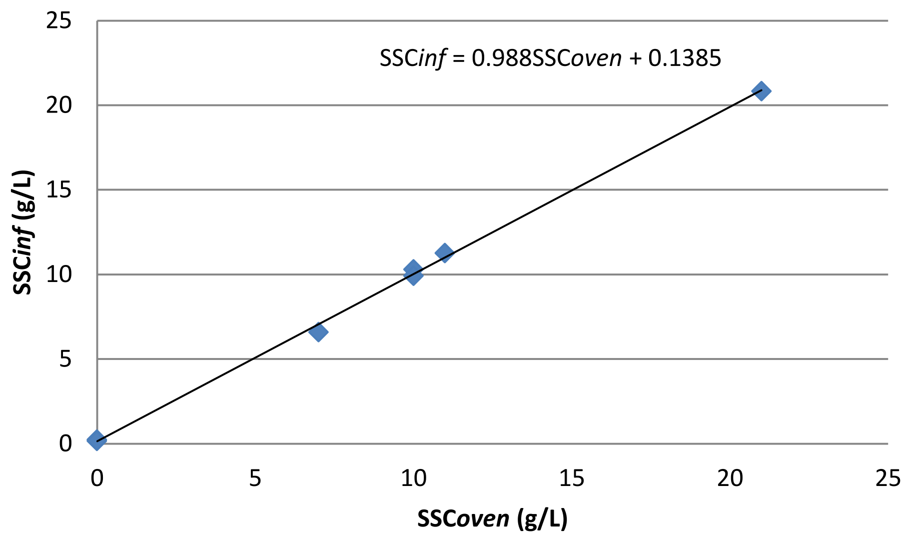

Fig. 4: Comparisons of SSC Obtained Using the Optical Sensor Instrument (SSC_{inf}) and Oven-Dry (SSC_{oven}) Methods

The linear regression equation obtained is given as:

$$SSCinf = 0.988SSCoven + 0.1385 \quad \text{.......2}$$

Where, SSCinf = suspended sediment concentration measurement obtained using the optical sensor system; SSCoven = suspended sediment concentration measurement obtained using oven-drying method.

4. CONCLUSION

In-situ measurement of suspended sediment provides an alternative and convenient means of estimating suspended sediment concentration in streams rather than the conventional oven-drying method. The optical sensor instrument developed, offers simple technology, relative low cost of components and ease of deployment. Light dependent resistor was adopted in this design instead of photodiode because of its high sensitivity to backscattered light.

However, regular maintenance is needed to keep this digital optical sensor instrument in good working shape. Regular cleaning of the infrared component after each use to avoid biofouling should be strictly adhered to. Also, the instrument should not be left on when not in use and battery should be replaceD as at when needed.

REFERENCES

Abrahams, A.D. and J.F. Atkinson 1993. Relation Between Grain Velocity and Sediment Concentration in Overland Flow. Water Res., 29: 3021 - 3028

Campbell, C.G., D.T. Laycak, W. Hoppes, N.T, Tran and F.G. Shi 2005. High Concentration Suspended Sediment Measurement Using a Continuous Fibre Optic In-Stream Transmissometer. J. Hydrol. 311: 244 - 253

Clifford, N.J. 1995. Laboratory and Field Assessment of an Infrared Turbidity Probe and its Response to Particle Size and Variation in Suspended Sediment Concentration. Hydrological Sciences Journal 40 (6): 771 - 791

Curtis, J.A. 2007. Summary of Optical-Backscatter and Suspended Sediment Data, Tomales Bay Watershed, California, Water Years 2004, 2005, and 2006. USGS Scientific Investigations Report

Downing, J.P. 2006. Twenty-five Years with OBS Sensors: The Good, The Bad and the Ugly. Continental Shelf Research 26 (17 – 18): 2299 – 2318
EPA 1999. Basic Turbidimeter Design and Concepts. Turbidity Guidance Manual.
Eder, A., P. Strauss, T. Kruger and J.N. Quinton 2010. Comparative Calculation of Suspended Sediment Loads with Respect to Hysteresis Effects in the Petzenkirchen Catchment, Australia. Journal of Hydrology 389: 168 - 176
Edwards, T.K. and G.D. Glysson 1999. Field Methods for Measurement of Fluvial Sediment. Techniques of Water Resources Investigation of the USGS, Bk 3, C2
Foster, I.D.L., R. Millington and R.G. Grew 1992. The Impact of Particle Size Controls on Stream Turbidity Measurements; Some Implications for Suspended Sediment Yield Estimation. Erosion and Sediment Transport Monitoring Programmes in River Basins. Proceedings of the Oslo Symposium. IAHS Publ. No. 210.
Guillen, J., A. Palanques, P. Puig, X. Durrieu, D. De Madron and F. Nyffeler 2000. Field Calibration of Optical Sensors for Measuring Suspended Sediment Concentration in the Western Mediterranean. Sci. Mar., 64 (4): 427 - 435
Hatcher, A., P. Hill, J. Grant and P. Macpherson 2000. Spectral Optical Backscatter of Sand in Suspension: Effects of Particle Size, Composition and Colour, Marine Geology 168: 115 - 128
Hay, A.E. and J. Sheng 1992. Vertical Profiles of Suspended Sand Concentration and Size from Multifrequency Acoustic Backscatter. J. Geophy. Res. 97: 15661 - 15677
Huang, B.S., T.L. Teng and Y.T. Yeh 1995. Numerical Modelling for Acoustic Scattering of 3-D Spherical Wavefronts: Implications on Near Basin Amplification. Terr. Atmos. Ocean. Sci. 6: 251 - 270
IAEA 2005. Fluvial Sediment Transport: Analytical Techniques for Measuring Sediment Load. IAEA – TecDOC-1461
Landers, M.N. 2010. Review of Methods to Estimate Fluvial Suspended Sediment Characteristics from Acoustic Surrogate Metrics. 2nd Joint Federal Interagency Conference, Las Vegas, June 27 – July 1
Lei, T., H. Wang, J. Zhao, Q. Liu and W. Xia 2002. Automatic System for Dynamical Determination for Sediment Concentration and Flow Rate in Runoff. Trans. CSAE 18: 48 - 51
Li, X., T. Lei, W. Wang, Q. Xu and J. Zhao 2005. Capacitance Sensors for Measuring Suspended Sediment Concentration. Catena 60: 227 - 237
Omar, A.F. and MatJafri, M.Z.B. 2009. Turbidimeter Design and Analysis: A Review on Optical Fibre Sensors for the Measurement of Water Turbidity. Sensors 9: 8311 - 8335
Orwin, J.F. and C.C. Smart 2005. An Inexpensive Turbidimeter for Monitoring Suspended Sediment. Geomorphology 68: 3 - 15
Shi, X. and F. Zhang 2012. A Preliminary Study on the Measurement of Sediment Concentration in Hillslope Runoff with an Electronic Tracer. Terr. Atmos. Ocean. Sci. 23(5): 597 - 604
Schlaberg, H.I., J.H. Baas, M. Wang, J.L. Best, R.A. Williams and J. Peakall 2006. Electrical Resistance Tomograpghy for Suspended Sediment Measurements in Open Channel Flows Using A Novel Sensor Design. Part. Part. Syst. Charact. 23: 313 – 320
Schoellhamer, D.H and S.A. Wright 2003. Continuous Measurement of Suspended Sediment Discharge in River by Use of Optical Backscatter Sensor. IAHS Pub. 283: 28 - 36
Sutherland, T.F., P.M. Lane, C.L. Amos and J. Downing 2000. The Calibration of Optical Backscatter Sensor for Suspended Sediment of Varying Darkness Levels. Marine Geology 162: 587 - 597
Thorne, P.D. and D.M. Hanes 2002. A Review of Acoustic Measurement of Small-Scale Sediment Procesess. Cont. shelf Res. 22: 603 - 632
Thorne, P.D., P.J. Hardcastle and R.L. Soulsby 1993. Analysis of Acoustic Measurements of Suspended Sediments. J. Geophy. Res. 98: 899 - 910
Vos, R.J., P.G.J. ten Brummelluis and H. Gerritsen 2000. Integrated Data-Modelling Approach for Suspended Sediment Transportation on A Regional Scale. Coast. Eng. 41: 177 – 200
Vousdoukas, M.I., S. Aleksiadis, C. Grenz and R. Verney 2011. Comparisons of Acoustic and Optical Sensors for Suspended Sediment Concentration Measurements under Non-homogeneous Solutions. Journal of Coastal Research, Special Issue 64: 160 - 164

Ziegler, A.C. 2002. Issues Related to Use of Turbidity Measurement as a Surrogate for Suspended Sediment. Turbidity and Other Surrogate Workshop, April 30 – May 2, Reno NV

Zobisch, M.A., P. Klingspor and A.R. Oduor 1996. The Accuracy of Manual Runoff and Sediment Sampling from Erosion Plots. J. Soil Water Conse. 51: 231 – 233

ESTIMATION OF RUNOFF AND SEDIMENT YIELD OF UPPER EBONYI RIVER WATERSHED USING *MWAGNPS*

G. I. Ezenne, E. L. Ndulue and V. Ogwo
Agricultural and Bioresources Engineering Department, University of Nigeria, Nsukka, Nigeria.
E-mail: gloria.ezenne@unn.edu.ng

ABSTRACT

Information about runoff and sediment exported from watersheds as well as related erosive processes are required by watershed managers and decision-makers. The event-based Agricultural Non-Point Source (AGNPS) pollution model is used extensively to simulate runoff, sediment yield and nutrient transport in agricultural watersheds. The present study estimated runoff and sediment yield of Upper Ebonyi River watershed using Mapwindow AGNPS (MWAGNPS). The materials used for the study include the Digital Elevation Map (DEM), the land use map and the soil map of the study area. The study was carried out using 13 rainfall-runoff events, 5 for calibration and 8 for validation, from Upper Ebonyi River watershed, Enugu State. The results obtained with MWAGNPS were compared with the observed data. After the analysis, the coefficient of performance between the observed and simulated runoff and sediment yield gave 1.3 and 1.4 respectively. Therefore, a calibrated MWAGNPS model could estimate runoff and sediment yield in the study area within an acceptable estimation error.

KEYWORDS: Watershed, runoff, sediment.

1. INTRODUCTION

The spatial distribution of water and the sediment it carries is difficult to assess. This is because normally the sediment concentration is measured at a point in the catchment, usually at an outlet where the sediments are lumped together. With the help of environmental models the spatial distribution of sediment can be considered. Simulations under various combinations of different factors of land and water management can provide comparative analysis of different options and then prove to be very useful guide as to what Best Management Practices (BMPs) can be adopted to minimize pollution from point and non-point sources (Shrestha, 2005). Many process-based models have been developed in the past for rainfall-runoff-erosion modelling. According to Rainis et al., (2002), these process-based models are advantageous as compared to the other methods of sediment yield estimation, particularly when the spatial and temporal distributions of net soil loss must also be determined for devising optimal soil conservation and management practices.

MWAGNPS is a MapWindow GIS interface for AGNPS. AGNPS (Agricultural Non-Point Source Pollution) Model was developed by the Agricultural Research Service, U.S. Department of Agriculture, in co-operation with Minnesota Pollution Control Agency and the Natural Resource Conservation Service (NRCS) (Rainis et al., 2002; Noor et al., 2012). The AGNPS model is an event-based model that simulates surface runoff, sediment, and nutrient transport primarily from agricultural watersheds. Borah and Bera (2003) summarized watershed-scale hydrologic and nonpoint-source pollution single-event models. Basic model components include hydrology, erosion, sediment, and chemical transport. In addition, the model considers point sources of water, sediment, nutrients, and chemical oxygen demand (COD) from animal feedlots, and springs. The model has the ability to output water results at intermediate points throughout the watershed network. This capability is based on the model's implementation of the 'cell'. Cells are uniformly square areas subdividing the watershed, and all watershed characteristics and inputs are expressed at the cell level. These Cells allows analysis at any point within the watershed. Each cell homogenously represents the environmental factors. Model components use equations and methodologies that have been well established. Runoff volume and peak flow rate are estimated using the SCS runoff curve number method. Upland erosion and sediment transport is estimated using a modified form of the Universal Soil Loss Equation, USLE. Sediment is routed from cell to cell through the watershed to the outlet using sediment transport and depositional relationship which is based on a steady-state continuity equation.

The AGNPS model is a simple routing runoff model based on the single storm event and very useful to identify the critical area, since the hydrologic components and nutrient loadings are provided based on the unit cell grids (Choi and Park, 1997). Kirnak (2002) compared Water Erosion Prediction Project (WEPP) model and the Agricultural Non-Point-Source Pollution Model (AGNPS) and found that there was no significant statistical difference between measured and predicted runoff and sediment data for both models (at $\mu = 0.05$ level). Parajuli et al., (2007) says that overall AGNPS model efficiency was found to be better than WEPP, especially in predicting sediment yields. Grunwald and Norton (1999), Panuska et al. (1991) concluded that sediment yield calculations were highly dependent on the quality of the peak flow calculations of the AGNPS model. The predicted sediment yield values ranged from a maximum under prediction of 60% to a maximum over prediction of 1.4% compared to measured sediment yield values. Though, testing and validation of AGNPS model using measured data is still scarce (Rainis et al., 2002; Grunwald and Norton, 1999).

Therefore, the objective of this study is to simulate runoff and sediment yield on Upper Ebonyi River watershed, Enugu state using MWAGNPS. The simulated values are compared with the observed data from the watershed.

2. METHODOLOGY

2.1 AGNPS Component Equations

Hydrologic Calculations

The peak flow is calculated using *TR55*. The *TR55* option uses the SCS unit hydrograph generation theory and assumes a rectangular shaped channel (top width and bankfull depth). The *TR55* method is an extension of the basic curve number theory including rainfall amount and distribution through the use of a unit hydrograph. The SCS curve number technique is a simplified method for estimating rainfall excess that does not require computing infiltration and surface storage separately. The excess rain volume (runoff) depends on the amount of precipitation and the volume of total storage (retention) predicted by the SCS (equation 1):

$$Q = \frac{(P - 0.2S)^2}{P + 0.8S} \quad \text{--------------------------------} \quad (1)$$

where Q is the runoff volume, P is the total rainfall from the storm and S is the retention factor, all with length dimensions [inches]. The retention factor S is obtained from (equation 2)

$$S = \frac{1{,}000}{CN} - 10 \quad \text{--------------------------------} \quad (2)$$

where CN is the curve number for the cell. These runoff curve numbers depend on the soil water content (moisture condition) and can be found as tabulated values for different land use descriptions. The SCS method uses the convolution of a triangular hydrograph for overland routing of excess rainfall where the peak time is the only parameter determining the shape of the hydrograph. The area under the unit hydrograph equals the unit volume of the rainfall excess.

Sediment Transport

Soil erosion affects downstream water bodies (Noor et al., 2012). The AGNPS model simulates the soil loss and sediment yield in a two-step process. For the soil erosion calculations it uses a modification of the Universal Soil Loss Equation, USLE. The modified USLE equation as used in AGNPS is (Young et al., 1989):

$$SL = (EI)\,KLSCP\,(SSF) \text{ ------------------------- } (3)$$

where SL is the soil loss, EI is the product of the storm total kinetic energy and maximum 30-minute intensity, K is the soil erodibility factor, LS is the topographic factor, C is the cover and management factor, P is the supporting practice factor, and SSF is a factor to adjust for slope shape within the cell.

2.2 Data Extraction

The process of extracting data from map sources is divided into two sections:

(a) topography related data using the DEM file,
(b) soil type and land cover data using the map files.

A digital elevation model (DEM) is used to derive slope, slope length, aspect, and other related parameters (He, 2003). For the DEM extraction, the calculations are performed in two steps. For the flow direction of each cell, the point of maximum flow accumulation within the intersection of the cell and the watershed is found. The cell with the largest of these maximum flow accumulations is the outlet cell for the watershed. Table 1 shows AGNPS variables as function of DEM and MAP.

Table 1: AGNPS Variables as Function of DEM and MAP

Variable	DEM[1]	LU[2]	S[3]
Receiving Cell Number	●		
Receiving Cell Subdivision	●		
Flow Direction	●		
SCS Curve Number		●	●
Land Slope	●		
Slope Shape (Def=1)	●		
Slope Length (Def=150)	●		
Overland Manning's		●	
K - Factor			●
C - Factor		●	
P - Factor (Def=1)		●	
Surface Condition Constant		●	
COD Factor		●	
Soil Texture ID			●

[1]DEM-Digital Elevation Model; [2]LU-Map File (landuse layer): [3]S-Map File (soil type layer)

2.3 The Study Area

Upper Ebonyi river watershed is shown as the study area in Figure 1 below. The gauging point is at Obollo-etiti, Nsukka. Two major landforms are found within the catchment: the sandstone escarpment of the Udi-Nsukka Cuesta; and the shale peneplains of the Cross River Plains (Campling et al., 2002). Meteorological data was collected from meteorological station, space centre, UNN. The main source files (in map form) of Upper Ebonyi river watershed used to implement MWAGNPS simulation are:

1) Watershed – polygon shape file (single boundary layer)
2) DEM – ascii raster file.
3) Soil – raster file and the plug-in converted it to a shape file.

4) Landuse – raster file and the plug-in converted it to a shape file.

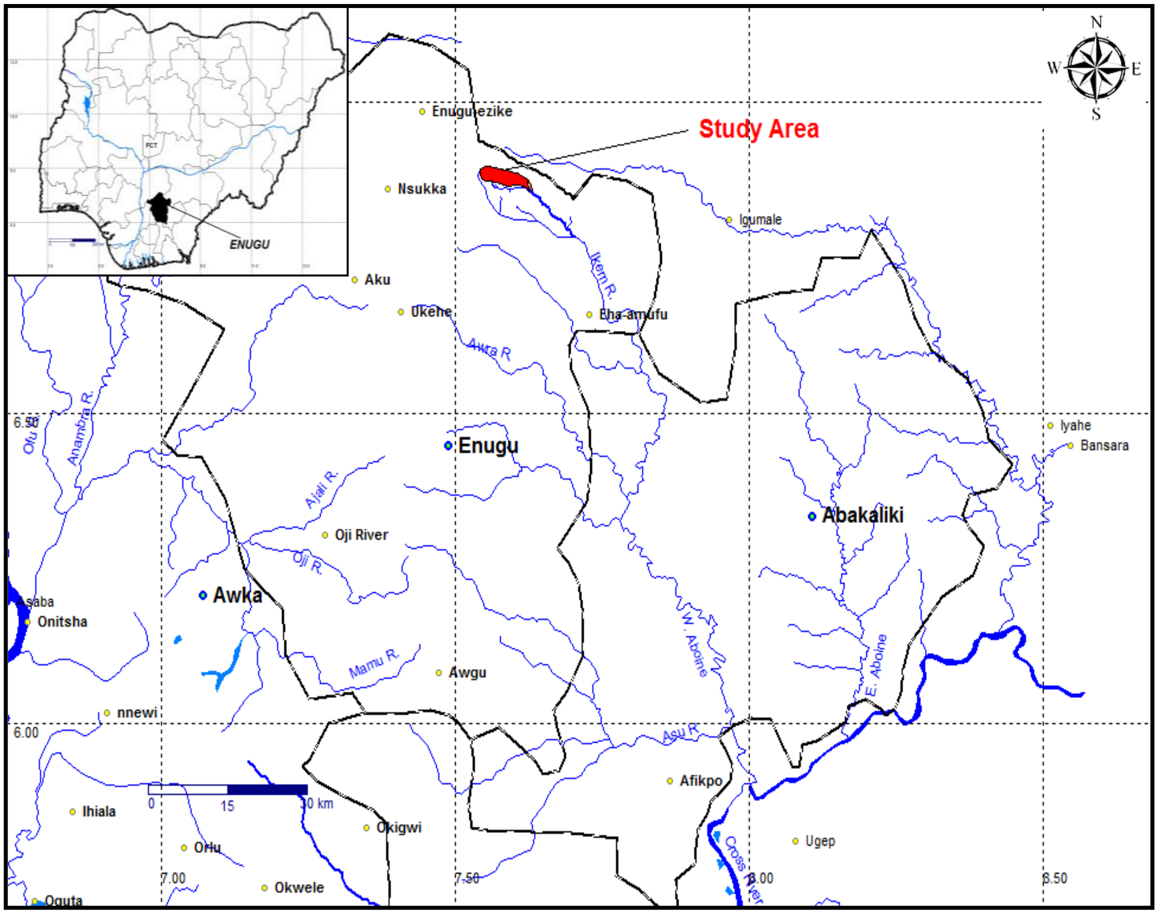

Figure 1: Map showing the study Area (Upper Ebonyi River Watershed)

2.4 Measurements and Model Parameters

MapWindow GIS serves as the main map engine used to display spatial information in the form of geographic layers and to extract the model data via the MWAGNPS plug-in. All the maps and the DEM data are stored in separate folders as shape and raster files. Also, all the modeled scenarios are stored as a combination of an Access database file with an associated grid as a shape file, both stored in the Scenarios folder. The model subdivides the study area into uniform grid cells similar to a raster-based GIS as specified. In this study, uniform grid system with cells was superimposed on the watershed, which generated 17 base cells. All watershed characteristics and inputs are expressed at the cell level. The cells are numbered consecutively from the upper left moving on the right direction and down automatically by the model.

The model requires two groups of input: watershed level and cell parameter (watershed element). At the watershed level, data required are as follows: watershed identification/description, precipitation (inches), precipitation duration, area of each cell (acres) and outlet cell number. For each watershed element (cell), AGNPS requires the following input data values (its distributed parameter information): cell number, number of the cell into which it drains, SCS curve number, average land slope (percent), slope shape factor (uniform, convex or concave), average field slope length (feet), average channel slope (percent), average channel side slope (percent), Mannings roughness coefficient for the channel, soil erodibility factor (K) for the USLE, cropping factor (C) for the USLE, practice factor (P) for the USLE, surface condition constant (factor based on land use), aspect (one of 8 possible directions indicating the principal drainage direction from the cell), soil texture (sand, silt, clay, peat), channel indicator (indicating existence of a defined channel within a cell). Geospatial databases built with geographic information systems (GIS) served as primary sources of input data to AGNPS. Elevation, land cover, and soil data for watershed are the base from which we extracted some input parameters required by the AGNPS.

Observed rainfall depth and the corresponding duration values were entered in the model (Table 2). Flow directions identified from digital elevation map (DEM) and field visits were assigned to the cells. The rainfall scenario for Upper Ebonyi River watershed was determined from rainfall recorded at the University of Nigeria Space Centre. From the records, rainfall events and their corresponding depth were selected with depths over 22.9mm. This approach was adopted because the AGNPS model, as input, uses rainfall depth and duration (hours) in each of its areal elements (Miklanek et al., 2004).

2.5 Model Calibration

The model was calibrated using 3 rainfall events and validated using 5 rainfall events as shown in Table 3. The surface runoff component of the model was calibrated by varying the 'Manning's roughness coefficient' parameter value. The sediment yield estimation was improved by proportionately varying the cropping factor (C) in the model.

Table 2: Observed rainfall depth and the corresponding duration values

Process	**Event**	**Date**	**Rainfall (mm)**	**Duration of Rain (hr.)**
Calibration	1	08-07-2013	32.8	7.6
	2	18-07-2013	32.9	2.4
	3	23-07-2013	45.4	3.7
Validation	4	25-07-2013	54.3	4.9
	5	08-08-2013	23	3.9
	6	21-08-2013	26.9	7.3
	7	27-08-2013	24.1	1.8
		28-08-2013	64.1	5.1

3. RESULTS AND DISCUSSION

For the purpose of calibration, the major results obtained after running the model are the peak runoff rate and the sediment yield. These results are shown in Tables 3 and 4 respectively.

Table 3: MWAGNPS model calibration and Validation results for Peak Flow

	Rainfall		**Peak flow (m^3/s)**	
	Event	**Depth(mm)**	**Simulated**	**Observed**
Calibration	1	32.8	0.0617	0.041
	2	32.9	0.0617	0.042
	3	45.4	0.1541	0.047
Validation	4	54.3	0.1204	0.105
	5	23	0.0014	0.036
	6	26.9	0.0210	0.030
	7	24.1	0.0085	0.034
	8	64.1	0.1031	0.134

Table 4: MWAGNPS model calibration and Validation results for Sediment Yield

	Rainfall		**Sediment (t)**	
	Event	**Depth(mm)**	**Simulated**	**Observed**
Calibration	1	32.8	0.45	0.758
	2	32.9	0.71	1.780
	3	45.4	9.84	3.461

Validation	4	54.3	8.11	3.241
	5	23	0.00	1.355
	6	26.9	0.03	1.877
	7	24.1	0.01	1.899
	8	64.1	10.10	9.210

The model performance was evaluated by calculating the coefficient of performance between observed and simulated parameters using Nash-Sutcliffe coefficient. The Nash-Sutcliffe coefficient describes how well the stream flows are simulated by the model. This efficiency criterion is commonly used for model evaluation, because it involves standardization of the residual variance, and its expected value does not change with the length of the record or the scale of runoff. The equation is described as follows:

$$NSE = 1 - \frac{\sum_{i=1}^{N}(Q_{Si} - Q_{Oi})^2}{\sum_{i=1}^{N}(Q_{Oi} - \overline{Q_O})^2} \quad \text{----------------------------- (4)}$$

After the analysis, the coefficient of performance between the observed and simulated runoff and sediment yield gave 1.3 and 1.4 respectively. A value of NSE = 1.0 indicates that the pattern of model estimation perfectly matches the measured data. The farther away from 1 the NSE value becomes, the larger the error in the predicted pattern when compared with the measurements. Based on the past studies of environmental model applications an NSE value of greater than 0.50 and mean relative error (MRE) value of less than 25% are considered numeric ratings for satisfactory model performance (Du et al., 2009). Hence from the analysis, the coefficient of AGNPS performance on Upper Ebonyi river watershed is not far from the value of NSE = 1. Though the results indicates that there are errors but is still within the acceptable limit.

4. CONCLUSION

The spatial distribution of water and the sediment it carries is difficult to assess. This is because normally the sediment concentration is measured at a point in the catchment, usually at an outlet where the sediments are lumped together. With the help of models like AGNPS, the spatial distribution of runoff and sediment can be considered. The event-based Agricultural Non-Point Source (AGNPS) pollution model interfaced in Mapwindow GIS is used in this study to simulate runoff and sediment yield in agricultural watersheds. The results obtained shows that calibrated MWAGNPS model can estimate runoff and sediment yield in the Upper Ebonyi river watershed within an acceptable estimation error. The coefficient of performance between the observed and simulated runoff and sediment yield gave 1.3 and 1.4 respectively.

REFERENCES

Borah D. K. and M. Bera 2003. Watershed-scale hydrologic and nonpoint-source pollution models: review of mathematical bases. Transactions of the American Society of Agricultural Engineers (ASAE), 46(6): Pp. 1553-1566

Campling Paul, Anne Gobin, Keith Beven and Jan Feyen 2002. Rainfall-runoff modelling of a humid tropical catchment: the TOPMODEL approach. Hydrological Processes 16;231–253

Choi Kyoung-Sik and Seok-Soon Park 1997. Comparison of two Non-point source Models (AGNPS and SWRRB) in urban coastal watershed. Environ. Eng. Res. 2, Pp.119-126

Du Bing, Xiaoyi Ji, R. Daren Harmel, and Larry M. Hauck 2009. Evaluation of a Watershed model for estimating daily flow using limited flow measurements. Journal of the American water resources association (JAWRA), 45, N0. 2. Pp. 475-484.

Grunwald S. and L. D. Norton 1999. An AGNPS-based runoff and sediment yield model for two small watersheds in Germany. Transactions of the American Society of Agricultural Engineers (ASAE), 42(6): 1723-1731

He Chansheng 2003. Integration of geographic information systems and simulation model for watershed management. Environmental Modelling & Software. 18, Pp. 809–813

Kirnak Halil 2002. Comparison of Erosion and Runoff Predicted by WEPP and AGNPS Models Using a Geographic Information System. Turk J Agric For, vol. 26, Pp. 261-268

Miklanek P., P. Pekarova, A. Konicek and P. Pekar 2004. Research Note: Use of a distributed erosion model (AGNPS) for planning small reservoirs in the Upper Torysa basin. Hydrology and Earth System Sciences, 8(6). Pp. 1186-1192

Noor Hamzeh, Somayeh Fazli, Seyde Maryam Alibakhshi 2012. Prediction of storm-related sediment-associated contaminant loads in a watershed scale. Ecohydrology and Hydrobiology. 12(3) 183-189 Panuska, J. C., 1. D. Moore, and L. A. Kramer 1991. Terrain analysis: Integration into the Agricultural Nonpoint Source (AGNPS) Pollution Model. J. *Soil & Water Conserv, I* (Jan/Feb.): Pp. 59-64.

Parajuli P.B., K.H. Yoo, D.A. Shannon and W.J. Jeon 2007. Application of WEPP and AGNPS to a Cattle grazing pasture with poultry litter application as a fertilizer. Journal of Environmental Hydrology, VOL. 15. Pp.1-12

Rainis Ruslan, Wan Ruslan Ismail and Noresah Mohd Shariff 2002. Estimating sediment yield of a small catchment in a tropical region using the AGNPS model: the waterfall river catchment, Penang, Malaysia. Journal of Environmental Hydrology, 10(9) 1-10.

Shrestha Sangam, Futaba Kazama, Mukand S. Babel and A. Das Gupta 2005. Use of ANNAGNPS for watershed modeling in Siwalik hills of Nepal. Proceedings of the 2005 International Conference on Simulation and Modeling. V. Kachitvichyanukul, U. Purintrapiban, P. Utayopas, eds.

Young R. A., C. A. Onstad, D. D. Bosch and W.P. Anderson 1989. AGNPS: A nonpoint-source pollution model for evaluating agricultural watersheds. Journal of Soil and Water Conservation, 44 (2) 168-173.

SPATIAL VARIATIONS OF THREE SELECTED RIVER WATERS QUALITIES IN EBONYI STATE FOR HUMAN CONSUMPTION

J. I. Awu, C. N. Madubuike, O. A. Ogunjirin and A. M. Adeyi
National Centre for Agricultural Mechanization (NCAM), Ilorin, Nigeria.
Federal University of Technology, Owerri, Imo State, Nigeria.
Email: awujohnibe4uk@yahoo.com, ntslola@yahoo.com

ABSTRACTS

The study focused on spatial quality evaluation of three selected rivers in Ebonyi State for human consumption. The rivers studied were Ubei, Idima and Iyioka rivers. Data was generated using Direct Reading Engineering Method (DREM), Gravimetric Method, Titrimetric Method, Spectrophotometric Method, Atomic Absorption Spectrophotometric Method, Total Viable count for physiochemical and Microbiological analysis respectively. The generated data was further subjected to a statistical analysis using one way analysis of variance (ANOVA) on difference between means of parameters and graphical method to determine the spatial variation of the water qualities.

The results showed that for some variables there is statistical difference between means of parameters with respect to space at various levels of significance. They include Sulphate (1%), Alkalinity (5%), Chemical Oxygen (5%), Nickel (1%), Arsenic (1%), Zinc (1%), Cadmium (1%), Bacteria (1%). Based on World Health Organization and Standard Organization of Nigeria guideline for drinking water, the results of microbiological analysis also indicated that the three selected rivers are polluted with disease causing microorganisms, such as E.Coliform, Salmonella, Bacillus Subtilis, all through the river course. Therefore, the river waters are not good for drinking. The consumers of this river waters are like to suffer the following: typhoid, fever, intestinal problem, diarrhea, skin rash, cholera. Necessary recommendations such as treating the water with Bio-Sand filter before use, amongst others, were made.

KEYWORD: Water quality, spatial, river water, drinking.

1. INTRODUCTION

Water is the most common, widely distributed and useful liquid on earth. No living thing can survive for long without a supply of water. This is because the reactions that go in the body to maintain life throughout the plant and animal world required the presence of water.

Water is a universal solvent. In other words, it has the ability of dissolving a great number of substances. Plants take food in water. Animals make their foods into solution before the body can use it, without water crop cannot grow, without crop animal cannot live and without crop and animal man cannot obtain food for survival. That is to say “no life without water”

Water is unique, it is the only substance that is found in the three states, liquid, solid (ice) and gaseous states. Earth’s water is constantly interacting, changing and in movement. Water freezes at 32^oF (0^oC) and boils at 212^oF (100^oC). In fact water freezing point and boiling point are the base line on which temperature is measured.

Although water is one of the most common thing on earth it is not equally distributed over the earth’s surface in terms of space and time (Abbasi, 1993). Water occurs on earth’s surface as surface water and below earth’s surface as ground water. Surface water include lakes, rivers, streams and natural open reservoir but for the purpose of this research, water inform of rivers or streams is being considered.
This work focused on the comprehensive and comparative quality analysis of Ubei, Idima, Iyioka rivers in Ebonyi State, with the view to detecting the spatial variations of the physiochemical and

microbiological parameters in the water, using these to determine the potability or otherwise of the river water.

The type, nature and concentrations of the pollutant in the river depends largely on the catchment characteristics, hydro-geological information, anthropogenic activities, magnitude of flow and level of aqua-bioactivities. For example surface water source that provide drainage outlet for farmland will surely have pollutants from fertilizer, pesticide and herbicides etc. Water can be classified as good or poor quality depending on the contaminants and it concentration.

The water in the natural environment always contains some level of impurities, this is so because water is said to be a universal solvent. It contains dissolved solids and gases and it host to a number of micro-organisms (Otuu, 2011). The water quality is defined by the level of its physical, chemical and microbiological quality and the water quality is also evaluated relative to the requirements for the waters intended used. The continues deterioration of these rivers by some impurities gotten from disposed wastewater from agricultural activities affect the normal life of a water and render it unacceptable and is said to be polluted (Fair et.al, 1996), often times lead to epidemics such as diarrhoea and cholera.

This project aims to analyse the water quality of Ubei, Idima and Iyioka rivers, all in south zone of Ebonyi State of Nigeria, with a view to establishing spatial variations of the water quality parameters with respect to drinking. The advent of industrialization in Ebonyi State has resulted in a large use and demand for Water, especially for agricultural and recreational activities, laundry and domestic use, amongst others. These and many others makes it imperative to carry out a study of the quality in order to know the extent to which these river quality parameters can vary over space with respect to drinking, having in mind that government can use them as a source of water scheme in future. This research study aims bringing into the fore, at given answers to the concentrations or potentials of the different water quality parameters that can impact negatively or positively on consumers. How does the concentration of these water parameters vary with space and to what level would these variations affect the quality of the waters?

2. MATERIALS AND METHOD

2.1 Project Site

The area of study is south zone of Ebonyi State of Nigeria. The study was carried out in three selected rivers, each with six distinct locations of 5kilometers apart. The rivers and their test locations are:

A. Ubei Rivers, with test locations at: (i) Ubei Amaiyi River. (ii). Ubei Etiti River (iii) Ubei Amangwu River (iv) Ubei River Extension 1 (v) Ubei River Extension 11(vi) Ubei River Extension 11
B. Idima Rivers , with test locations at: (i) Idima Okporojo River (ii) Idima Oko River (iii) Idima Amaiyi River (iv) Idima River Extension 1 (v) Ubei River Extension 11 (vi) Ubei River Extension 111
C. Iyioka Rivers, with test locations at: (i) Iyioka by Okwukwo River (ii) Iyioka River Extension 1 (iii) Iyioka River Extension 11 (v) Iyioka River Extension 111 (vi) Iyioka River Extension 1V

2.2 Water Sampling

Water samples were collected from the three different rivers, each having six selected distinct locations of about five (5) kilometres apart. The water samples were collected in January 2011. A total of eighteen (18) river locations / data points were carried out for each parameter (Each parameter test was replicated and an average was taken as the true value of the parameter). The samples collected were properly labelled and transferred to the pharmaceutics laboratory of the Department of Pharmaceutics, university of Nigeria Nsukka for preservation and analysis. The methods employed are as described in the following subsections.

2.3 Direct Reading Engineering Method (DREM)

This was done in situ and was used mainly for the analysis of physical parameters such as total dissolved solid (TDS), pH, Salinity, Electrical Conductivity (E.C), Dissolved Oxygen, Chemical Oxygen and temperature.

A 50ml volume of the water sample was drawn from each container with 50ml glass syringe and introduced into 100ml glass beaker and the physical parameter were activated by pressing gently on the Hacc multimeter (model C150) soft touch button. The value displayed at the LCD panel of the Hacch multimeter stand as the true value of the activated parameter.

2.4 Titrimetric Methods:

This method deals with tritrating the water sample with ethylene diamine tetra-acetic acid (EDTA) with solution for water hardness.

2.5 Spectrophotometeric Methods

This was used in the analysis of nitrate (NO3), Carbonate (CO_3), Sulphate (So_4), and Phosphate (PO_4). This method deals with the absorbance of light path length into the curvette which is directly proportional to the concentrations for a particular compound.

2.6 Gravimetric Methods

The Total Suspended Solid (TSS) was determined by this method. A glass fiber was dried in oven at $100^{O}C$ to obtain a known constant weight W_1, A 50ml volume of each water sample taken at the same dept was filtered through fiber bed. The fiber was dried in desiccator and weighed immediately to obtain the second weight W_2. The total suspended solid was calculated using the equation $TSS= (W_2-W_1)/50$
Where: W_2 = constant weight of solid on the fiber; W_1 = weight of the empty dried glass fiber; 50 = volume of water sample used.

The **Total Solid** (TS) was obtained by calculating the arithmetic sum of the total dissolved solid (TDS) and the total suspended solid (TSS)
$TS = TDS + TSS$

However, turbidity was obtained direct from the total suspended solid (TSS), using the relationship
Turbidity = TSS/ 50 (Otuu, 2011)

2.7 Atomic Absorption Spectrophotometric Method

This was used in the determination of all the metallic elements such as Lead (Pb), Copper (Cu), Iron (Fe), Nickel (Ni), Magnesium (Mg), Manganese (Mn), Arsenic (As), Zinc (Zn), Cadmium (cd) (Ajali, 2007).
For microbial analysis, the procedure includes the following:-

1. Preparation of media
2. Preparation of sterile petri-dish and oven-dried agar plate
3. Preparation of counting which includes dilution and counting.

For the purpose of biochemical test, a special growth media was employed for quicker identification. In this case some gram negative bacteria was grown on macconkey agar so as to select coliform through cultural features. Their reactions to glucose and lactose determines the type of disease causing organism present. The results of the analysis are tabulated and shown below for easy study of the variations of the river parameters with the help of descriptive compound line chart. The analysis was replicated to obtain the average value for each analysis. The generated data was further subjected to statistical analysis using one way analysis of variance (ANOVA) on difference between mean of parameter and a graphical method to determine its quality spatial variations.

3. RESULTS AND DISCUSSION

The behaviour of the physical chemical and microbial parameter test are shown in Figure 1.

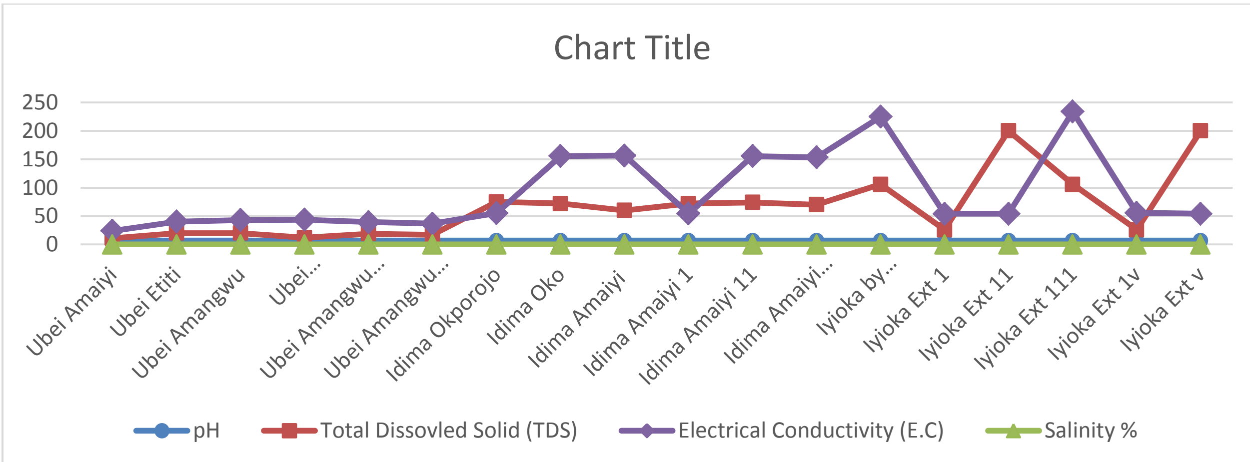

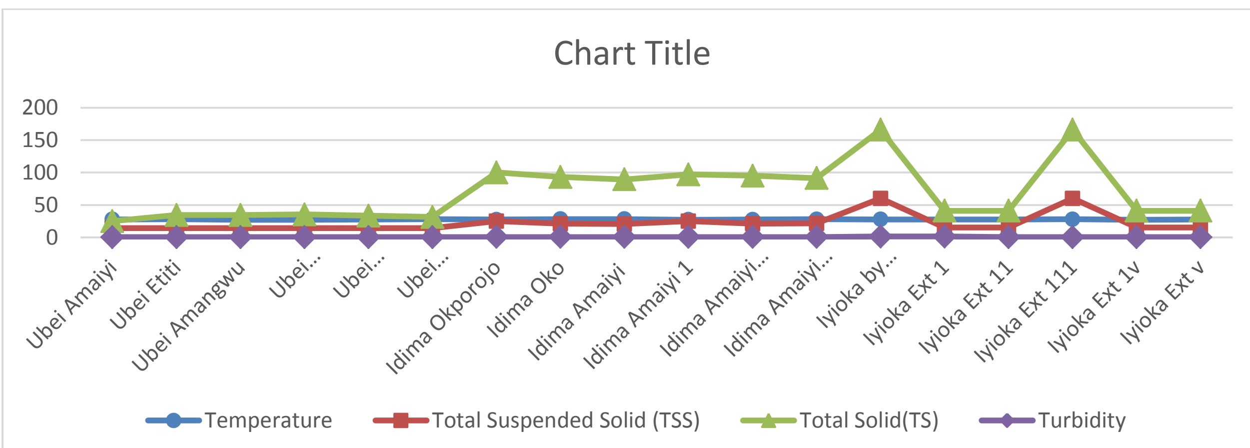

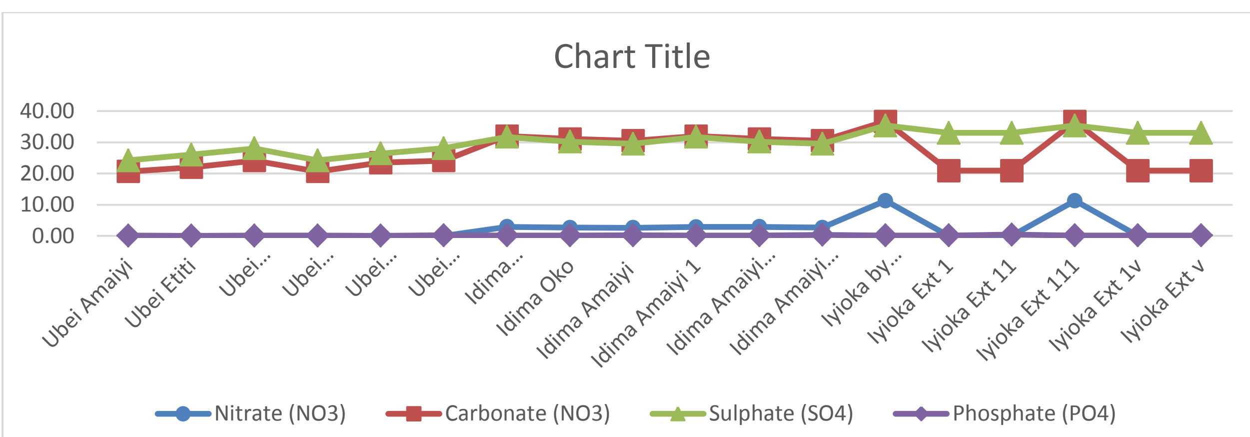

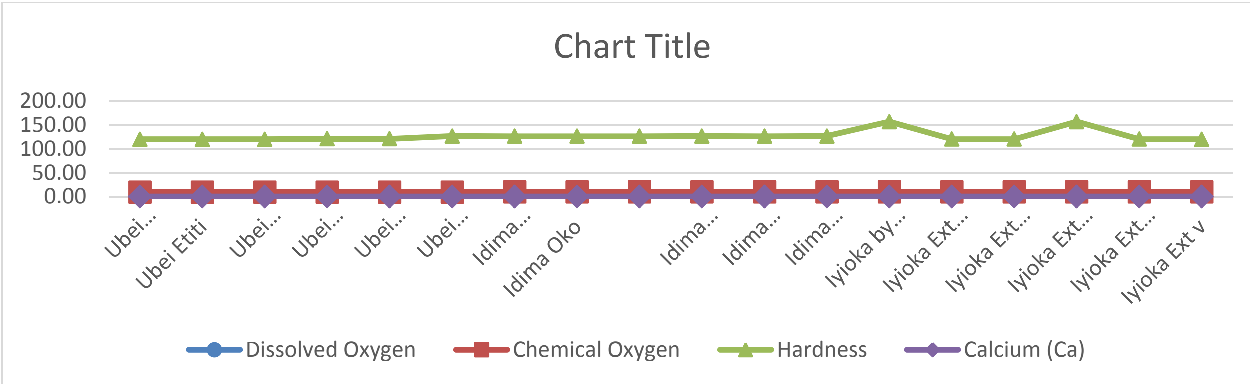

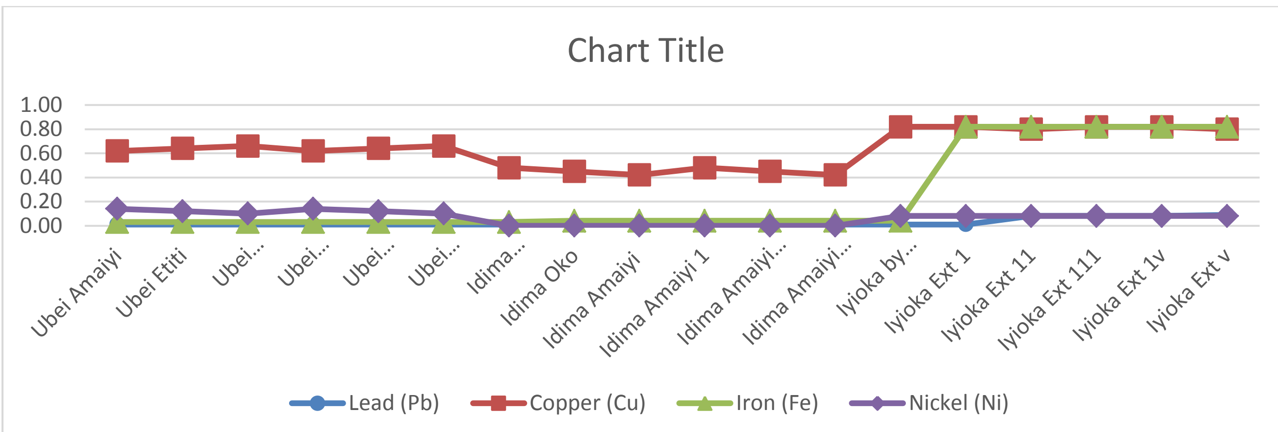

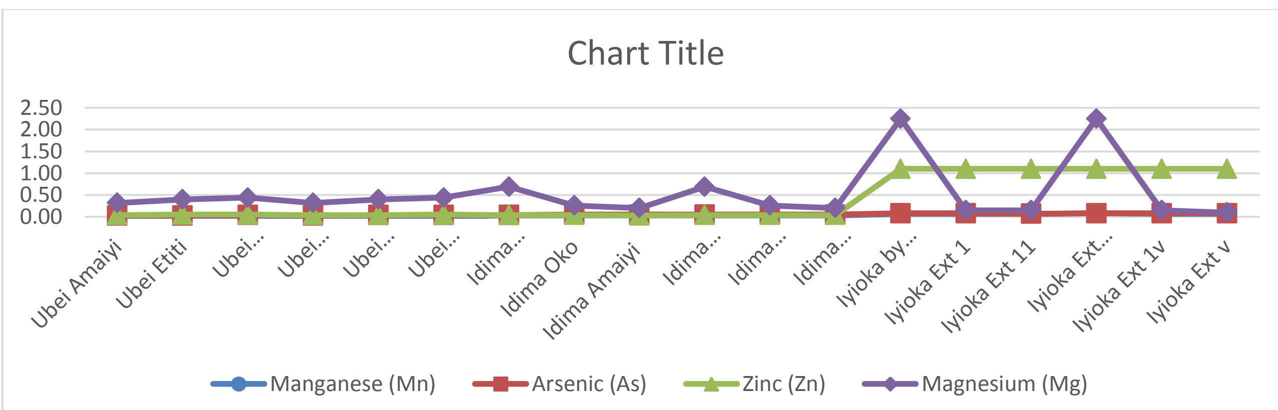

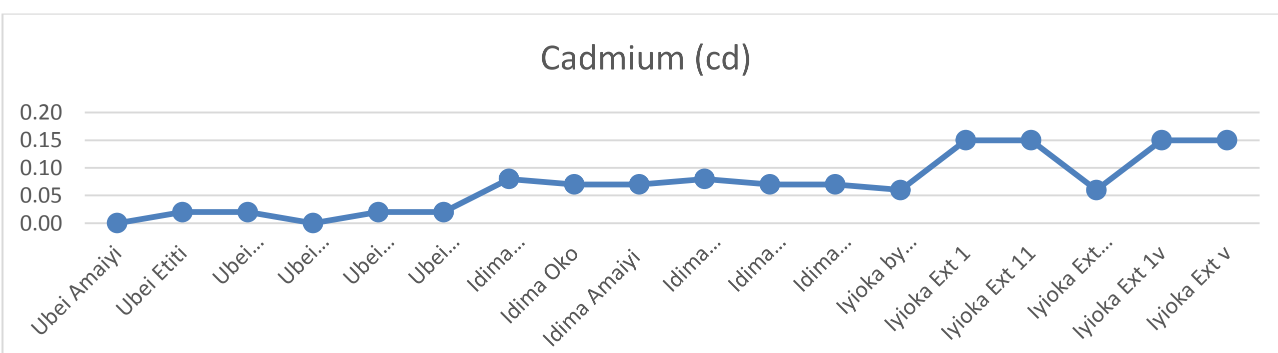

Figure 1: The behaviour of the tested physical, chemical and microbial parameter test

On comparing the water quality of the rivers studied with World Health Organization (WHO) and Standard Organization of Nigeria (SON, 2007) guideline for drinking water, it was observed that the sampled water pH (6.81 – 6.90), Electrical Conductivity (39.80 – 399.11%). Turbidity (0.29 – 1.42 NTU) and Total dissolved solid (26 – 200.17mg/ml), (0.00 – 11.25), copper (0.42 – 0.82), manganese (0.01 – 0.07) fall within a safe range. But Sulphate (24.20 – 35.38), chemical oxygen (9.60 – 10.39), nickel (0.00 – 0.14), arsenic (0.03 – 0.08), zinc (0.04 – 1.10), cadmium (0.00 – 0.15) fall above safe range. The summary of the ANOVA is shown in Table 1.

Table 1: summary of tested ANOVA result with respect to space during dry season

Parameters	F-CAL	F-TAB	Level Of Significant	Decision
pH	-0.535	-5.76	NS	Accept
Total Dissovled Solid (TDS)	-2.565	-5.76	NS	Accept
Salinity %	-23.915	-5.76	NS	Accept
Electrical Conductivity (E.C)	-1.409	-5.76	NS	Accept
Temperature	-0.439	-5.76	NS	Accept
Total Suspended Solid (TSS)	-0.827	-5.76	NS	Accept
Total Solid(TS)	-1.874	-5.76	NS	Accept
Turbidity	-1.47	-5.76	NS	Accept
Nitrate (NO3)	-0.805	-5.76	NS	Accept
Carbonate (NO3)	-1.971	-5.76	NS	Accept
Sulphate (SO4)	-18.933	-5.76	1%	Reject
Phosphate (PO4)	-1.293	-5.76	NS	Accept
Dissolved Oxygen	-0.564	-5.76	NS	Accept
Chemical Oxygen	-7.34	-5.76	5%	Reject
Hardness	-0.72	-5.76	NS	Accept
Calcium (Ca)	-0.9	-5.76	NS	Accept
Lead (Pb)	-1.532	-5.76	NS	Accept
Copper (Cu)	-0.455	-5.76	NS	Reject
Iron (Fe)	0	-5.76	NS	Reject
Nickel (Ni)	-84	-5.76	1%	Reject
Manganese (Mn)	-283	-5.76	1%	Reject
Arsenic (As)	-133	-5.76	1%	Reject
Zinc (Zn)	-1000492	-5.76	1%	Reject
Magnesium (Mg)	-0.404	-5.76	NS	Accept
Cadmium (cd)	-0.404	-5.76	5%	Reject
Bacteria	-1.107	-5.76	1%	Reject
Fungi	-2.68	-5.76	NS	Accept

Table 1 shows that there were significant differences in the area of some variables between space at various levels of significance, these includes: sulphate (1%), Sulphate (1%), Alkalinity (5%), Chemical Oxygen (5%), Nickel (1%), Arsenic (1%), Zinc (1%), Cadmium (1%), Bacteria (1%). But, other variables were not statistically different in their mean values within the period of study. Though, numerical difference may exist but statistical difference did not exist. This is because their F-Calculated (F-CAL) was less than F-Tabulated (F-TAB). On comparing the microbial river qualities of the three selected rivers studied to World Health Organization and Standard Organization of Nigeria (SON) guidelines for drinking water. It was discovered that the three rivers are not good for drinking because of the presence of some organisms such as E.coli., salmonella, bacillus subtilis.

4. CONCLUSIONS AND RECOMMENDATIONS

Iyioka River is the highest polluted river with Iyioka by Okwukwo as the highest polluted location. This is followed by Idima and Ubei River respectively. Generally it was found that there was continuous variation of all the river qualities. Microbiologically the three selected rivers are not good for drinking because of the presence of the bacteria and fungi. Use of Bio-Sand filter together with disinfectant amongst other methods are hereby recommended**.**

REFERENCE

Abbasi S.A. 1998. Water quality sampling and analysis, discovery publishing house, new delhi-110002 India.

Ajali, U et al 2007. Spectroscopic Methods and Techniques for Life and applied science. First edition published by Mason Production Ltd, Enugu State of Nigeria.

Armstrong F.A.J. 1963. Determination of nitrate in water by ultraviolet spectrophotometry. Anal. Chem. 35:1292

Emmanuel O.O. 2006. Statistic for Agricultural and Biological Science. First edition Published by Cheston Agency Ltd. Enugu State of Nigeria.

McGuire et al M.J. 2002. Information collection rule Data analysis. Denver, colo:water research foundation.

Okere C.D 2006. Environmental Pollution Control, First Edition. Published by Barloz Publishers Inc. Owerri, Imo State, Nigeria.

Otuu F.C 2011. Antimicrobial and Flocculant Properties of Moringa Oleifera Aqueous and Ethanolic Seed Extract in some Hand dug Well Water in Enugu State Metropolis for the award of Fellowship of Nigeria Institute of Science Laboratory Technology, Unpublished.

SON's and WHO's 2007. Guideline for drinking water.

Westeot, D.W. et al 1976. water quality for agriculture. Vikas Publishing House, New Delhi, FAO. Irrigation drainage paper No.29.

GUIDE FOR AUTHORS

Publication Schedule: The Journal of Agricultural Engineering and Technology (JAET) is published annually (four issues) by the Nigerian Institution of Agricultural Engineers (NIAE), A division of the Nigerian Society of Engineers (NSE).

Published articles can be viewed at the Institution's website: www.niae.net.

Manuscript: The manuscript should be typed double spaced on A4 paper (216mm x 279mm) on one side of the paper only, with left, right and top-bottom margins of 25.4mm. The original and three copies are required for initial submission. The paper should not exceed 20 pages including Figures and Tables. Manuscripts are also accepted as attached file in MS word.

Organization of the Manuscript: The manuscript should be organized in the following order; Title, Author's name and address including E-mail address and telephone number; Abstract; Keywords; Introduction; Materials and Methods; Results and Discussion; Conclusion; Notation (if any); Acknowledgements; References. The main headings listed above should be capitalized and left justified. The sub-headings should be in lower case letters and should also be left justified. Sub-sub headings should be in italics. All headings, sub-headings and sub-sub-headings should be in bold font. Headings and sub-headings should be identified with numbers such as 1; 1.1; 1.1.1 etc. For the sub headings, the first letter of every word should be capitalized.

Title: The title should be as short as possible, usually not more than 14 words. Use words that can be used for indexing. In the case of multiple authors, the names should be identified with superscripted numbers and the addresses listed according to the numbers, e.g. A. P. Onwualu[1] and G. B. Musa[2].

Abstract: An abstract not exceeding 400 words should be provided. This should give a short outline of the problem, methods, major findings and recommendations.

Keywords: There should be keywords that can be used for indexing. A maximum of 5 words is allowed.

Introduction: The introduction should provide background information on the problem including recent or current references to work done by previous researchers. It should end with the objectives and contribution of the work.

Materials and Methods: This section can vary depending on the nature of the paper. For papers involving experiments, the methods, experimental design and details of the procedure should be given such that another researcher can verify it. Standard procedures however should not be presented. Rather, authors should refer to other sources. This section should also contain description of equipment and statistical analysis where applicable. For a paper that involves theoretical analysis, this is where the theory is presented.

Results and Discussion: Results give details of what has been achieved, presented in descriptive, tabular or graphical forms. Discussions on the other hand, describe ways the data, graphs and other illustrations have served to provide answers to questions and describe problem areas as previously discussed under introduction.

Conclusion: Conclusion should present the highlights of the solutions obtained. It should be a brief summary stating what the investigation was about, the major result obtained and whether the result were conclusive and recommendations for future work, if any.

Notation: A list of symbols and abbreviation should be provided even though each of them should be explained in the place where it is used.

References: Follow the name-date system in the text, example: Ajibola (1992) for a single author; Echiegu and Ghaly (1992) for double authors and Musa et al. (1992) for multiple authors. All references cited must be listed in alphabetical order. Reference to two or more papers published in the same year by the same author or authors should be distinguished by appending alphabets to the year e.g. Ige (1990a, 1992b). All references cited in the text must be listed under section "References". For Journal, the order of listing should be author's name, year of publication, title of paper, name of journal, volume number, pages of the article: for books, the author's name comes first followed by the date, title of book, edition, publisher, town or city of publication and page or pages involved. Examples are as follows:

Journal Articles: Ezeike, G. O. I. 1992. How to Reference a Journal. J. Agric Engr. and Technology. 3(1): 210-205

Conference Papers: Echiegu, E. A. and Onwualu A. P. 1992. Fundamentals of Journal Article Referencing. NSAE paper No 92-0089. Nigerian Society of Agricultural Engineers Annual Meeting, University of Abuja, Abuja – Nigeria.

Books: Ajibola O. 1992. NSAE: Book of abstracts. NSAE: Publishers. Oba. Abakaliki, Nigeria.

Book Chapter: Mohamed S. J., Musa H. and Okonkwo, P. I., Ergonomics of referencing. In: E. I. U. Nwuba (Editor), Ergonomics of Farm Tools. Ebonyi Publishing Company, Oshogbo, Osun State, Nigeria.

Tables: Tables should be numbered by Arabic numerals e.g. Table 3 in ascending order as reference is made to them in the text. The same data cannot be shown in both Table and Figure. Use Table format to create tables. The caption should be self explanatory, typed in lower case letters (with the first letter of each word capitalized) and placed above the table. Tables must be referred to in the text, and positioned at their appropriate location, not at the end of the paper.

Figures: Illustrations may be in the form of graphs, line drawings, diagrams schematics and photographs. They are numbered in Arabic numerals e.g. Figure 5.m. The title should be placed below the figure. Figures should be adequately labeled. All Figures and photographs should be computer generated or scanned and placed at their appropriate locations, not at the end of the paper.

Units: All units in the text, tables and figures must conform to the International System of units (SI)

Reviewing: All papers will be peer reviewed by three reviewers to be appointed by the Editors. The editors collate the reviewers' reports and add their own. The Editor-In-Chief's decision on any paper is final.

Off Prints: A copy of the journal is supplied free of charge to the author(s). Additional reprints can be obtained at current charges.

Page Charges: The journal charges a processing fee of N1000 and page charges are currently N1000 per journal page. When a paper is found publishable, the author is advised on the page charges but processing fee (non refundable) must be paid on initial paper submission. These charges are subject to change without notice.

Submission of Manuscript: Submission of an article for publication implies that it has not been previously published and is not being considered for publication elsewhere. Four copies of the manuscript and N1000 processing fee should be sent to:

The Editor-In-Chief
Journal of Agricultural Engineering and Technology (JAET)
C/o The Editorial Office
National Centre for Agricultural Mechanization (NCAM)
P.M.B. 1525, Ilorin, Kwara State
Nigeria.

Papers can also be submitted electronically to any member of the Editorial Board and to the Technical Assistant to the Editor In Chief at ifeeolife@yahoo.com.